

## Durham E-Theses

---

### *Morphology of block copolymers from neutron scattering*

Gary Welsh

#### How to cite:

---

Welsh, Gary (1992) Morphology of block copolymers from neutron scattering. Doctoral thesis, Durham University.

#### Use policy

---

The full-text may be used and/or reproduced, and given to third parties in any format or medium, without prior permission or charge, for personal research or study, educational, or not-for-profit purposes provided that:

- a full bibliographic reference is made to the original source
- a <https://etheses.durham.ac.uk/id/eprint/5606/> is made to the metadata record in Durham E-Theses
- the full-text is not changed in any way

The full-text must not be sold in any format or medium without the formal permission of the copyright holders.

Please consult the [full Durham E-Theses policy](#) for further details.

3931

The copyright of this thesis rests with the author.  
No quotation from it should be published without  
his prior written consent and information derived  
from it should be acknowledged.

**MORPHOLOGY OF BLOCK COPOLYMERS FROM  
NEUTRON SCATTERING**

GARY WELSH

Department of Chemistry  
University of Durham

PhD Thesis 1992

The copyright of this thesis rests with the author.  
No quotation from it should be published without his  
prior written consent and information derived from it  
should be acknowledged.

No material contained in this thesis has previously  
been submitted for a degree in this or any other  
University.



16 APR 1993

**For my wife, Teresa - Thank you**

## ACKNOWLEDGEMENTS

I would like to thank the S.E.R.C. for funding this thesis and Professors M.L. Hitchman and J.W. Feast, at Strathclyde and Durham Universities respectively, for allowing me to work in their Departments.

I would especially like to acknowledge the contribution of my Supervisor, Dr. R.W. Richards, but for whose help and cajoling this thesis would not have been written.

I wish to thank all the people who helped me carry out my experiments at the Rutherford-Appleton laboratory, Oxford and the Institut Lave-Langevin, Grenoble especially Dr. A. Rennie and Dr. H. Stanley/Dr. R. Heenan.

My gratitude also extends to Mrs. S. Wallbank for her tireless work on typing this thesis.

Finally I would like to thank family and friends for their support during my studies and thank my wife, Teresa, for helping me retain my sanity.

MORPHOLOGY OF BLOCK COPOLYMERS FROM NEUTRON  
SCATTERING

Gary Welsh

PhD Thesis 1992

Abstract

Block copolymers are widely used commercially and so a complete understanding of these systems requires that the nature of the polymer interface, the effect of deformation and the interaction between polymer substituents are known. Triblock copolymers of poly(styrene-isoprene-styrene) were synthesised and used in a Small Angle Neutron Scattering (SANS) study of deformation (Ch. 3). Three sets of samples were made and, of these, two sets were found to have degraded giving unexpected results (Ch. 3.2). The third set, SPH150 series, however, did exhibit the expected anisotropy on deformation (Ch. 3.3). In these samples, the extension parallel to the stretch direction was affine for all elongation ratios studied and, perpendicular to the stretch direction, the extension was non-affine. The interaction between polymer substituents was examined using SANS on an isotopic diblock copolymer of polystyrene to ascertain if the mixing of hydrogenous and deuterated species was ideal (Ch. 4). The results obtained showed the mixing between these species could be assumed to be ideal. The nature of the polymer-polymer interface was studied on the CRISP reflectometer using poly(styrene-isoprene) diblock samples (Ch. 5). The results obtained for unannealed samples showed that a 'pseudo-equilibrium' had been achieved in these samples which was lost on annealing.

## CONTENTS

	<u>Page</u>	
<u>CHAPTER 1 - INTRODUCTION</u>		
<u>1.1. Block Copolymers</u>		
1.1.1. Introduction	2	
1.1.2. Block Copolymer Morphology	4	
1.1.3. Techniques Used to Study Block Copolymers	6	
<u>1.2. Small Angle Neutron Scattering</u>		
1.2.1. Introduction	6	
1.2.2. Block Copolymer Dimensions for SANS	10	
<u>1.3. Theories of Rubber Elasticity</u>		16
References	20	
<u>CHAPTER 2 - EXPERIMENTAL</u>		
<u>2.1. Polymer/Copolymer Preparation</u>		
2.1.1. Vacuum Line	22	
2.1.2. Monomer and Solvent Purification	23	
2.1.3. Calibration of Initiator	24	
2.1.4. Polymerisation of Copolymers	24	
<u>2.2. Polymer/Copolymer Characterisation</u>		
2.2.1. Weight Average Molecular Weight and Polydispersity	29	
2.2.2. Number Average Molecular Weight	30	
2.2.3. Ultra Violet Spectroscopy	31	
<u>2.3. Small Angle Neutron Scattering</u>		
2.3.1. SANS Instrument	33	
2.3.2. Sample Preparation	35	
2.3.3. Data Correction	38	
<u>2.4. Neutron Reflectometry</u>		
2.4.1. Instrumentation	40	
2.4.2. Samples for Reflection Studies	41	
References		
<u>CHAPTER 3 - STUDY OF DEFORMATION IN A TRIBLOCK COPOLYMER</u>		
<u>3.1. SANS Study of a Cylindrical Domain Triblock Copolymer</u>	44	

	<u>Page</u>
3.1.1. Introduction	44
3.1.2. Previous Work	46
<u>3.2. Experimental</u>	52
3.2.1. Results and Discussion	56
<u>3.3. SANS Study of a Spherical Domain Triblock Copolymer</u>	
3.3.1. Introduction	71
3.3.2. Experimental	73
3.3.3. Results	74
3.3.4. Discussion	84
3.3.5. Future Work	88
<u>3.4. SANS Study of Extruded Samples</u>	
3.4.1. Introduction	90
3.4.2. Experimental	90
3.4.3. Results and Discussion	91
References	95
<u>CHAPTER 4 - THE INTERACTION BETWEEN COMPONENT BLOCKS OF AN ISOTOPIC DIBLOCK COPOLYMER</u>	
<u>4.1. Introduction</u>	98
4.1.1. Background	99
4.1.2. R.P.A. Theory	100
4.1.3. Experimental	106
<u>4.2. Results and Discussion</u>	
4.2.1. Isotopic Diblocks of Polystyrene	109
4.2.2. Discussion of Results	117
<u>4.3. Polymer Blends</u>	
4.3.1. Introduction	122
4.3.2. Experimental	122
4.3.3. Results	123
References	124
<u>CHAPTER 5 - NEUTRON REFLECTIVITY STUDIES OF THE ORDERING IN A SERIES OF DIBLOCK COPOLYMER FILMS</u>	
<u>5.1. Introduction</u>	125
5.1.1. Background	126

	<u>Page</u>
<u>5.2. Results and Discussion</u>	
5.2.1. Results	128
References	148
<u>CHAPTER 6 - GENERAL DISCUSSION</u>	150
<u>APPENDICES</u>	
1 'RPOLLY' PROGRAM FOR SANS DATA CORRECTION	
2 'SASFIT' PROGRAM FOR DATA ANALYSIS	
3 LECTURES AND COLLOQUIA LIST	

## CHAPTER 1 - INTRODUCTION

### 1.1. Block Copolymers

#### 1.1.1. Introduction

Block copolymers are macromolecules made up of terminally connected, chemically different segments. The sequential arrangement of block copolymers can be one of three types, Figure (1.1.):

- (i) A-B diblock structure containing only two segments.
- (ii) A-B-A triblock structure containing three segments.
- (iii)  $(A-B)_n$  multiblock structure containing many segments.

In general, most polymer mixtures are incompatible leading to a two-phase morphology at the microscopic level in block copolymers. The domains formed are of the order of tens of nanometers since the intersegment linkage present in block copolymers restricts the extent to which the segments can separate. This microdomain formation is the source of the unique properties of many block copolymers and led to the development of the new technology of thermoplastic elastomers.

These two terms had previously been mutually exclusive in polymer science but it was found that A-B-A and  $(A-B)_n$  block copolymers (Figure 1.1) are characterised by their thermoplasticity together with rubber-like

behaviour. To obtain a thermoplastic elastomer a two-phase network has to be developed where the copolymer is made up of a minor fraction of hard block (glass transition temperature,  $T_g$ , greater than room temperature) and a major fraction of a soft block ( $T_g$  less than room temperature). In such a system the hard blocks microphase separate to form small domains which act as physical cross-linking and reinforcement sites. Only copolymers containing two or more hard blocks per macromolecule can do this.

Due to their thermoplastic and rubber-like characteristics block copolymers find a great deal of use commercially. In the car industry for instance, block copolymers of styrene-isoprene and styrene-butadiene are used in making tyres.

Figure 1.1. Block Copolymer Structures

A-A-A.....-A-A-A-B-B-B.....-B-B-B

A-B diblock copolymer

A-A-A.....-A-A-A-B-B-B.....-B-B-B-A-A-A.....-A-A-A

A-B-A triblock copolymer

(A-A-A.....-A-A-A-B-B-B.....-B-B-B)<sub>n</sub>

(A-B)<sub>n</sub> multiblock copolymer

The investigation of block copolymer behaviour under various conditions and the effect at the molecular as well as the macromolecular level is of great interest since it enables predictions of copolymer behaviour to be made. This would allow block copolymers to be made that would best achieve the properties required for a particular use.

1.1.2. Block Copolymer Morphology

The morphology of a block copolymer is dependent on the volume fraction of each component<sup>1</sup> and on the method of copolymer synthesis. The major component normally exists as the continuous phase and the minor component forms discrete domains. These domains can

be divided into three general morphologies:-

(i) Spherical - Volume fraction of minor component is less than 20%.

(ii) Cylindrical - Volume fraction of minor component is somewhat greater than 20%.

(iii) Lamellar - The two phases are present in nearly equal volume fractions.

It is often the case that the microphases form regular arrays where the periodic structure is of a macrolattice and the submicroscopic domains are the repeating element. In this case spheres give rise to a cubic lattice, cylinders form a two-dimensional hexagonal lattice and lamellae form a regularly repeating lamellar sequence. The type, size and arrangement of domains have a great influence on the physical properties of the copolymer that are dependent on the nature of the continuous phase.

In the interfacial region, where the two segments mix, the morphology of the structure can be either very sharp or diffuse depending on the nature of the phase boundary. The more chemically compatible the segments the more diffuse the interfacial layer will be. A measure of the compatibility of copolymer components is given by the interaction parameter,  $\chi$ . If  $\chi$  is negative then mixing between substituents was favoured but if  $\chi$  is positive mixing was unfavourable and substituents would be phase separated.

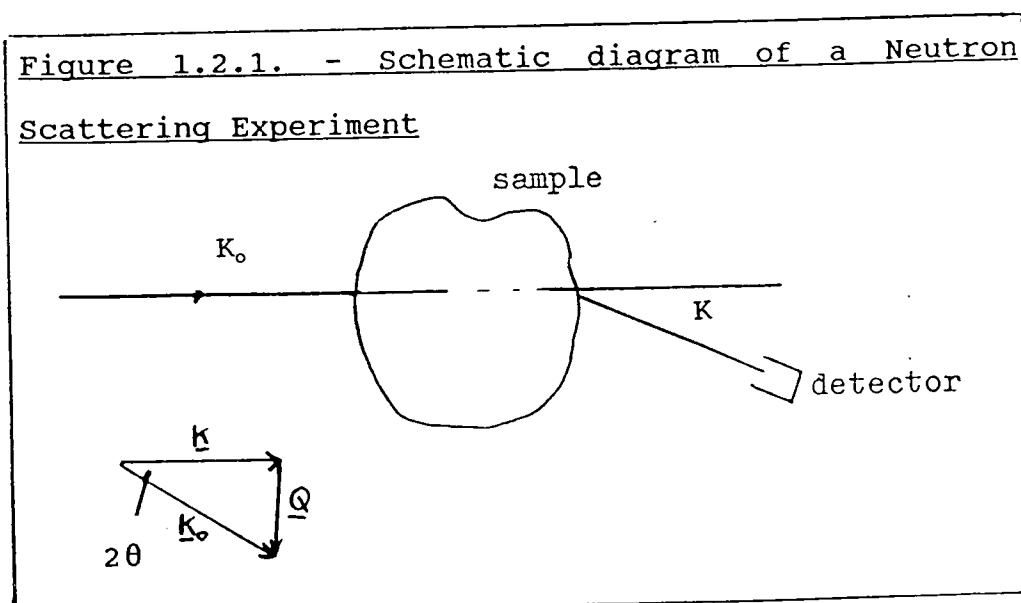
### 1.1.3. Techniques used to study Block Copolymers

The technique used to study a block copolymer or any polymer system depends on two main factors. Firstly what facilities are available and secondly what particular aspect of the sample is of interest. Before the advent of Small Angle Neutron Scattering the main techniques were electron microscopy, birefringence, light scattering and Small Angle X-Ray Scattering. These are still used, though to a lesser extent, today.

### 1.2. Small Angle Neutron Scattering (SANS)

#### 1.2.1. Introduction

The fundamentals of SANS have been extensively dealt with in the literature<sup>2</sup> so there is little point in covering the ground. It is, however, germane to give a brief account of a typical neutron scattering experiment. Figure 1.2.1. shows a schematic diagram of a neutron scattering experiment.



The incident neutron beam is of intensity  $I_0$  with wave vector,  $\underline{K}_0$ . Now  $\underline{K}_0$  equals  $(2\pi/\lambda)$  where  $\lambda$  is the wavelength of neutrons used. The scattered intensity,  $I$ , of wave vector  $\underline{K}$  at an angle  $2\theta$  to the incident beam is the result of neutron-neutron interaction between the beam and specimen. In SANS there is no transfer of energy between neutron and specimen and so SANS is an elastic scattering method where  $\underline{K} = \underline{K}_0$ . This means the scattering vector,  $\underline{Q}$ , is given by  $(4\pi/\lambda \sin\theta)$ . The scattered intensity,  $I$ , can then be written as:-

$$I = I_0 N (d\sigma/d\Omega) \Delta\Omega \quad \text{EQ. (1)}$$

where:

$N$  = number of nuclei in the scattering volume.

$\Delta\Omega$  = the solid angle subtended by the detector at the sample.

$(d\sigma/d\Omega)$  = differential scattering cross section of the specimen.

The  $(d\sigma/d\Omega)$  term contains both structural information on the scattering material and scattering which provides no information on the sample and can be regarded as a background signal which has to be subtracted from the data to give the required information. The two components of  $(d\sigma/d\Omega)$  have been identified as the differential coherent scattering cross-section which contains the structural

information and the incoherent scattering cross-section which is the source of the background scattering. This leads to an expression for the differential scattering cross-section using a two-phase model where:-

$$I(Q) = I_o \frac{N}{V} \Delta\Omega \left[ \frac{V_p^2}{N} N_p (\rho_p - \rho_m)^2 S(Q) + \frac{\sigma_{inc}}{4\pi} \right] \quad \text{EQ. (2)}$$

where:

V = scattering volume;  $V_p$  = scattering particle volume.

$N_p$  = number of particles in volume, V.

$\sigma_{inc}$  = incoherent scattering cross-section.

$\rho_p, \rho_m$  = coherent scattering length density for the scattering particle and the matrix in which particles are dispersed respectively.

$(\rho_p - \rho_m)^2$  = contrast factor

$S(Q)$  = scattering law for material being investigated. The contribution of  $S(Q)$  is increased when the contrast factor is made as large as possible. In SANS this is usually achieved by using a fully deuterated material as the scattering particle. This is because scattering length densities,  $\rho$ , can be calculated from:-

$$\rho = bN_A d / M \quad \text{EQ. (3)}$$

where:      b = coherent scattering length

                  d = physical density

                  M = segment molecular weight

$N_A = \text{Avogadro's Number}$

For hydrogen,  $b = - 0.374 \times 10^{-12}\text{cm}$

For deuterium,  $b = 0.667 \times 10^{-12}\text{cm}$

So by using deuterated material the contrast factor, and hence  $S(Q)$ , can be increased. So when a few deuterated macromolecules are dispersed in a hydrogenous matrix:

$$S(Q) = 1 / (Q^2 \langle Rg^2 \rangle^2) \exp [ (-Q^2 \langle Rg^2 \rangle) - 1 + Q^2 \langle Rg^2 \rangle ] \quad \text{EQ. (4)}$$

where:

$\langle Rg^2 \rangle = z\text{-average mean square radius of gyration.}$

In the case of a triblock copolymer equation (2) becomes more complex due to the contribution to the overall scattering intensity caused by ordering of the domain-forming blocks. For a triblock copolymer the Debye equation only holds if this contribution in equation (5) can be eliminated.

$$I(Q) \propto (X\rho_D + (1-X)\rho_H - \rho_0)^2 S(Q) + X(1-X)(\rho_D - \rho_H)^2 P(Q) \quad \text{EQ. (5)}$$

where:

$I(Q) = \text{scattered intensity}$

$\rho_d, \rho_H = \text{scattering length densities of the deuterated and hydrogenous isoprene respectively.}$

$\rho_o = \text{scattering length density of hydrogenous styrene.}$

$S(Q) = \text{total scattering law for block copolymer}$

$P(Q) = \text{scattering law due to deuterioisoprene block}$

$X = \text{weight fraction of deuterioisoprene in block copolymer}$

For the elimination of the scattering due to  $S(Q)$  from

equation (5) then:

$$X\rho_D + (1-X)\rho_H - \rho_o = 0 \quad \text{EQ. (6)}$$

For poly(styrene-isoprene-styrene) the value of X in equation (6) was calculated to be 0.16.

### 1.2.2. Block Copolymer Dimensions from SANS

In studies of block copolymers the copolymer dimensions of most interest are the radius of gyration, the domain morphology, the nature of the interfacial region, the domain size and interdomain distance. These may all be determined by SANS study and compared with the predictions of domain formation theories.

The two main theories of microdomain formation have come from Meier<sup>3</sup> and Helfand<sup>4-7</sup> though others have carried out theoretical work<sup>8,9</sup>. The theories of both Helfand and Meier are statistical thermodynamic in nature and are based on equilibrium considerations. Consequently both theories have a fair amount of common statistical thermodynamic principle.

The crux of any statistical thermodynamic approach to microphase separation is that the most favourable conformation is the one that minimises the total free energy, G, from:

$$dG = dH - TdS$$

where:

G = Gibbs Free Energy (J)

dH = enthalpy change (J)

T = temperature (K)

$dS$  = entropy change ( $J K^{-1}$ )

In his theory, Meier states that the relative free energy difference between the domain structure and the homogeneous mixture is made up of several terms which limit entropy and segment conformation.

Helfand's approach is similar but by making an assumption, that the interphase is narrow and molecular weight independent, he obtained a simplified formula for the free energy difference. Helfand has criticized Meier's theory on several points including its inability to describe sufficiently the interface between two homopolymers.

Despite this both theories showed that the free energy of the domains vary with segment weight fraction so that there are regions where the minimum free energy is associated with one particular morphology. Both theories also predict that domain size and interdomain distance are proportional to molecular weight though they show a different degree of proportionality. Helfand predicts domain size is proportional to  $M_d^{2/3}$  whereas Meier has it as  $(\alpha M_d^{1/2})$ . The parameter,  $\alpha$ , the chain expansion parameter, of Meier may be dependent on molecular weight of the block,  $M_d$ , but it is not made clear if this is the case.

There is, however, disagreement between the two theories on the question of the dependence of the interfacial thickness and copolymer volume fraction on the molecular weight. Meier's theory predicts that

the interfacial thickness is inversely proportional to molecular weight whereas Helfand assumes that it is invariant with molecular weight. As a result, Meier's theory predicts much larger volume fractions in the interphase at low molecular weight.

#### 1.2.2.1. Interdomain Distance, Domain Size and Ordering

Assuming copolymer samples are composed of  $N_p$  identical domains with coherent scattering length density,  $\rho_p$  and volume,  $V_p$  dispersed in a matrix of coherent scattering length density,  $\rho_m$ , then the coherent cross-section,  $d\sigma/d\Omega$ , may be written as:

$$\frac{d\sigma}{d\Omega} = \frac{C_f V_p^2 N_p}{N} (\langle F_p^2(Q) \rangle - \langle F_p(Q) \rangle^2) + \langle F_p(Q) \rangle^2 A(Q) \quad \text{EQ. (7)}$$

where:

$C_f$  = contrast factor

$N$  = number of nuclei illuminated by the beam

$F_p(Q)$  = single particle form factor (SPFF)

$A(Q)$  = interparticle interference function

Where the scattering particles are of reasonably uniform shape and size then it is found that  $\langle F_p^2(Q) \rangle = \langle F_p(Q) \rangle^2$  and exact equality is obtained from spherical particles. As a result equation (1) may be simplified and the scattering intensity,  $I(Q)$ , obtained can be written as:

$$I(Q) = K' \cdot C_f \cdot \langle F_p(Q)^2 \rangle \cdot A(Q) + K' I_{inc} \quad \text{EQ. (8)}$$

where:

$K'$  = a constant

Consequently the scattering spectra consist of a coherent factor composed of contributions due to  $\langle F_p(Q)^2 \rangle$  and  $A(Q)$  superimposed on a flat incoherent background. For particles arranged periodically then the  $A(Q)$  contribution will be manifest as a series of discrete peaks in an  $I(Q)$  vs  $Q$  plot, and the intensity of these peaks will be modified by the shape of the SPFF. If, on the other hand, particle arrangement is local, then interference peaks at high  $Q$  will disappear and any structure in the scattering profile will be due to  $\langle F_p(Q)^2 \rangle$  only.

In general, it is found that domain ordering is a local effect and the lattice does not extend far through the sample. The domains are ordered locally in small grains which are randomly oriented throughout the sample. Annealing samples has been shown to increase the number of resolvable peaks. Resolution is affected by three factors:

- (i) Grain size
- (ii) Lattice distortion within the grain
- (iii) Spectrometer resolution

Interplanar spacing,  $d_{int}$  is obtained from Bragg's Law

$$d_{int} = 2\pi / Q_{int} \quad \text{EQ. (9)}$$

By comparing the value of the ratio of the spacings from subsidiary peaks to that of the first with

characteristic ratios for simple regular domain arrangements, each sample may be assigned a structure. At higher  $Q$  Bragg maxima disappear and a series of minima and broad maxima due to SPFF become apparent. From their position, domain size can be obtained. Figures 1.2.2. and 1.2.3. show this graphically.

Figure 1.2.2. Scattering Profile At Low  $Q$

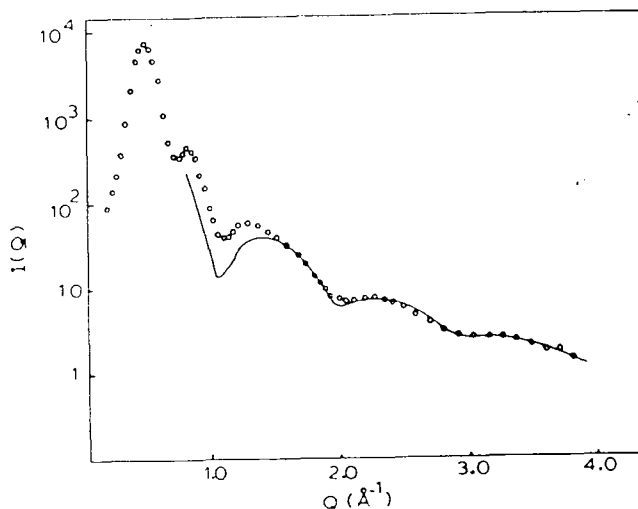
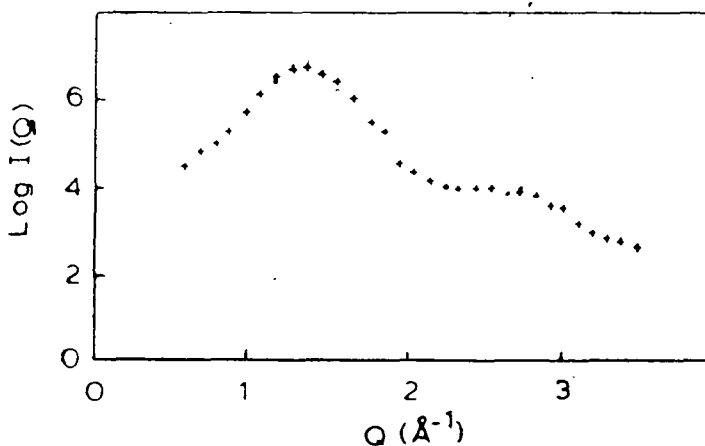


Figure 1.2.3. Scattering Profile at Intermediate  $Q$



For lamellar domains it has been shown that<sup>1</sup>

$$d_{\text{int}} = 2\pi/Q_{\text{max}}$$

$$F_p(Q) = (\pi/QL)^{1/2} J_{1/2}(QL/2) \quad \text{EQ. (10)}$$

where:

$J_{1/2}(QL/2)$  is a Bessel function of order  $1/2$ . L is the length of lamellae.

For cylindrical domains<sup>1</sup>

$$d_{\text{int}} = 4\pi/\sqrt{3}Q_{\text{max}}$$

$$F_p(Q) = 2J_1(QR_c)/QR_c \quad \text{EQ. (11)}$$

where:

$J_1(QR_c)$  is a Bessel function of order 1.  $R_c$  = cylinder radius.

For spherical domains<sup>1</sup>

$$d_{\text{int}} = \sqrt{6}\pi/Q_{\text{max}}$$

$$F_p(Q) = (9\pi/2)^{1/2} J_{3/2}(QR_s)^{3/2} \quad \text{EQ. (12)}$$

where:

$J_{3/2}(QR_s)$  is a Bessel Function of order 3/2.

$R_s$  = sphere radius.

Typical scattering profile for a spherical system shows it is less well ordered than either lamellar or cylindrical systems. The main peak is lower and broader and subsidiary peaks are indistinct. This is to be expected since the displacement of domains from the perfect lattice positions causes a decrease in intensity and a broadening of Bragg peaks. For spheres this effect is most marked.

### 1.3. Theories of Rubber Elasticity

The elastic nature of block copolymers has led workers to examine the applicability of classical theories of rubber elasticity in these systems. The first steps in producing models to describe the interactions in polymers were made in the Rotational Isomeric State (R.I.S.) model developed by Volkenstein, Birshtein and Flory. This model classified interactions between chain substituents into two groups and by assigning the most probable population of conformational states the R.I.S. model is obtained. Detailed calculations for R.I.S. models involve matrix algebra and large computers.

The affine model<sup>10</sup> put forward by Flory stated that the displacement of cross-links was affine with macroscopic deformation. At the opposite extreme to the affine model, is the 'phantom network' approach postulated by James and Guth<sup>11,12</sup>. The 'phantom network' states that the network deforms affinely so that the macroscopic deformation of the sample and of the mean vectors connecting cross-link points are the same. Monomer units between cross-link points are free to move consistent with constraints imposed at the cross-links. Neither the volume occupied by monomer units nor the blocking of one chain's deformation by the material presence of other chains is directly taken into account in calculating chain statistics on deformation. Submolecules with the same

number of monomer units have very different mean end-to-end distances. This occurs because of topological constraints and because of the volume displaced by other parts of the network. This distribution of mean end-to-end distances is Gaussian and junction points, fluctuating due to Brownian motion, are dependent on the network functionality. They are isotropic and independent of mean distances between chain ends and sample deformation.

$$z = \bar{z} + \delta z \quad \text{EQ. (13)}$$

$$\langle z^2 \rangle = \langle \bar{z}^2 \rangle + \langle \delta z^2 \rangle \quad \text{EQ. (14)}$$

where:

$z$  =  $z$  component of vector connecting ends of a submolecule.

$\delta z$  = instantaneous fluctuation from position.

Thus  $\langle z^2 \rangle$  does not deform affinely.

Neutron scattering experiments showed evidence of microscopic transformations that were below those obtained using the phantom model<sup>13,14</sup>. This led Bastide et al<sup>15</sup> to put forward the network unfolding hypothesis. According to this hypothesis there are  $f$ -topological neighbours, ( $f$  is the cross-link functionality), which are directly linked to a reference cross-link. There are, however,  $n$  other cross-links that are spatially closer to the reference cross-link but whose topological connection is much longer and passes through several cross-links. It is argued that, on deformation, the spatial neighbours

will move to a much greater extent than topological neighbours and consequently network deformation will be less than affine. This is only strictly valid, however, for end-linked chains.

These theoretical studies mentioned previously have investigated the effect of macroscopic deformation on the transformation of the mean-squared radius of gyration. It may, alternatively, be analysed in terms of the transformation of the mean-square end-to-end chain vector which is related to, but is different from, the transformation of the mean-squared radius of gyration. Birefringence and segmental orientation in deformed networks have been analysed in terms of the transformation of the mean-squared chain vectors.

Birefringence in polymers is normally associated with molecular orientation and so should give information about molecular arrangement as opposed to arrangement of the submicroscopic particles. Birefringence can be defined as the separation of a ray of light on passing through a crystal into two unequally refracted, plane-polarized rays (of orthogonal polarizations). This effect occurs in crystals in which the velocity of light is not the same in all directions i.e. refractive index is anisotropic. Uniaxial crystals have one direction in which double refraction does not occur. McIntyre et al<sup>16</sup>, described the long range structure of block copolymers as that of a macrolattice made up of microphases which are often

formed into regular arrays. Erman and Flory<sup>17</sup> put forward a theory of strain birefringence of amorphous polymer networks. This theory was based on an analysis of strain birefringence according to the Gaussian theory of phantom networks put forward by James and Guth<sup>11,12</sup>. The theory of strain birefringence had, previously, been based on the affine network model in which the transformation of chain vectors was directly proportional to the macroscopic strain. This model was discredited experimentally by Erman and Flory<sup>18</sup> and theoretically by Flory<sup>19</sup>. Erman and Flory<sup>17</sup> predicted that the change in refractive index,  $\Delta n$  for real networks is non-linear with the stress,  $T$ , for uniaxial extension ie. the stress-optical coefficient  $\Delta n/\tau$  should decrease with elongation. They went on to produce experimental data to back this up<sup>20</sup>. They carried out birefringence and stress measurements on two networks of varying degrees of cross-linking swollen in a variety of solvents (eg. dodecane, carbon tetrachloride). The networks used were poly(dimethylsiloxane).

Flory and Erman<sup>21</sup> put forward a constrained junction model of networks based on the phantom model. They produced experimental results to back up this approach<sup>11</sup>.

## Chapter 1 - References

1. Thomason, J.L.; PhD Thesis, Strathclyde (1981)
2. Maconnachie, A.; Richards, R.W.; Polymer; 19, 739, (1978)
3. Meier, D.J.; J. Polym. Sci. Part C, 26, 81 (1969)
4. Helfand, E.; Wasserman, Z.R.; Macromolecules; 13, 994, (1980)
5. Helfand, E.; Wasserman, Z.R., in "Developments in Block Copolymers" Ed. I. Goodman, Applied Science Publishers Ltd., London (1982)
6. Helfand, E., Macromolecules; 9, 879, (1976)
7. Helfand, E.; Macromolecules; 8, 552, (1975)
8. Leibler, L.; Macromolecules; 13, 1602, (1980)
9. Hong, K.M.; Noolandi, J.; Macromolecules; 16, 1083 (1983)
10. Flory, P.J.; in "Principles of Polymer Chemistry" - Cornell Univ. Press. Ithaca, NY, (1953)
11. James, H.M.; Guth, E.; J. Chem. Phys.; 15, 669 (1947)
12. James, H.M.; Guth, E.; J. Chem. Phys.; 21, 1039 (1953)
13. Benoit, H. et al; J. Polym. Phys. Ed.; 14, 2119 (1976)
14. Bastide, J. et al; Macromolecules; 17, 83 (1984)
15. Bastide, J. et al; J. Macro. Sci. Phys.; B19, 13 (1981)

16. McIntyre, et al; *Macromolecules*; 3, 322, (1970)
17. Erman, B.; Flory, P.J.; *Macromolecules*; 16, 1601 (1983)
18. Erman, B.; Flory, P.J.; *Macromolecules*; 15, 806, (1982)
19. Flory, P.J.; *J. Chem. Phys.*; 66, 5720 (1977)
20. Erman, B.; Flory, P.J.; *Macromolecules*; 16, 1607, (1983)
21. Erman, B.; Flory, P.J.; *Macromolecules*; 15, 800 (1982)

## CHAPTER 2 - EXPERIMENTAL

### 2.1. Polymer/Copolymer Preparation

#### 2.1.1. Vacuum Line

All polymer and copolymer samples were polymerised anionically under high vacuum. The vacuum line used to carry out these polymer syntheses is shown in Figure 2.1.1.. The line was evacuated by means of a rotary/Diffstak diffusion pump combination connected in series.

The rotary pump was model ED100 and the 'Diffstak' diffusion pump was model 63/150M, both supplied by **Edwards**. The pressure in the lines was measured using a **Pirani** PR10C gauge head with a **Pirani** II meter up to  $1 \times 10^{-2} \text{ Nm}^{-2}$  and a **Penning** CP252 gauge head with a **Penning** 8 meter up to  $4 \times 10^{-6} \text{ Nm}^{-2}$ . No sample syntheses were attempted until the pressure was less than  $2 \times 10^{-6} \text{ Nm}^{-2}$ . As Figure 2.1.1. shows, the main vacuum line consisted of four manifolds each of which was connected to three submanifolds. The submanifolds allowed distillation of monomers and solvents to be performed in isolation from the main vacuum line. The 'O' ring taps and joints, Figure 2.1.2., used in

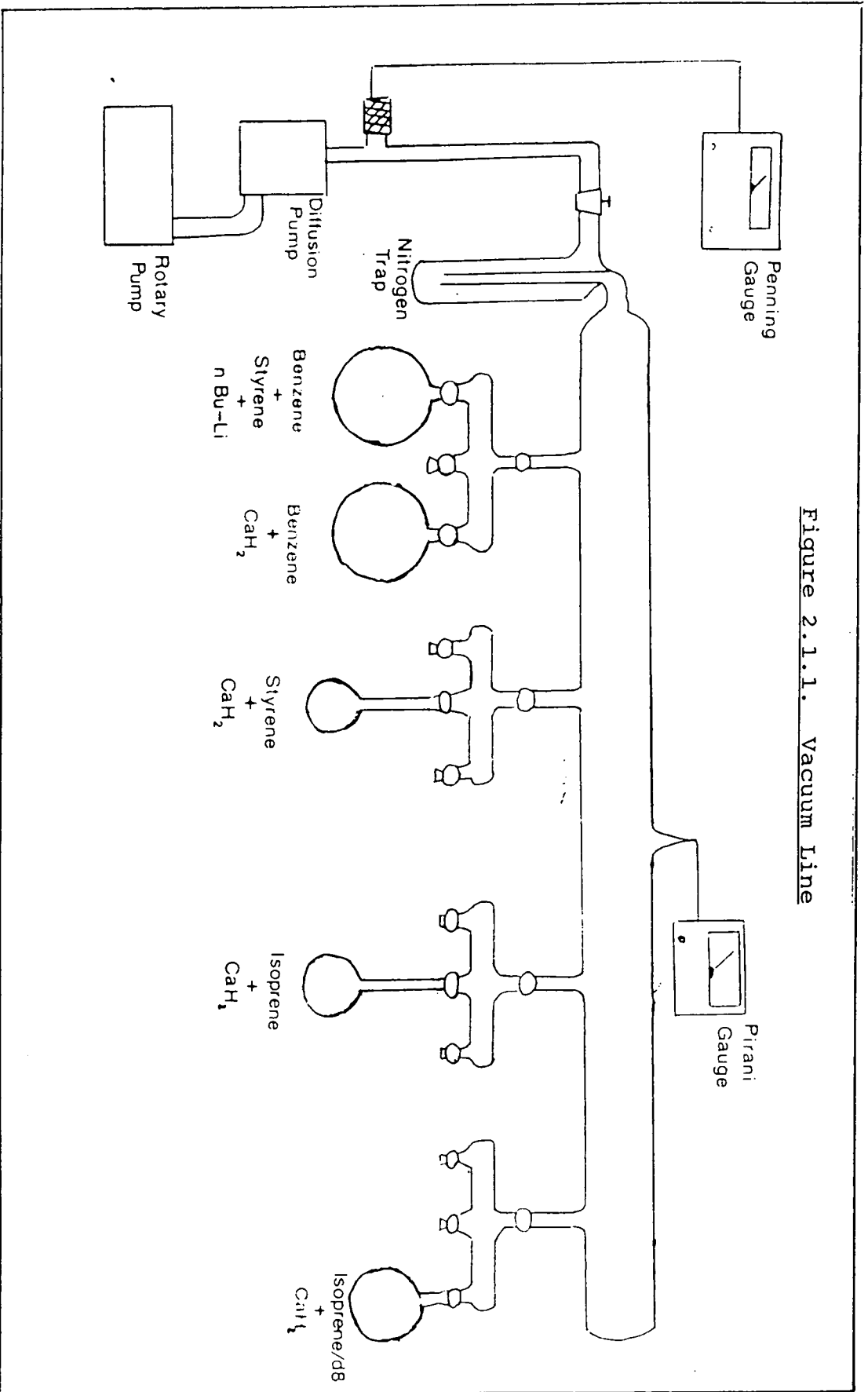
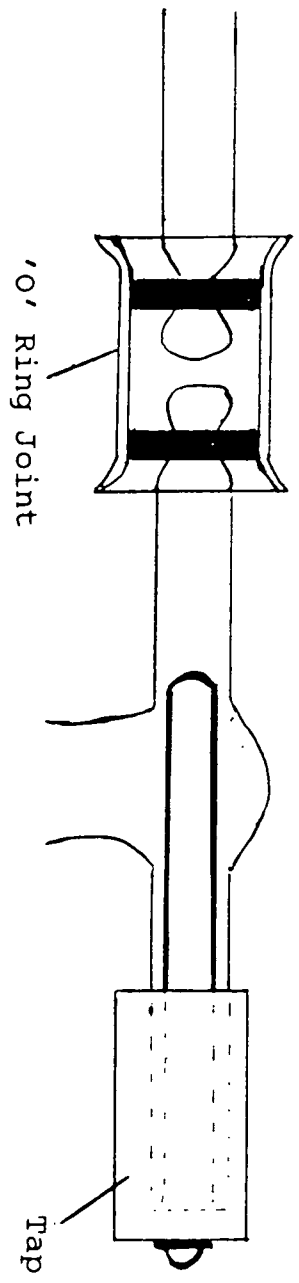


Figure 2.1.1. Vacuum Line

Figure 2.1.2. The 'O' Ring Joint and Taps used in Polymer Synthesis



syntheses were PTFE and were supplied by Youngs. The initiator used for polymerisation was Aldrich - supplied 2.5M n-butyllithium in 100ml of hexane.

#### 2.1.2. Monomer and Solvent Purification

Prior to placing them on the vacuum line, inhibitors and/or impurities in monomers and solvents were removed. For this purpose Aldrich - supplied styrene was washed with a 10% (w/v) aqueous NaOH solution and then rinsed several times with distilled water to remove the inhibitor (tert-butyl catechol,  $(\text{CH}_3)_3\text{CC}_6\text{H}_3-1,2-(\text{OH})_2$ ). The washed monomer was then stored over  $\text{CaCl}_2$  for a day before being distilled, under reduced pressure, into a flask containing  $\text{CaH}_2$  and a stirring bar. After this final purification stage the styrene monomer was attached to the vacuum line using Apiezon 'N' vacuum grease. Once attached to the line it was stirred and degassed for at least a week, as were all monomers, before being used in polymer syntheses. Aldrich - supplied isoprene and Promochem - supplied isoprene-d8 (96%) were poured directly onto  $\text{CaH}_2$  and attached to the line for stirring and degassing. The solvent used was Aldrich - supplied benzene. This was first washed with concentrated  $\text{H}_2\text{SO}_4$  and then rinsed several times with distilled water. After being left to dry over  $\text{CaCl}_2$  for 12 hours, the benzene was distilled into a flask containing  $\text{CaH}_2$ . The flask was then placed

on the vacuum line to be stirred and degassed for at least a week before it could be distilled into a second flask containing 'living' polystyryllithium anions to remove any remaining impurities which might have terminated the polymerisation.

### 2.1.3. Calibration of the Initiator

Prior to sample polymerisation the initiator was tested by polymerising five polystyrene samples using a known weight of monomer and 25  $\mu$ l, 50  $\mu$ l, 75  $\mu$ l, 100  $\mu$ l and 150  $\mu$ l of initiator respectively. The five polystyrene samples obtained were analysed by Gel Permeation Chromatography (G.P.C.), (Section 2.2.1), to obtain their weight-average molecular weights, ( $M_w$ ) and polydispersities ( $M_w/M_n$ ). From these results the amount of initiator required to obtain a specific molecular weight was calculated from the following relationship:-

$$V_i = W_m / (M_w \cdot V_i) \quad \text{EQ. (1)}$$

where :  $V_i$  = initiator volume, l

$W_m$  = weight of monomer, kg

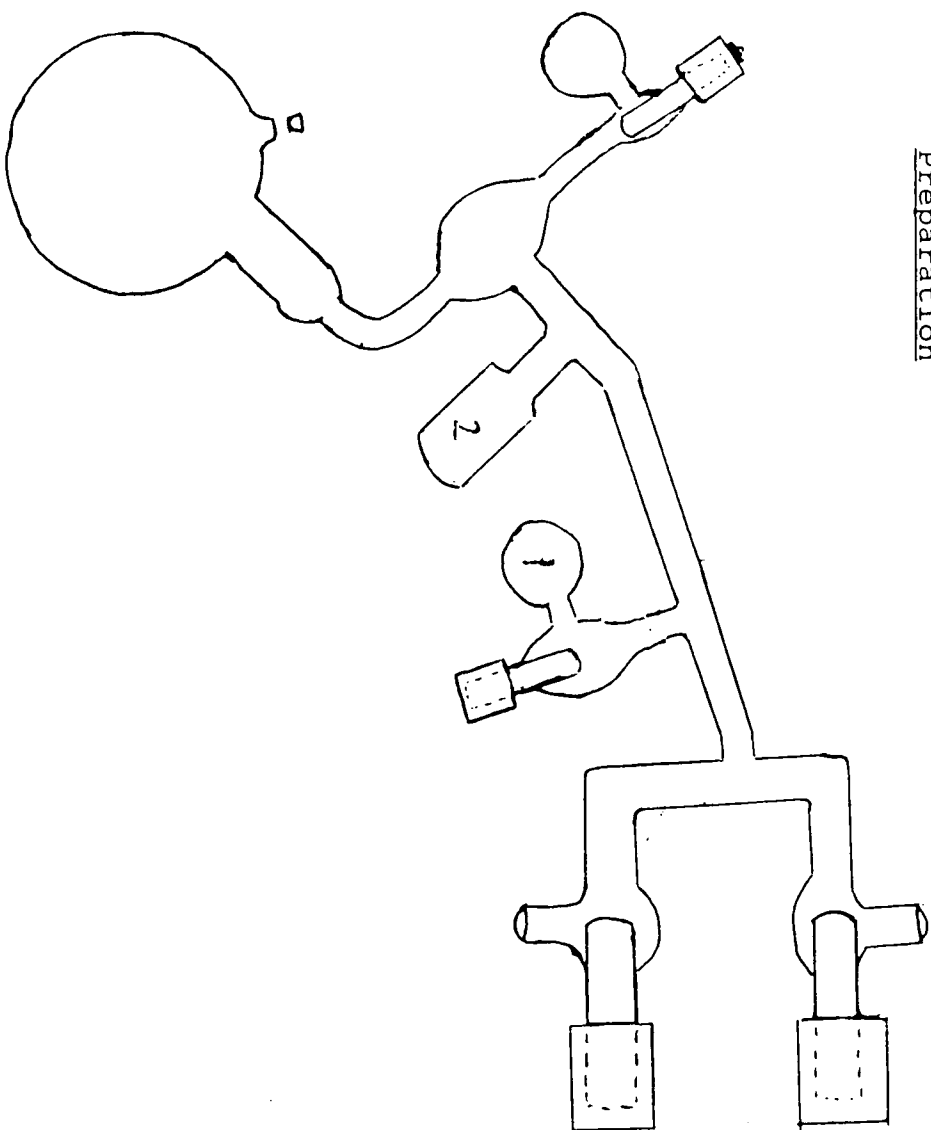
$M_w$  = molecular weight, kg

### 2.1.4. Polymerisation of copolymers

#### 2.1.4(a) Hydrogenous Copolymers

Hydrogenous copolymers were prepared in the reaction flask shown in Figure 2.1.3.. The flask was fitted with a new **Aldrich** rubber septum for each reaction. Once the flask was fitted to the vacuum line it was

Figure 2.1.1.3. Reaction Flask for Copolymer/Polymer Preparation



evacuated and 'flamed out' with an oxy-methane torch to remove any impurities that may have adsorbed to the glass surface. Once this had been done the flask was isolated from the line for around four hours to check that there was no appreciable loss of vacuum.

Assuming there was no appreciable loss of vacuum, 0.1g of thoroughly stirred and degassed styrene was distilled into the reaction flask. Benzene (15 ml) was distilled from the flask containing the 'clean' solvent and polystyryllithium solution into the reaction flask. Once the reaction solution had reached room temperature a large excess of n-butyllithium (circa 500  $\mu$ l) was injected. This 'living' solution was then rinsed around the inside of the whole reaction vessel before being returned to the side-flask (No. 1 in Figure 2.1.3.). Any traces of the 'living' solution still present in the reaction vessel were removed by rinsing out with benzene, which was distilled into the finger (No. 2 in Figure 2.1.3.), from the 'living' solution. This procedure was repeated until the benzene remained colourless after wetting the whole of the reaction vessel. Once this had been achieved the whole assembly was weighed and replaced on the vacuum line. The pre-determined weight of styrene monomer was then distilled into the reaction flask. Benzene was then distilled into the reaction flask from the on-line

solvent flask containing 'living' polystyryllithium to make a 10% (w/v) solution of monomer in benzene. The reaction vessel was then removed from the vacuum line and brought up to room temperature as quickly as possible. Then, with the reaction solution covering the septum, the pre-determined volume of initiator was carefully injected using a **Hamilton** gas-tight syringe. After injection the solution quickly turned a yellow/orange colour. The colour was an indication that polymerisation was proceeding. The lower the molecular weight the more orange the solution colour was. The polymerisation was then allowed to proceed for at least ninety minutes before addition of the isoprene. Prior to addition, the isoprene was pre-polymerised to remove any impurities that may still have been present. Prepolymerisation of isoprene involved the monomer being distilled into a flask fitted with a rubber septum, which was placed in an ice/water bath, and 100  $\mu$ l of initiator was added to the monomer. The prepolymerisation was allowed to proceed for between thirty minutes and two hours since, after two hours, the prepolymerised isoprene became potentially explosive. Any excess prepolymerised isoprene was destroyed with 0.5 ml of thoroughly degassed methanol. After thirty minutes the required amount of prepolymerised isoprene was distilled into a flask which

was then connected to the reaction vessel.

The whole assembly was then connected to the vacuum line and the connection was evacuated. The isoprene was then distilled into the small finger (No. 2 in Figure 2.1.3.), where it was allowed to come up to room temperature before being added to the reaction solution. On addition of the isoprene this solution became almost colourless. The reaction vessel was then isolated from the line and left overnight. The polyisoprene adopts the cis 1-4 conformation using this synthetic route. If the polymerisation had proceeded the reaction solution should have undergone a significant increase in viscosity overnight. At this point the reaction was either, terminated if a diblock copolymer was required, or, if a triblock copolymer was required, more styrene was added. The reaction was terminated by injecting 0.5ml of thoroughly degassed methanol and shaking vigorously for a few seconds.

After termination the solution was precipitated into an excess of methanol with stirring. The methanol was then decanted off and the copolymer precipitate was placed in a vacuum oven at room temperature to dry until constant weight was achieved.

For hydrogenous polymerisations between 10 and 20g of polymer was normally synthesised and a small amount of

this was taken for analysis. The remainder was placed in Aldrich Sure-Seal bottles and stored in a freezer at 280 K.

#### 2.1.4(b) Polymerisation Techniques for Deuterated and Random Copolymers

The polymerisation of deuterated and random copolymers followed, for the most part, the synthetic route applied to hydrogenous copolymers. The differences occurred in monomer purification where deuterio-monomers were not vacuum distilled but, after washing and drying, were placed directly over  $\text{CaH}_2$  and attached to the vacuum line for stirring and degassing. The reason for this being the relatively large cost of deuterated materials which meant losses in purification could be very expensive. The synthesis of polymers containing fully deuterated polyisoprene blocks was then the same as that for the fully hydrogenous polymerisations as was the isolation technique (see Section 2.1.4(a)). The synthesis of the random copolymers was complicated by the fact that a specific amount of hydrogenous and deuterated prepolymerised isoprene monomer had to be mixed in a reaction flask before being added to the 'living' polystyryllithium in the reaction vessel. Once this step had been successfully achieved then the polymerisation proceeded as for a completely hydrogenous polymerisation.

## 2.2. Polymer/Copolymer Characterisation

### 2.2.1. Weight Average Molecular Weight ( $M_w$ ) and Polydispersity by Gel Permeation Chromatography (G.P.C.)

All polymer samples had their weight-average molecular weight, ( $M_w$ ), and polydispersity, ( $M_w/M_n$ ), measured using G.P.C.<sup>1</sup>. The solvents used were tetrahydrofuran (THF) or chloroform at room temperature. These measurements were carried out on two different instruments.

The first was in the Department of Chemistry, Strathclyde University. This instrument had four 0.3 m, 10 $\mu$ m **Polymer Lab.** columns with nominal pore sizes 10<sup>2</sup>, 10<sup>3</sup>, 10<sup>4</sup>, 10<sup>5</sup>nm respectively. The samples were run at ambient temperature using chloroform or THF as the solvent and were detected using a **Cecil** U.V. detector. The second, at Durham University, was used to measure the  $M_w$  of the low molecular weight isotopic block copolymers of polystyrene/polystyrene-d8. The instrument used to make these measurements was a **Viscotek** differential refractometer/viscometer Model 100 using THF as the solvent. Since both instruments were calibrated using polystyrene standards the results obtained for those samples which also contain polyisoprene have to be corrected for the fraction of polyisoprene in the sample<sup>2</sup>.

2.2.2. Number Average Molecular Weight ( $M_n$ ) from Membrane Osmometry

For the S15150 samples the number average molecular weight ( $M_n$ ) was obtained using a **Knauer** Membrane Osmometer. This measured the osmotic pressure of a polymer as a height (h) of solvent necessary to oppose osmotic flow through a membrane. The following relationship is obtained:

$$\pi/c = TR(1/M_n + A_2c + A_3c^2) \quad \text{EQ. (2)}$$

where:

$$\pi = h\rho g$$

h = osmotic height (m)

$\rho$  = solvent density ( $\text{kg m}^{-3}$ )

g = gravitational acceleration ( $\text{m s}^{-2}$ )

$A_2, A_3$  = second and third virial coefficients respectively

c = concentration ( $\text{kg mol}^{-1}$ )

T = Temperature (K)

$M_n$  = Number average molecular weight ( $\text{kg mol}^{-1}$ )

Krigbaum and Flory<sup>3</sup> expressed the third virial coefficient as

$$A_3 = K\rho A_2^2 M_n \quad \text{EQ. (3)}$$

where :

$K\rho$  is related to the polymer solvent interaction parameter.

Since  $K\rho = 0.25$  in good solvent<sup>4</sup> then a plot of  $(\pi/c)^{1/2}$  vs.  $c$  should give a straight line with intercept  $(RT/M_n)^{1/2}$  and slope  $(RTM_n)^{1/2} A_2/2$ .

Distilled toluene was used as the solvent. Polymer samples were made up to a stock solution of  $0.01 \text{ g cm}^{-3}$  in distilled toluene. The stock solution was then left overnight to ensure complete dissolution and was then used to make up five dilutions;  $0.001 \text{ g cm}^{-3}$ ,  $0.002 \text{ g cm}^{-3}$ ,  $0.004 \text{ g cm}^{-3}$ ,  $0.006 \text{ g cm}^{-3}$  and  $0.008 \text{ g cm}^{-3}$  respectively.

These samples, in ascending order of concentration, were then injected into a **Knauer** membrane osmometer.

### 2.2.3. Styrene Weight Fraction from Ultra-Violet Spectroscopy

Polystyrene has two strong absorption maxima at 262nm and 268nm respectively. At these wavelengths polyisoprene absorbs only slightly. By measuring the absorbance of polystyrene, polyisoprene and copolymer at these wavelengths it is possible to calculate the weight fraction of styrene ( $W_S$ ) in the copolymers using the following relationship:-

$$W_s = \frac{K_{CP} - K_{PI}}{K_{PS} - K_{PI}}$$

where:

$K_{CP}$ ,  $K_{PI}$ ,  $K_{PS}$  = extinction coefficient for copolymer, polyisoprene and polystyrene respectively.

The values of  $K_{PI}$  and  $K_{PS}$  at 262nm and 268nm were obtained from literature<sup>5</sup>.

The samples were made up to  $5 \times 10^{-4}$  g cm<sup>-3</sup> in volumetric flasks using spectroscopic grade chloroform as the solvent. They were then left overnight to ensure complete dissolution of the polymer.

The measurements were made on a **Perkin Elmer 551** Spectrometer, with a 1 mm slit width, scanning from 275 to 250 nm at 1 nm s<sup>-1</sup>. Prior to measuring the sample the Spectrometer was zeroed using the solvent as both sample and reference cells. Once this had been done the sample cell containing solvent was replaced by one containing polymer and solvent. This was allowed to stabilise for ten minutes after which time two scans were recorded. Before adding the next sample the sample cell was rinsed out several times with fresh solvent before adding the next sample for measurement.

$K_{CP}$  was measured at both 262nm and 268nm for the copolymers and the average value was taken.

## 2.3. Small Angle Neutron Scattering

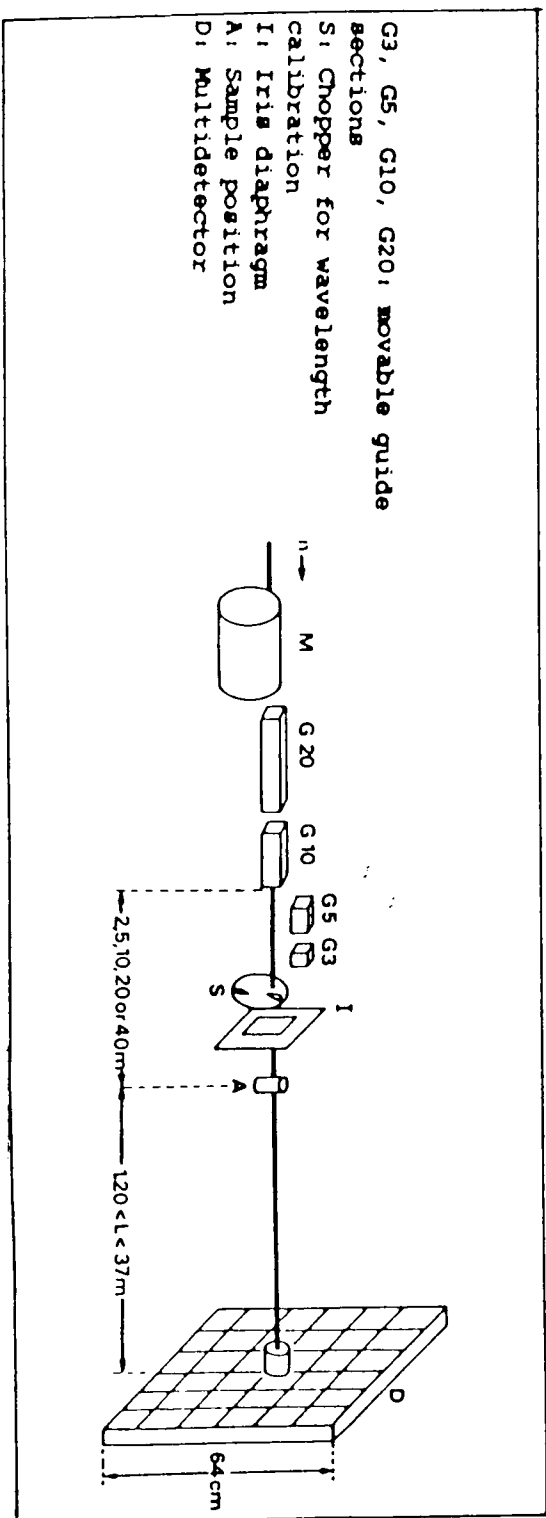
### 2.3.1. SANS Instruments

#### 2.3.1.(a) Institut Laue-Langevin, (I.L.L.), Grenoble

Small Angle Neutron Scattering, (SANS), experiments were carried out on both D11 and D17 diffractometers at the I.L.L., Grenoble. These use neutrons of constant wavelength to give a combined Q-range of  $0.001 - \text{Å}^{-1}$  to  $1.000 \text{ Å}^{-1}$  for these measurements. Figure 2.1.4. shows a schematic diagram of a typical small angle diffractometer, in this case D11 instrument.

At the I.L.L., thermal neutrons from the nuclear reactor passed from a cold source, with enhanced longer wavelength flux, through a window in the reactor wall to an evacuated guide tube. Here, due to the slight curvature in the guide tube, neutrons are passed to the diffractometer by total internal reflection whilst fast neutrons and  $\gamma$ -ray background are reduced. The 'white' neutron beam was then monochromated by a velocity selector which only allows neutrons of a preselected velocity to pass. This means, in practice, the neutrons leave the monochromator with a reduced wavelength spread. The incident neutron flux is monitored by fission monitors on either side of the velocity selector allowing the normalisation of all experiments to the same flux. The monochromatised beam

Figure 2.1.4. Schematic Diagram of a typical diffractometer



is then passed through a collimator and a cadmium diaphragm to define the beam size. Cadmium is used because of its capacity to absorb neutrons.

After traversing the sample, the scattered neutron beam passes down an evacuated tube to a  $\text{BF}_3$  - filled detector. The x and y coordinate of each neutron is recorded by an array of 1 cm x 1 cm cells. Since, however, the directly transmitted beam is of such great intensity the central detector cells have to be protected. This is accomplished by placing a cadmium beamstop in front of the detector.

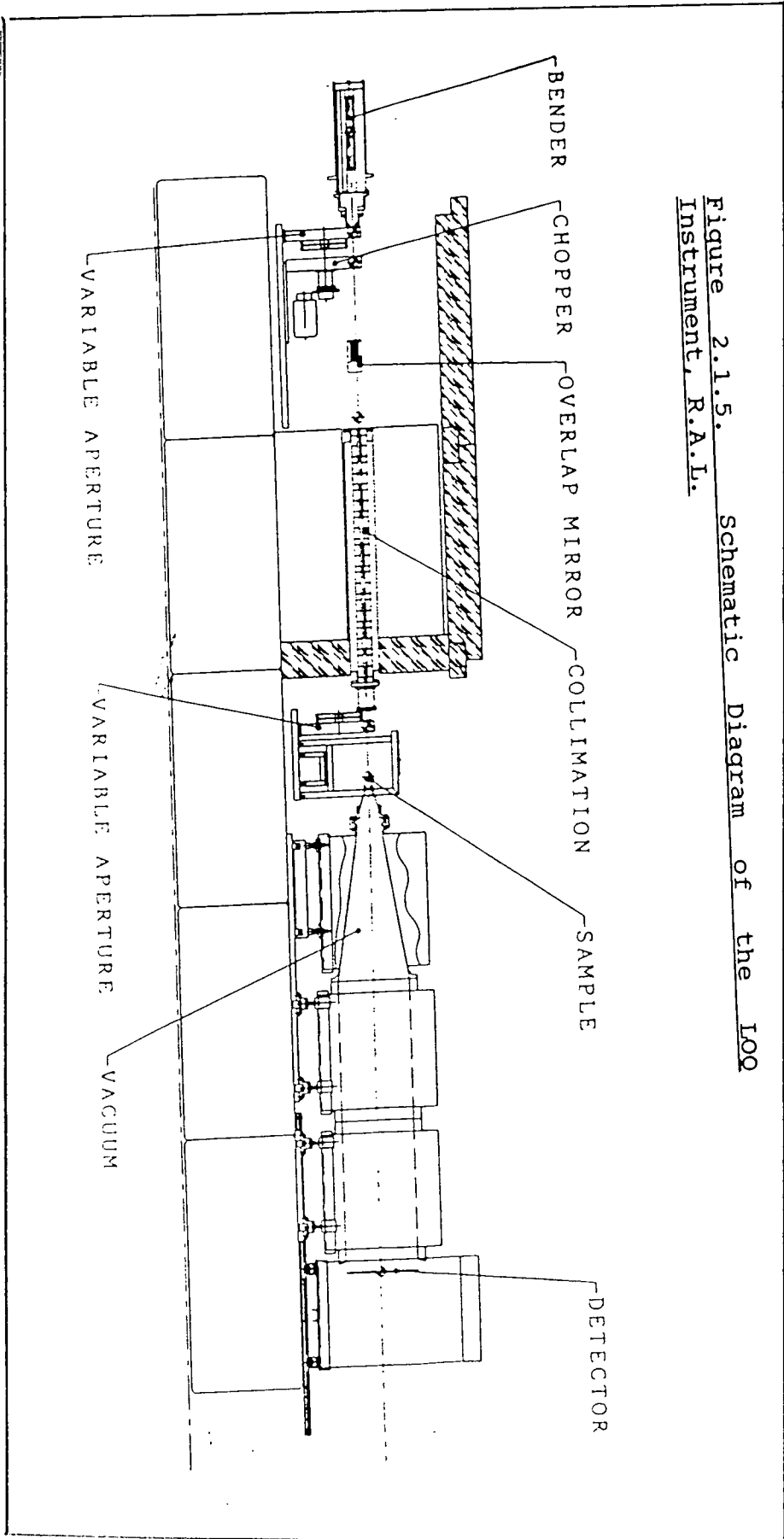
It was necessary to perform transmission measurements of short duration to enable absolute analysis of the scattering results to be achieved.

2.3.1.(b) Rutherford-Appleton Laboratory, R.A.L., Oxford

The LOQ instrument at the R.A.L. is a 'time-of-flight' Spectrometer. It has a Q-range of  $0.005 \text{ \AA}^{-1}$ - $0.22 \text{ \AA}^{-1}$ . Figure 2.1.5. shows a schematic diagram of LOQ.

At the R.A.L., neutrons from the reactor passed through a Superminor Soller bender where neutrons with wavelengths less than 2 were removed. After removing these low wavelength neutrons, those neutrons with wavelengths greater than 12A were removed by the frame overlap minor. The neutron beam now contains neutrons with wavelengths between 2A and 12A and is then

Figure 2.1.5. Schematic Diagram of the IOO Instrument, R.A.L.



collimated. The beam size was set by adjusting the aperture dials which allow a diameter range of 0.2cm to 2.0cm in the beam size. The beam then passes through the sample where it is scattered. The scattered beam travels down an evacuated tube to a BF<sub>3</sub>-filled detector at a fixed distance from the sample. For similar reasons to those given for the D11/D17 Spectrometers it was necessary to perform short transmission measurements on samples studied on the LOQ instrument.

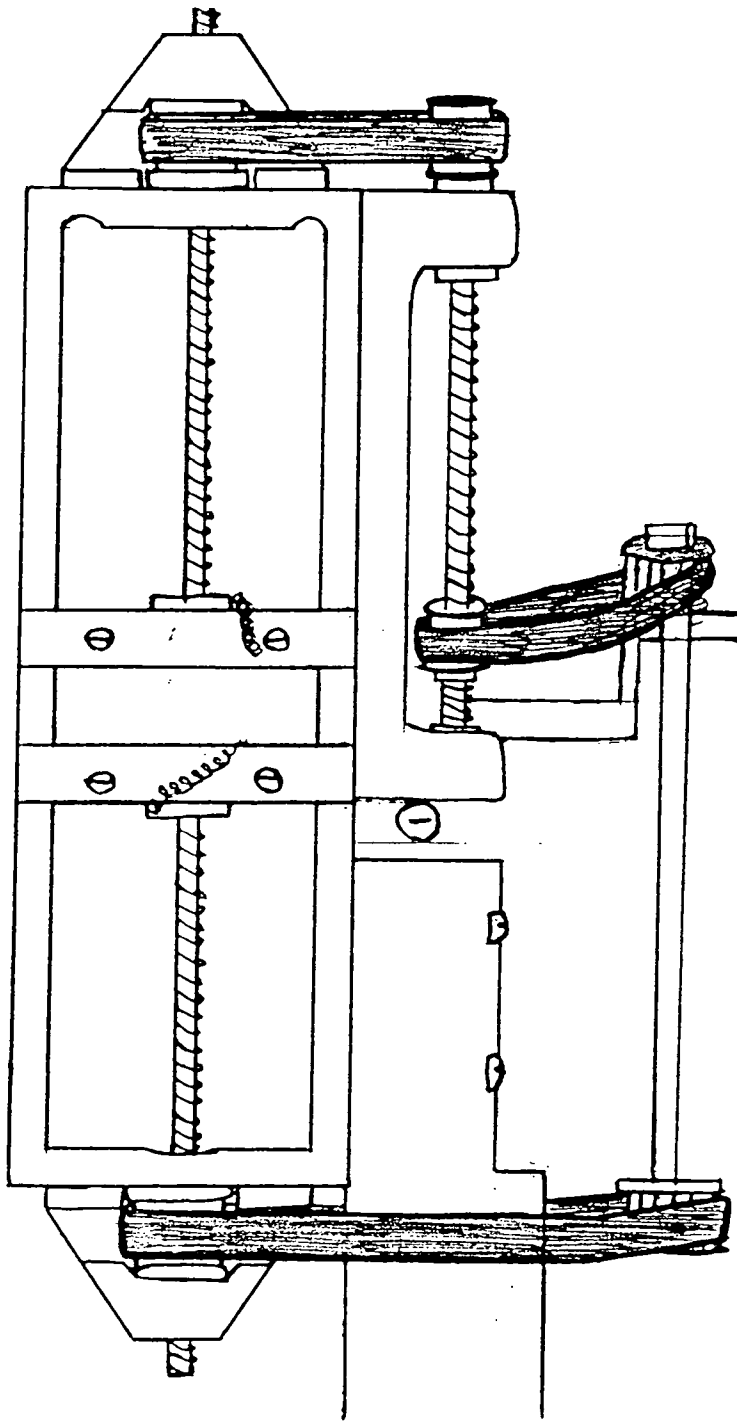
### 2.3.2. Sample Preparation for neutron scattering experiments

The preparation of samples prior to use in neutron scattering experiments can be divided into two possible methods:

#### 2.3.2.(a) Samples for deformation experiments

Samples for deformation experiments were cast from toluene in PTFE casting blocks. These had a casting volume of 7 cm x 7 cm x 0.3 cm, and sample thicknesses of 0.5 mm - 1.5 mm were obtained. The solvent was allowed to evaporate slowly over a period of 2 weeks whereupon the samples were placed in a vacuum oven at 298 K to remove any remaining solvent. Once all of the solvent had been evaporated the resulting cast polymer sample was cut into strips of around 5 cm x 1 cm x 0.1 cm so that they could be fitted in the stretching rig (Figure 2.1.6.). The stretching rig is designed

Figure 2.1.6. Stretching Rig

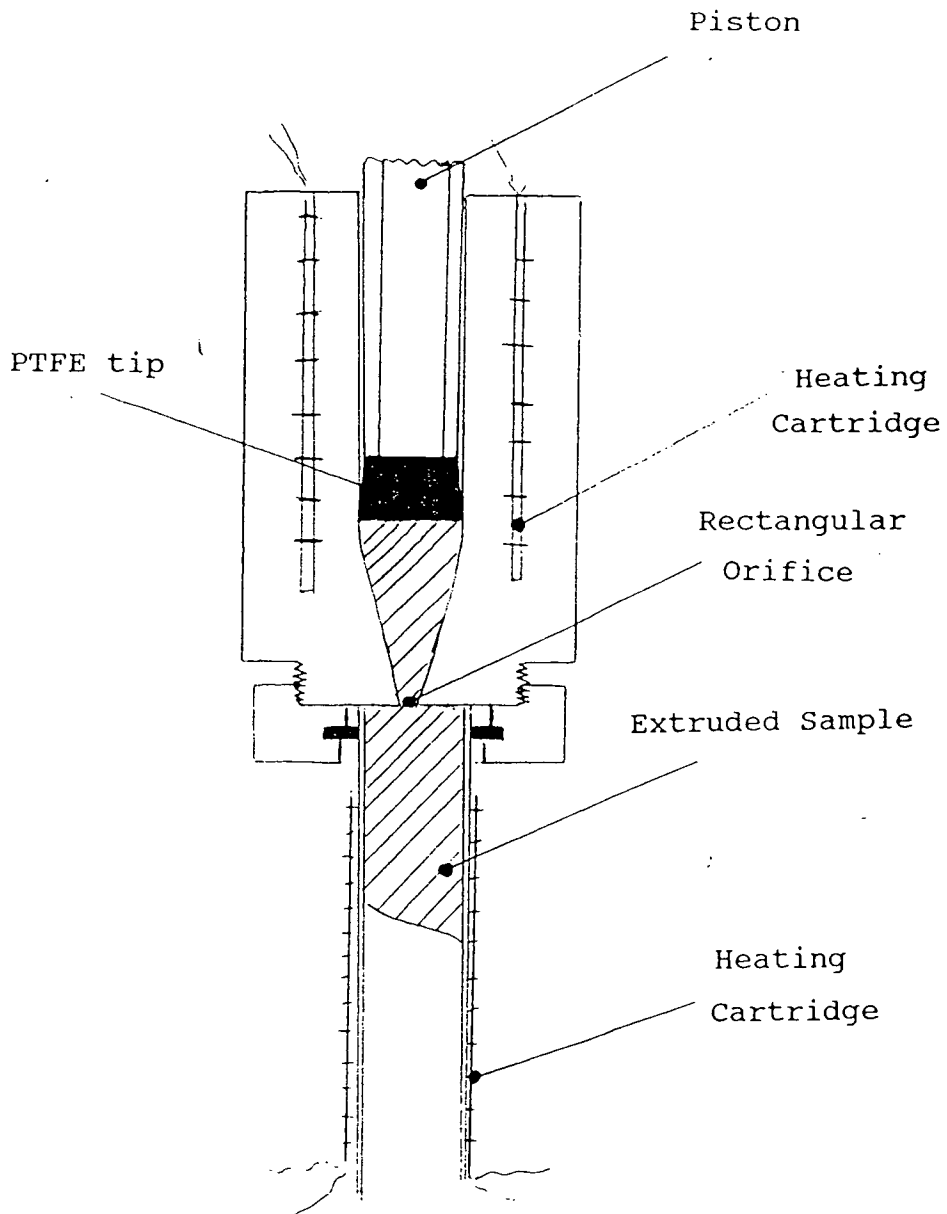


such that the same region of the sample is illuminated by the beam for each extension ratio. The sample thicknesses were measured using a micrometer before the sample was clamped in the rig.

The rig was then positioned squarely in the beam. At the I.L.L. this was achieved using clamps and the sample was aligned in the beam using a laser light. At the R.A.L. clamps were also used but the sample was aligned in the beam using an aluminium nose-guide.

Extension ratios examined were between 1.0 and 2.2. Some samples were used in studies of extruded triblock copolymers which form so-called "single-crystals". This involved using the extrusion apparatus shown in Figure 2.1.7. which was based on a design by Folkes and Keller<sup>6</sup>. Copolymer samples were placed in the sample chamber and the piston was fitted above it. The upper half of the apparatus was then heated to 423 K and held at this temperature for three hours. After this time a force of  $8.5 \text{ kg cm}^{-2}$  was applied to the piston. This then forced the sample through the 1 mm diameter aperture at the end of the sample chamber. The lower half of the apparatus was held at 323 K and the interior was coated with a layer of PTFE spray to facilitate removal of the extruded sample.

Figure 2.1.7. Cross-Section of the Extrusion Apparatus



2.3.2.(b) Samples for use in Examining the Applicability of the Random Phase Approximation (R.P.A.)

Samples for use in neutron scattering experiments to examine the applicability of the R.P.A. were isotopic diblock copolymers of polystyrene/deuteropolystyrene. These experiments were carried out on the LOQ instrument at R.A.L.. Samples were prepared using the following method.

Samples were pressed into discs of around 1 mm thickness using a heating press. The sample was placed in the heating jacket and was then held under pressure in the apparatus. The heating jacket was then pumped down to remove any trapped air and the jacket was heated to 423 K. The pressure and temperature were maintained at these levels for around 15 minutes after which time they were removed and the disc was removed from the heating jacket.

The discs were then placed in a heating rack. This was then mounted in the beam, ensuring the beam passed through the centre of the sample. Temperatures between 310 K and 473 K were examined. The temperature was measured and controlled using platinum resistance thermometers placed in close proximity to the samples themselves. Temperature control was  $\pm 1$  K of the

selected temperature. All samples were allowed to equilibrate at each temperature for at least twenty minutes prior to commencing measurements.

### 2.3.3. Data Correction

Data correction can be split into the correction required for LOQ data and that required for D11/D17 data.

#### 2.3.3.1. LOQ Data Correction

A detailed mathematical description of data corrections carried out by the COLETTE program at RAL can be found in reference (7). A LOQ data correction followed the steps shown below:-

(a) ALL scattering runs had an empty beam run subtracted from them.

(b) ALL scattering runs were corrected to a thickness of 1 mm and were corrected for monitor counts and sample transmission.

These are shown in Equation (5)

$$I = \frac{S_s}{t_s T_s} - \frac{S_{eb}}{t_{eb} T_{eb}}$$

EQ. (5)

where:

I = corrected scattering intensity.

$S_s$ ,  $S_{eb}$  = scattering intensity of sample and empty beam respectively

$T_S, T_{eb}$  = transmission of sample and empty beam respectively.

$t_S, t_{eb}$  = thickness of sample and empty beam respectively. (mm)

For the empty beam run,  $T_{eb} = 1, T_{eb} = 1$ , and so equation (5) is simplified. All these corrections are carried out at LOQ using the COLETTE program. This accounts for any monitor count differences between runs.

#### 2.3.3.2. ILL Data Correction

Data correction for ILL data broadly follows that for LOQ data. A detailed description has been published<sup>8</sup> and so only a brief outline will be given here.

In order that absolute intensities may be calculated such that the results are instrument-independent, the following measurements have to be made:-

(a) Measure the water sample holder (WB) and transmission,  $T_{WB}$

(b) Measure the water (W) in its sample holder and transmission,  $T_{W+WB}$

(c) Measure the background (random) sample (SB) and Transmission,  $T_{SB}$

(d) Measure the sample (S) and transmission,  $T_{S+SB}$

All the above are normalised for the same incident flux by dividing by the monitor counts.

The corrections then required are shown below:-

EQ. (6)

$$I_f = \frac{I_c}{V_f} \cdot \frac{T_{(W+WB)}}{T_{(S+SB)}} \cdot \frac{N_v d\sigma_v}{N_s d\Omega}$$

where:

$I_f$  = absolute scattering cross section

$I_c$  = (sample) - (sample background)

$V_f$  = Detector corrections

$N_v d\sigma_v$  = self shielding due to bulk microscopic cross section

$N_s d\Omega$  = section of sample and water

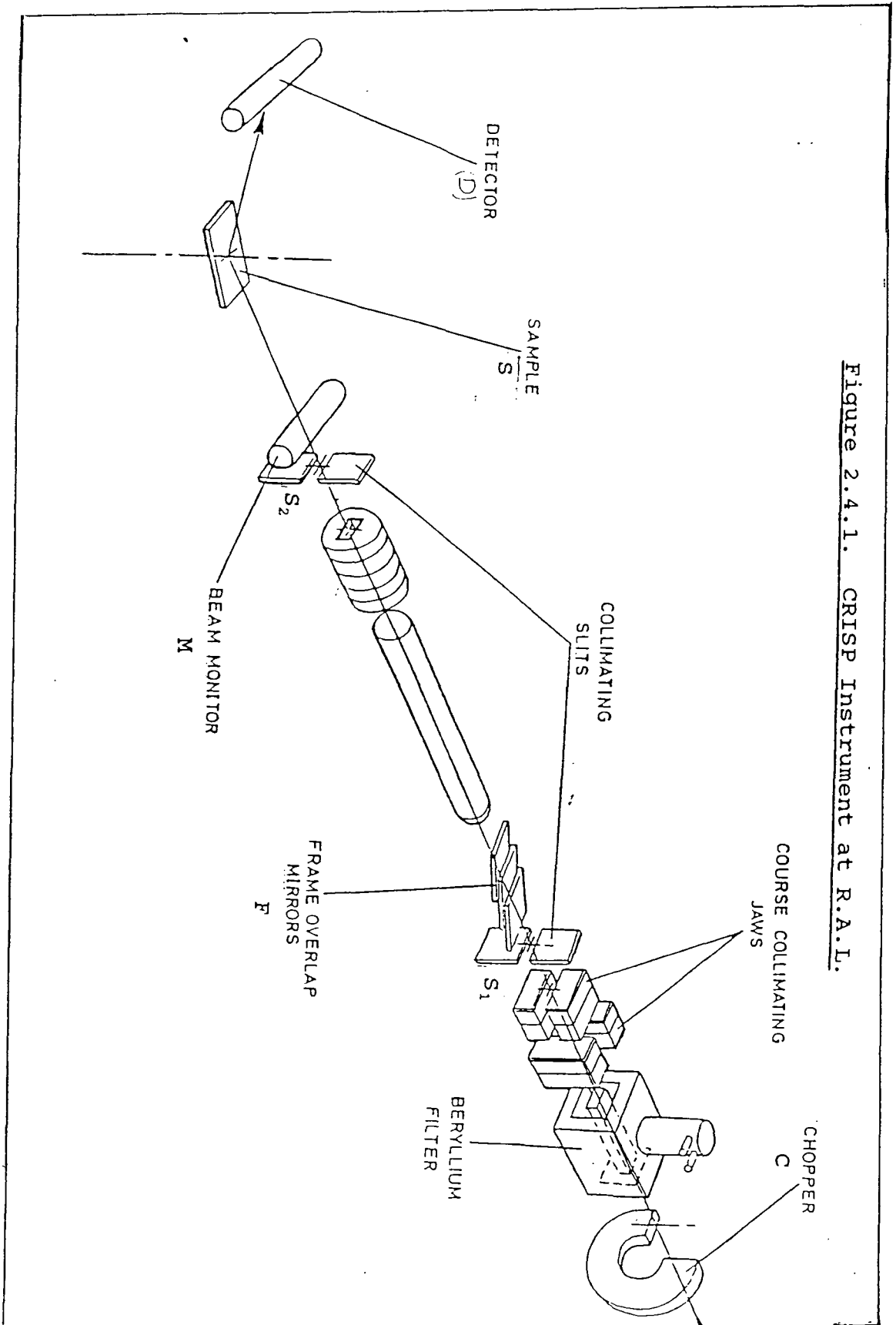
## 2.4. Neutron Reflectometry

### 2.4.1. Instrumentation

CRISP is a time-of-flight spectrometer at the R.A.L. used to examine solid and liquid surface phenomena. A schematic plan of the instrument is shown in Figure 2.4.1.. The incident beam is inclined to the horizontal, to enable liquid surfaces to be investigated, and the optimum reflection angle chosen is  $1.5^\circ$ . The incident beam is around 40 mm wide x 2-6 mm high and is determined using a horizontal slit geometry.

The wavelength band,  $\Delta\lambda$ , is defined by a single disc chopper (C) located 6.29 m from the hydrogen moderator. By operating the chopper at 25 Hz with a  $90^\circ$  phasable aperture a  $\Delta\lambda$  between 0.05 nm and 2.6 nm is obtained and some frame overlap contamination due to high wavelength neutrons is eliminated. Further suppression of long wavelength neutrons is provided by three mirrors

Figure 2.4.1.1. CRISP Instrument at R.A.L.



(F) mounted in series. These mirrors are made from single crystal silicon wafers with evaporated nickel coatings which, when inclined at  $3^\circ$  to the incident beam, reflect out long wavelength neutrons.

The sample position (S) is 1.75 m from the detector (D). The detector is a single  $\text{He}^3$  gas detector in a  $\text{B}_4\text{C}$ /resin housing whose acceptance aperture is defined by an adjustable cadmium slit. Coarse beam collimation is given by the bulk target station shielding and final beam size and collimation is defined by two horizontal cadmium slits ( $S_1$ ,  $S_2$ ).

A neutron beam monitor placed in front of the first defining slit is used to monitor the neutron spectrum incident on the reflectometer. A second beam monitor (M) positioned after the final defining slit is used to normalise the measured reflectivity data to the incident neutron spectrum.

#### 2.4.2. Samples for Reflection Studies

Samples used in Neutron Reflection Experiments were styrene/isoprene diblock copolymers. Once these samples had been isolated, around 1g was dissolved in distilled toluene. This was then allowed to equilibrate overnight.

The solution was then taken to a laminar flow station where samples were spun-cast onto optical flats. The speed of rotation was varied until a sample thickness

of around 100 nm was obtained. It was found that a speed of around 1000 r.p.m. gave the required thickness. Samples were then placed in a vacuum oven at 333 K to remove any excess toluene. Sample thicknesses were measured using a DEKTAK instrument. The DEKTAK instrument also gave a microscopic view of the surface which gave an indication of the uniformity of the film. The DEKTAK instrument used a diamond tipped stylus to explore the surface of the film. By making a small scratch through the film to the flat surface the DEKTAK instrument can measure this difference in height to give the film thickness.

The samples were then taken to RAL for use on the CRISP reflectometer.

## Chapter 2 - References

1. Moore, J.C.; J. Polym. Sci.; Polym. Symp.; 21, 1, (1968)
2. Tung, L.H.; J. App. Polym. Sci.; 24, 953, (1979)
3. Krigbaum, W.R., Flory, P.J.; J. Polym. Sci. 9, 503, (1952)
4. Kurata, M, Stockmeyer, W.H.; Fortschr. Hochpolym. Forschl, 3, 196, (1963)
5. Thomason, J.L.; PhD Thesis, Strathclyde University, (1981)
6. Folkes, M.J., Keller, A., Scalisi, F.P.; Kolloid-Zeitschrift, 251, 1, (1973)
7. "LOO data treatment-draft" - R.K. Heenan, R.A.L. (1987)
8. "A Computing Guide for Small Angle Scattering Experiments" - R.E. Ghosh, I.L.L. (1989)

## CHAPTER 3 - STUDY OF DEFORMATION IN A TRIBLOCK

### COPOLYMER

#### 3.1. SANS Study of a Cylindrical Domain Triblock Copolymer

##### 3.1.1. Introduction

Two triblock copolymer series of poly(styrene-isoprene-styrene) were anionically polymerised in the laboratory and are characterised in Table 3.1. These copolymers were:-

- i) A fully hydrogenous triblock copolymer (HYD1, HYD2).
- ii) A 'Random' triblock copolymer where the deuterated isoprene was distributed randomly throughout the polyisoprene matrix (RAN1, RAN2).
- iii) A 'MIX' triblock copolymer where hydrogenous triblock copolymers were mixed with a calculated amount of triblock copolymer with the isoprene portion fully deuterated (DEU1, DEU2).

It was important that the total molecular weights and weight fractions of polystyrene were as close as possible. As can be seen from Table 3.1. this was achieved for both sets of triblock copolymers. The SANS studies were carried out on the LOQ instrument at the Rutherford-Appleton Laboratory, Oxford and on the D11/D17. Spectrometers at the Institut-Lave Langevin, Grenoble. Detailed descriptions of these instruments are given in Ch. 2.

From the weight fractions of polystyrene in each sample it was calculated that the S15150 and S15150B series were made up of cylindrical polystyrene domains in a regular two-dimensional hexagonal lattice in a polyisoprene matrix<sup>1</sup> (Ch. 1).

Table 3.1. - Characteristics of Cylindrical Poly(styrene-Isoprene-Styrene) Triblock Copolymers

SAMPLE	$M_w$ ( $\times 10^{-3}$ )	$M_w/M_n$	$W_s$
<u>S15150</u>			
HYD1	88.0	1.08	0.28
RAN1	87.0	1.09	0.24
DEU1	88.0	1.08	0.24
<u>S15150B</u>			
HYD2	108.0	1.08	0.25
RAN2	110.0	1.12	0.26
DEU2	112.0	1.10	0.25

where:

$M_w$  = weight-average molecular weight

$M_n$  = number-average molecular weight

$W_s$  = weight fraction of polystyrene

### 3.1.2. Previous Work

The unique properties of block copolymers described in Ch. 1 led to the development of new technology for thermoplastic elastomers. Due to their thermoplastic and rubber - like characteristics block copolymers are widely used commercially in, for instance, the car tyre industry where styrene-isoprene and styrene-butadiene copolymers are of importance. The examination of block copolymers using neutron scattering techniques could give information about the interaction between substituent molecules, the interfacial region and the molecular and macromolecular arrangement of these species. This broad study would enable copolymer behaviour under specific conditions to be predicted and lead to the 'custom-made' block copolymer for a specific use. As well as this practical use for neutron scattering results, the various theories of rubber elasticity could be tested using these results to ascertain if any are valid for the particular copolymer system under scrutiny.

#### 3.1.2.1. Previous Experimental Studies of Block Copolymers

With the relatively recent advent of the SANS technique, there has been much attention focused on the nature of the interaction between constituents of unstressed block copolymer species. In the case of the poly(styrene-isoprene) block copolymer system

examined here, Richards and Thomason<sup>2</sup> studied both diblock and triblock systems in the unextended state and found some agreement with the thermodynamic theory of Helfand. For the extended systems, Hadziioannou et al<sup>3</sup> used low angle scattering techniques and found that the results obtained for the mean square distance of scattering elements relative to a plane gave values that lay between those predicted by the affine and phantom models. This was in contrast to work done on amorphous polystyrene in a high density polyethylene billet by the same workers<sup>4</sup> which showed good agreement with the affine model up to a draw ratio of 10.0. These observations led Hadziioannou et al to conclude that for samples where the molecular weight was greater than the entanglement molecular weight the molecular extension mirrored the macroscopic extension. This, however, proved to be the exception rather than the rule with the affine model being an extreme model.

Berney et al<sup>5</sup> studied a series of poly(styrene-butadiene) diblock copolymers using SANS, SAXS and electron microscopy. They found the results obtained for the mean radius of the polybutadiene spheres from SANS and SAXS were comparable but those obtained using electron microscopy were much smaller. This led Berney to conclude that truncation of the polybutadiene spheres occurred on sample preparation for electron microscopy. This showed one advantage of

the scattering techniques over other techniques. Hasegawa<sup>6</sup> stated that for a better understanding of microdomain structure, it was necessary to consider perturbation of chains in the domain space. Lateral perturbations may have an important effect on dynamical properties through molecular entanglements in microdomain space. Hasegawa<sup>6</sup> and co-workers used poly(styrene-isoprene) diblock copolymers for SANS and SAXS studies of the molecular conformation in microdomain space and the effect of strong chain perturbations on it. From SAXS studies of these alternating lamellar microdomains of polystyrene and polyisoprene these workers found that there were ten to a hundred times more lamellae with normal perpendicular to the film surface rather than parallel to it. These results were confirmed by SANS studies of the same sample. Hashimoto et al<sup>7</sup> reported that the uniformity of microdomain sizes of poly(styrene-isoprene) block copolymers was much higher than that for the molecular weights of the block copolymers comprising the domains. In previous work<sup>8</sup> these same workers found that the relationship between the domain period and the molecular weight from experiment was consistent with the theoretical results based upon random flight chain statistics in the confined domain space.

### 3.1.2.2. Previous Work on Triblock Copolymers

In 1971 Folkes and Keller<sup>9</sup> examined the poly(styrene-butadiene-styrene) (SBS) system using infra-red radiation and obtained information on molecular orientation using infra-red dichroism. The results obtained showed no dichroism for either phase indicating molecular isotropy over a 'unit cell' of the macrocrystal within specified limits. Folkes and Keller<sup>10</sup>, using a birefringence method, also studied a 'single crystal' prepared by extension of an (SBS) triblock copolymer. They found that on rotating a small sample between crossed polars a sharp extinction was observed when the extrusion direction was parallel or perpendicular to the plane of polarization of the incident light indicating that there was anisotropy in this sample.

With the advent of SANS and SAXS, work began on investigating block copolymers in the solid state. Pakula et al<sup>11</sup> used SAXS technique to examine structural changes in poly(styrene-butadiene-styrene) triblock copolymers caused by annealing in the highly oriented state. The triblock copolymers were composed of lamellar polystyrene domains in a matrix of polybutadiene. The sample was deformed to a draw ratio of six and then annealed. The results showed that, depending on the annealing temperature, various morphological changes were observed.

Where the annealing temperature was less than the

glass transition temperature of polystyrene, the resultant morphology was influenced by non-recoverable reorientation of the polystyrene microdomains was the dominant factor.

For annealing temperatures greater than the order-disorder transition temperature, the morphology of the microdomains with macroscopically random orientation was re-formed from the block polymers in disordered state. These workers then went on to perform a SAXS study on the same triblock copolymer system but with cylindrical morphology<sup>12</sup>. Samples were deformed parallel, perpendicular and at 45° to the direction of the original domain orientation. The results showed that, at room temperature, the SAXS pattern changes were similar to those previously observed for lamellar triblock copolymers. At small deformations from the meridional scattering it was found that the interdomain distance had increased along the stretching direction but, at the same time, the scattering intensity decreased due to increasing disorder in interdomain distances or to reorientation of the microdomains from the direction perpendicular to the stretching direction. When elongations were near to the yield point the maximum in the meridional direction disappeared indicating that almost all microdomains originally oriented perpendicular to the stretching direction changed their orientation. At higher elongations a well developed four point pattern

was observed indicating microdomains assumed preferential orientations inclined to the stretching direction. These patterns changed with increasing deformation possibly due to changes in particle length and orientation. Finally at elongations close to fracture, all maximum in the scattering pattern disappeared suggesting that a proportion of the cylinders fractured on extension and then relaxed back to their equilibrium separation. Richards and Mullin<sup>13</sup> conducted a time resolved SAXS and SANS study of poly(styrene-isoprene-styrene) triblock copolymers in extension. The copolymer had cylindrical domain morphology and was subjected to uniaxial deformation. The SAXS studies showed the lattice plane extension ratios were severely non-affine as a function of the bulk extension ratio in contrast to the findings of Pakula et al<sup>11,12</sup>. The domain dimensions were found to be unchanged by uniaxial extension. From SANS, the effect of uniaxial extension of the diffuse interfacial layer thickness parallel and perpendicular to the stretch direction was determined. They found there was no detectable change in lattice plane spacings perpendicular to the stretch direction but the diffuse layer apparently thickened. Parallel to the stretch direction, the interfacial layer disappeared immediately the lattice plane separation increased.

The results described above for uniaxial extension of

the block copolymers was attributable to two sources. Firstly, the non-affine lattice plane separation and the disappearance of the diffuse interfacial layer could have been due to some of the bulk strain being accommodated by the polyisoprene blocks. The polyisoprene blocks interconnect separate polystyrene domains and so could 'unravel' to accommodate the bulk strain. Secondly, the application of a bulk deformation may lead to a partial orientation of cylindrical domains gave rise to the fragmented scattering patterns observed. In order to facilitate an examination of the effect of deformation on the central polyisoprene block the very strong scattering,  $S(Q)$ , due to the long range order of the polystyrene domains had to be eliminated as described in Chapter 1.2.3.. This technique had previously been successfully applied by other workers<sup>15,18</sup> examining various copolymer systems.

### 3.2. Experimental

Since the LOQ instrument at R.A.L. was relatively new a series of experiments using 'standard' polystyrene samples were carried out. These samples are characterised in Table 3.2.. Samples were mounted on optical discs and placed in a sample holder in the neutron beam where they were exposed to the beam until sufficiently good statistical data was obtained. The results obtained were used to construct Kratky plots, (Figure 3.2.1(a)), and calculate radii of

Figure 3.2.1 (a) Kratky Plot Obtained for MIX3 Sample on LOQ Instrument, R.A.L.

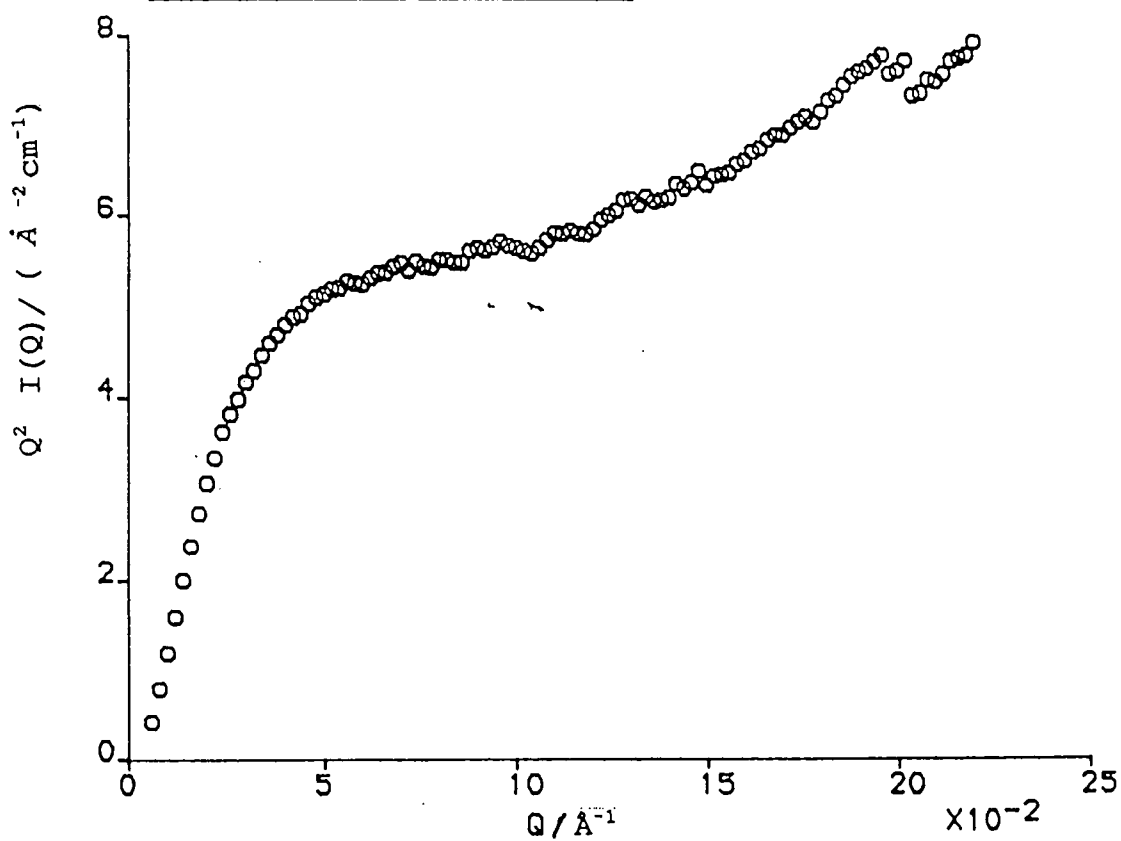
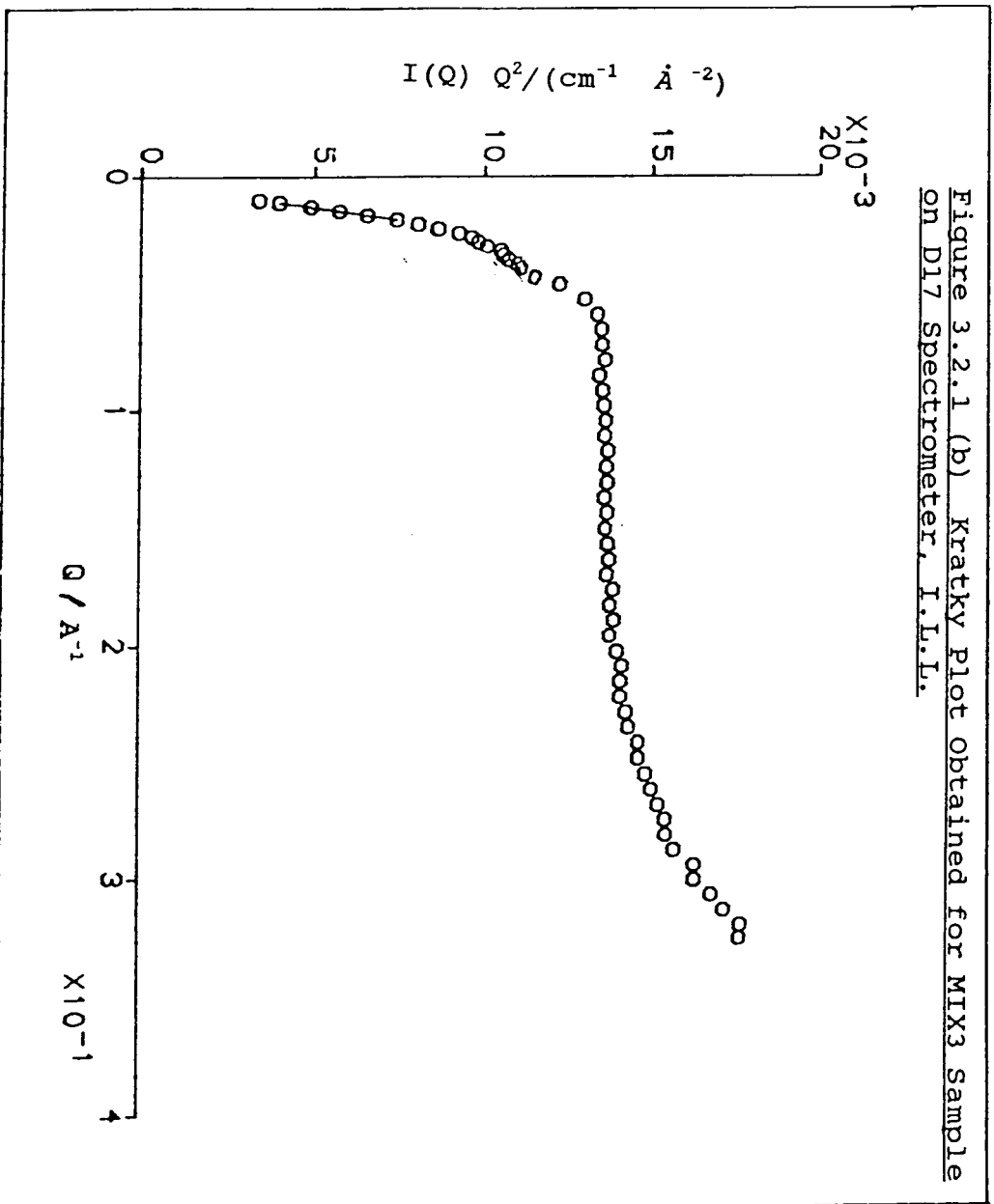


Figure 3.2.1 (b) Kratky Plot Obtained for MIX3 Sample on D17 Spectrometer, I.L.L.



gyration for the polystyrene samples. The same set of polystyrene samples were then taken to the D11/D17 Spectrometers at the Institut-Lave Langerin where they were put through the same experiments as carried out on LOQ instrument.

These results were used to construct Kratky plots, (Figure 3.2.1 (b)), and obtain radii of gyration. Table 3.3. shows the results obtained for radii of gyration ( $R_g$ ) from both instruments. From the Kratky plots and radii of gyration results it was clear that some adjustments were necessary to the LOQ instrument set-up. These adjustments were made before the triblock copolymer samples were studied 'on the' LOQ instrument. On all subsequent visits to perform experiments using the LOQ instrument a check of the instrument configuration was made using one of these 'standard' polystyrene samples and once this was assessed and the results were acceptable, the samples to be studied were placed in the beam and examined. This caution was deemed unnecessary at the ILL due to the excellent results obtained from the 'standard' polystyrene samples when run on D11 and D17 spectrometer.

Block copolymer samples to be used were cut from copolymer films cast in PTFE blocks. The first set of experiments was carried out on the S15150 series of triblock copolymers using the D11 Spectrometer at the ILL and the LOQ instrument at R.A.L..

Table 3.2. Sample Characteristics of 'Standard' Polystyrenes

SAMPLE	$M_w$	$M_w/M_n$
MIX1	38082	1.02
MIX3	87328	1.02
MIX4	152312	1.03

$M_w$  refers to the molecular weight of the deuterated portion of the polymer blend.

Table 3.3. Radii of Gyration and Molecular Weights for Standard Polystyrene samples at RAL AND ILL, Grenoble

SAMPLE	Rg (Å)		Rg theoretical (Å)	M <sub>w</sub> from SANS	
	RAL	ILL		ILL	RAL
MIX1	43.9 ± 8.2	50.8 ± 6.5	55.0	35.1	31.6
MIX3	70.0 ± 9.8	82.0 ± 2.4	82.7	84.0	102.0
MIX4	108.0 ± 12.2	119.4 ± 8.4	109.4	107.0	130.7

These samples were approximately 5cm long x 4cm wide x 1cm thick and great care was taken not to stress them whilst placing them in the stretching frame (Ch. 2). The samples themselves were noted to be very sticky on both sides and when they were placed in the neutron beam and were elongated, the sample surface rippled and as the stretching increased these ripples became more widespread and appeared to be penetrating into the sample itself. This had the direct consequence that the maximum elongation ratio ( $\lambda$ ) achieved for the S15150 series was 2.0 due to the sample shearing as one of these ripples penetrated the whole sample thickness. Once the sample had sheared it was removed from the stretching frame and it appeared to have no elastic qualities as it retained the length it last had in the stretching frame.

The scattering data obtained for the S15150 samples on LOQ and D11 instruments were corrected as described in Ch. 2 and the results were used in further analysis.

### 3.2.1. Results and Discussion

Zimm plots were made for each extension ratio studied for each instrument and the radius of gyration,  $R_g$ , and molecular weight,  $M_w$  were calculated (Figures 3.2.2(a),(b)). These are shown in Table 3.4.. It was interesting to note, however, that the 'contrast-matching' technique appeared to have been very successful as Figures 3.2.3 and 3.2.4. show.

The Bragg scattering associated with the long range

Figure 3.2.2 (a) Zimm Plot Obtained for 515150 Sample at Extension Ratio 1.5m 100 Instrument, R.A.L.

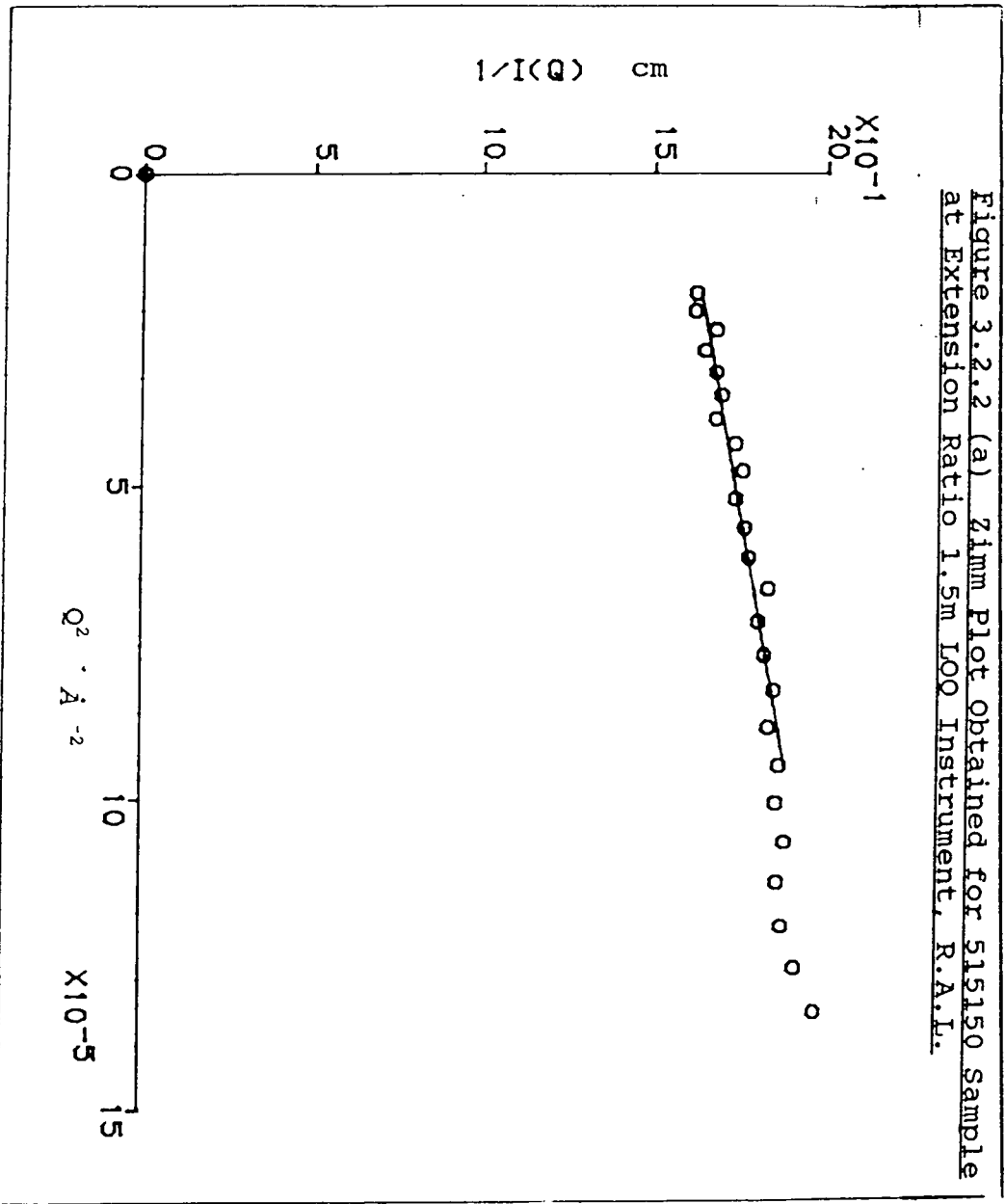


Figure 3.2.2 (b) Zimm Plot Obtained for 515150 Sample  
at Extension Ratio 1.3 on D11 Instrument, I.L.L.

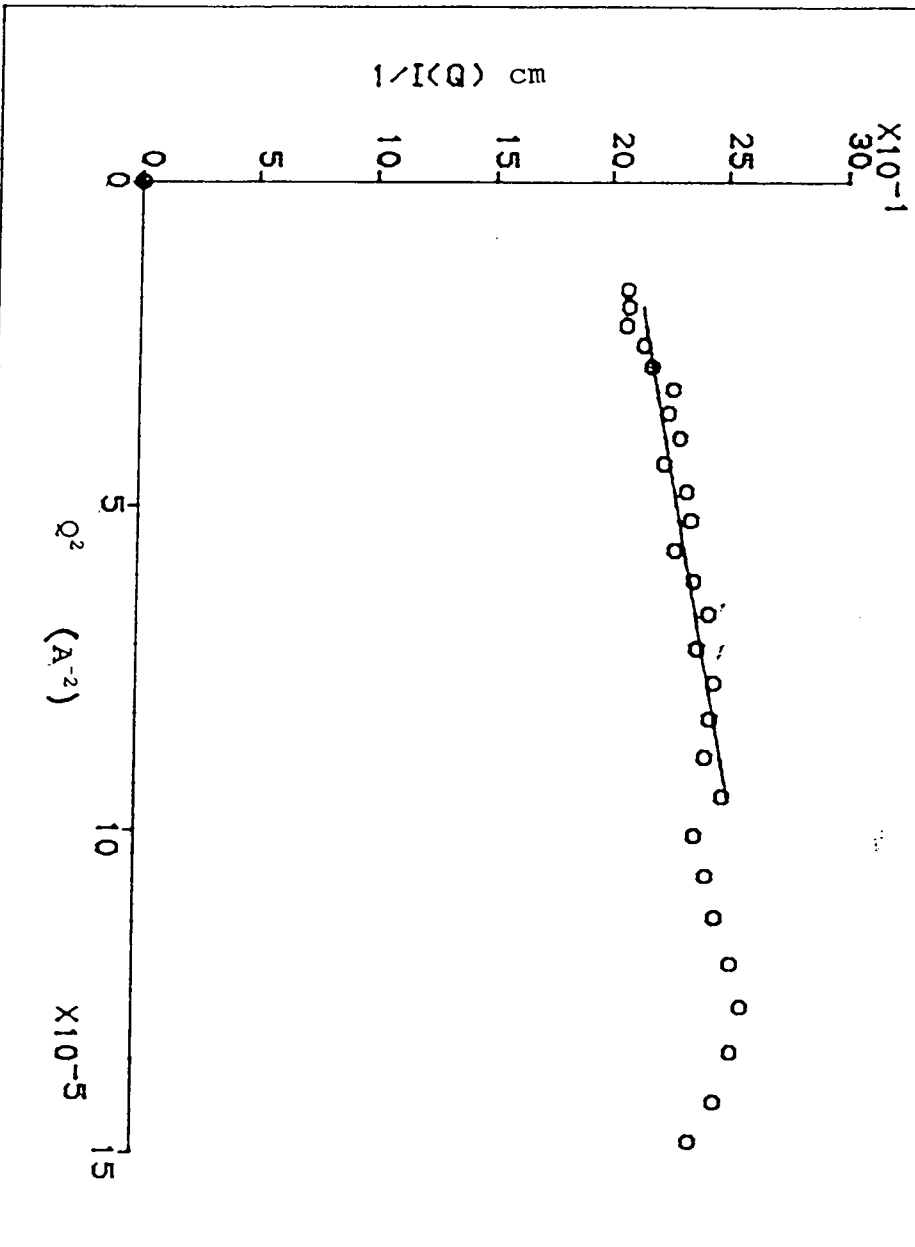


Figure 3.2.3. Scattering Intensity  $I(Q)$  vs  $Q$  Obtained for 'MIX' Sample of 515150 series on LOQ Instrument, R.A.L.

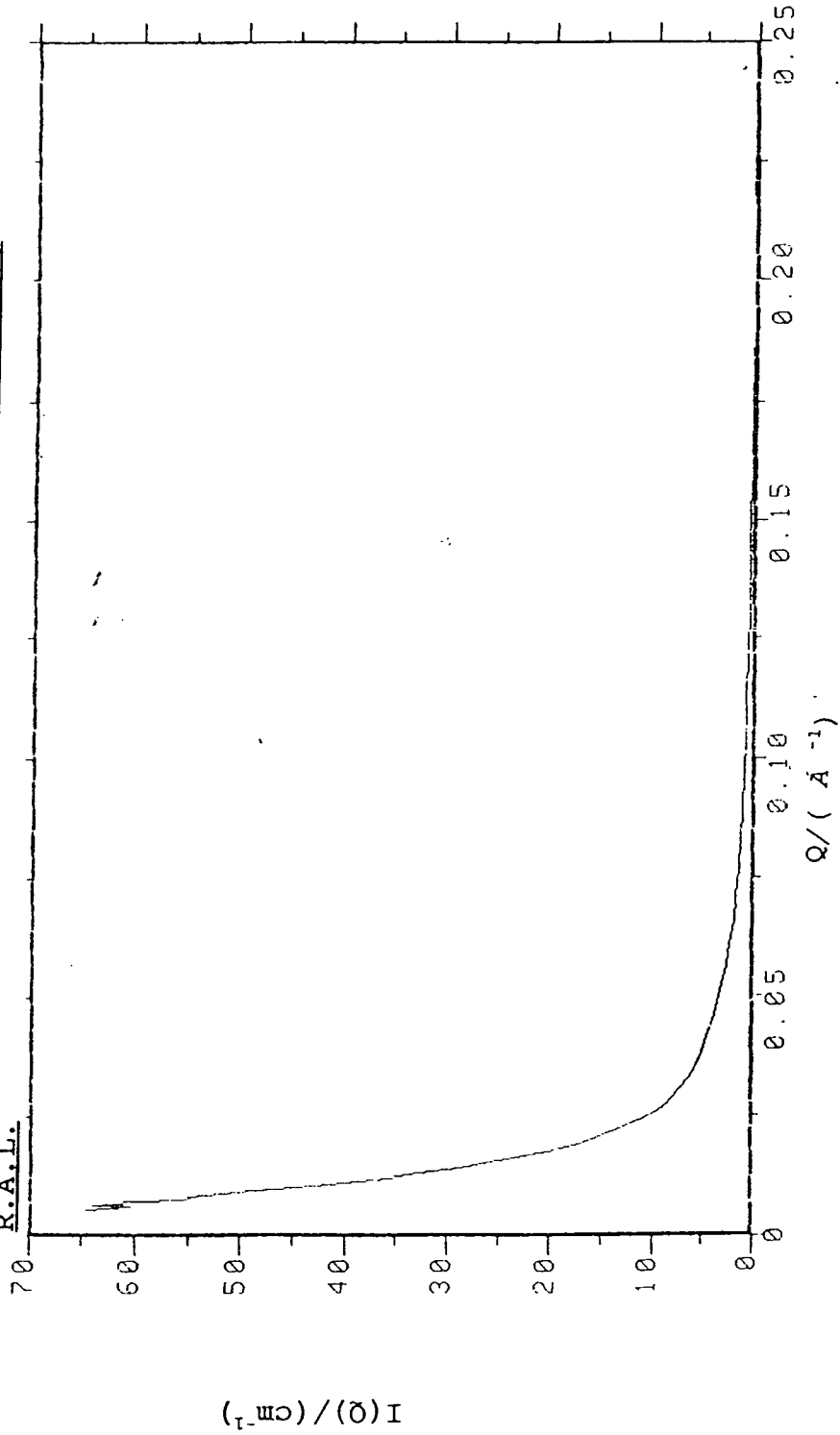
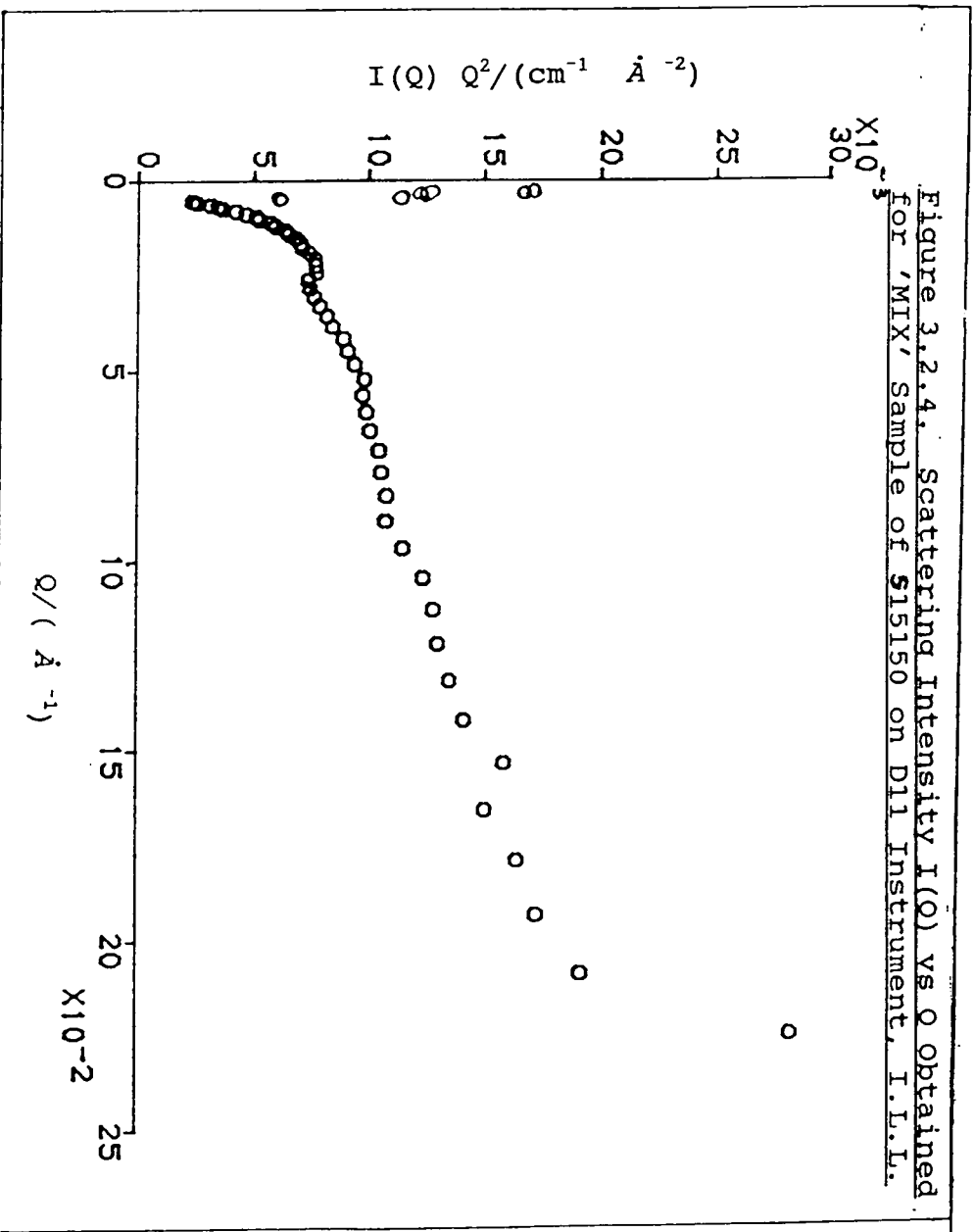


Figure 3.2.4. Scattering Intensity  $I(Q)$  vs  $Q$  obtained for 'MIX' Sample of S15150 on D11 Instrument, I.L.L.



order of the polystyrene domains was virtually eliminated and allowed the examination of the effect of elongation on the central polyisoprene block to be less complicated. The scattering profile obtained for the S15150 series on both instruments, however, was not as expected. The scattering profiles obtained for all elongation ratios studied did not show any evidence of anisotropy as had been expected. An explanation for this was sought by examining the results obtained from Zimm plots for  $R_g$  and  $M_w$  in Table 3.4..

For a triblock copolymer of poly(styrene-isoprene-styrene) with cylindrical styrene monophology the theoretical  $R_g$  is given by:-

$$R_g = 0.31 M_w^{\frac{1}{2}} \quad \text{EQ. (5)}$$

where:  $M_w$  = molecular weight of the polyisoprene block.

This is for the unextended sample and for S15150  $R_g$  was calculated to be 80 Å.

Table 3.4. - SANS results obtained for S15150 samples on D11 and LOQ instruments

EXTENSION RATIO, $\lambda$	Rg ( $\text{\AA}$ )		Rg <sub>affine</sub> ( $\text{\AA}$ )	M <sub>w</sub> (gx10 <sup>-3</sup> )		M <sub>w</sub> (gx10 <sup>-3</sup> ) from GPC
	LOQ	D11		LOQ	D11	
1.0	80.9 ± 4.9	81.9 ± 3.7	80	40.4 ± 4.3	46.6 ± 4.5	53.2
1.1	81.0 ± 4.7	83.4 ± 3.8	88	38.7 ± 4.1	44.8 ± 4.2	
1.3	89.9 ± 5.1	86.3 ± 3.9	104	43.6 ± 4.8	47.7 ± 4.7	
1.5	94.1 ± 5.7	79.2 ± 4.1	120	41.2 ± 4.4	43.9 ± 4.1	
2.0		91.4 ± 5.3	160	-	43.8 ± 4.6	

In Table 3.4.  $M_w$  calculated using the following equation<sup>36</sup>

$$\log M_{w(GPC)}^{cop} = \log M_{w(true)}^{cop} + W_{isoprene} \log K \quad \text{EQ. (6)}$$

where:

$\log M_{w(GPC)}^{cop}$  = molecular weight of triblock copolymer from G.P.C. measurement.

$\log M_{w(true)}^{cop}$  = true molecular weight of triblock copolymer

$W_{isoprene}$  = weight fraction of isoprene

$K$  = constant

Thomason found  $K = 1.35$  for a styrene-isoprene block copolymer and this was used to obtain the  $M_w$  from GPC in Table 3.4..

From Table 3.4., the unextended radius of gyration for S15150 from both LOQ and D11 instrument are close to this value. When the values obtained for  $R_g$  at each extension ratio are examined it is clear that for the majority of cases both D11 and LOQ results are very similar in magnitude. Table 3.4. also shows the radius of gyration at each elongation ratio if the stretching was affine. The other classical theories of rubber elasticity described in Ch. 3.1.2. were compared with the scattering results obtained for the S15150 series but none was found to be a 'good' match. The intercept of the Zimm plot at  $Q=0$  was used to calculate the molecular weight of the polyisoprene

block at each extension ratio. The calculated results are shown in Table 3.4..

The molecular weight of the central polyisoprene block determined by Gel Permeation Chromatography was 53200, and the results obtained from Zimm plots are all of that magnitude, it can be concluded that the deuterated portion is spread uniformly throughout the polyisoprene part of the triblock copolymer mix as expected.

The range of  $Q$  covered by LOQ instrument (Ch. 2) allowed a Kratky plot to be made for S15150 results obtained on this instrument at each elongation ratio. These were all of the same form as shown in Figure 3.2.4.. The general shape of this plot is not similar to the classical Kratky plot shown in Figure 3.2.5. due to the maxima in the low  $Q$  region just before the plateau part of the graph. The presence of these two maxima was ascribed one of the following:-

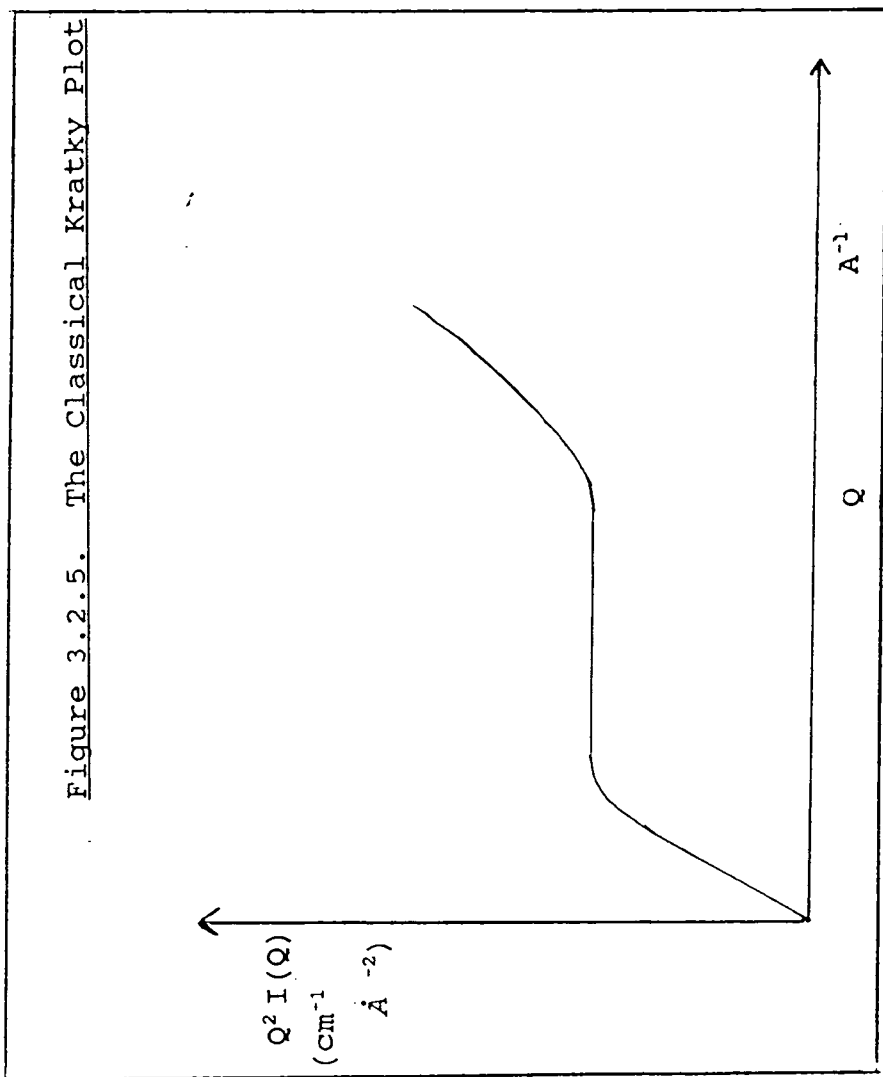
(i) The deuteropolyisoprene had degraded causing the copolymer to lose its elasticity and give the unusual scattering profile obtained.

(ii) The relatively low molecular weight of the S15150 series resulted in the apparent lack of elasticity and the unusual scattering profile.

(iii) The unusual scattering in the low  $Q$  region of the Kratky plot was caused by void scattering.

(iv) There was a complex molecular reaction to elongation in the S15150 series which had not been

Figure 3.2.5. The Classical Kratky Plot



previously described by any other works.

These appeared to be the four most probable reasons and of the four the first, sample degradation, seems most likely due to two factors. Firstly, the discrepancy between the molecular weights calculated from SANS and GPC could indicate degradation had occurred and secondly the 'tacky' nature of the samples themselves. To eliminate one of the four possibilities listed above, low molecular weight, it was decided to synthesise a second series of triblock copolymers with a higher molecular weight but the same proportion of polystyrene and polyisoprene. The target was a total molecular weight of 120000. These samples are characterised in Table 3.1.. Samples were cast from toluene in PTFE casts as for S15150 samples and were wrapped in silver foil and placed in a freezer at 280K prior to being taken to Oxford or Grenoble for SANS studies. The experiments were carried out in the same manner as described previously for the S15150 series of samples.

For the S15150B series, however, the D17 Spectrometer was made available for analysing the effect of deformation at higher  $Q$  values. This data when combined with D11 data, allowed the  $Q$  range  $0.005 \text{ \AA}^{-1}$  to  $0.30 \text{ \AA}^{-1}$  to be covered with good statistics on the scattering profile obtained. For both LOQ and D11/D17 data, however, the same isotropic scattering pattern was observed as had been obtained for the S15150

series (Figures 3.2.6, 3.2.7). The S15150B samples however, felt tacky on one side and looked shiny and felt smooth on the other whereas the S15150 series samples were tacky on both sides. When the 'Random' and 'MIX' samples were placed in the stretching frame and subjected to elongation the same pattern observed for the S15150 series was found (Figures 3.2.8 and 3.2.9). Firstly, samples would not stretch beyond an elongation ratio of 2.2. Secondly, samples showed the same 'ripple effect' on the surface as noted for the S15150 series as soon as any stress was placed on the samples themselves. Various attempts were made to try to prevent samples from shearing at the point at which they were clamped in the stretching frame. These included bonding the sample to the sample holder with glue in the stretching frame and affixing a piece of sandpaper to the sample holders and clamping the sample on top of it. These both met with failure so the deformation study was limited to a maximum extension ratio of 2.2. This was a slight improvement on that achieved for the S15150 series and may have been due to the higher total molecular weight of the S15150B.

Figure 3.2.8 shows that, for the 'Random' sample there was a distinct maximum in the scattering profile. When, however, this 'random' scattering was subtracted from the 'MIX' scattering to give the corrected scattering intensity for the triblock copolymer sample

Figure 3.2.6. Kratky Plot obtained for 515150B sample at Extension Ratio 2.0 on IQQ Instrument, R.A.L.

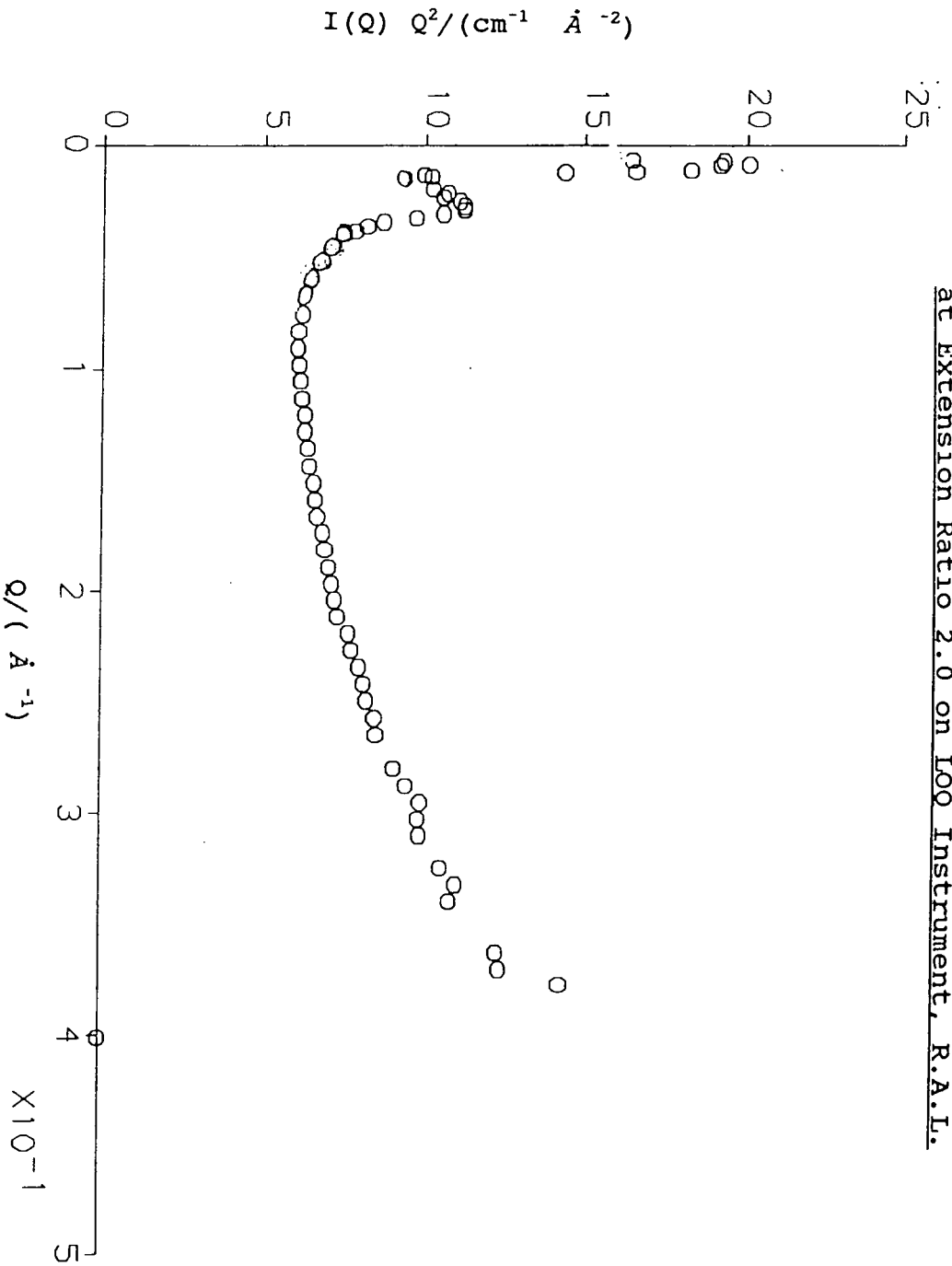


Figure 3.2.7. Kratky Plot Obtained on 515150B Sample at Extension Ratio 2.0 on D11/D17 Instruments, I.L.I.

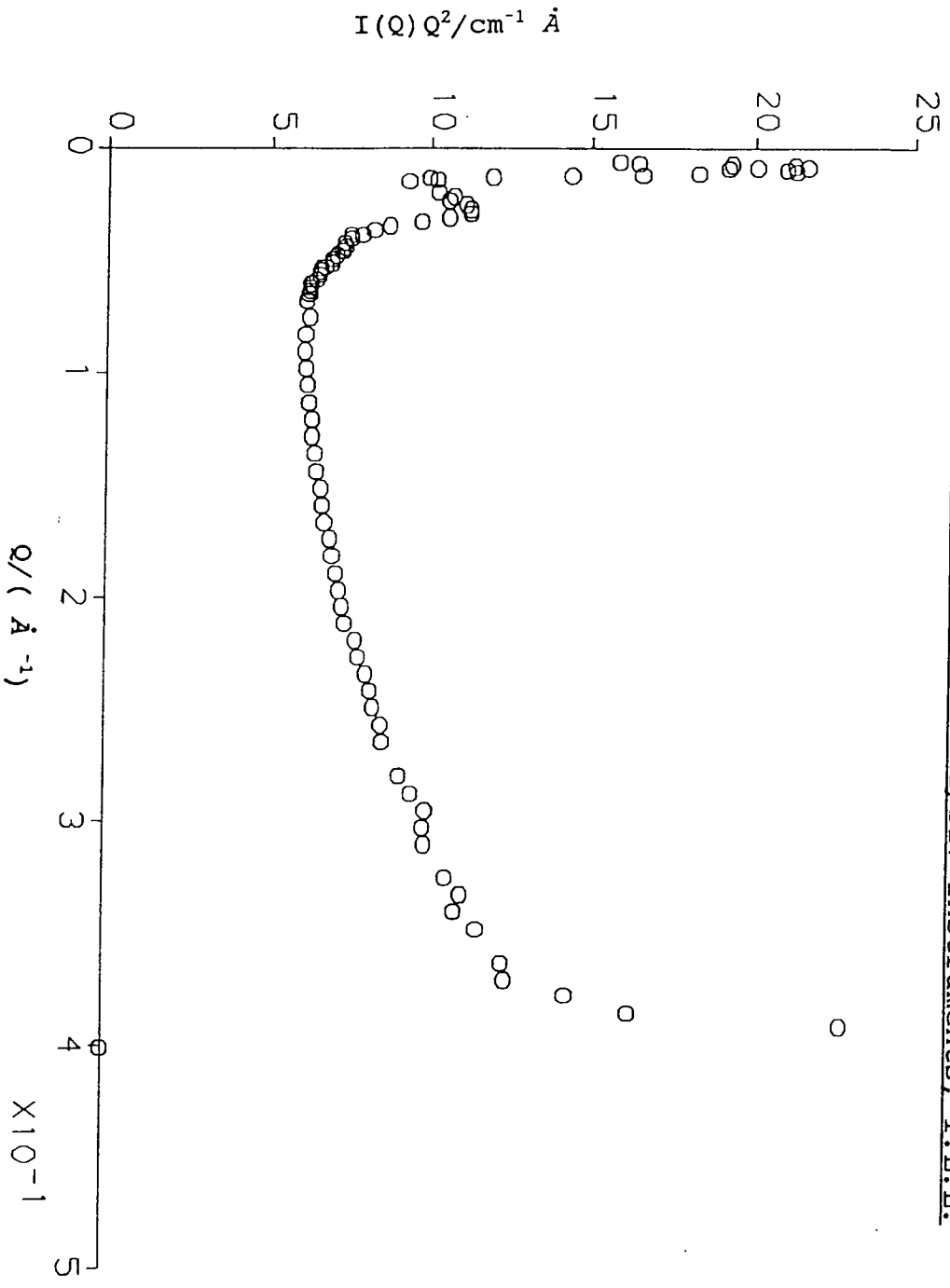
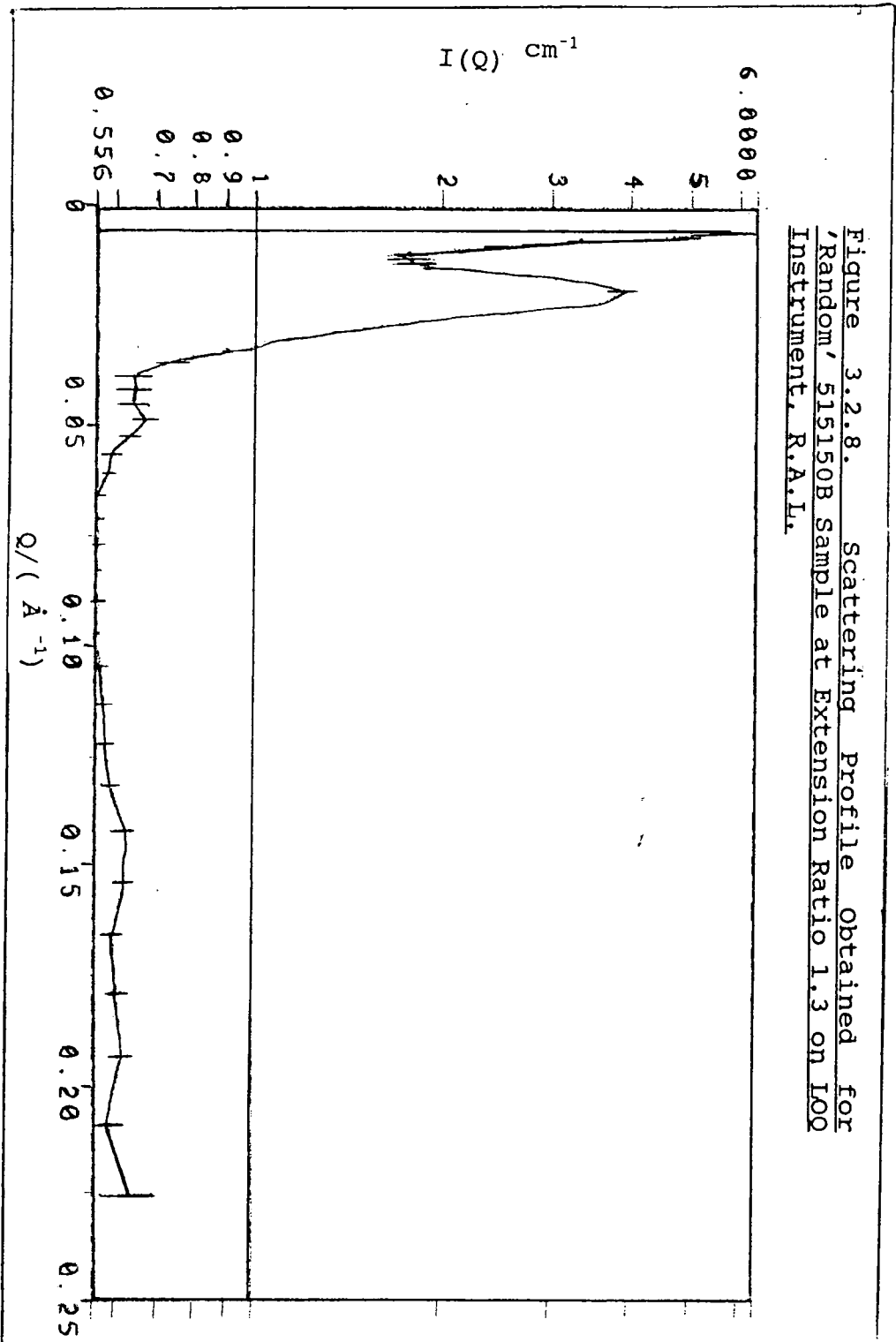
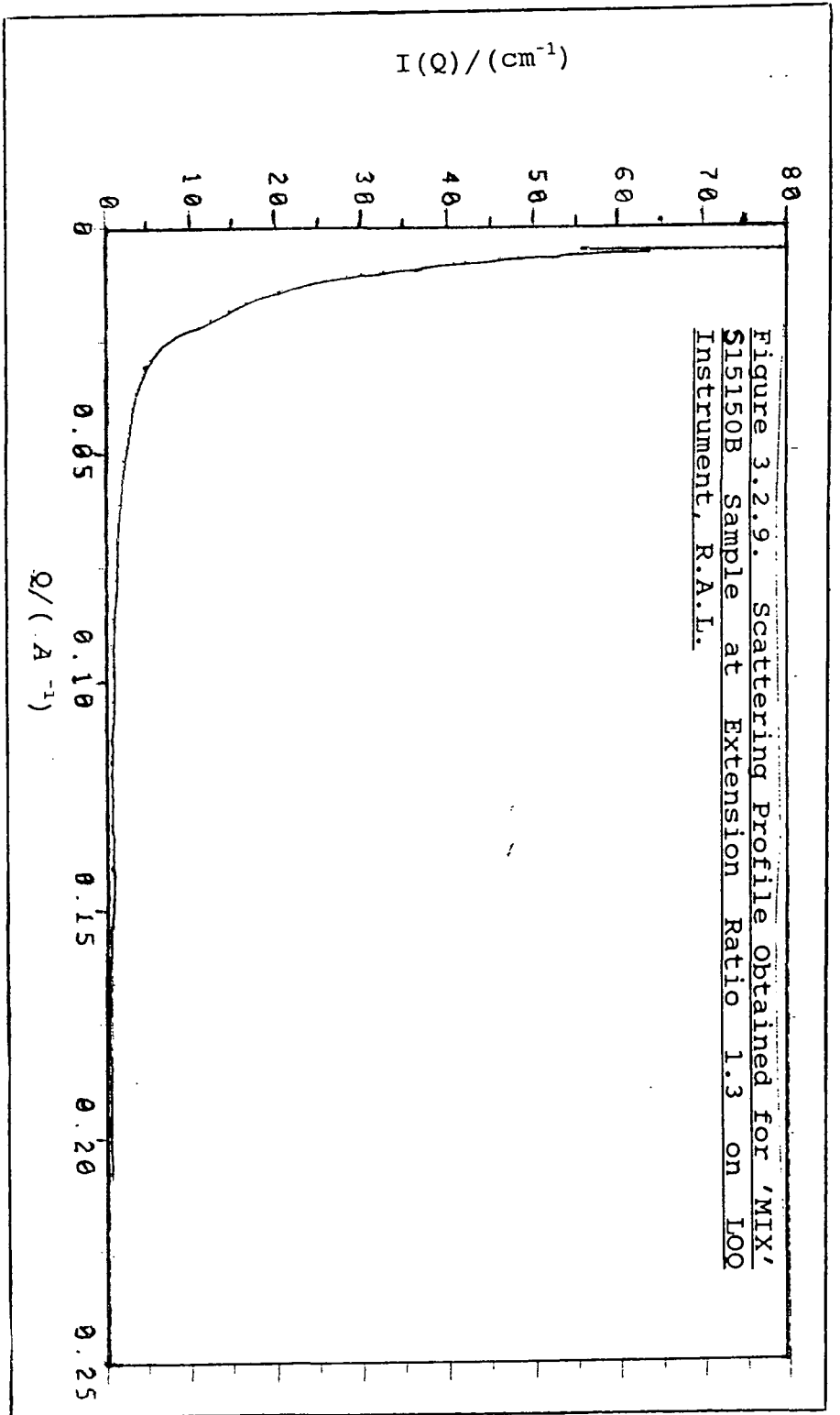


Figure 3.2.8. Scattering Profile Obtained for 'Random' 515150B Sample at Extension Ratio 1.3 on IQQ Instrument, R.A.L.





at the extension ratio under examination, then this maximum was not apparent (Figure 3.2.9). Due to the much greater scattering intensity obtained from the 'MIX' sample the scattering from the 'Random' sample was a very small proportion and so the maximum. On close examination of Figure 3.2.9. it is clear that the maximum, though not obvious, is still there. This indicates that the 'contrast matching' technique had not been quite perfect and some Bragg scattering due to the ordering of the polystyrene domains had not been removed.

Zimm plots of LOQ and D11 data were used to obtain radii of gyration and molecular weights of the deuterated portion of the polymer at each extension ratio studied. These results are shown in Table 3.5., and are consistent with the results obtained from the S15150 series but not what was expected based on work carried out previously by other workers and theoretical calculations. The lack of anisotropic scattering was not due to molecular weight phenomenon since a triblock copolymer of similar molecular weight with the polystyrene position deuterated did exhibit anisotropic scattering<sup>15</sup>.

The results obtained for S15150B radius of gyration at each elongation ratio studied show that the unstretched sample has an experimental radius of gyration, calculated using the molecular weight obtained from G.P.C. measurements, which is very close

to that predicted from theory.

This is consistent with the S15150 series which also showed good agreement between the theoretical and experimentally obtained  $R_g$  for the unstressed material. As the extension ratio was increased the radii of gyration did increase as expected but not affinely. The deformation of the S15150B series showed that it was non-affine for all extension ratios studied. As before this is the same result as that obtained for the S15150 series. The fact, however, that the maximum elongation ratio achieved for the S15150B series was slightly greater than that achieved for the S15150 series was not regarded as being an indication of some molecular weight dependence for several reasons.

Table 3.5. SANS Results Obtained for S15150B series on LOQ and D11/D17 Instruments

EXTENSION RATIO $\lambda$	Rg ( $\text{\AA}$ )		Rg <sub>affine</sub> ( $\text{\AA}$ )	M <sub>w</sub> ( $\times 10^{-3}$ )		*M <sub>w</sub> ( $\times 10^{-3}$ ) from G.P.C.
	LOQ	D11		LOQ	D11	
1.0	85.3 $\pm$ 4.8	88.3 $\pm$ 3.7	89.0	51.5 $\pm$ 4.0	46.8 $\pm$ 4.2	66.8
1.1	88.1 $\pm$ 5.3	91.3 $\pm$ 4.1	97.9	49.9 $\pm$ 3.9	53.9 $\pm$ 4.0	
1.3	92.3 $\pm$ 6.1	93.4 $\pm$ 5.0	115.7	53.7 $\pm$ 4.7	45.1 $\pm$ 4.4	
1.5	104.5 $\pm$ 8.0	98.1 $\pm$ 5.3	133.5	58.4 $\pm$ 5.8	49.0 $\pm$ 5.3	
2.0	110.8 $\pm$ 9.4	107.5 $\pm$ 8.0	178.0	58.9 $\pm$ 6.1	55.3 $\pm$ 4.9	

\* M<sub>w</sub> from G.P.C. calculated as for 515150 series.

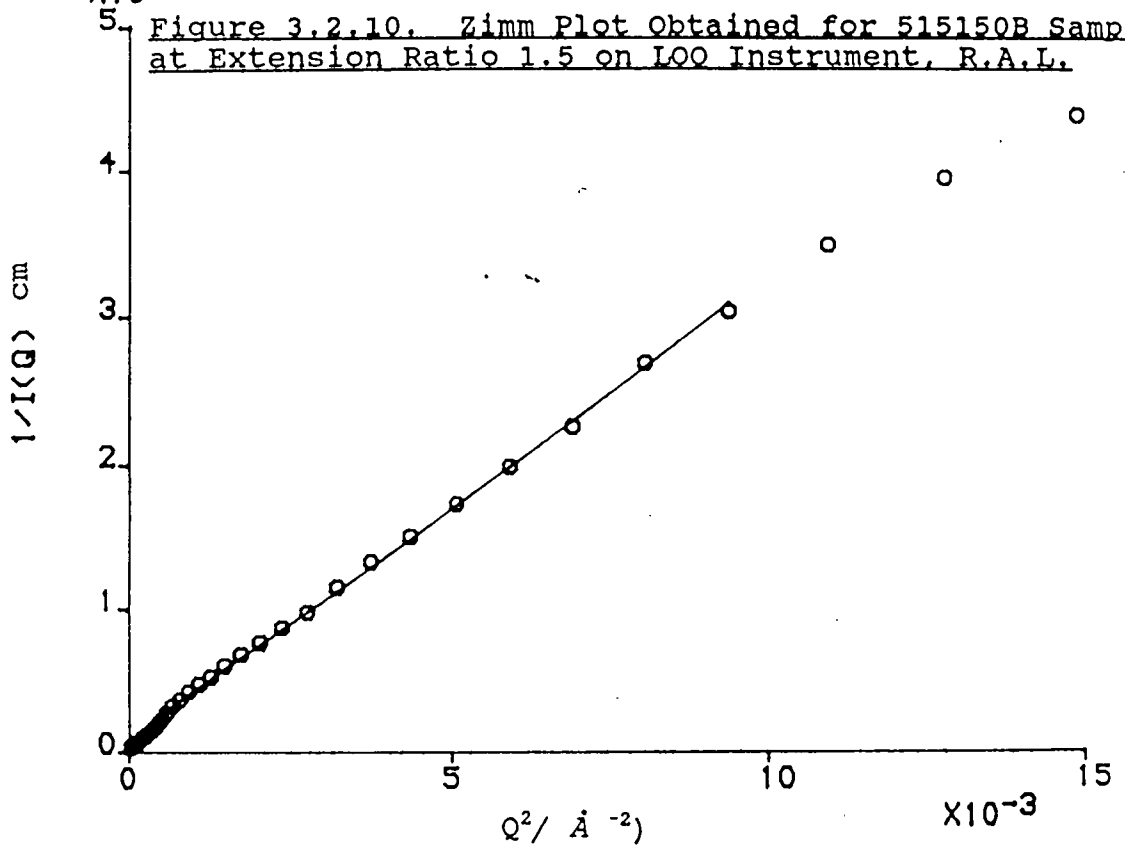
Firstly, the samples' history - the S15150B samples were two to three weeks old when they were studied first and the final experiments were carried out on them when they were approximately 3 months old.

The S15150 samples, however were two to three months old when they were first studied and almost a year old when they were last examined. This wide difference in the age of the sample could have accounted for the greater deterioration in the S15150 samples than in the newer set resulting in the slightly greater elongation ratios achieved for the S15150B series. Secondly, the elongation ratios were determined by physically measuring the length of the unextended sample and then multiplying these by the required extension ratio to give the required sample length. This obviously had a degree of error associated with it and with only a 10% better elongation ratio being achieved the human error associated with this measurement could account for this 10% increase achieved for S15150B samples.

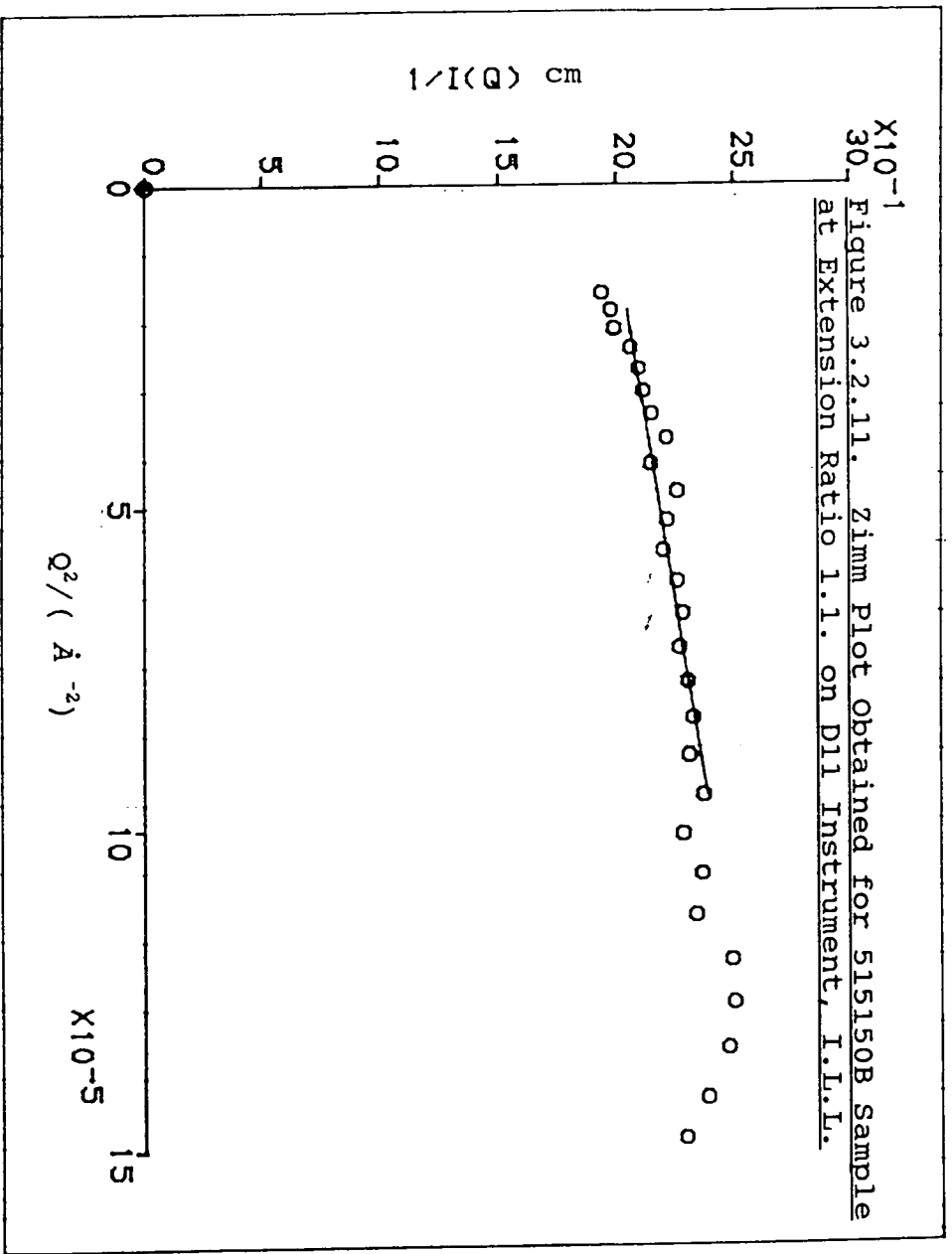
As for the S15150B series, the LOQ and D11/D17 sets of results are very similar, (Table 3.5.). This is as expected but does prove that uniform data can be obtained from the two different types of Spectrometer. Zimm plots were also used to calculate the molecular weight of the deuterated portion of the S15150B copolymer similar to those shown in Figures 3.2.10 and 3.2.11. The results obtained are shown in Table 3.5.

X10<sup>-1</sup>

Figure 3.2.10. Zimm Plot Obtained for 515150B Sample at Extension Ratio 1.5 on LOO Instrument, R.A.L.



30  $\times 10^{-1}$  Figure 3.2.11. Zimm Plot Obtained for 515150B Sample at Extension Ratio 1.1. on D11 Instrument, I.L.I.



As for the S15150 series all results are within 10% of each other for all elongation ratios. The experimentally obtained  $M_w$  are less than that obtained from G.P.C. at all extensions but are of the same magnitude, similar once again to that found for the S15150 series of samples.

In conclusion, the S15150 and S15150B samples showed several differences compared to results obtained on similar polymer samples by other workers (Ch. 3.1.2.). Firstly, the S15150 and S15150B series of samples did not show any anisotropic scattering at any extension ratio studied. This is in contrast to the anisotropic scattering reported from various polymer systems by other workers and is not what was theoretically predicted. Secondly, on physical examination of the samples themselves it was apparent that there was not a great deal of elasticity present. When this sample was compared to a similar one synthesised by Mullin in which the polystyrene portion was deuterated, it was clear these samples still retained their elasticity despite being several years old.

Besides the differences noted above between theoretically and experimentally obtained data the results obtained for the S15150 and S15150B series of samples were consistent in other areas. The radii of gyration calculated at each extension ratio for the S15150 and S15150B series showed deformation was non-

affine for all extension ratios studied. For both series of samples the unextended radius of gyration calculated from experimental data and theory were in very close agreement.

The lack of anisotropy for either set of samples at any of the extension ratios studied led to the assumption that the most probable cause of this was the degradation of the deuteropolyisoprene portion of the triblock copolymers S15150 and S15150B. As a consequence of this conclusion, the scattering profiles obtained for the S15150 and S15150B samples and, in particular, the two sharp maxima in the low Q region of the scattering spectrum were caused by the degradation of the central deuteropolyisoprene block and the relaxation of the molecules at each extension ratio. Samples of HYD1, RAN1, and 'MIX' triblock copolymers were sent for electron microscopy examination in America.

Only the HYD1 samples was studied using electron microscopy and this showed there was indeed a degree of ordering in the sample but this was not as great as had been expected and there appeared to be some 'contamination' of the sample. This 'contamination' could have occurred before shipment to America or whilst in America awaiting study. The absence of electron microscopy results for the RAN1 and 'MIX' triblock copolymer samples meant that conclusions would only be based on one result which would be

inappropriate. The source of the 'contamination' in the HYD1 sample could not be identified.

In summary, the S15150 and S15150B series of triblock copolymers were very similar. The physical appearance and elasticity of the samples was not as expected from previous triblock copolymer samples synthesised on the same equipment. In a study of a poly(styrene-butadiene) diblock copolymer DiCorleto et al<sup>21</sup> examined the effect of ageing on diblock copolymer samples. These authors found that samples, when subjected to a stress, after being quenched, slow cooled or isothermally aged showed a craze-pattern growth. This is very similar to what was observed for the S15150 and S15150B series of samples. The S15150 and S15150B samples were not, however, quenched, slow-cooled or isothermally aged but were relatively old and had been used in studies at ambient temperatures for several days and then stored in a freezer at 280K until required again. With this sort of thermal history it is possible that some sort of ageing occurred in these copolymers resulting in the craze growth observed as these samples were stretched.

Despite the work done on ageing of block copolymers it would appear that the major contribution to the loss of elasticity and the absence of anisotropic scattering of the S15150 and S15150B series of triblock copolymer was due to the oxidative

degradation of the deuterioisoprene portion of these samples.

### 3.3. SANS Study of a Spherical Domain Triblock Copolymer

#### 3.3.1. Introduction

The studies of the S15150 and S15150B series of polystyrene-isoprene-styrene) triblock copolymer systems described previously were made up of cylindrical polystyrene domains in a polyisoprene matrix. As a follow up to these experiments another triblock copolymer of poly(styrene-isoprene-styrene) was synthesised by Polymer Laboratories with spherical polystyrene domains. These samples are characterised in Table 3.3.1.. As Table 3.3.1. shows the total molecular weights were in the same region as those of the S15150B series. The SPH150 series was made up in the same way as the S15150 and S15150B series by casting films from toluene solutions of the copolymer (Ch. 2).

When these samples of SPH150 were removed from their PTFE casting blocks the physical and mechanical properties of the films were different to the S15150 and S15150B series.

Firstly, the films were not tacky and secondly they appeared to be much more elastic than either the S15150 or S15150B had been.

Table 3.3.1. - Characteristics of SPH150 samples prepared by Polymer Laboratories

SAMPLE	TOTAL $M_w$ ( $\times 10^{-3}$ )	$M_w/M_n$	WT. FRACTION STYRENE, $W_s$
<u>SPH150</u>			
Hydrogenous	117	1.02	0.16
'MIX'	158	1.02	0.17
'Random'	124	1.02	0.16

$M_w$ ,  $M_w/M_n$  - determined by G.P.C. analysis

$W_s$  - determined by U.V. Spectrometry

This apparent difference in the samples could have been caused by one of three factors; (i) the method of preparation, (ii) the different source of deuterioisoprene used or, (iii) the increased content of isoprene in the samples prepared by Polymer laboratories. Of the three, the method of preparation seems most likely since G.P.C results for S15150 and S15150B samples indicated that the samples were indeed triblock copolymers with a fairly narrow polydispersity.

### 3.3.2. Experimental

'Random', 'MIX' and Hydrogenous films were taken for examination on the D11 Spectrometer. In view of the relatively short amount of time available for this experiment it was not possible to examine the fully hydrogenous film. When the stretching frame had been positioned correctly in the beam, the 'MIX' and 'Random' samples were attached to the stretching frame in turn in the unextended state to ascertain how much time would be required for each sample to yield statistically significant data. As had been found for the S15150 and S15150B series previously it was found that the 'MIX' sample was a much stronger scatterer than the 'Random' sample for the SPH150 series. The scattering from the 'MIX' sample was around fifty times greater than that of the background 'Random' sample. As a result, the scattering due to the

'Random' sample was so small as compared to the 'MIX' sample as to be insignificant (Figures 3.3.1 and 3.3.2). Consequently after the first few extension ratios had been studied the 'Random' sample was no longer examined.

The 'MIX' sample was studied at extension ratios of 1.0, 1.2, 1.4, 1.6, 1.8, 2.0 and 2.2. Higher extension ratios could not be examined due to the mechanical limits of the stretching frame which reached its upper limit for this particular sample at that point. Once the 'MIX' sample had been studied at the elongation ratios listed above, it was removed from the stretching frame and immediately went back to its original unextended length indicating the rubber-like nature of the SPH150 sample.

### 3.3.3. Results

The most obvious result of this study was the anisotropic nature of the scattering as the sample was extended. The anisotropic scattering data obtained was corrected using the appropriate programs at the I.L.L.<sup>22</sup> by dividing the scattering profile into 30° sectors to give six sectors in all. (Figure 3.3.3). In Figure 3.3.3, sectors 3 and 5 are equivalent as are sectors 2 and 6. Consequently for each extension ratio, six sets of corrected data were obtained and this was reduced to four when the data from equivalent sectors were combined. The data were then used, after taking account of sample thickness, monitor counts

Figure 3.3.1. Scattering Profile Obtained for Background 'Random' SPH150 sample at elongation ratio 1.6 on D11 instrument, I.L.L.

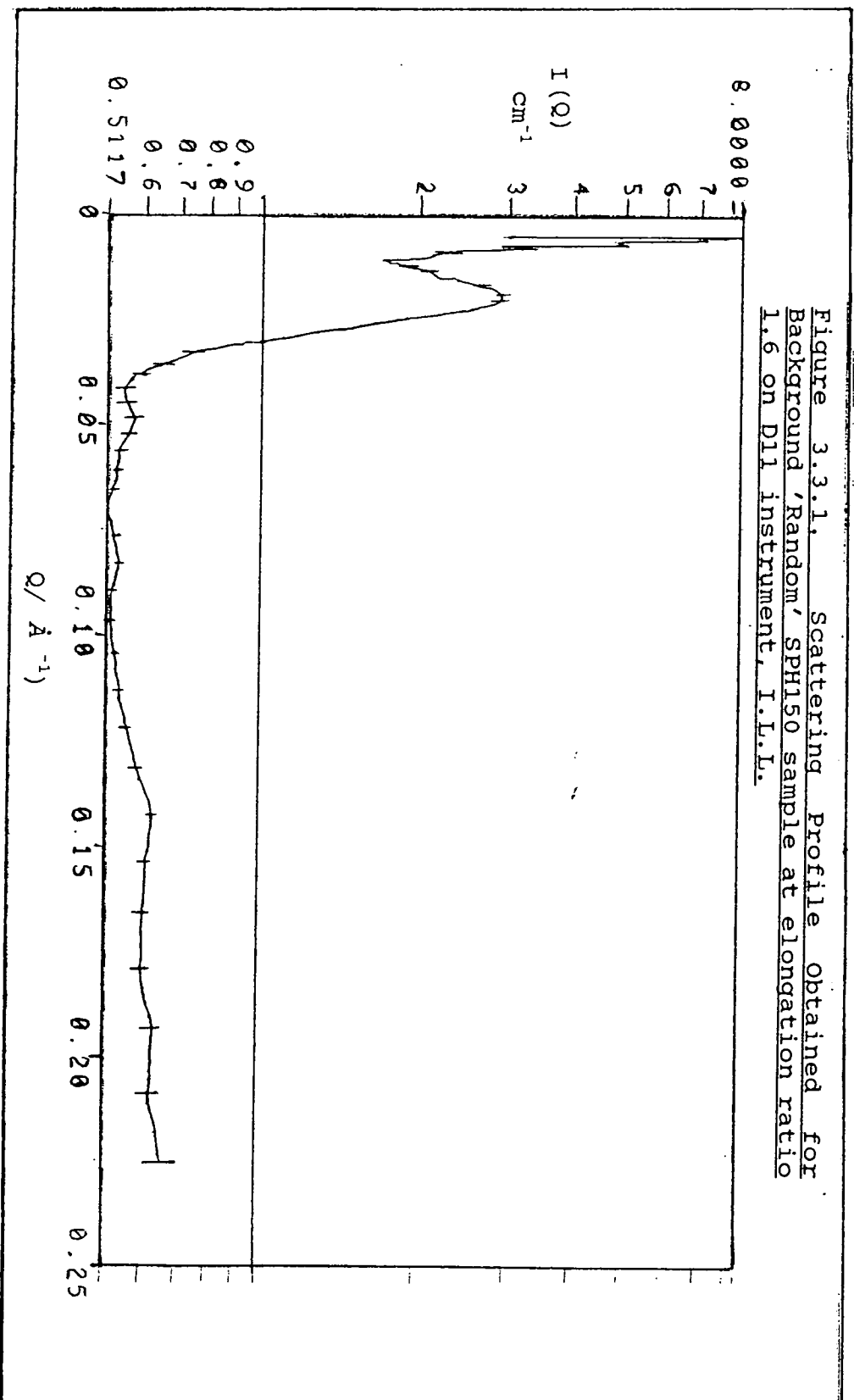


Figure 3.3.2. Scattering Profile obtained for 'MIX' SPH150 sample at elongation ratio 1.6 on D11 Instrument, I.L.L.

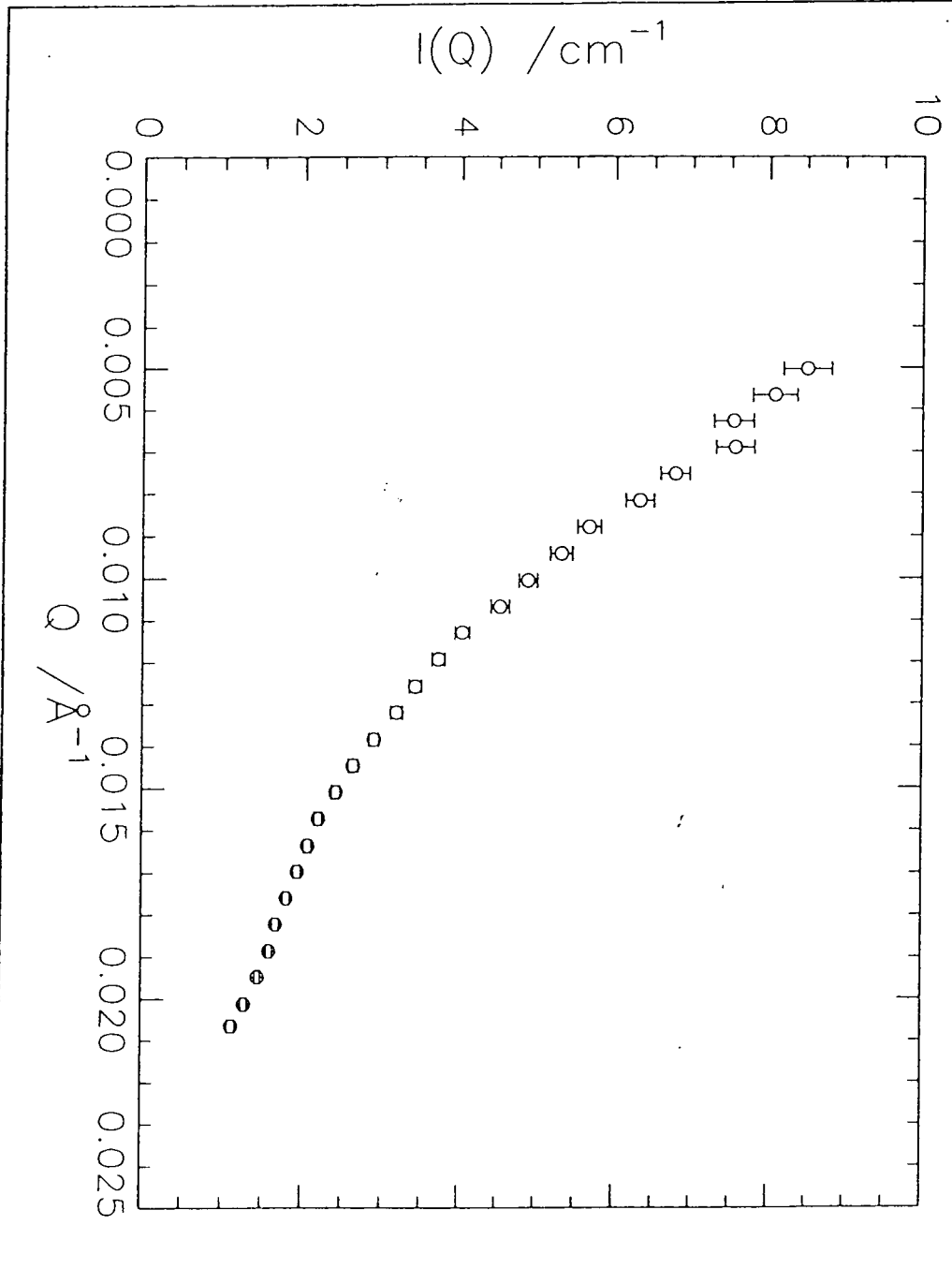
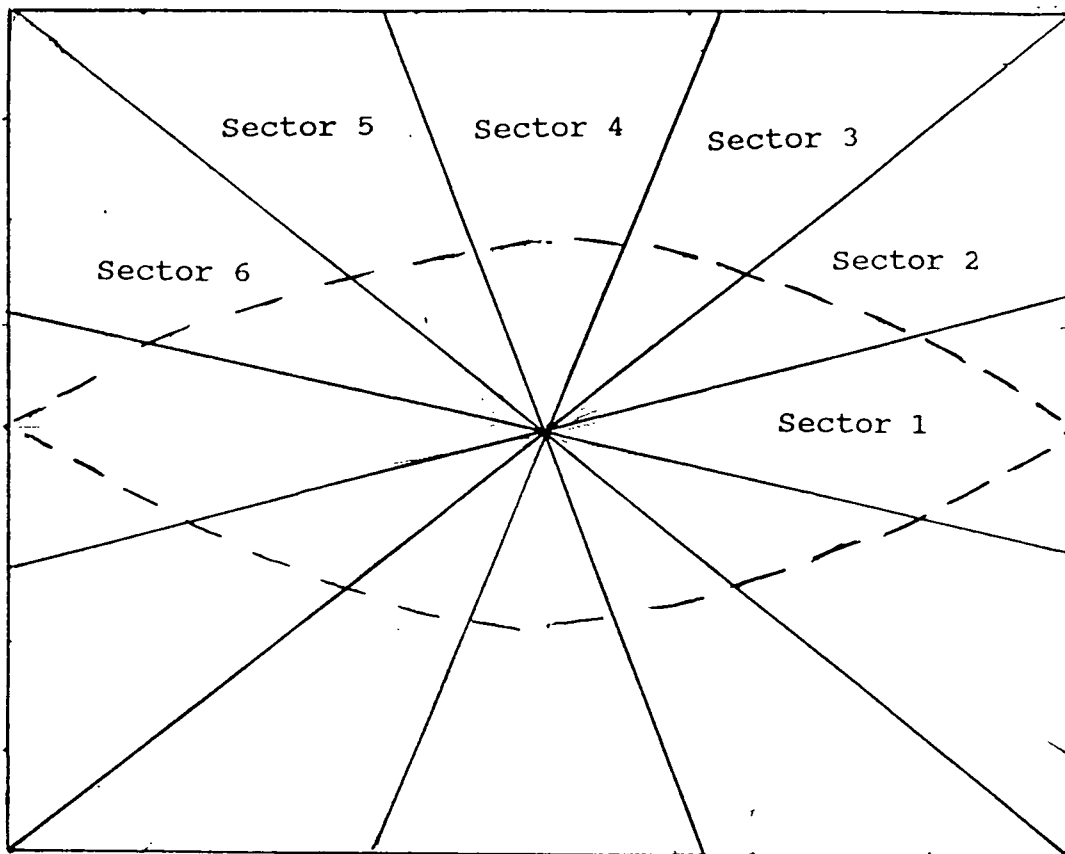


Figure 3.3.3. The Arrangement of Sectors In an Anisotropic Scatterer to be analysed at I.L.L. with 30° sectors



--- EXAMPLE CONTOUR LINE

etc. as described in Ch. 2, to obtain information regarding the effect of uniaxial extension on the central polyisoprene block by analysis of the radii of gyration and molecular weights obtained from Zimm plots for each extension ratio. Figures 3.3.4 to 3.3.10 show the scattering profiles obtained for the 'MIX' sample at each elongation ratio studied. Figures 3.3.11 to 3.3.14 show the typical Zimm plots obtained parallel and perpendicular to the stretch direction. The results obtained for the four different sectors are shown in Tables 3.3.2 to 3.3.5 respectively. From these results it is clear that, as the elongation ratio increased in the direction of the applied stress, the radius of gyration also increased but, perpendicular to the applied stress the corresponding radius of gyration decreased as the elongation ratio increased. This would appear to indicate that the affine model was applicable to the stretching of the polyisoprene molecules. The applicability of this model was tested using the equations:-

$$(Rg^{\parallel})^2 = Rg_0^2 (\lambda^{\parallel})^2$$

$$(Rg^{\perp})^2 = Rg_0^2 / \lambda^{\perp}$$

where:

$Rg^{\parallel}, Rg^{\perp}$  = calculated radius of gyration parallel and perpendicular to the stretch direction ( $\text{\AA}$ )

$Rg_0$  = calculated radius of gyration for the unstressed

Figure 3.3.4.  $I(Q)$  vs  $Q$  Scattering Profile obtained for 'MIX' Sample at Elongation Ratio 1.0 parallel to stretch direction

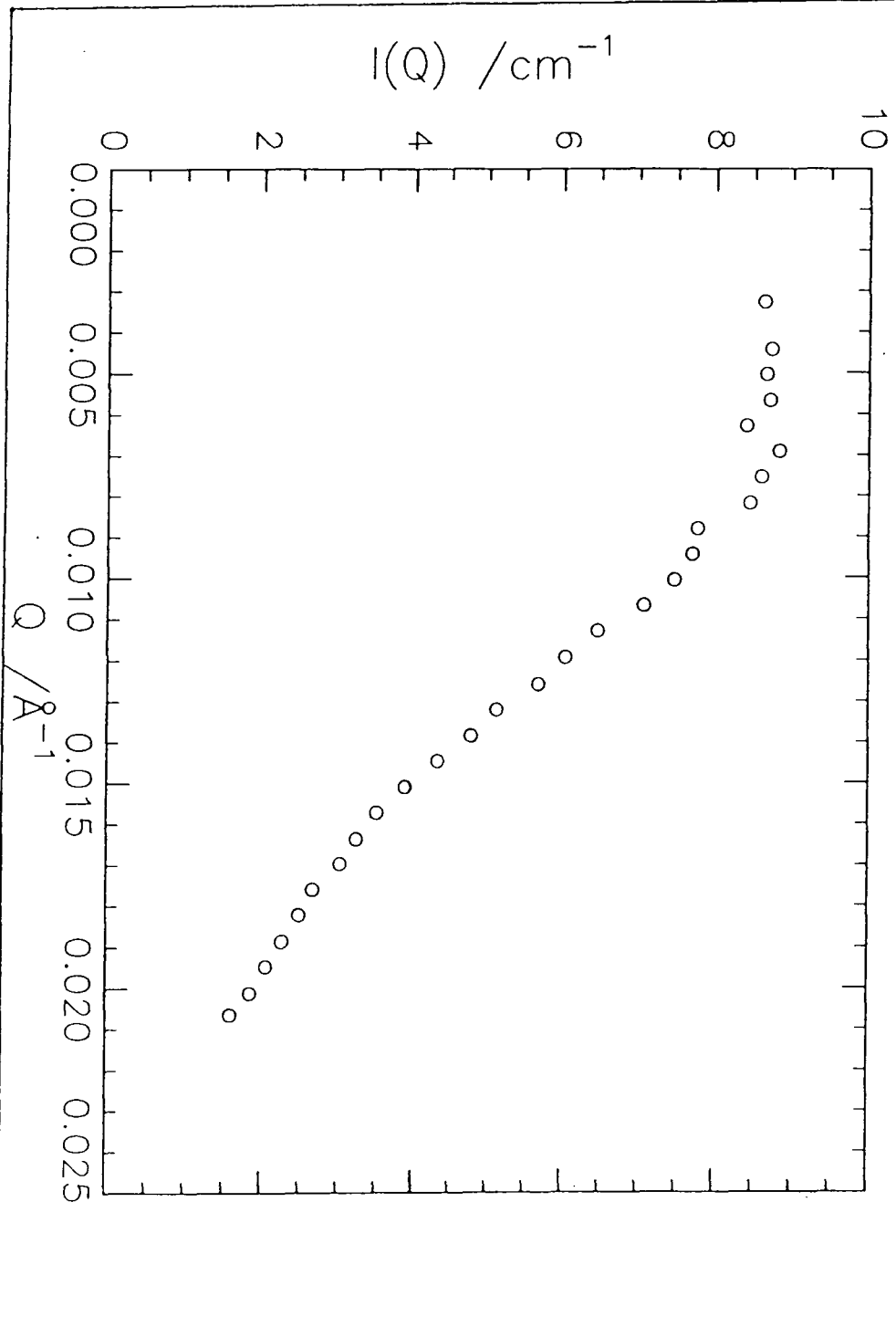


Figure 3.3.5  $I(Q)$  vs  $Q$  Scattering Profile obtained for 'MIX' Sample at Elongation Ratio 1.2 parallel to stretch direction

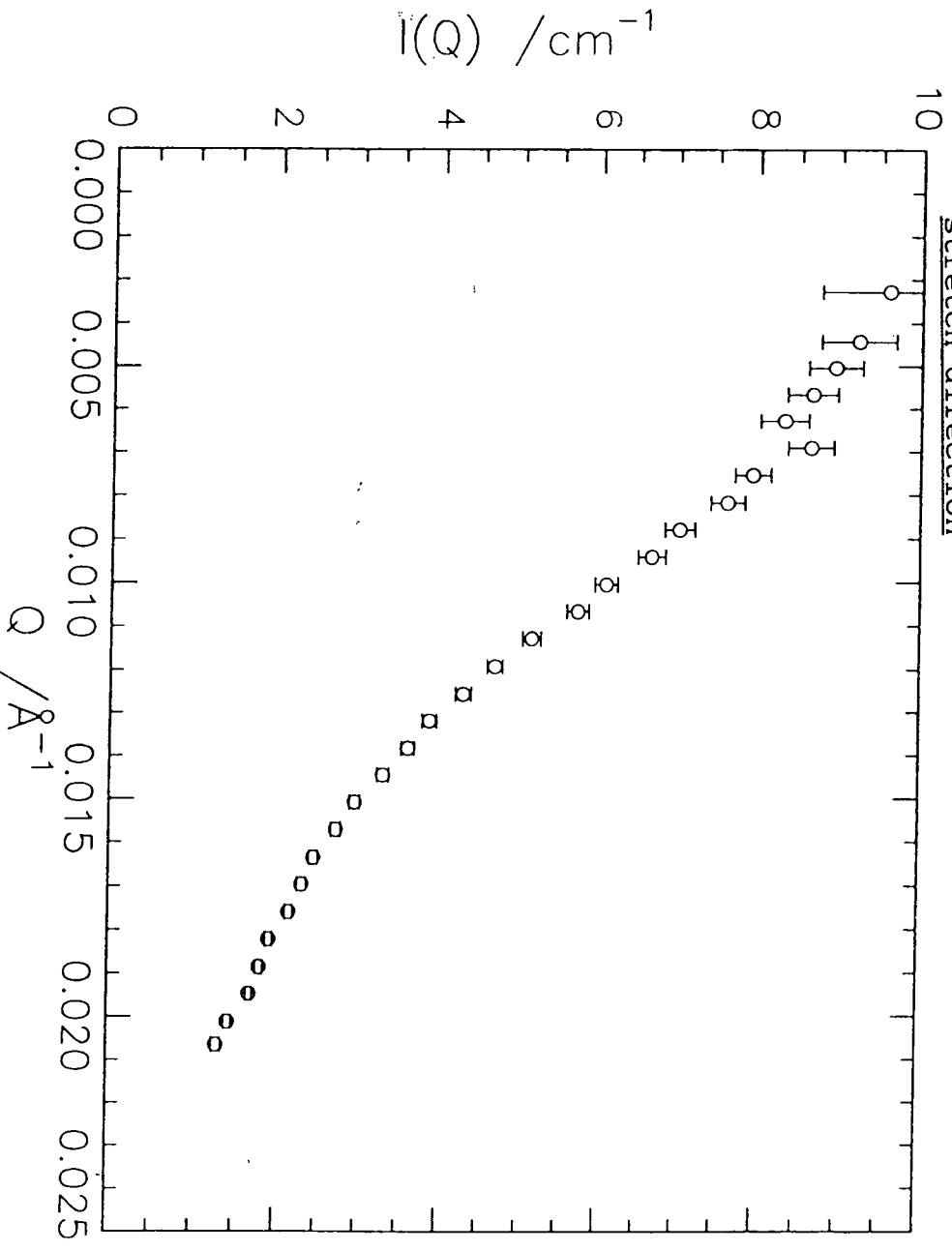


Figure 3.3.6  $I(Q)$  vs  $Q$  Scattering Profile obtained for 'MIX' Sample at Elongation Ratio 1.4 parallel to stretch direction

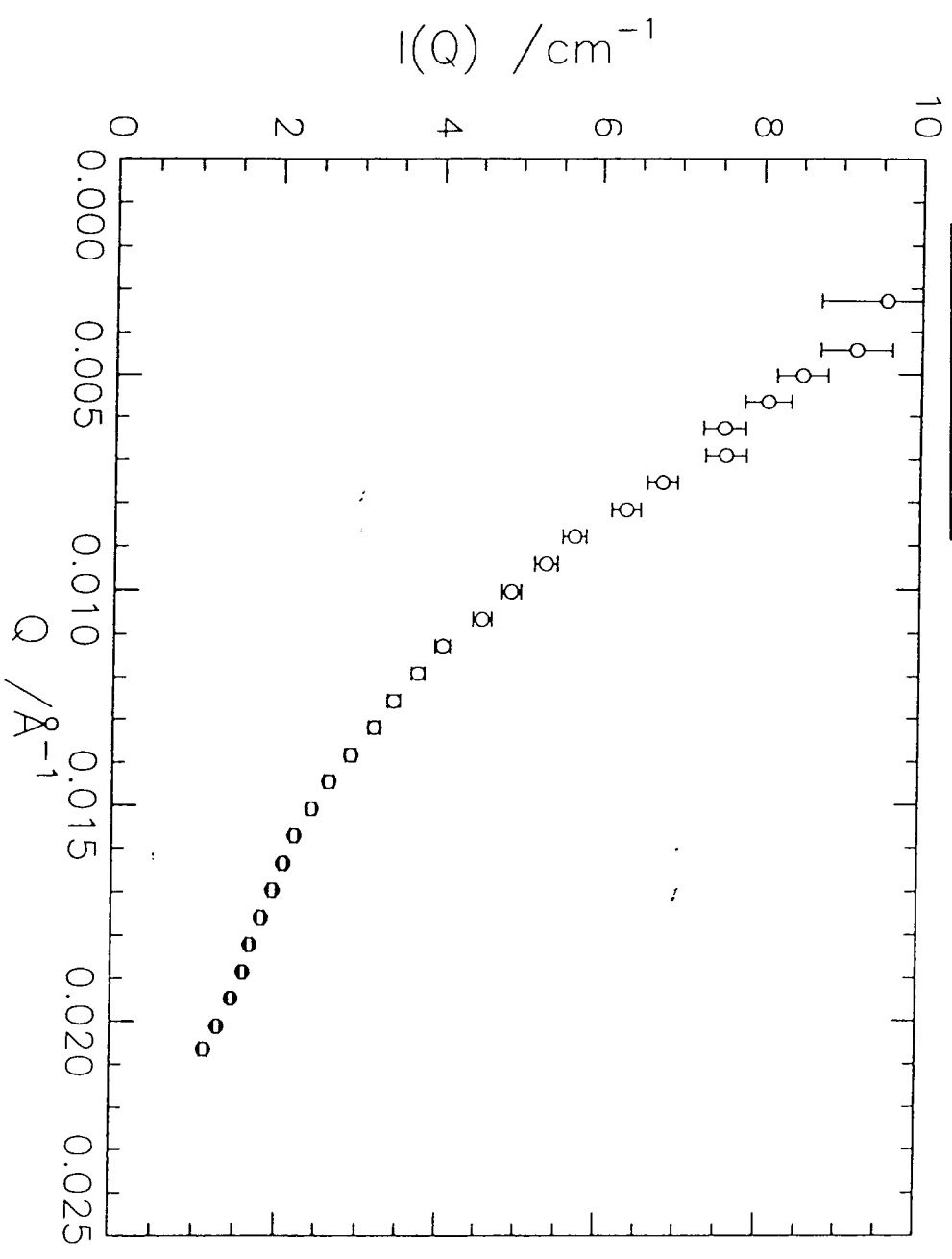


Figure 3.3.7  $I(Q)$  vs  $Q$  Scattering Profile obtained for 'MIX' Sample at Elongation Ratio 1.6 parallel to stretch direction

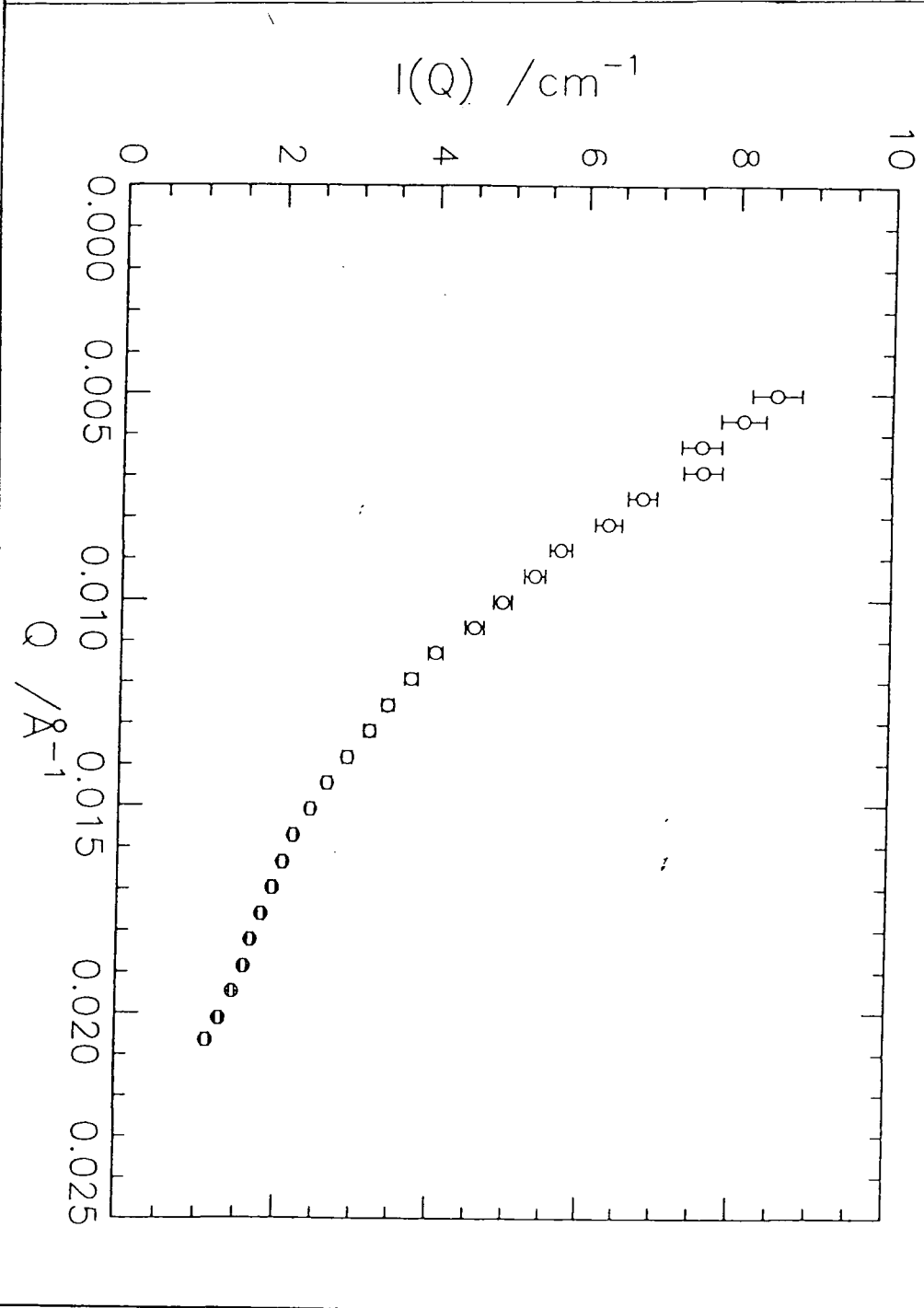


Figure 3.3.8  $I(Q)$  vs  $Q$  scattering profile obtained for 'MIX' Sample at Elongation Ratio 1.8 parallel to stretch direction

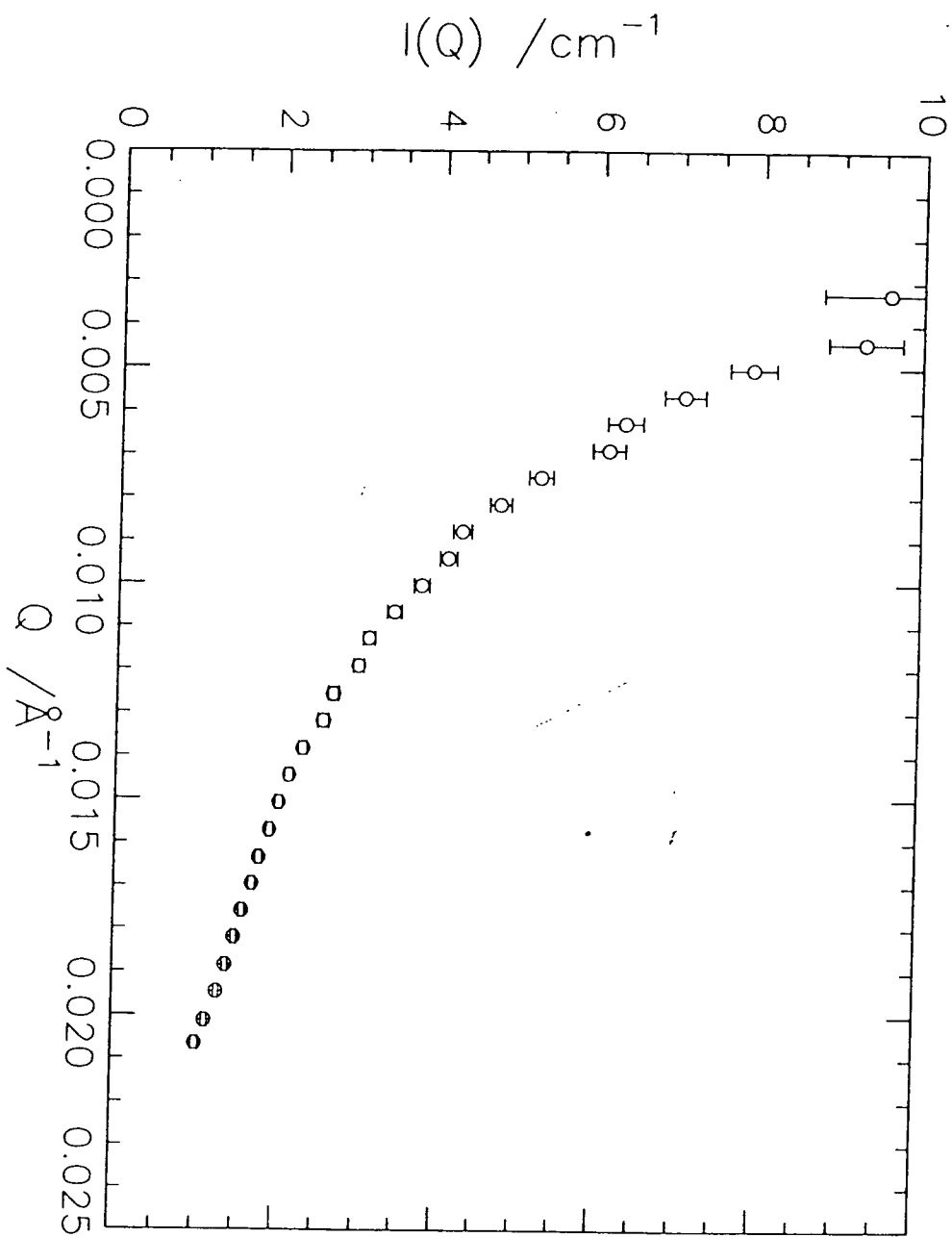


Figure 3.3.9  $I(Q)$  vs  $Q$  Scattering Profile obtained for 'MIX' sample at Elongation Ratio 2.0 parallel to stretch direction

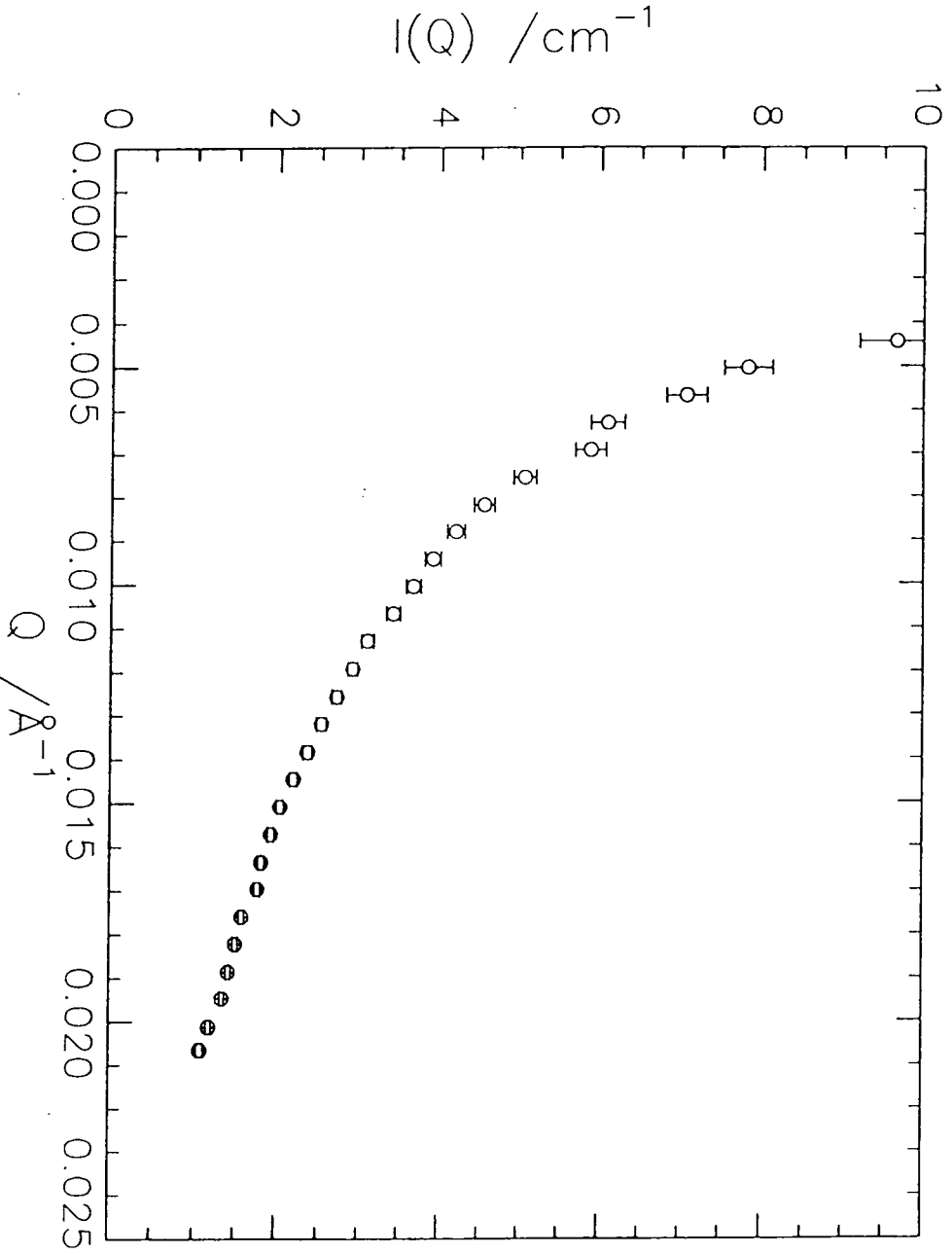


Figure 3.3.10 I(Q) vs Q Scattering Profile obtained for 'MIX' Sample at Elongation Ratio 2.2 parallel to stretch direction

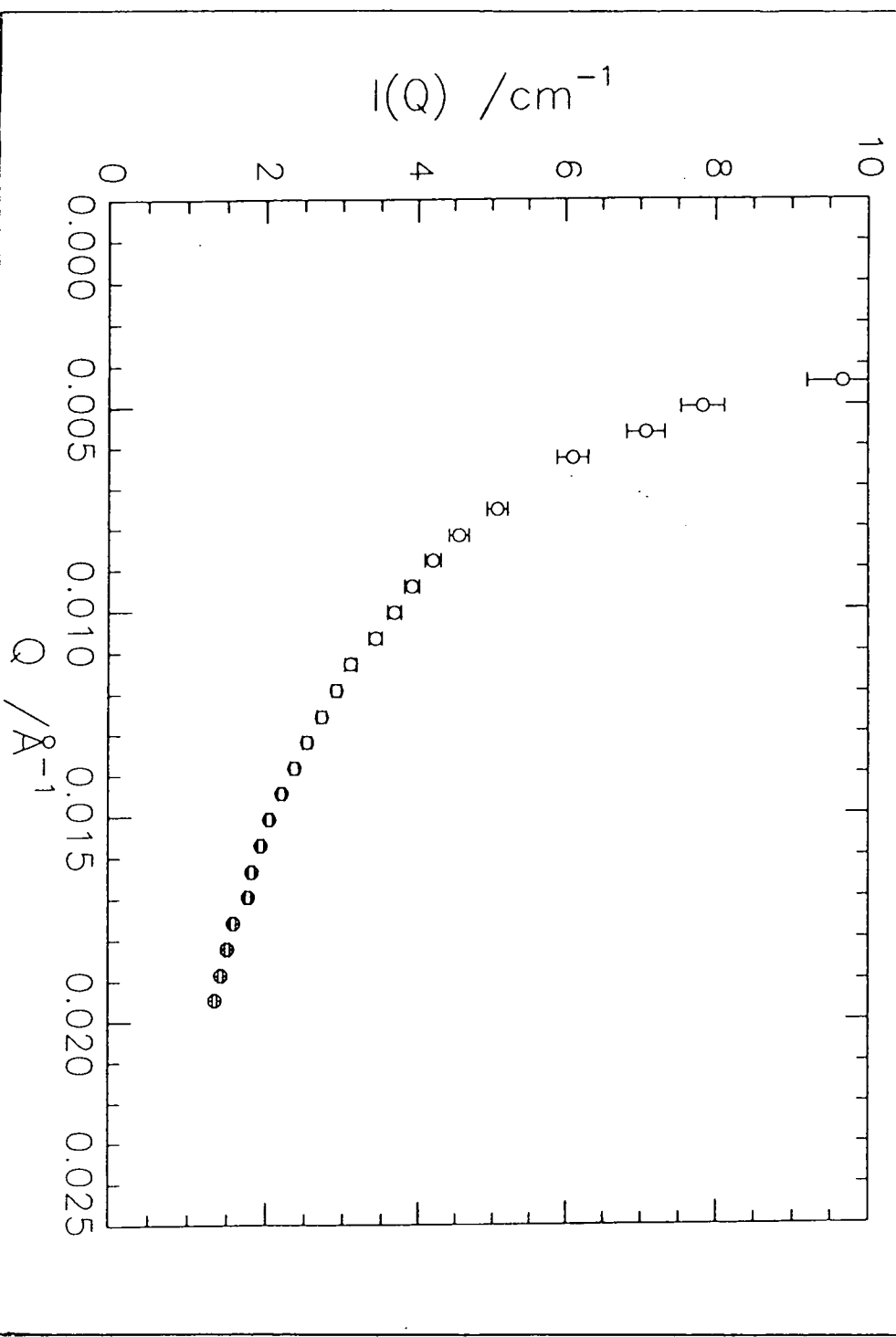


Figure 3.3.11 Zimm Plot obtained for 'MIX' Sample at Elongation Ratio 1.4 parallel to stretch direction

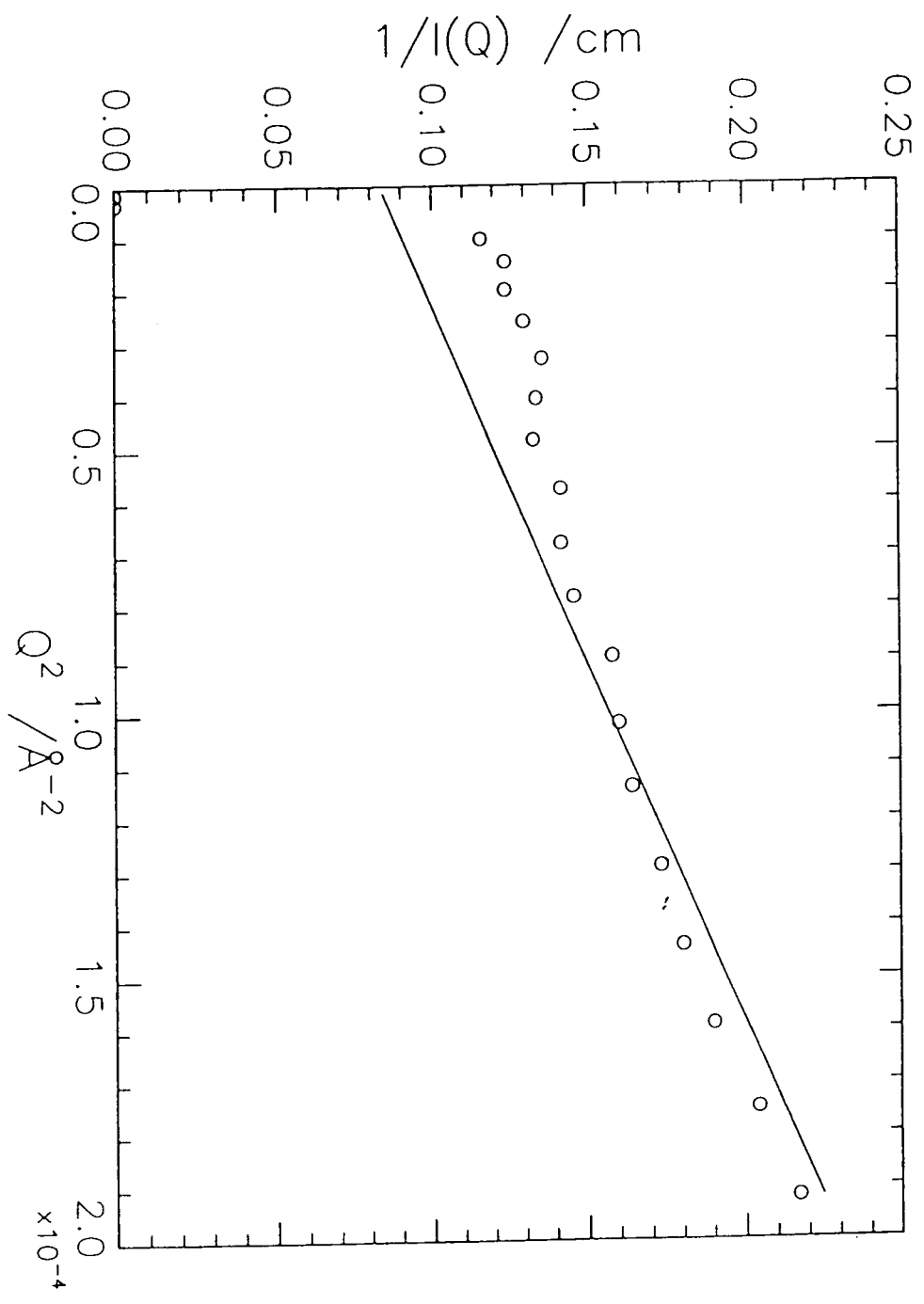


Figure 3.3.12 Zimm Plot Obtained for 'MIX' sample at Elongation Ratio 2.2 parallel to stretch direction

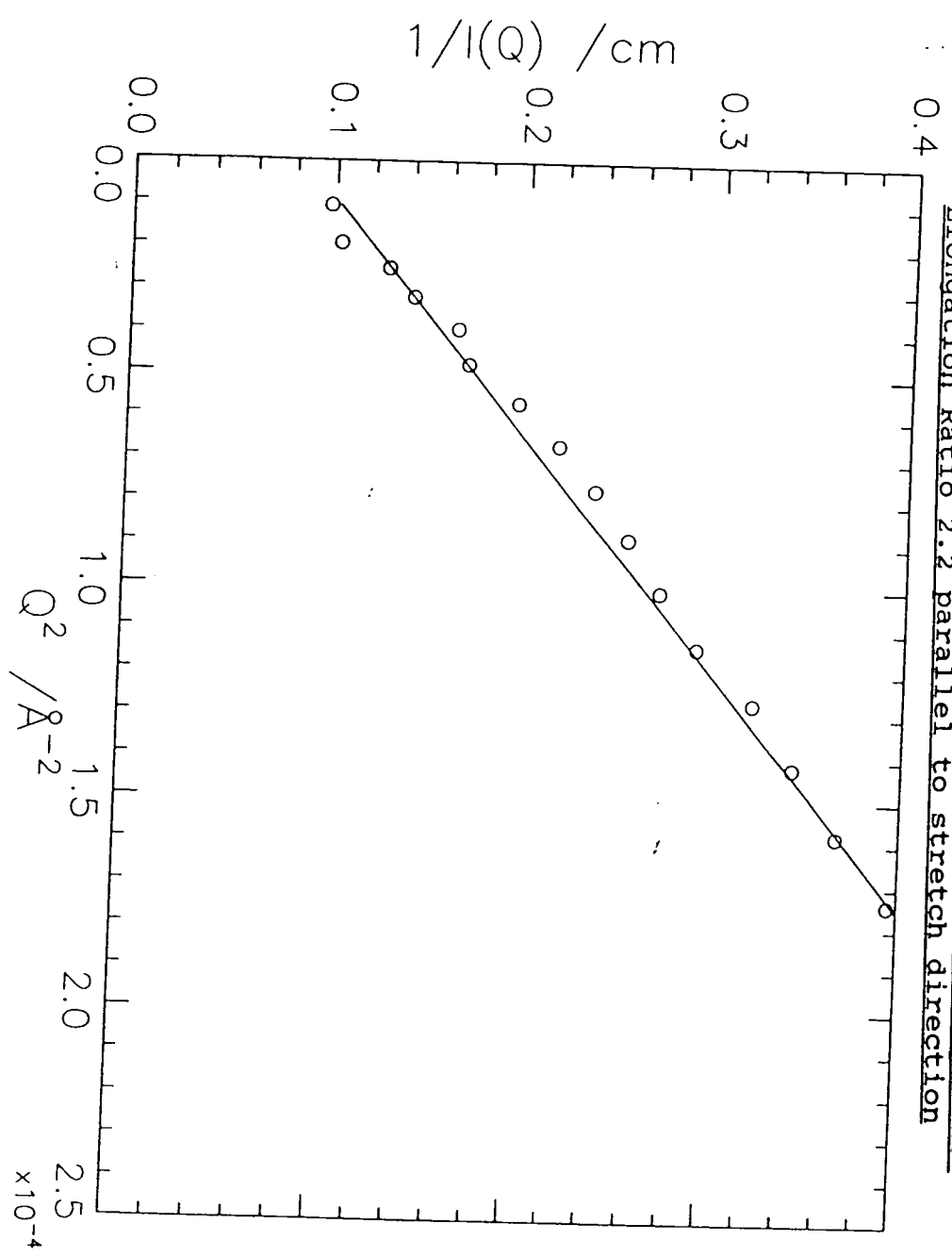


Figure 3.3.13 Zimm Plot obtained for 'MIX' sample at Elongation Ratio 1.4 perpendicular to stretch direction

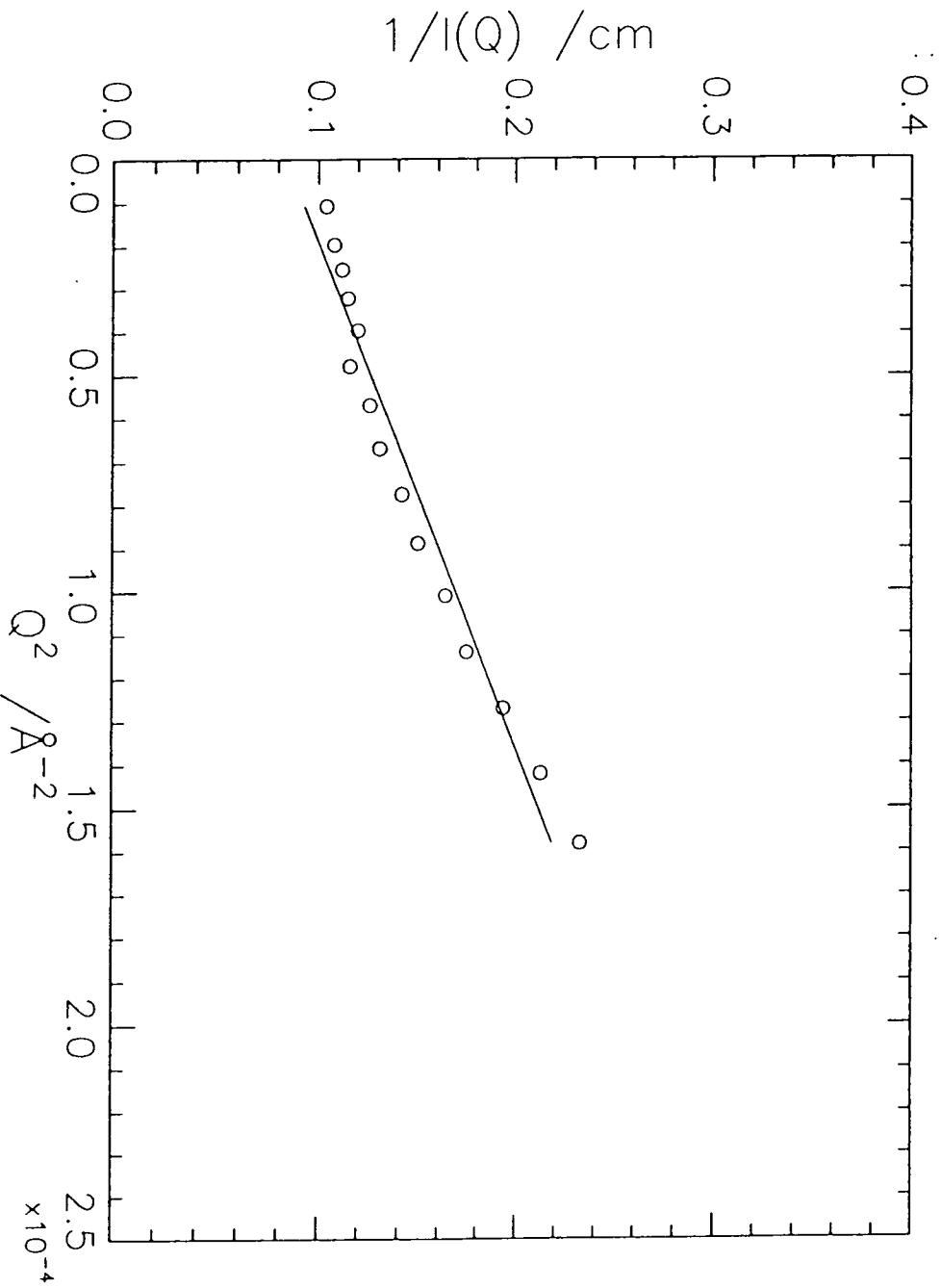
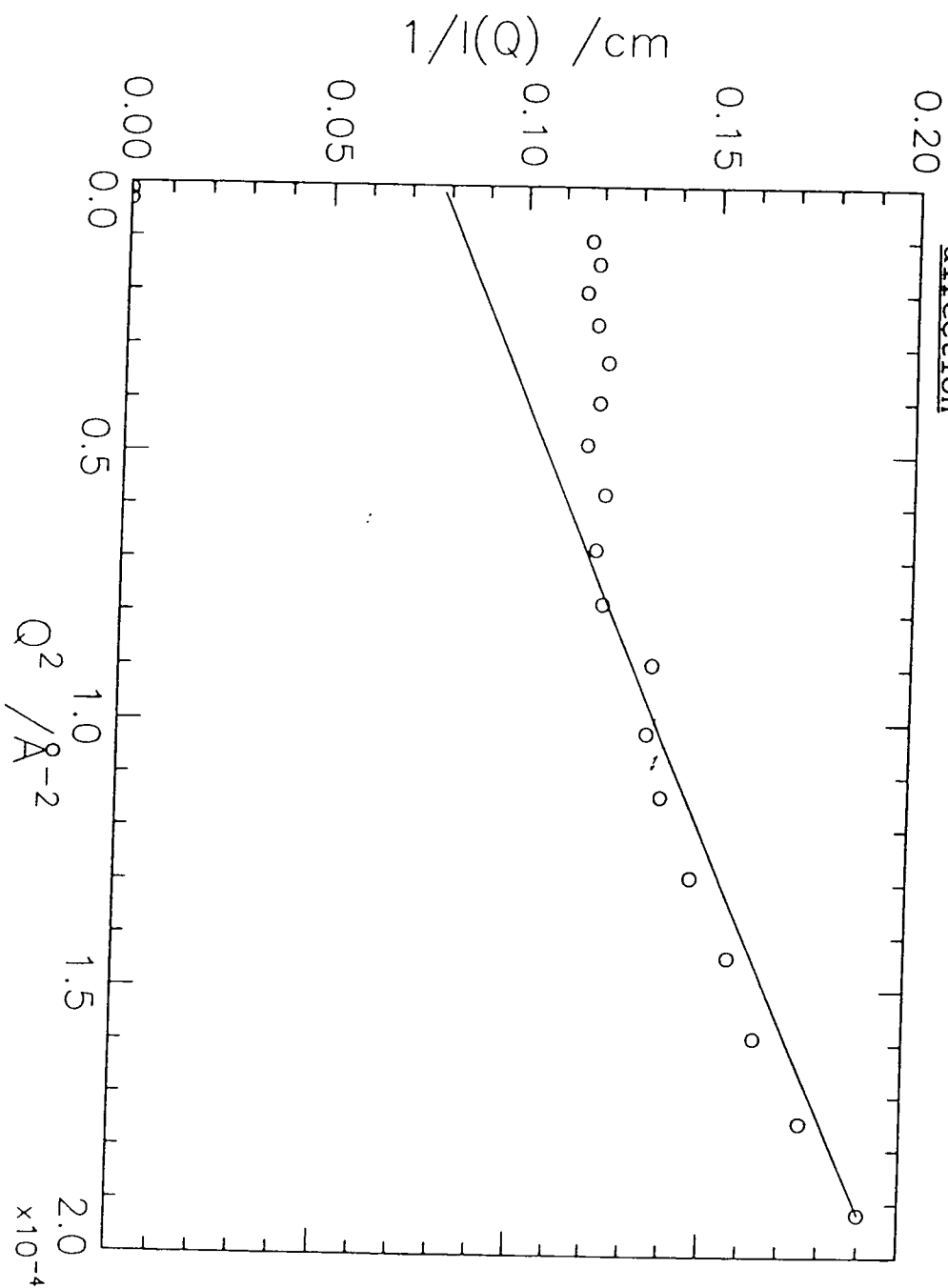


Figure 3.3.14 Zimm plot obtained for 'MIX' sample at Elongation Ratio 2.2 perpendicular to stretch direction



copolymer ( $\text{\AA}$ )

$\lambda^{\parallel}, \lambda^{\perp}$  = elongation ratio parallel and perpendicular to  
the stretch direction

These results are shown in Table 3.3.6.

Table 3.3.2. - Radii of Gyration (Rg) and Molecular Weights (M<sub>w</sub>) obtained for SPH150 series (Sector 1)

ELONGATION RATIO (λ)	Rg (Å)	M <sub>w</sub> (x10 <sup>-3</sup> )	M <sub>w</sub> (GPC) (x10 <sup>-3</sup> )
1.0	87.0 ± 4.1	101.2 ± 5.3	102.8
1.2	85.8 ± 3.9	103.6 ± 5.1	
1.4	84.1 ± 3.8	104.5 ± 5.0	
1.6	82.1 ± 4.2	103.4 ± 4.8	
1.8	78.7 ± 3.8	103.8 ± 4.5	
2.0	76.5 ± 4.1	104.3 ± 6.3	
2.2	74.4 ± 4.6	108.1 ± 4.8	

$M_w^{GPC}$  - molecular weight of polyisoprene block obtained from G.P.C. after correction similar to that undertaken for S15150 and S15150B series.

Table 3.3.3 - Radii of Gyration (Rg) and Molecular Weights (M<sub>w</sub>) obtained for SPH150 series (Sector 2)

ELONGATION RATIO ( $\lambda$ )	Rg ( $\text{\AA}$ )	M <sub>w</sub> ( $\times 10^{-3}$ )
1.0	87.4 $\pm$ 3.9	108.9 $\pm$ 6.1
1.2	89.3 $\pm$ 4.1	106.2 $\pm$ 6.3
1.4	93.1 $\pm$ 4.3	103.4 $\pm$ 5.7
1.6	97.2 $\pm$ 4.7	106.1 $\pm$ 5.9
1.8	98.3 $\pm$ 7.2	107.4 $\pm$ 7.0
2.0	100.5 $\pm$ 7.2	104.3 $\pm$ 6.9
2.2	104.2 $\pm$ 8.3	102.6 $\pm$ 5.8

Table 3.3.4 - Radii of Gyration (Rg) and Molecular Weights (M<sub>w</sub>) obtained for SPH150 series (Sector 3)

ELONGATION RATIO, (λ)	Rg (Å)	M <sub>w</sub> x10 <sup>-3</sup>
1.0	89.4 ± 4.4	109.0 ± 5.3
1.2	97.5 ± 5.0	107.4 ± 5.1
1.4	110.6 ± 6.4	104.9 ± 5.2
1.6	137.1 ± 8.1	106.6 ± 6.7
1.8	151.5 ± 9.8	100.5 ± 5.8
2.0	170.9 ± 11.3	105.6 ± 5.5
2.2	190.3 ± 13.5	108.3 ± 6.4

Table 3.3.5 - Radii of Gyration (R<sub>g</sub>) and Molecular Weights (M<sub>w</sub>) obtained for SPH150 series (Sector 4)

ELONGATION RATIO ( $\lambda$ )	R <sub>g</sub> (Å)	M <sub>w</sub> (x10 <sup>-3</sup> )
1.0	93.6 ± 5.5	108.1 ± 4.7
1.2	108.5 ± 6.1	102.4 ± 4.9
1.4	125.7 ± 7.5	102.1 ± 5.8
1.6	148.6 ± 9.9	105.1 ± 5.4
1.8	179.3 ± 11.0	108.3 ± 5.5
2.0	195.1 ± 13.4	108.1 ± 5.7
2.2	204.3 ± 15.8	100.4 ± 5.9

Table 3.3.6 - Radii of Gyration parallel, (Rg<sup>||</sup>) and perpendicular, (Rg<sup>⊥</sup>) to the stretch direction and the corresponding affine radius of gyration (Rg<sup>affine</sup>)

ELONGATION RATIO ( $\lambda$ )	Rg <sup>  </sup> (Å)	Rg <sup>affine</sup> (Å) (Parallel)	Rg <sup>⊥</sup> (Å)	Rg <sup>affine</sup> (Å) (Perpendicular)
1.0	93.6 ± 7.9	93.6	87.0 ± 6.0	87.0
1.2	108.5 ± 8.3	112.3	85.8 ± 6.2	79.4
1.4	123.7 ± 8.7	131.0	84.1 ± 6.0	73.5
1.6	148.6 ± 9.5	150.0	82.1 ± 6.1	68.6
1.8	179.3 ± 11.6	168.5	78.7 ± 5.9	64.8
2.0	195.1 ± 13.5	187.2	76.5 ± 5.7	61.5
2.2	204.3 ± 16.0	205.9	74.4 ± 5.8	58.7

NOTE: The values of  $Rg^{\text{affine}}$  parallel and perpendicular in Table 3.3.6. was based on that calculated from this data at elongation ratio 1.0 rather than any theoretical equations.

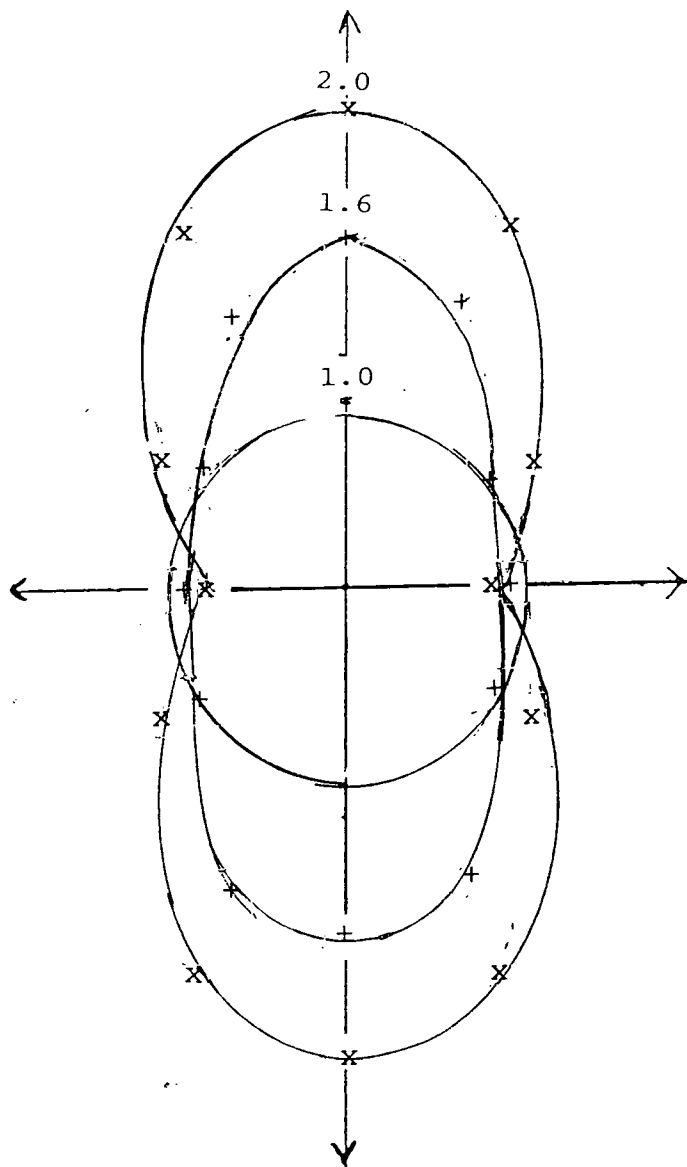
From Table 3.3.6. it can be concluded that the stretching was affine for the SPH150 series up to elongation ratio 2.2 parallel to the stretch direction but not in the direction perpendicular to the stretch direction.

These results are in complete contrast with those obtained using the S15150 and S15150B series which showed that samples simply relaxed during elongation. Since this experiment was only carried out on the D11 Spectrometer at I.L.L., it was not possible to obtain Kratky plots to examine the effects of elongation at higher  $Q$  values due to the narrow  $Q$  range of the instrument used. The results obtained for the radii of gyration showed that the unextended radii of gyration was similar for each sector i.e. there was no residual stress on the sample.

The radii of gyration showed an increase as the elongation ratio increased gradually from Sector 1 to Sector 4. These results were used to draw the distribution of segments in the scattering ellipsoid (Figure 3.3.15) for extension ratios 1.0, 1.6 and 2.0 which clearly demonstrates the changes in shape of the polyisoprene blocks.

The data obtained for SPH150 samples were used to

Figure 3.3.15 - Scattering Distribution of segments in SPH150 sample at elongation ratios 1.0, 1.6 and 2.0

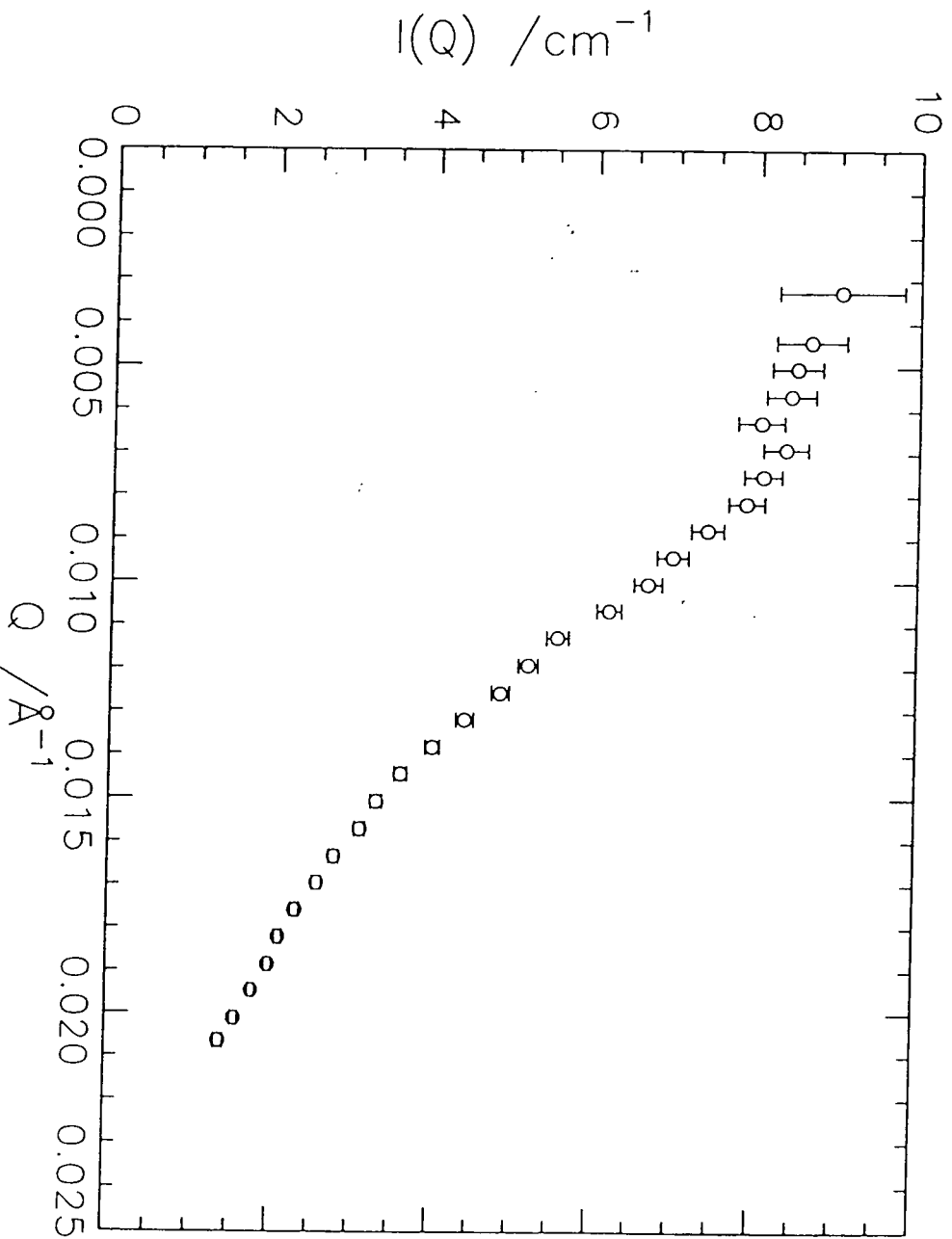


determine the molecular weight of the deuterated polyisoprene part of the SPH150 series and compare this to the corrected result obtained from G.P.C. measurement. The calculated molecular weights from SANS are very close to those obtained from G.P.C. and so it may be concluded that the deuterioisoprene is randomly distributed in the triblock copolymer. This is a similar result to that obtained for the S15150 and S15150B series.

The molecular weight of the deuterated SPH150 sample shown in Table 3.3.1 was, however, 25% greater than that of the Hydrogenous and Random SPH150 samples. Consequently, the molecular weight match for the 'MIX' SPH150 sample was not as good as that obtained for either the S15150 or S15150B 'MIX' samples. The polydispersity  $M_w/M_n$  for all SPH150 samples were, on the other hand, very similar. The scattering profile obtained for the 'MIX' sample of SPH150, (Figure 3.3.16), showed that the 'contrast-matching' technique had been successful due to the absence of Bragg peaks associated with the ordering of polystyrene blocks and in this case, the importance of matching the molecular weights of the Hydrogenous and Deuterated samples was small.

In summary the SPH150 series gave different results to those obtained from the S15150 and S15150B series

Figure 3.3.16  $I(Q)$  vs  $Q$  Plot Obtained for 'MIX'  
SPH150 Sample at Elongation ratio 1.8 on D11  
Instrument, I.L.L.



though the total molecular weights of these samples were in the same region as that of the SPH150.

Though the results obtained for the SPH150 series were different they were much closer to what had been previously expected. The scattering profile did become anisotropic as the 'MIX' sample was deformed. However, analysis of the radii of gyration at each elongation ratio parallel and perpendicular to the stretch direction revealed that deformation in the sample could be described as affine parallel to the applied stress and non-affine perpendicular to the applied stress.

#### 3.3.4. Discussion

Since the SPH150 sample was only studied on the D11 instrument at the I.L.L., the scope of discussion on the results obtained is limited. The relatively small  $Q$  range covered meant that the Kratky plots for this sample did not cover the  $Q$  range required to determine if the SPH150 sample followed the classical Kratky profile, or deviated in some way from this. Despite this limitation the results obtained for SPH150 samples were of great interest.

The anisotropic nature of the scattering data obtained for the SPH150 sample was not unexpected. The affine nature of the scattering data parallel to the stretch direction, however, was.

The earliest SANS studies of deformation of polymers were carried out on homopolymers. Picot et al<sup>23</sup>

uniaxially deformed a sample of hot stretched polystyrene and found that at elongation ratios below 1.7 affine deformation was the dominant mechanism. At elongation ratios greater than 3.0, however, the affine model did not hold. These results were accounted for by using a model where affine behaviour held only for distances separating effective cross-links. Boué et al<sup>24</sup> found that the transverse coil radius of gyration of a hot stretched linear polystyrene was affine in behaviour, up to an elongation ratio of 10.0 for an extrusion oriented high molecular weight polystyrene ( $M_w \approx 500000$ ) though for lower molecular weights the deformation was less than affine.

From the above examples it is clear that there have been some experiments carried out using SANS on homopolymers that have found affine behaviour on deformation.

Alongside these SANS studies deformation was studied in polymer systems using polymers swollen in solvents and the radii of gyration in these equilibrated systems was measured. Davidson<sup>20</sup> carried out a series of swelling experiments on polystyrene gels swollen in cyclohexane and found little variation in polymer dimensions up to volumetric swellings of 30 times that of unswollen polymer and Bastide et al<sup>28</sup> studied polystyrene networks swollen in benzene up to a volumetric swelling of 17.4. Bastide et al obtained

similar results to those of Davidson and interpreted them as supporting the disinterpenetration theory that chain dimensions were determined by local interactions ie. excluded volume effects.

As well as obtaining some results which appeared to support the affine model on deformation of a polystyrene homopolymer<sup>23,24</sup>, other workers found conflicting results when working on the same polymer system Clogh et al<sup>26</sup> studied polystyrene samples that had been cross-linked using  $\gamma$ -radiation, then stretched at 418K to elongation ratios of 2.3.

These results showed that the calculated radii of gyration in the direction of stretch were in good agreement with the phantom network approach but perpendicular to the stretch direction were consistent with the end-to-end pulling theory. These results all show that for homopolymer systems, particularly polystyrene, all the various theories of rubber elasticity have some support depending on the molecular weight of the polymer studied and the temperature at which the experiment is carried out.

For a block copolymer system, however, where there is a more complex arrangement of molecules the simple affine model would not appear to be the appropriate one. Previous work<sup>26</sup> has shown that the affine model may only be applicable to polymer networks where the deformation of the sample is carried out at temperatures close to the glass transition

temperature.

The classical theories of rubber elasticity predict that the phantom model or the end-to-end pulling models would be the most appropriate for describing the effect of deformation on a triblock copolymer of poly(styrene-isoprene-styrene). Relatively few papers on the study of block copolymers using SANS have been published.

Richards and Mullin<sup>27</sup> studied the effect of deformation on a poly(styrene-isoprene-styrene) triblock copolymer where the polystyrene blocks were examined and found that none of the classical theories of rubber elasticity applied to the data obtained. The polystyrene was arranged in cylindrical domains in this study with a total molecular weight of 120000 which is very similar to the S15150B series studied as part of this thesis.

From the results obtained by other workers as detailed previously it is clear that the affine nature of the data obtained parallel to the direction of the uniaxial stress is unique. In the direction perpendicular to the applied stress the results are less than affine and closely approximate the junction affine model which would be closer to that expected from theoretical considerations.

Comparison of the results obtained for the SPH150 series and the S15150 and S15150B series is limited by two facts. Firstly, the latter were synthesised in

the laboratory by this author, whereas the SPH150 series were synthesised by an outside agency. The deuterioisoprene used to synthesise the SPH150 samples was also from a different source to that used to synthesise the S15150 and S15150B samples. Secondly, the morphologies of the SPH150 and the S15150/S15150B samples were different. The S15150 and S15150B samples were triblock copolymers with cylindrical polystyrene domains arranged on a hexagonally close packed array whereas the SPH150 samples had spherical polystyrene domains arranged on a cubic lattice. The response of the spherical polystyrene domain would be quite different to that of the cylindrical domains on uniaxial extension since considerable alignment could occur in the cylindrical system but not in the case of the spherical system. In addition spherical polystyrene regions are ductile and deform in response to stress.

Despite these limitations some comparisons are possible and these have been described earlier.

#### 3.3.5. Future Work

The immediate task for the SPH150 series would be to obtain results at larger  $Q$  values to enable a Kratky plot to be drawn and get a fuller understanding of the deformation process in this sample. Kratky plots have been made from the results obtained using the D11 Spectrometer (Figure 3.3.17 and 3.3.18), but do not reach sufficient  $Q$  values to draw any conclusions.

Figure 3.3.17 Kratky Plot Obtained for 'MIX' SPH150  
Sample at Elongation Ratio 1.0 on D11 Instrument,  
I.L.L.

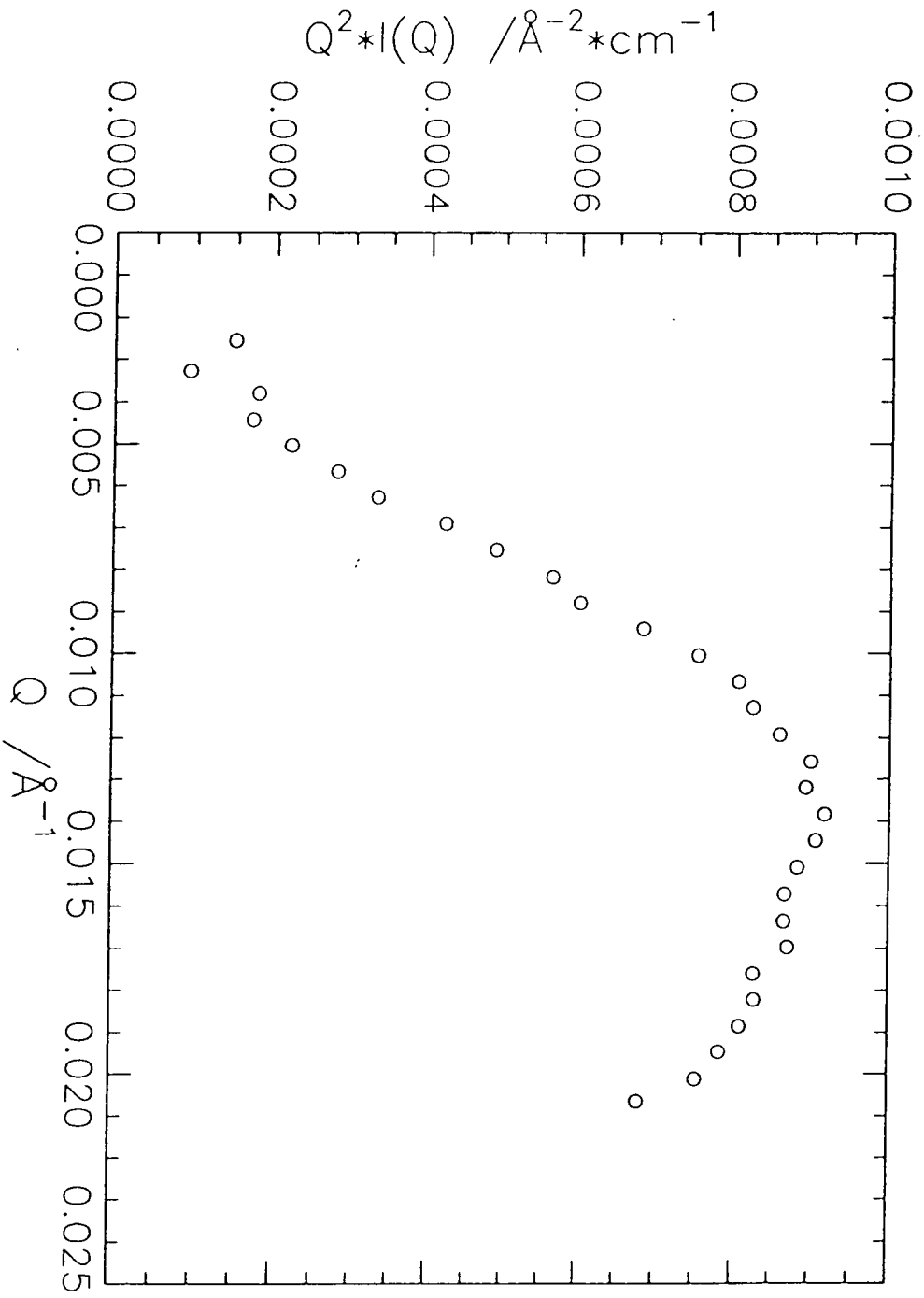
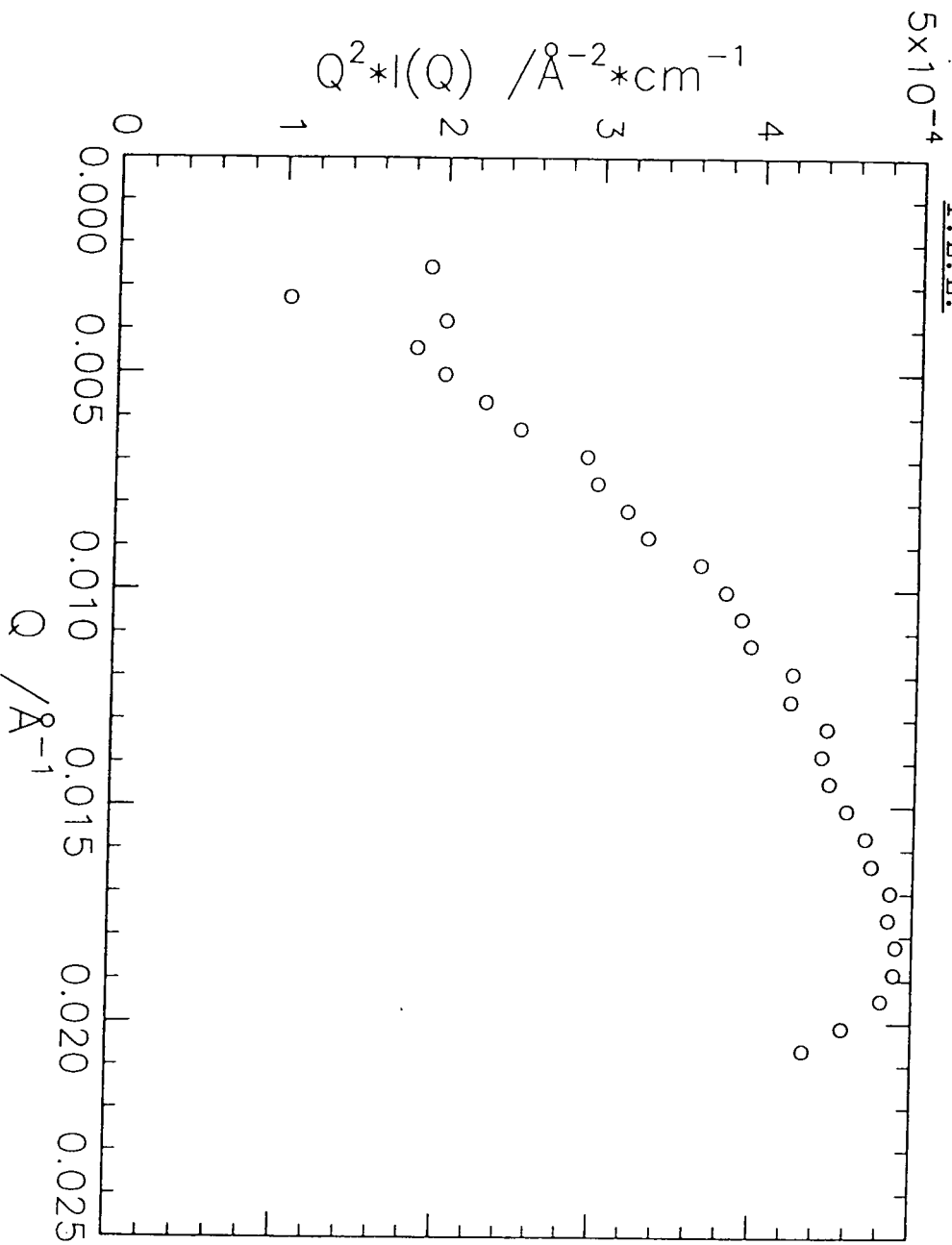


Figure 3.3.18 Kratky Plot Obtained for 'MIX' SPH150  
Sample at Elongation Ratio 2.0 on D11 Instrument,  
I.L.I.



The extension ratios covered for the SPH150 series were limited to a maximum of 2.2 due to the equipment used. This is a relatively small extension ratio range and future work should seek to examine the effect on the spherical polystyrene domains in the SPH150 sample at much greater extension ratios to ascertain if the affine nature of the deformation up to 2.2 parallel to the stretch direction, in particular, still holds.

### 3.4. SANS Study of Extruded S15150 Samples

#### 3.4.1. Introduction

The study of unextruded S15150 samples at various elongation ratios has been described in Ch. 3.1. In conjunction with this study it was decided to use some of the S15150 triblock copolymers in a study of extruded copolymer systems subjected to uniaxial extension.

The main purpose of extrusion in a triblock copolymer is to uniaxially align the polystyrene domains. This is achieved by extruding the block copolymer melt through a narrow orifice. The result is a 'single crystal' block copolymer similar to that described by Folkes and Keller<sup>17</sup>. In such oriented systems the lattice plane separation has been found not to be at the equilibrium values predicted by statistical thermodynamic theory<sup>29,30,31</sup> which were observed experimentally on solution cast samples<sup>2,32</sup>. This leads to the question of the effect on the configuration of the isoprene blocks in a poly(styrene-isoprene-styrene) triblock copolymer which was being deformed. As a result S15150 samples were extruded using the apparatus shown in Ch. 2, Figure 2.1.7. to determine unambiguous radii of gyration parallel and perpendicular to the stretch direction.

#### 3.4.2. Experimental

The extruded S15150 samples were prepared as described in Ch. 2. The extruded samples appeared more elastic

than their unextruded solution-cast equivalents and were not tacky in texture. Due to limitations in the extrusion apparatus, it was only possible to obtain samples 3cm length x 1cm depth x 2cm width. The major problem associated with the experiment was the tacky nature of the triblock copolymer which made it adhere strongly to the metal wall of the extrusion apparatus and consequently prevent large samples of extruded material being synthesised. Attempts were made to alleviate this problem by spraying the walls of the extrusion apparatus with a non-stick spray but this had limited success and time restraints prevented further solutions being sought. The extruded S15150 samples were studied on the D11 Spectrometer, I.L.L.. The samples were placed in the stretching frame and aligned in the beam as described previously for S15150 and S15150B samples. The 'Random' extrudate was used as a background sample and subtracted from the 'MIX' Extrudate scattering.

Due to sample limitations it was possible to examine the samples at elongation ratios 1.0 and 1.1 only.

#### 3.4.3. Results and Discussion

The SANS results obtained for the extrudate samples show the anisotropic nature of the data clearly (Figure 3.4.1 and Figure 3.4.2.). These figures also show, however, that the alignment of the cylindrical polystyrene domains was not parallel to the extrusion direction as had been expected. These domains appear

Figure 3.4.1. Contour Plot Obtained for Extruded  
515150 Sample at Elongation Ratio 1.0

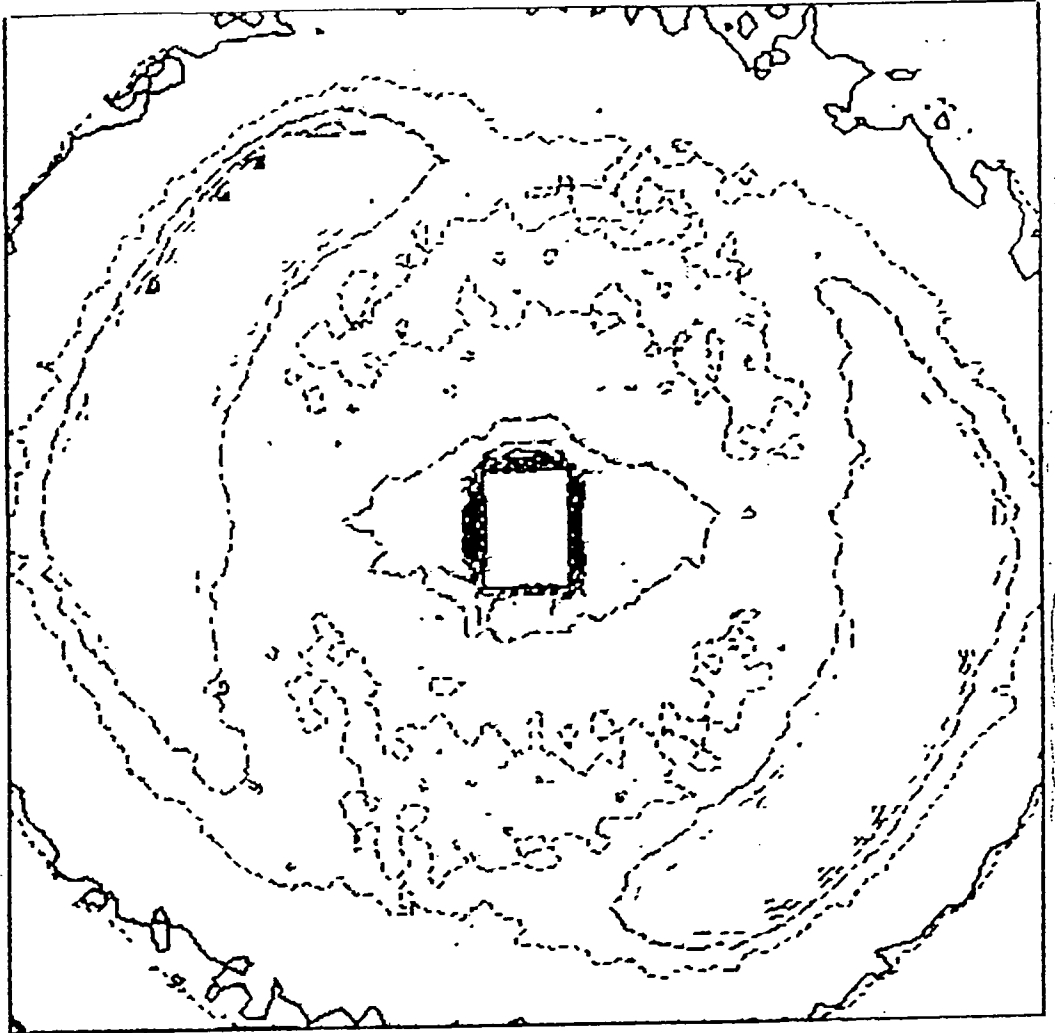
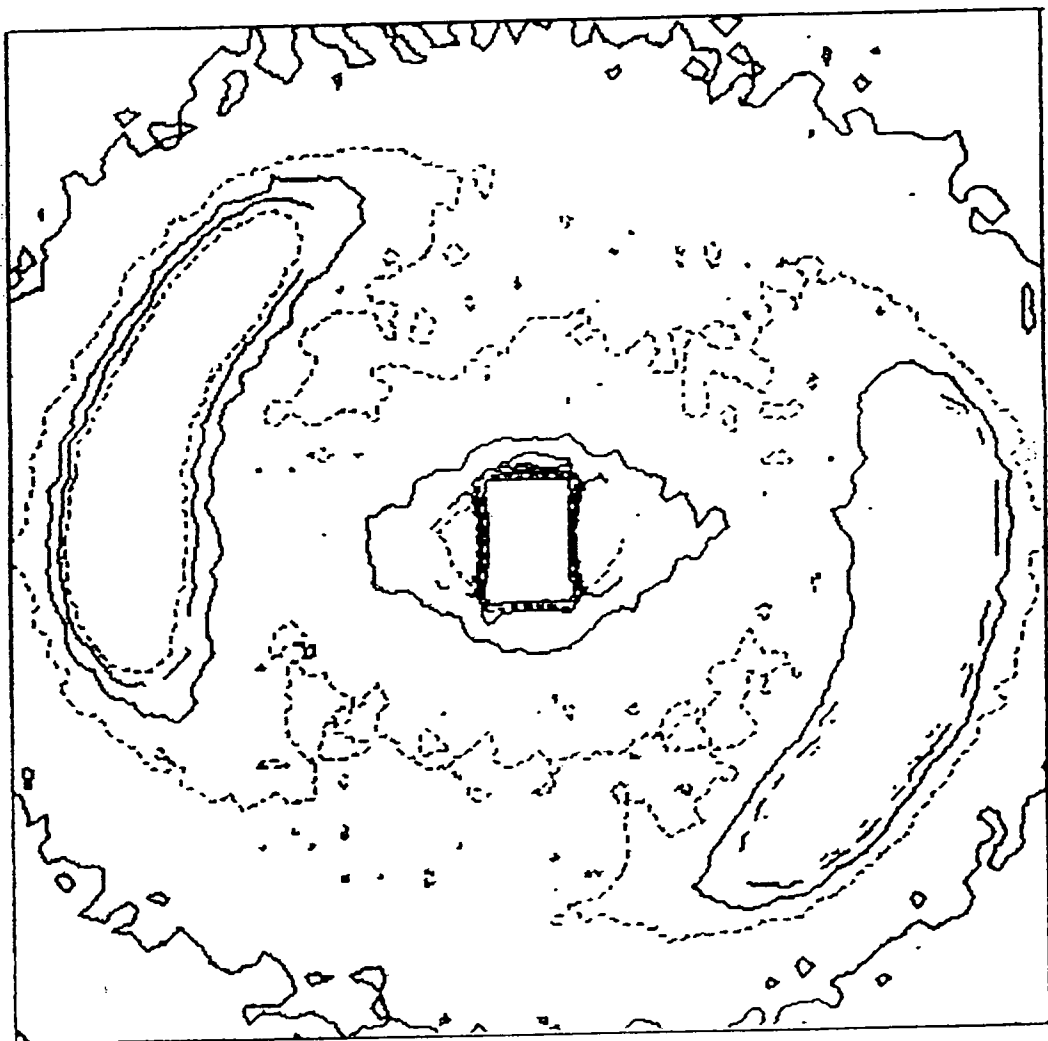


Figure 3.4.2. Contour Plot Obtained for Extruded  
S15150 Sample at Elongation Ratio 1.1



to have aligned slightly off parallel to the direction of extrusion which can be explained by the limitations of the extrusion apparatus. When the weight was applied to the piston to extrude the molten block copolymer as described in Ch. 2. there was some lateral movement in the piston which meant the weight was not applied directly downwards but some degrees off this.

The scattering data obtained, being anisotropic, was corrected and studied in sectors similar to that described for the SPH150 series previously (Ch. 3.3). The  $I(Q)$  vs.  $Q$  profiles for each sector were plotted for elongation ratio 1.1, (Figure 3.4.3 to 3.4.6.), and showed the presence of a Bragg peak at  $Q \approx 0.03 \text{ \AA}^{-1}$  in all sectors though of varying intensity. The presence of this Bragg peak made it difficult to determine radii of gyration,  $R_g$ , and molecular weights  $M_w$  from Zimm plots. The Bragg peak was least well resolved in the direction parallel to the applied stress and so a Zimm plot was made for data obtained in this sector, and  $R_g$ ,  $M_w$  were calculated (Figure 3.4.7.) for the extrudate at elongation ratio 1.1. The value of  $R_g$  obtained was  $87.3 \pm 5.7 \text{ \AA}$  and the  $M_w$  was  $(31.1 \pm 2.8) \times 10^3$ . The calculated  $M_w$  from SANS was similar to that obtained from G.P.C. measurement indicating that the deuterioisoprene was distributed randomly throughout the copolymer system. The bragg

Figure 3.4.3.  $I(Q)$  vs  $Q$  Scattering Profile obtained for Extruded S15150 at Elongation Ratio 1.1, Sector 1

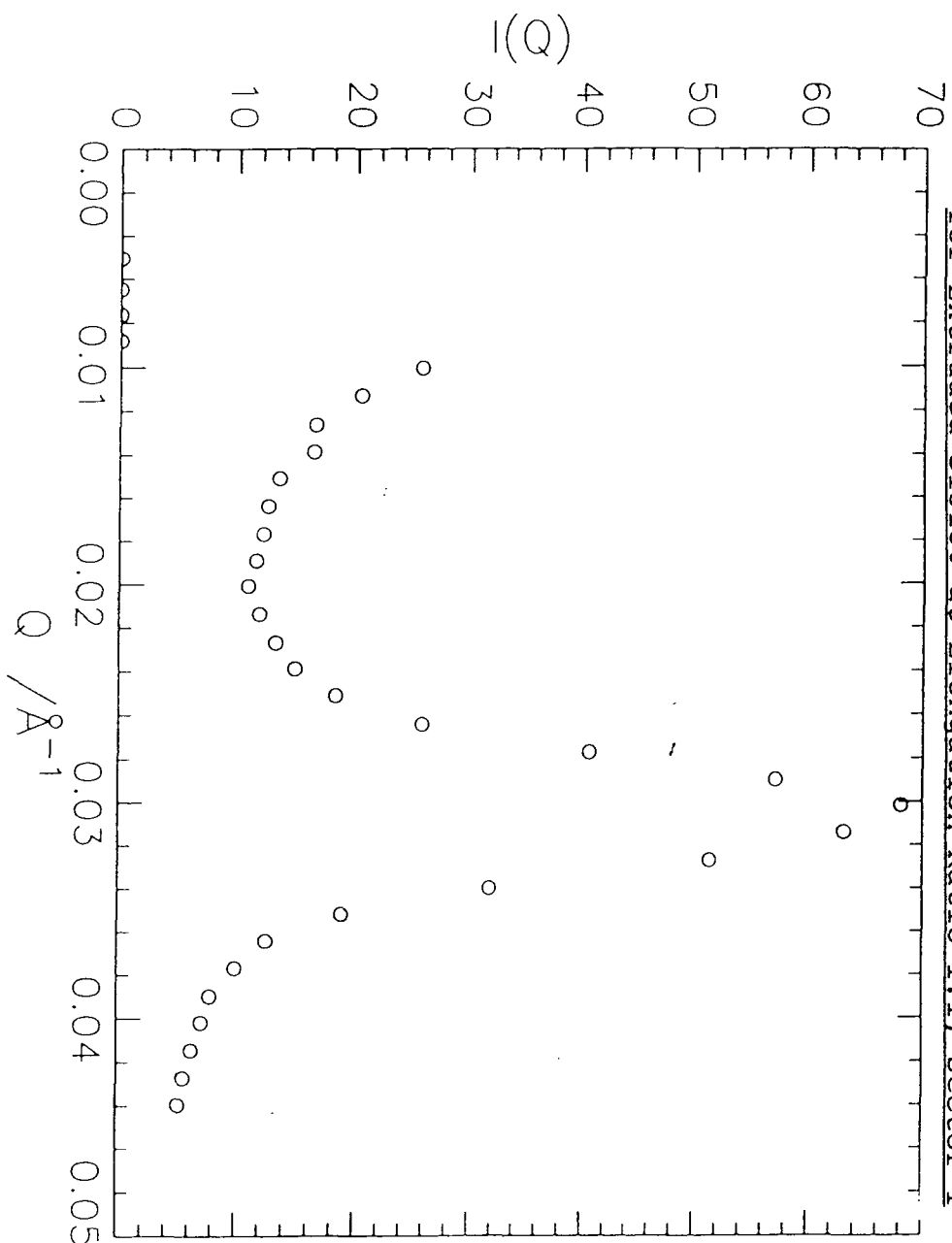


Figure 3.4.4.  $I(Q)$  vs  $Q$  Scattering Profile Obtained for Extruded S15150 at Elongation Ratio 1.1, Sector 2

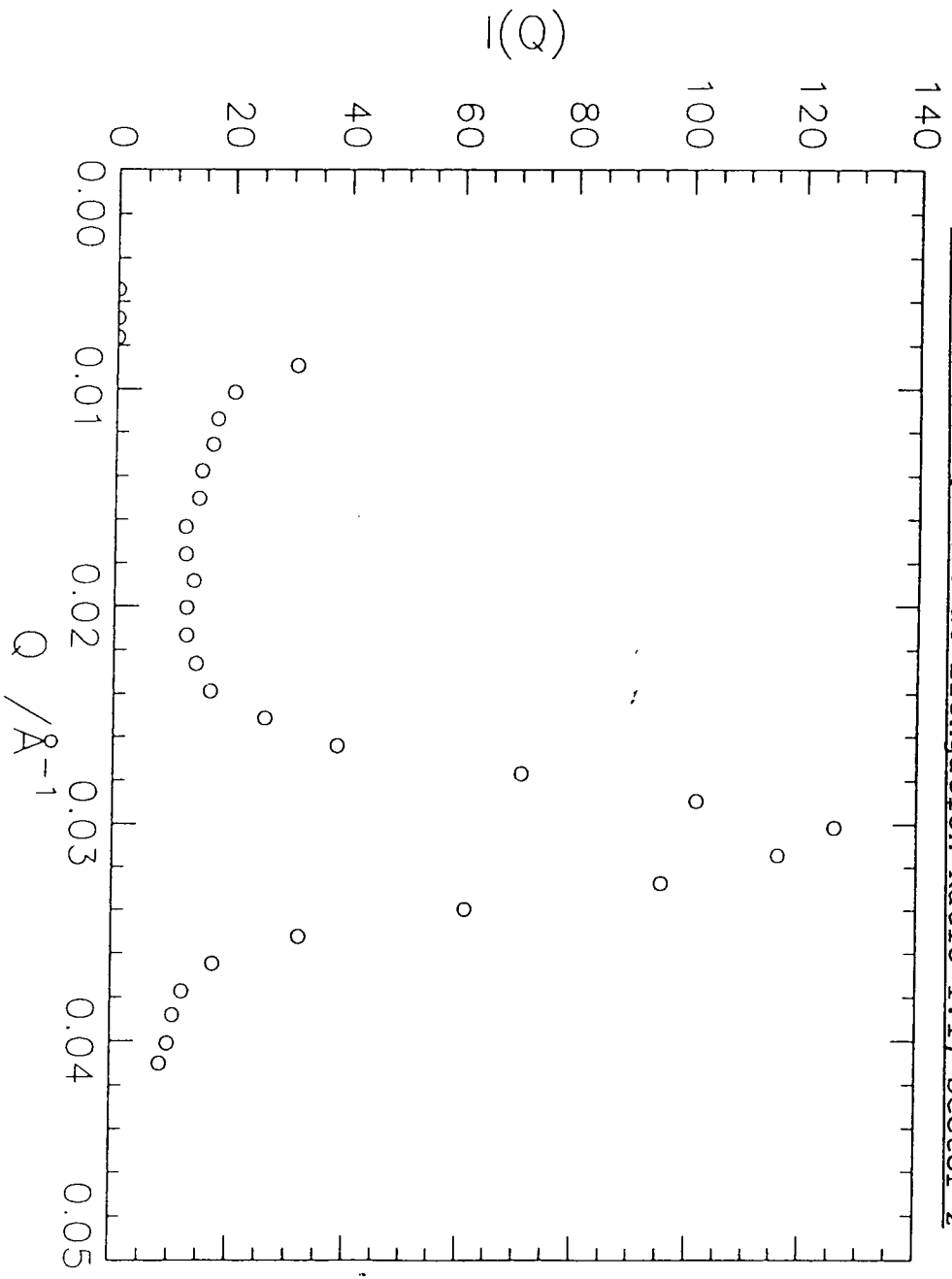


Figure 3.4.5.  $I(Q)$  vs  $Q$  Scattering Profile Obtained for Extruded S15150 at Elongation Ratio 1.1, Sector 3

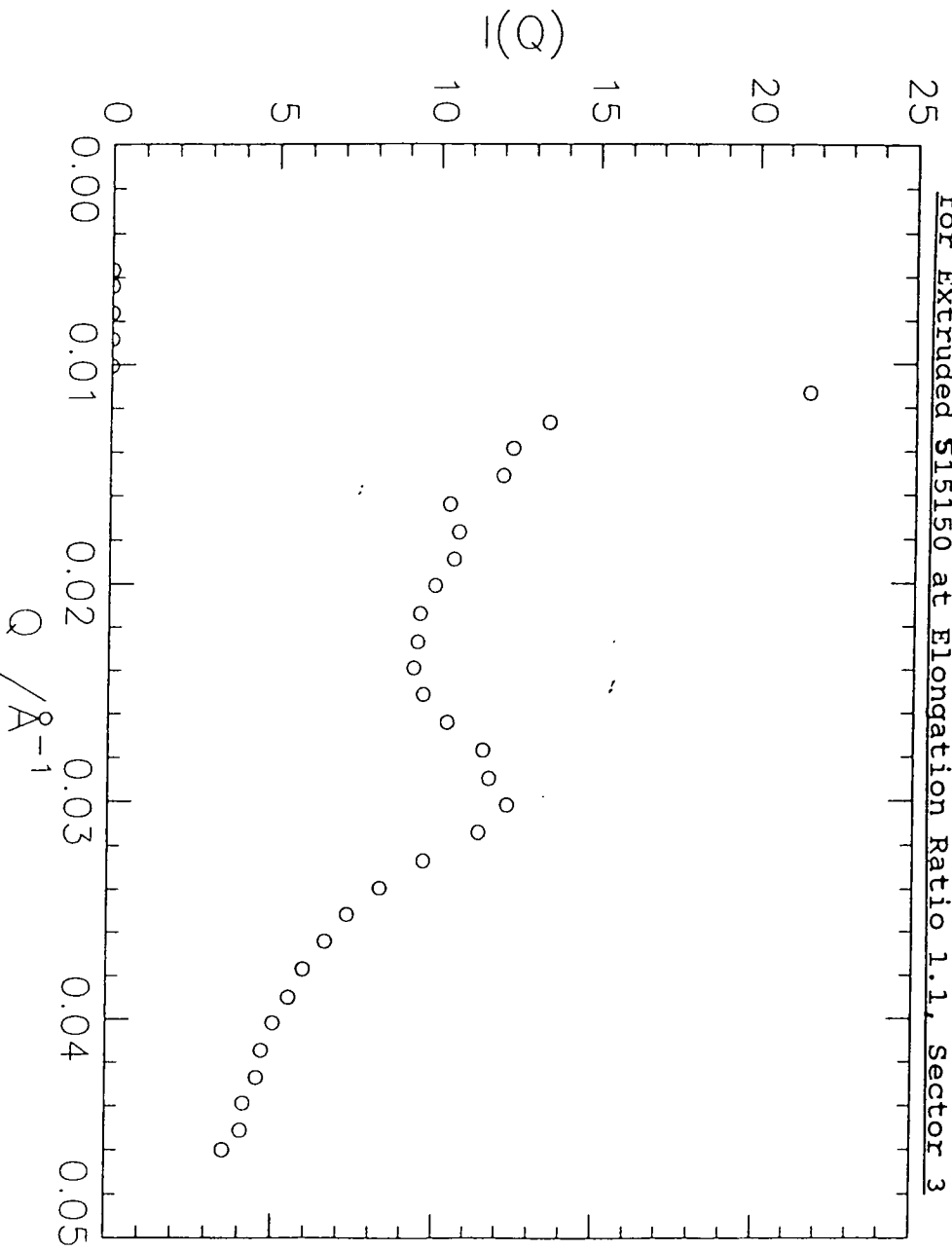


Figure 3.4.4.6.  $I(Q)$  vs  $Q$  Scattering Profile Obtained for Extruded 515150 at Elongation Ratio 1.1, Sector 4

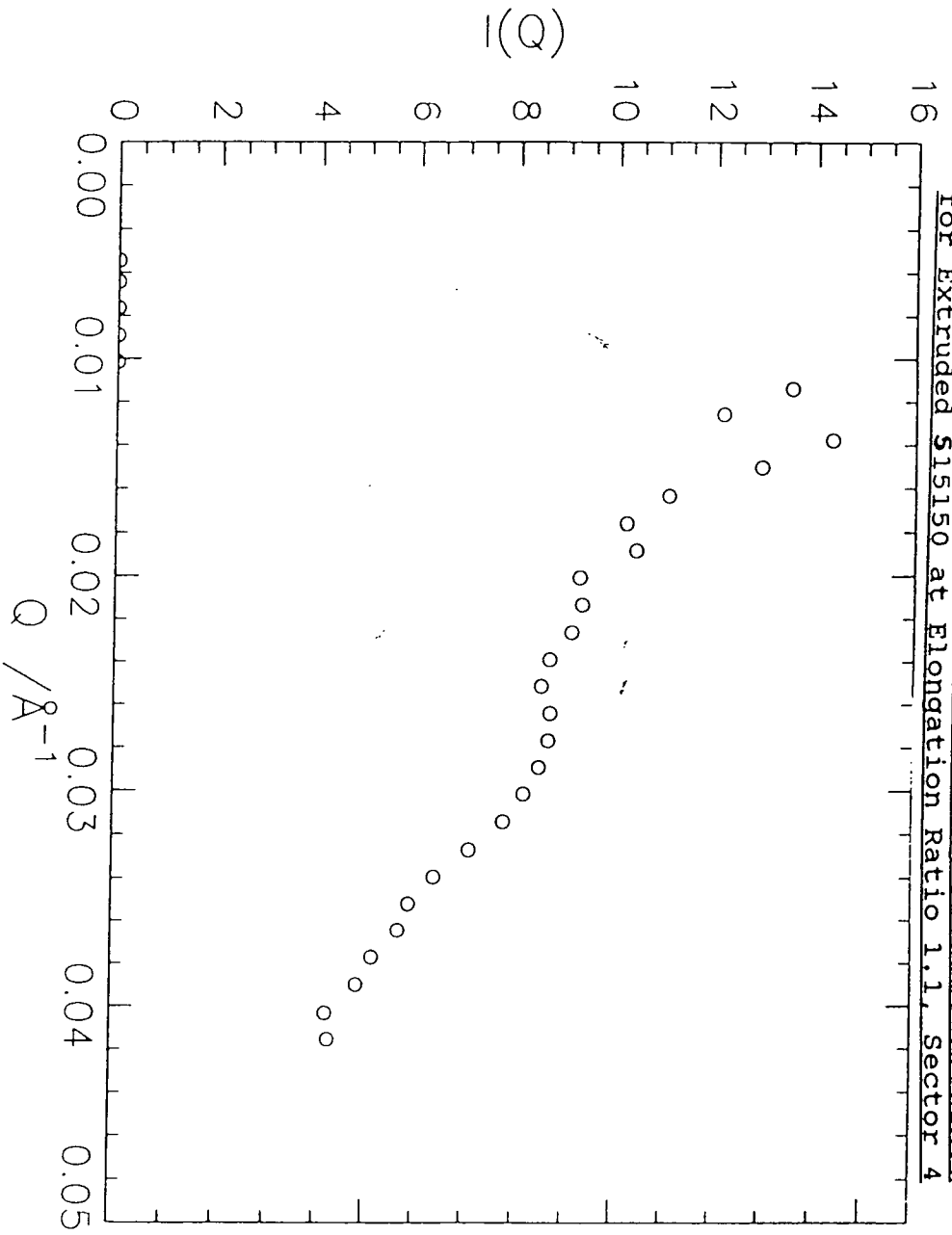
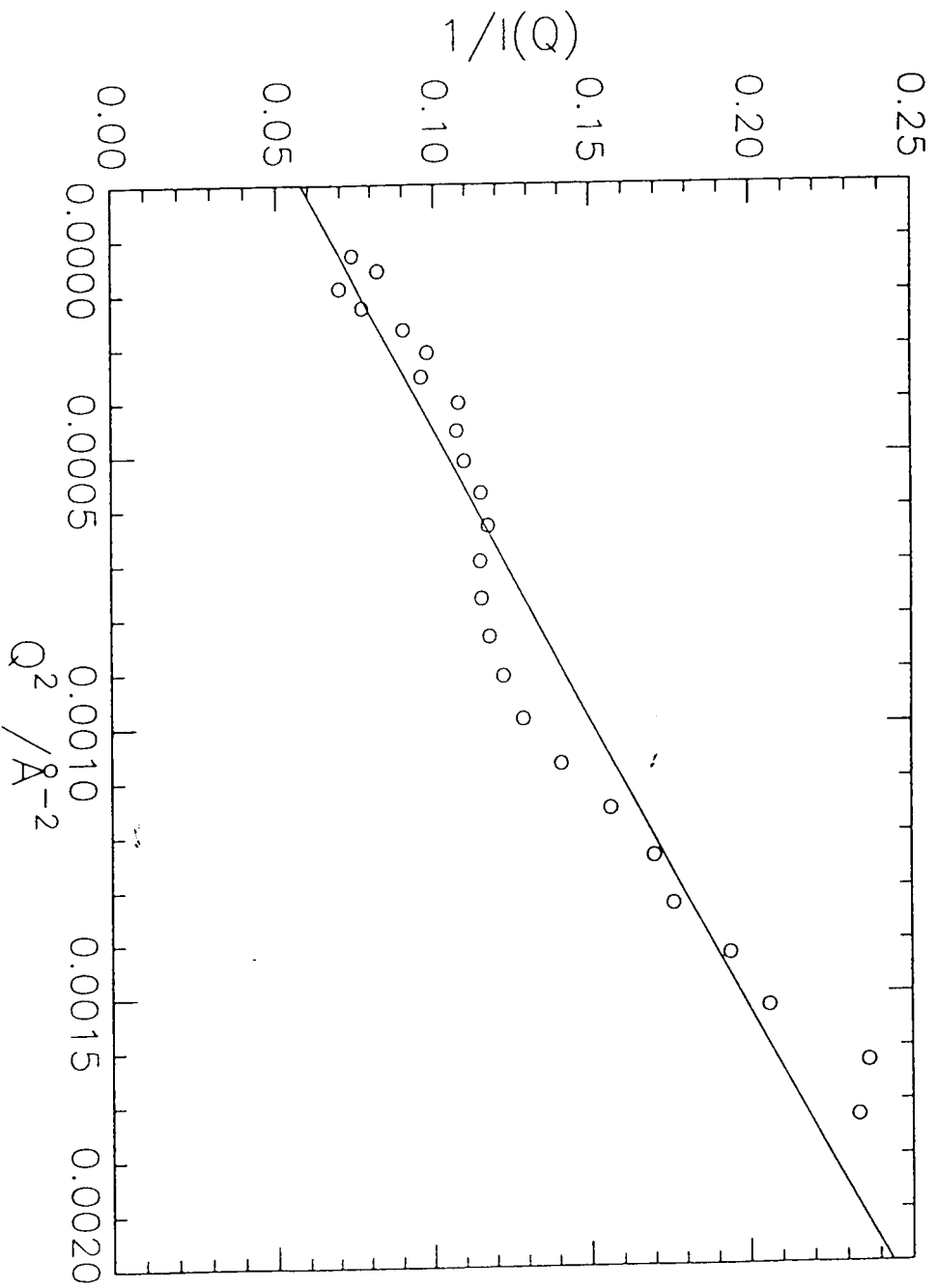


Figure 3.4.7. Zimm Plot Obtained for Extruded 515150  
at Elongation Ratio 1.1, Sector 4



peak at  $Q \simeq 0.03 \text{ \AA}^{-1}$  indicates that the 'contrast-matching' technique had not been 100% successful (Ch. 1). The position of this Bragg peak, however, would correspond to an interdomain spacing of 25.6nm using equation (7) below:

$$d_{int} = \sqrt{6\pi} Q_{max} \quad \text{EQ. (7)}$$

where:

$d_{int}$  = Interdomain spacing (nm)

$Q_{max}$  = position of primary Bragg peak (nm)

There is no suggestion however that there may be any Bragg peaks present at lower  $Q$  values, so this one at  $Q \simeq 0.03 \text{ \AA}^{-1}$  is the primary Bragg peak. Richards and Thomason<sup>2</sup> have reported a  $d_{int}$  of around 38nm for a poly(styrene-isoprene-styrene) triblock copolymer with spherical morphology in the unextruded state which was approximately the same total molecular weight of the S15150 copolymer. This is almost double that obtained for the more highly-oriented extrudate studied here. Richards and Thomason did report, however, that there was some evidence that there could have been at least one Bragg<sup>2</sup> peak at a lower  $Q$  than observed in their study but further work using a spectrometer with a lower  $Q$  range would have been necessary to verify this. As a result comparison between the results obtained by these workers and the work carried out here on the extruded S15150 sample is not possible. In conclusion, the results obtained for the extruded

S15150 were relatively disappointing. The samples were clearly anisotropic but due to sample size limitations it was not possible to extend the samples beyond an elongation ratio of 1.1 parallel to the extrusion direction.

The Zimm plots obtained for each sector of the extruded S15150 scattering data showed the presence of a large Bragg peak indicating that the 'contrast-matching' technique described in Ch. 1 had not been fully effective. The presence of this peak also led to the radii of gyration and molecular weights being immeasurable in general, though one calculation was attempted. This showed that the deuterioisoprene was indeed statistically spread throughout the copolymer system since the calculated molecular weight from SANS was very close to that obtained from G.P.C. measurement. The radius of gyration,  $R_g$ , calculated was very similar to that obtained for the non-extruded S15150 sample described in Ch. 3.1.

For future work, larger samples required to be synthesised so that a much wider range of elongation ratios can be studied and allow determination of  $R_g$  parallel and perpendicular to the extrusion direction.

### Chapter 3 - References

- 1) Thomason, J.L.; PhD Thesis, Strathclyde (1981)
- 2) Richards, R.W.; Thomason, J.L.; Macromolecules; (1983), 16, 982
- 3) Hadziioannou, G.; et al, Macromolecules; 15, 263, (1982)
- 4) Hadziioannou, G.; Wang L.H.; Stein, R.S.; Porter, R.S.; Macromolecules; 15, 880, (1982)
- 5) Berney, C.V.; Cohen, R.E.; Bates, F.S.; Polymer; 23, 1222, (1982)
- 6) Hasegawa, H.; Hashimoto, T.; Kawai, H.; Macromolecules; 18, 67, (1985)
- 7) Hashimoto, T.; Tanaka, H.; Hasegawa, H.; Macromolecules; 18, 1864, (1985)
- 8) Hashimoto, T.; Shibayana, M.; Kawai, H.; Macromolecules; 13, 1237, (1980)
- 9) Folkes, M.J.; Keller, A.; Scalisi, F.P.; Polymer; 12, 793, (1971)
- 10) Folkes, M.J.; Keller, A.; Polymer; 12, 222, (1971)
- 11) Pakula, T.; Saijo, K.; Hashimoto, T.; Macromolecules; 18, 2037, (1985)
- 12) Pakula, T.; Saijo, K.; Kawai, H.; Hashimoto, T.; Macromolecules; 18, 1294, (1985)
- 13) Richards, R.W.; Mullin, J.T.; Materials Research Society Symposium Proceedings, Vol. 79, 299.

- 14) Akcasu, A.Z.; et al, J. Polym. Sci. Polym. Phys. Ed.; 18, 863, (1980)
- 15) Miller, J.A.; Cooper, S.L.; Han, C.C.; Pruckmayr. G.; Macromolecules; 17, 1073, (1984)
- 16) Richards, R.W.; Thomason, J.L.; Polymer; 22, 581, (1981)
- 17) Hadziioannou, G.P.; Skoulios, A.; Macromolecules; 15, 258, (1982)
- 18) Hadziioannou, G.P.; Skoulios, A.; Macromolecules; 15, 267, (1982)
- 19) Bastide, J.; Duplessix, R.; Picot, C.; Candau, S.; Macromolecules; 17, 83, (1984)
- 20) Davidson, N.S.; PhD Thesis, University of Strathclyde, 1984.
- 21) DiCorleto, J.A.; Cohen, R.e.; Polymer; 29, 1240, (1988)
- 22) "A Computing Guide for Small Angle Scattering Experiments, Ghosh, R.E.; I.L.L. (1989).
- 23) Picot, C.; et al, Macromolecules; 10, 436, (1977)
- 24) Boué, F.; Nierlich, M.; Jannink, G.; Ball, R.; J. Physique; 43, 137, (1982)
- 25) Hadziioannou, G.; Wang, L.; Stein, R.S.; Porter, R.S.; Macromolecules; 15, 1594, (1982)
- 26) Clough, S.B.; Maconnachie, A.; Allen, G.; Macromolecules; 13, 774, (1980)
- 27) Richards, R.W.; Mullin, J.T.; Materials Research Symposia; 16, (1987).
- 28) Tung, L.H.; J. Appl. Polym. Sci., 24, 953 (1979)

- 29) Helfand, E.; "Developments in Block Copolymers"  
Ed. I. Goodman, Applied Science (1982)
- 30) Hadziioannou, G.; PhD Thesis, Strasburg, (1980)
- 31) Bates, F.S. et al; Polymer; 24, 519 (1983)
- 32) Richards, R.W.; Adv. Polym. Sci.; 71, 1, (1985)

CHAPTER 4 - THE INTERACTION BETWEEN COMPONENT  
BLOCKS OF AN ISOTOPIC DIBLOCK COPOLYMER

4.1. Introduction

For Small Angle Neutron Scattering studies involving the use of selective deuteration technique described in Chapter 1 it has been assumed that this technique had no effect on the mixing of hydrogenous and deuterated species. This meant there was no excess free energy of mixing associated with deuteration but work carried out by Bates et al <sup>1,2</sup> on mixtures of hydrogenous and deuterated isomers of high molecular weight ( $500 \times 10^3$  -  $1000 \times 10^3$ ) polymers, suggested this was not a reasonable assumption. This set of experiments sought to investigate this matter and resolve it using isotopic diblock copolymers of deuterated and hydrogenous polystyrene. These experiments were carried out at the Rutherford Appleton Laboratory, Oxford using the LOQ instrument. Alongside studies of diblock copolymers some time was spent carrying out experiments on blends of deuteropolystyrene and hydrogenous polystyrene. These two studies are quite different and therefore are discussed separately.

#### 4.1.1. Background

Prior to the advent of Small Angle Neutron Scattering (SANS) to examine polymer-polymer interactions, the techniques used were slow and in some cases led to large errors in the calculated interaction parameters,  $\chi$ . The techniques applied included microcalorimetry<sup>3,4</sup> electron microscopy<sup>5</sup> and Small Angle X-Ray Scattering<sup>6,7</sup>. All of these techniques have limitations - for electron microscopy studies the preparation of samples is critical and is a major source of error in the results obtained for this technique. Small Angle X-Ray Scattering relies on their being sufficient electron density contrast between substituents.

Green and Doyle<sup>8</sup> used the Forward Recoil Spectrometry technique to investigate polymer-polymer interactions in blends of hydrogenous and deuterated polystyrene of high ( $700 \times 10^3$ - $800 \times 10^3$ ) molecular weight. The results obtained for the interaction parameter,  $\chi$ , by this method had an associated error of  $\pm 50\%$  due to the scattered nature of the data. Similarly, with the SANS data obtained by Bates et al<sup>1,2</sup> the background subtraction was made somewhat arbitrarily which may account for the results they obtained. This SANS study used isotopic diblock copolymers of polystyrene and great care was taken in ensuring that the background ('Random') sample was subtracted from the sample ('MIX')

properly. With these provisions it was hoped that this series of experiments would give a clear indication whether the conclusions of Bates et al were upheld.

#### 4.1.2. The Random Phase Approximation Theory (R.P.A.)

Much of the early work investigating polymer-polymer interactions was carried out on blends of homopolymers. De Gennes<sup>9</sup> put forward a mean field theory to describe the scattering profiles obtained for polymer blends. This was known as the Random Phase Approximation (R.P.A.) and involves the parameter,  $\chi$ . The Flory-Huggins interaction parameter,  $\chi$  is indicative of the degree of mixing of polymer substituents. If  $\chi$  is negative then mixing between substituents was favoured but if  $\chi$  is positive mixing was unfavourable and phase separation occurs. A detailed description of R.P.A. theory can be found in the literature<sup>9</sup> but it is Leibler's<sup>10,11</sup> extension of R.P.A. theory so that it covered block copolymers that is relevant here. A brief summary of this extension is given below but full details can be found in Reference (10). In particular, the application of the R.P.A. theory to an A-B diblock copolymer will be discussed.

For an A-B diblock copolymer of composition,  $f$ , in the molten state the system may be regarded as incompressible.

$$\rho_A(\underline{r}) + \rho_B(\underline{r}) = 1 \quad \text{EQ. (1)}$$

where:

$r$  = any point in the liquid

$\rho_A, \rho_B$  = ratio of local monomer density to the average monomer density.

At equilibrium a balance between two opposing effects is reached:

(i) Monomers A and B repel each other leading to a decrease in A-B contacts.

and (ii) The subsequent entropy decrease in the system due to (i) above leads to an increase in the free energy.

Mixing of A and B constituents is probable if the enthalpy of interaction,  $\Delta H$ , between unlike monomers is small or negative. The enthalpy of interaction,  $\Delta H$  is defined as:

$$\Delta H = \kappa T \chi \rho_A \rho_B \quad \text{EQ. (2)}$$

where:

$\kappa$  = Boltzmann Constant ( $\text{JK}^{-1}$ )

$T$  = temperature (K)

If the value of  $\chi$  becomes sufficiently large and positive (eg. on cooling the system) then microphase separation is favoured. In such a system, the distribution of A and B segments is not uniform throughout. To char-



acterise this deviation of monomers from a uniform system an order parameter,  $\psi(\underline{r})$ , is introduced and may be described by a density-density correlation function:

$$\overline{S}(\underline{r}-\underline{r}') = \frac{1}{K} T \langle \psi_A(\underline{r}) \psi_A(\underline{r}') \rangle \quad \text{EQ. (3)}$$

where:  $\psi_A(\underline{r}) = \langle \rho_A(\underline{r}) - f \rangle$  at  $\underline{r}$

$\psi_A(\underline{r}') = \langle \rho_A(\underline{r}') - f \rangle$  at  $\underline{r}'$

The Fourier Transform of Equation (3) is measured in an elastic neutron scattering experiment.

$$I(q) \propto \overline{S}(q) \quad \text{EQ. (4)}$$

where:

$I(q)$  = scattered neutron intensity as a function of scattering vector,  $q$ .

$$q = \frac{4\pi}{\lambda} \sin(\theta/2)$$

$\lambda$  = wavelength of radiation

$\theta$  = scattering angle

For a molten diblock copolymer the correlation function  $\overline{S}/q$  is given by:

$$\overline{S}(q) = W(q) / S(q) - 2\chi W(q) \quad \text{EQ. (5)}$$

$$\text{where: } S(q) = S_{AA}(q) + S_{BB}(q) + 2S_{AB}(q) \quad \text{EQ. (6)}$$

$$W(q) = S_{AA}(q) - S_{BB}(q) - S_{AB}^Z(q) \quad \text{EQ. (7)}$$

For an A-B diblock copolymer

$$S_{AA}(q) = Ng(f, u) \quad \text{EQ. (8)}$$

$$S_{BB}(q) = Ng(I - f, u) \quad \text{EQ. (9)}$$

$$S_{AB}(q) = \frac{N}{2}[g(I, u) - g(f, u) - g(I - f, u)] \quad \text{EQ. (10)}$$

where:

$g(f, u)$  is the Debye function

$$g(f, u) = 2[fu + \exp(-fu) - I]/u^2 \quad \text{EQ. (11)}$$

$$u = q^2 Rg^2$$

$$Rg^2 = Na^2/b$$

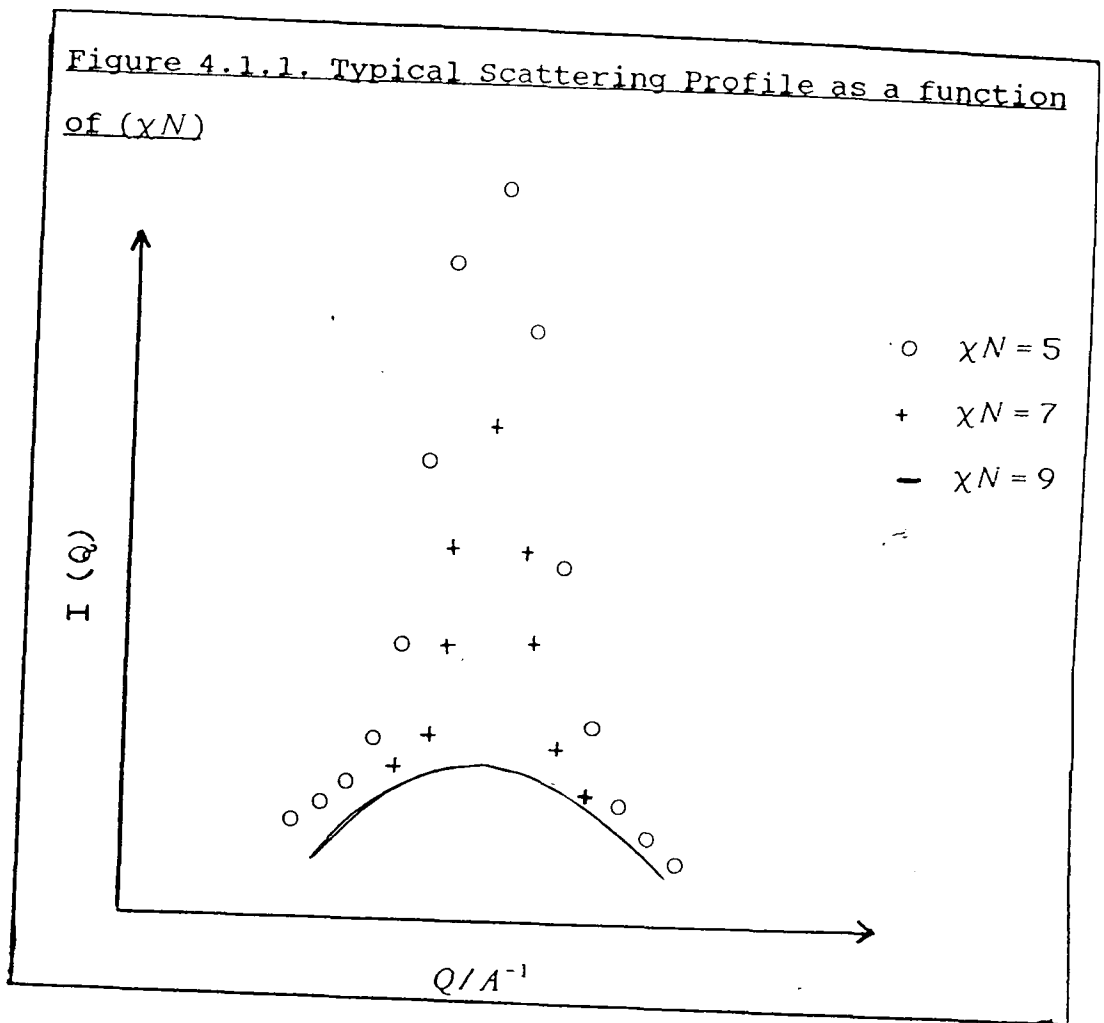
$a$  = Kuhn statistical length

$N$  = total number of monomers

For low  $q$  values, ( $q Rg \ll 1$ ), the scattering intensity decreases due to the systems' incompressibility, whereas for high  $q$  values ( $q Rg \gg 1$ ) the monomer density fluctuations are like those of an ideal chain and  $I(q)$  decreases as  $1/q^2$ . The net result is a peak at an intermediate  $q$  value giving a similar result to the 'correlation hole' effect described by De Gennes<sup>9</sup>.

The equations (4) to (11) show that the intensity profile in the disordered region may be fitted using  $Rg$  and  $\chi$  as fitting variables since  $N$  and  $f$  are constants. The shape of the intensity profile is strongly dependent on the product  $\chi N$  (Figure 4.1.1).

Figure 4.1.1. Typical Scattering Profile as a function of  $(\chi N)$



As the value of  $\chi N$  increases, the maximum increases in amplitude but does not move from its initial value of  $(Q \text{ max. } R_g)$ . for diblock copolymers R.P.A. theory predicts:

- i) The peak maximum will be situated at  $Q \approx 2/R_g$  where  $R_g$  is the radius of gyration of the whole copolymer.
- ii) As  $\chi$  decreases the peak amplitude decreases but the peak width increases. A decrease in  $\chi$  is usually obtained by increasing the temperature for more favourable mixing.

iii) The full width at half height is determined by  $\chi$ . It is interesting to compare this behaviour with that for a homopolymer blend<sup>12</sup> (Figure 4.1.2.). For A-B mixtures the intensity maximum is evidently at  $q=0$  and  $\chi$  is determined by extrapolating the data back to  $q=0$ . For a diblock copolymer Leibler<sup>10</sup> suggested that in the disordered regime the equilibrium state is determined by two factors :

(i) the chain composition ( $f$ )

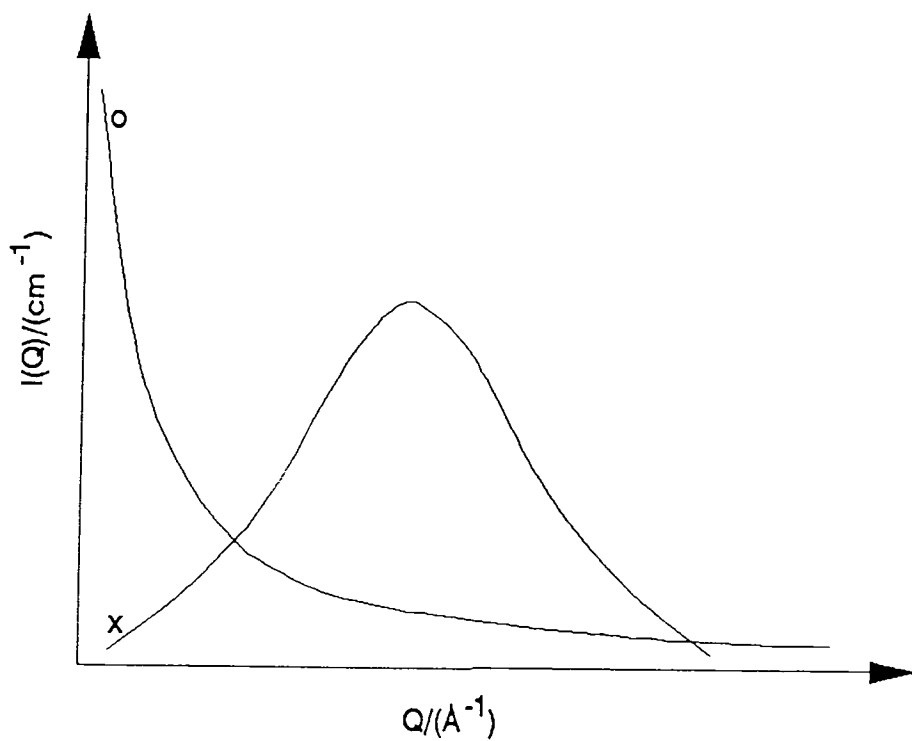
and (ii) the Product ( $\chi N$ )

At the spinodal point,  $(\chi N)_s$ , the critical point for unmixing of substituents occurs.

$$1/l = S(q)/W(q) - 2\chi = 0 \quad \text{EQ. (12)}$$

This corresponds to a minimum in the function  $S(q)/W(q)$  and allows the interaction parameter at the spinodal point ( $\chi_s$ ) to be calculated. For an A-B diblock copolymer the spinodal point occurs at  $(\chi N)_s = 10.5$  whereas for the equivalent homopolymer blend  $(\chi N)_s = 2$ . Thus at some temperatures an A-B diblock copolymer would be homogeneous ( $(\chi N) < 10.5$ ), whereas the corresponding homopolymer blend would phase separate ( $(\chi N) > 2$ ) in agreement with the work of Krause et al<sup>4</sup>

Figure 4.1.2. Typical Scattering Profiles for an A-B homopolymer blend (o) and A-B Diblock Copolymer (x)



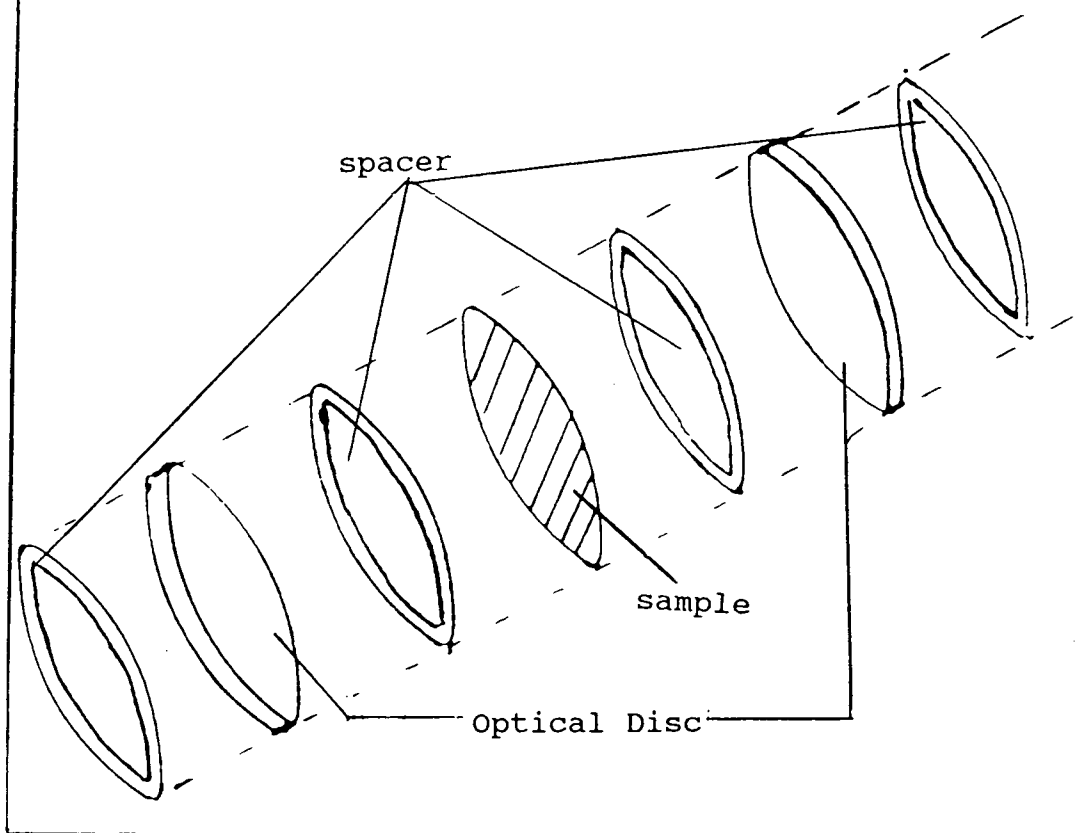
#### 4.1.3. Experimental

Diblock copolymers of polystyrene/deuteropolystyrene and polystyrene/deuteropolystyrene blends were synthesised as described in Ch. 2. The sample characteristics are shown in Tables (4.2.1 and 4.2.2). These samples were then taken to the Rutherford Appleton Laboratory, Oxford for study on the LOQ spectrometer after being pressed into discs as described in Ch. 2.3.2.(b). The discs were placed between optical flats in a mounting assembly as shown in Figure 4.2.1 and arranged in a heating rack. The heating rack was then placed in the beam and a laser light was used to ensure the samples were exposed to the beam. The samples were then heated to 393K and allowed to equilibrate for 30 minutes before measurements began. Samples were then studied at 10K intervals up to 473K allowing the same equilibration period as for the first studies.

The initial temperature was chosen by examining the glass transition temperature,  $T_g$ , of polymer substituents and ensuring studies commenced 20K above the highest one. This was to ensure any possible effects due to being too close to the  $T_g$  of one substituent were eliminated.

During the course of the study it was noted that all the samples started to form air bubbles as the tem-

Figure 4.2.1. Arrangement of Sample in Sample Holder for use in LOQ instrument



perature increased. For the lower molecular weight samples (Table 4.2.2) the samples seeped out of the sample holders at all the temperatures studied. Attempts to alleviate this problem, using PTFE tape as a barrier to leakage and tightening up the sample holder at every new temperature studied, had limited success as sample losses were still obtained.

Every sample was studied at each temperature until good statistics had been obtained to allow the data to be of use in subsequent analysis.

Table 4.2.1. - Characteristics of high molecular weight  
Isotopic Diblock Copolymers of Polystyrene

SAMPLE	$M_W$ ( $\times 10^{-3}$ )	$M_W/M_n$
PSH80PSD20	94.2	1.11
PSH60PSD40	91.2	1.16
PSH40PSD60	93.9	1.20
PSH20PSD80	91.8	1.23

Table 4.2.2. - Characteristics of low molecular weight  
Isotopic Diblock Copolymers of Polystyrene

SAMPLE	$M_W$ ( $\times 10^{-3}$ )	$M_W/M_n$
PSH80PSD20B	11.9	1.22
PSH50PSD50B	16.6	1.16
PSH20PSD80B	16.3	1.23

## 4.2. Results and Discussion

### 4.2.1. Isotopic Diblock Copolymers of Polystyrene

The first set of experiments were carried out using the high molecular weight ( $100 \times 10^{-3}$ ) series. Figure 4.2.2. and Figure 4.2.3. show the typical scattering profile obtained from this set of samples. It is evident that there is a single maximum in the profile but it is not fully resolved. This was due to the limited  $Q$  range of the LOQ instrument in the low  $Q$  region of the scattering profile. Despite this limitation, the main predictions of the R.P.A. theory were obtained. Firstly, there was a single maximum and secondly as the temperature increased the peak amplitude decreased and the peak width increased (Figure 4.2.4.). Since the peak was not fully resolved it was, however, not possible to ascertain if the peak maximum was situated at  $Q \simeq 2/Rg$ .

The limited resolution of the peak for each copolymer sample led to great difficulty in obtaining a fit to the data. The relatively few data points in the low  $Q$  region of the scattering profile had the highest errors associated with them (up to 50% in some cases) and so could not be used when attempting to fit the data. As a consequence of this only two diblock copolymer samples, PSH20PSD80 and PSH80PSD20, gave fits of reasonable statistical significance. These results

Figure 4.2.2. Scattering Profile obtained for PSH20PSD80 sample at 393K

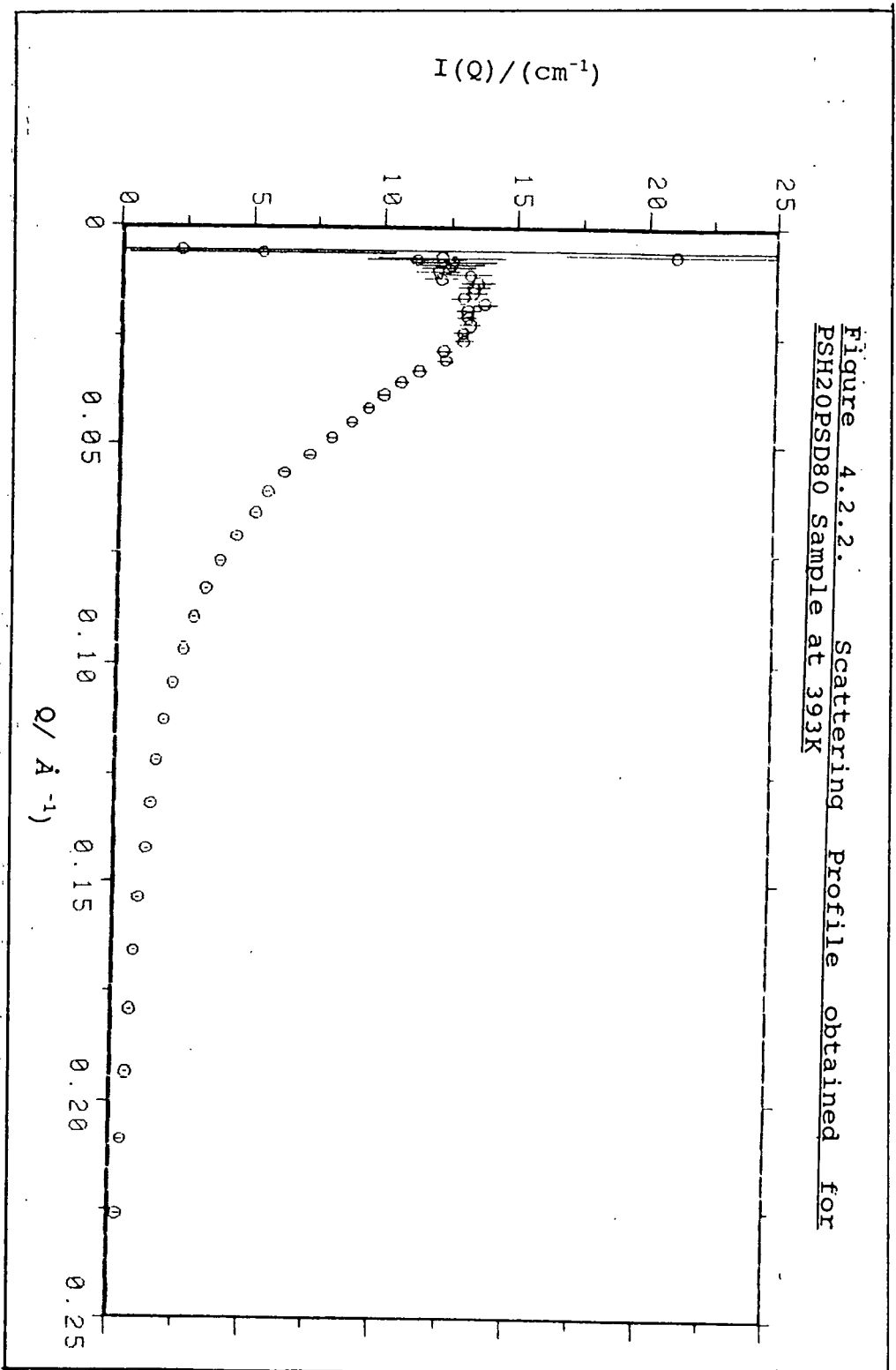
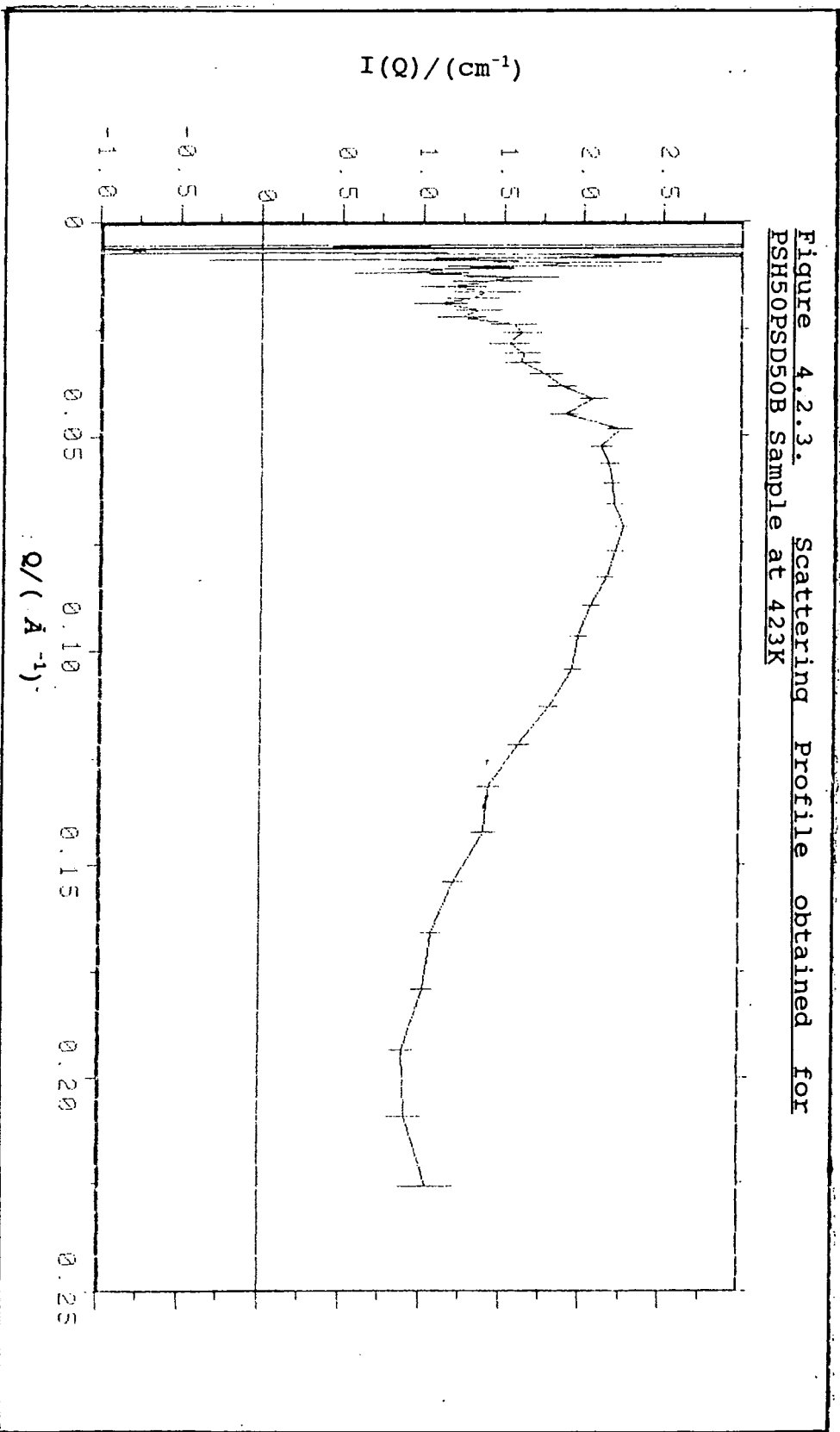


Figure 4.2.3. Scattering Profile obtained for PSH50PSD50B Sample at 423K



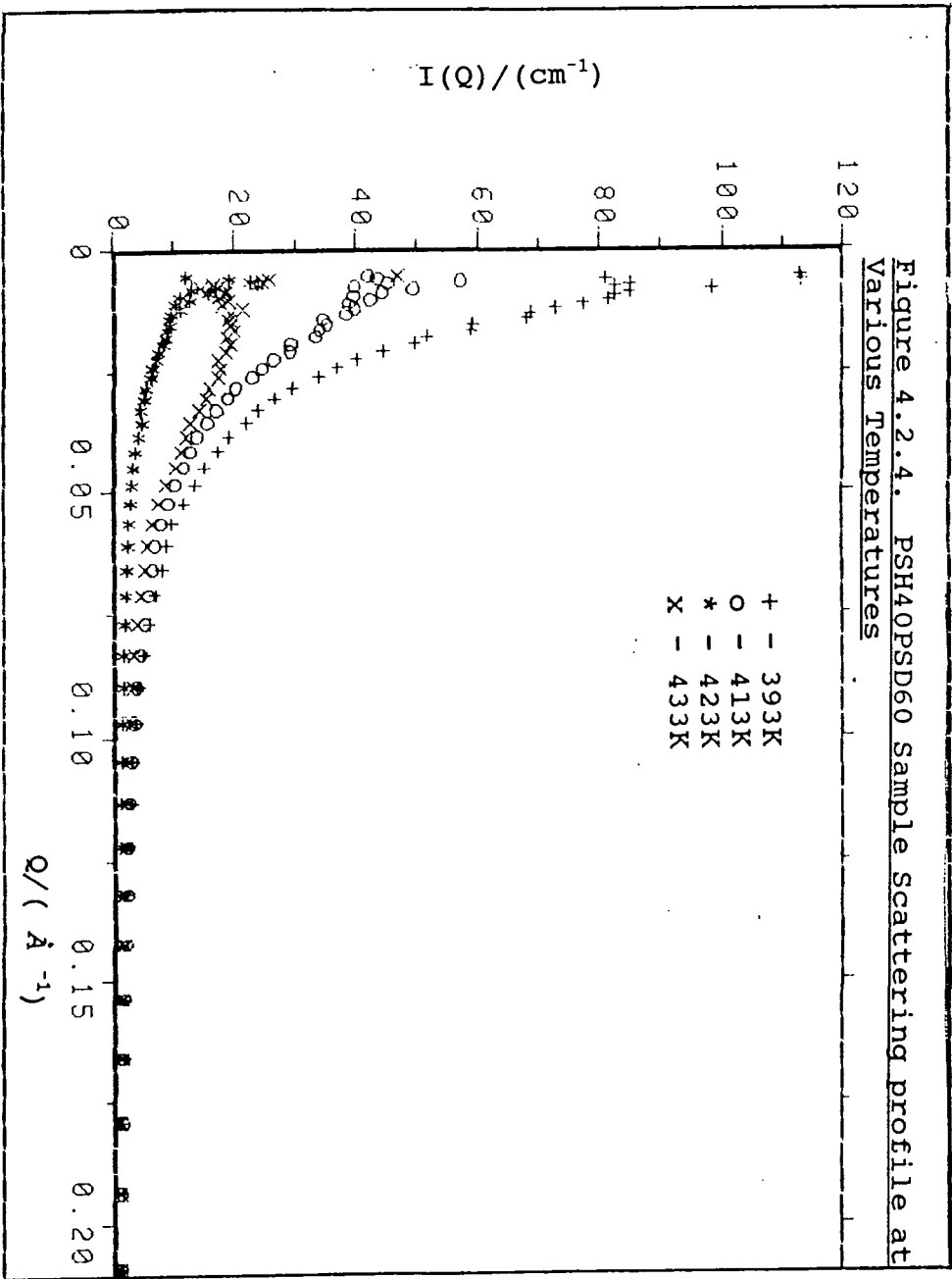


Figure 4.2.4. PSH40PSD60 Sample Scattering profile at Various Temperatures

are shown in Tables 4.2.3 and 4.2.4 and were obtained using a computer program that 'fixed' the value of  $R_g$  from the maximum intensity in the scattering profile and then varied the value of  $\chi$  until the best statistical fit was obtained. Tables 4.2.3 and 4.2.4 clearly show that the radii of gyration obtained for each sample at each temperature studied using this fit were similar. These showed, in general, an increasing favourability of mixing of polymer constituents as indicated by an increasingly negative interaction parameter,  $\chi$ . Figures 4.2.5(a)-4.2.5(d) show typical fits to sets of experimental data obtained from PSH80PSD20 sample at various temperatures.

The results obtained for the interaction parameter,  $\chi$  at various temperatures,  $T$ , for the PSH20PSD80 and PSH80PSD20 samples were used to find the values of the constants  $A$  and  $B$  in the following relationship:

$$\chi = A + \frac{B}{T}$$

EQ. (13)

A graph of  $1/\chi$  vs  $T$  was plotted for each sample and a least squares fit was used to obtain the best straight line through the data (Figures 4.2.6 and 4.2.7). The values have a large error associated with them due to the relatively small number of data points.

Figure 4.2.5(a) Scattering Profile and best fit for PSH80PSD20 Sample at 393K

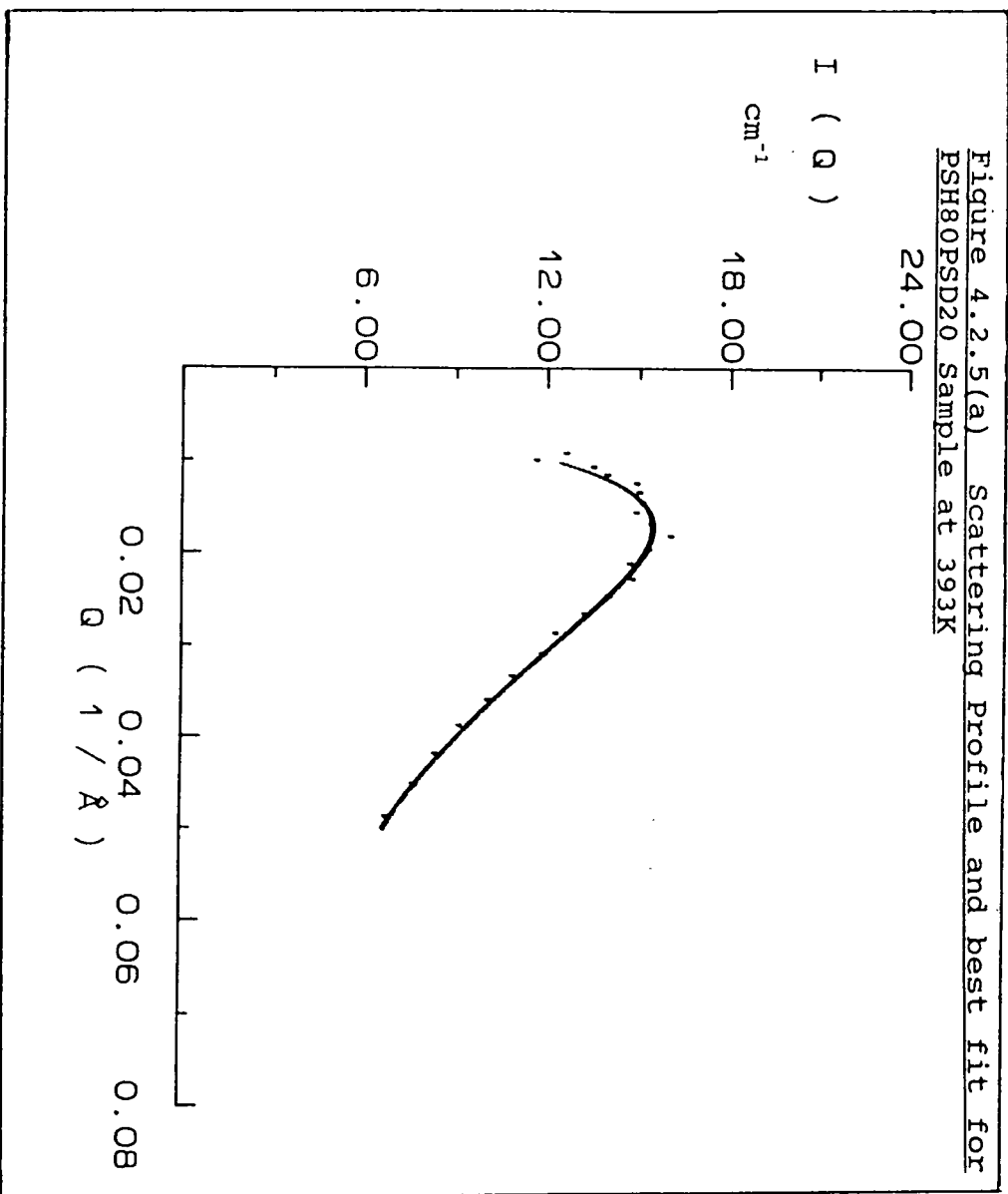


Figure 4.2.5(b) Scattering Profile and best fit for PSH80PSD20 Sample at 403K

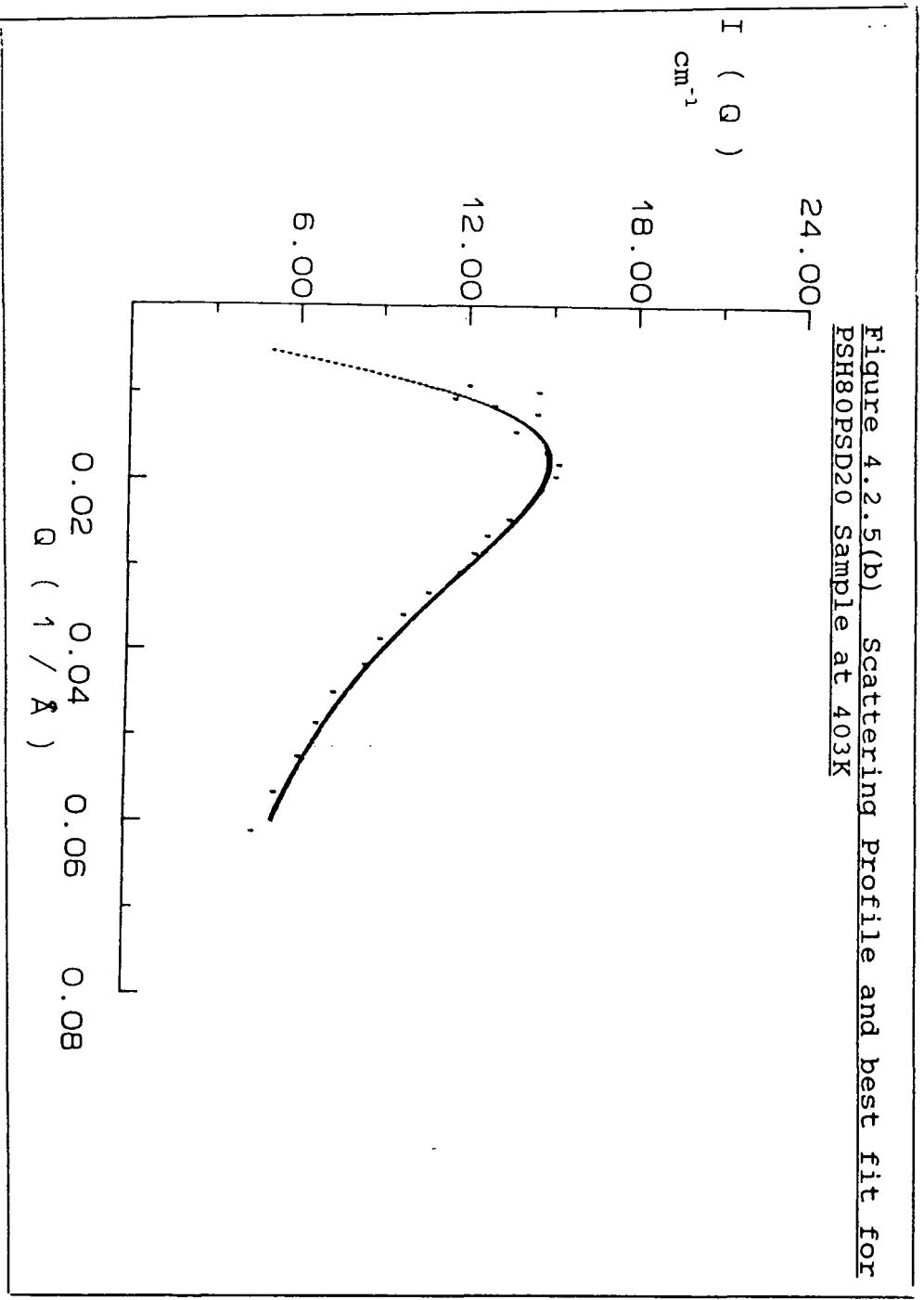


Figure 4.2.5(c) Scattering Profile and best fit for PSH80PSD20 Sample at 413K

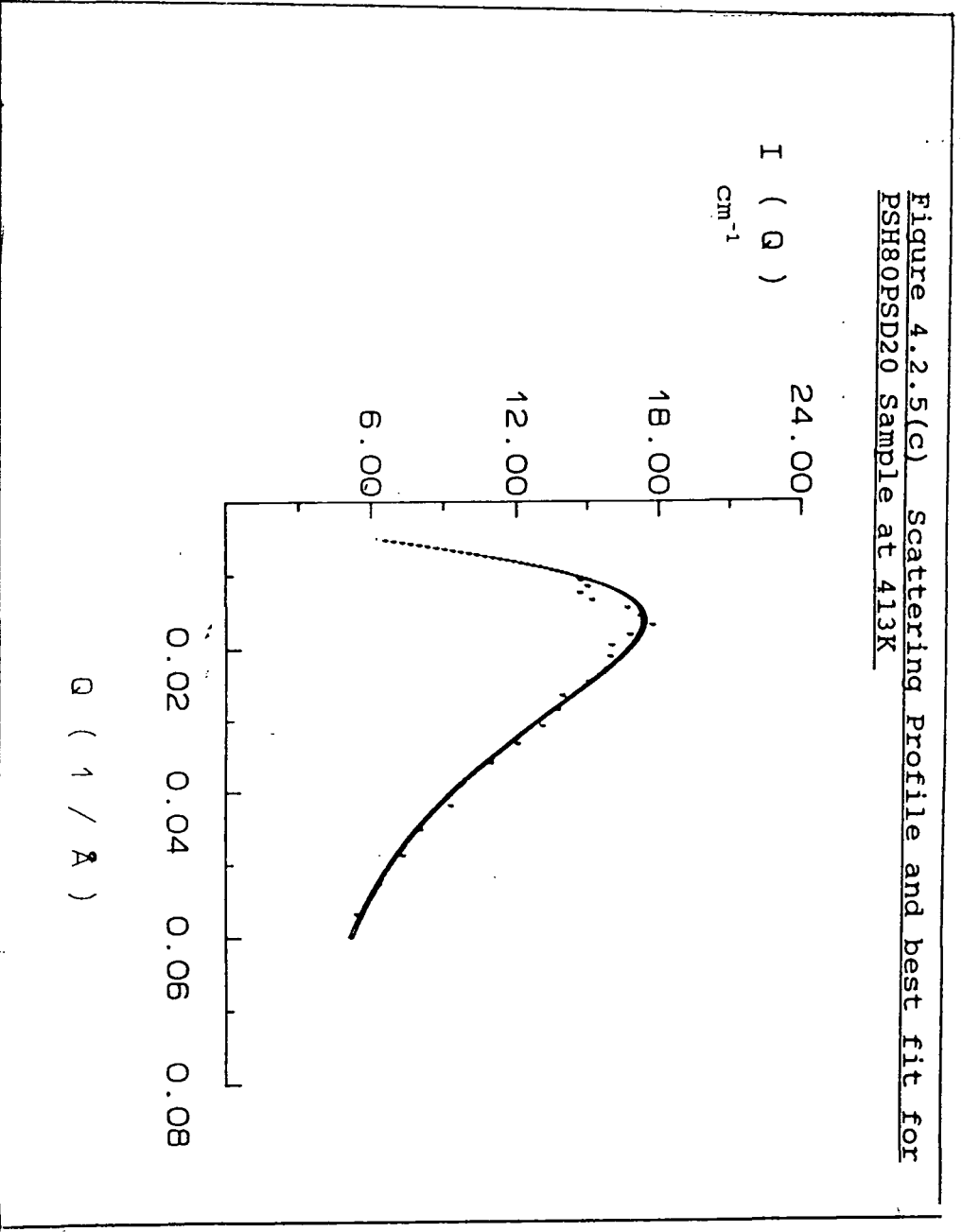


Figure 4.2.5(d) Scattering Profile and best fit for PSH80PSD20 Sample at 423K

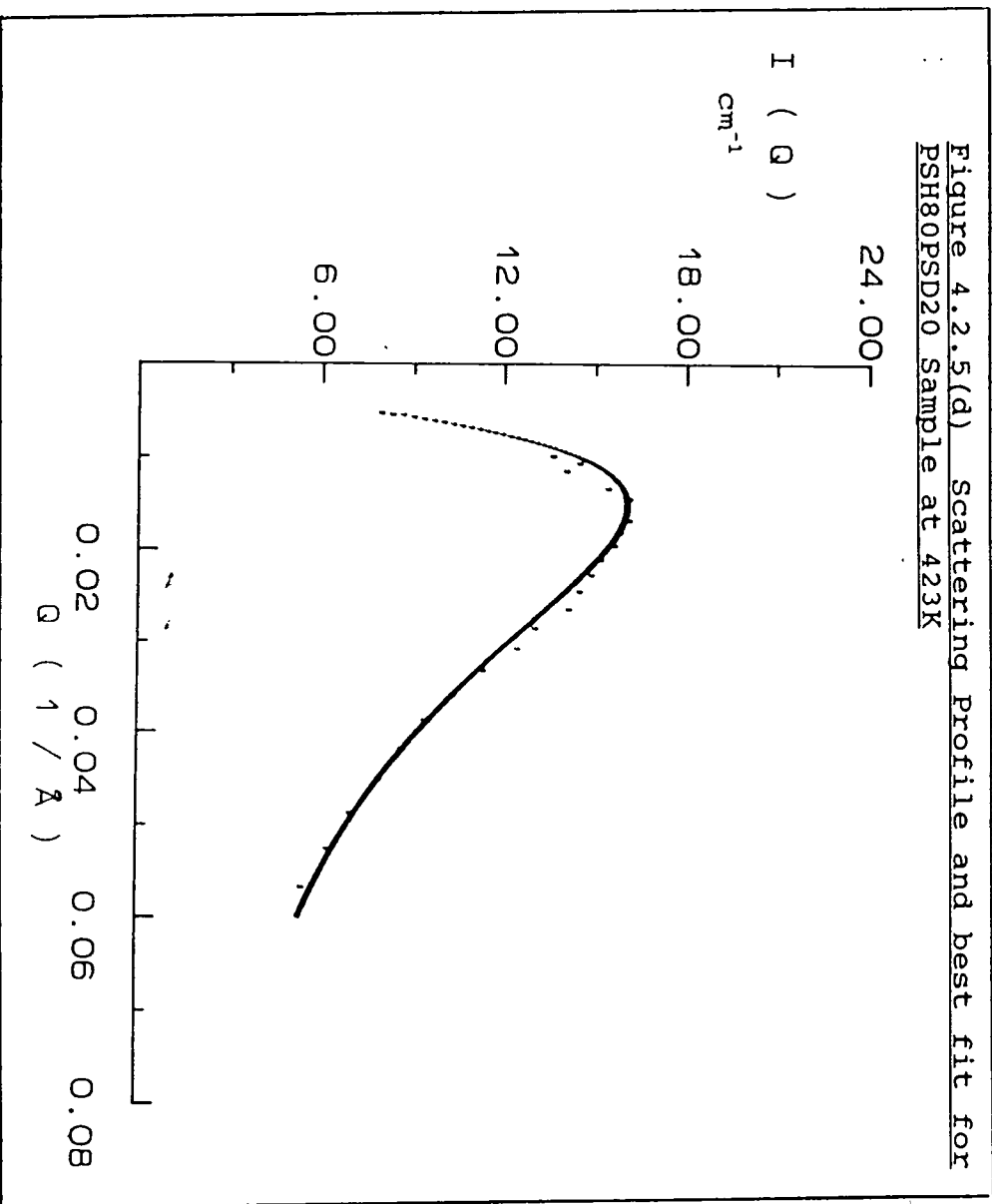


Figure 4.2.6. Plot of  $\chi$  vs  $1/T$  for PSH20PSD80 Sample

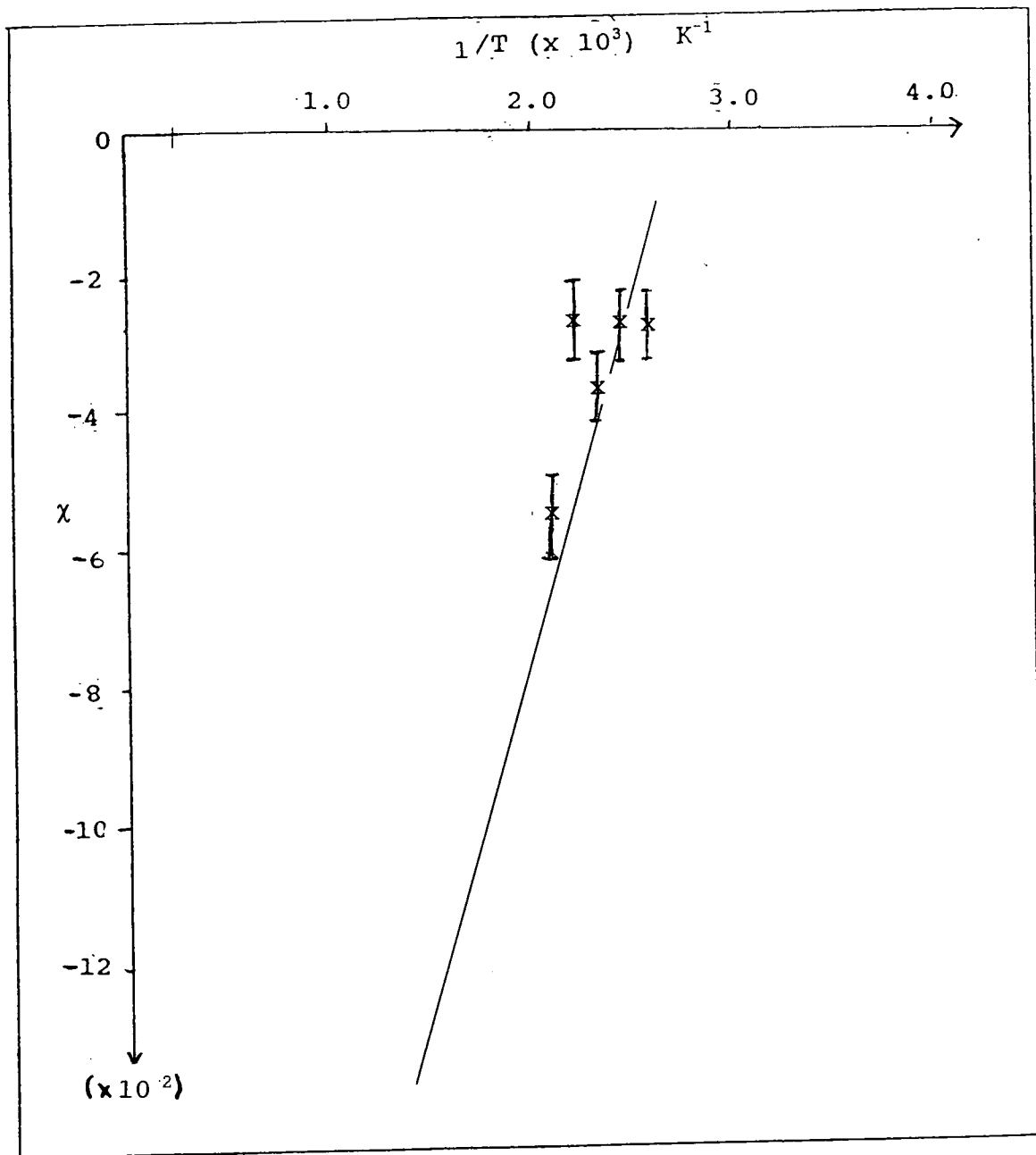


Figure 4.2.7. Plot of  $\chi$  vs  $1/T$  for PSH80PSD20 Sample

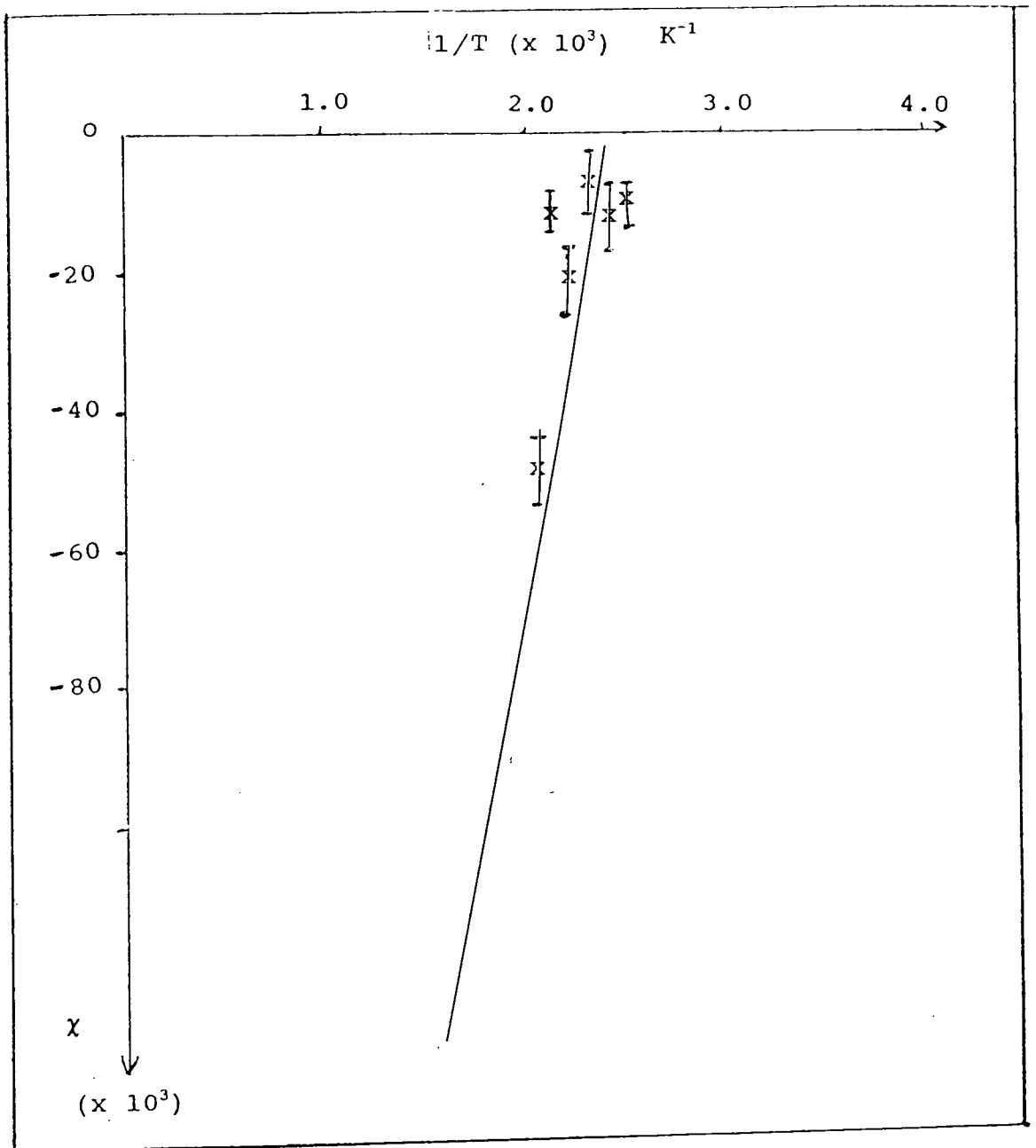


Table 4.2.3 - Results obtained for PSH20PSD80 copolymer sample

	Temperature (K)			
	393	403	413	423
Interaction Parameters, $\chi$ ( $\times 10^2$ )	$-2.78 \pm 0.62$	$-2.89 \pm 0.66$	$-3.82 \pm 0.77$	$-2.62 \pm 0.59$
Radius of gyration, $R_g$ ( $\text{\AA}$ )	118.0	117.9	127.3	118.0
				433
				$-5.78 \pm 1.08$
				137.6

Table 4.2.4.4. Results obtained for PSH80PSD20 copolymer sample

	Temperature (K)					
	393	403	413	423	433	453
Interaction Parameters, $\chi$ ( $\times 10^3$ )	-9.17 ( $\pm$ )	-9.56 ( $\pm$ )	-7.94 ( $\pm$ )	-22.80 ( $\pm$ )	-9.82 ( $\pm$ )	-49.70 ( $\pm$ )
Radius of gyration, $R_g$ ( $\text{\AA}$ )	121.1	121.0	133.0	142.0	125.3	143.9

Table 4.2.5. - Constants A and B obtained from a  $\chi$  vs  $1/T$  plot

Sample	A	B
PSH20PSD80	-0.37	137.2
	$\pm$	$\pm$
	0.04	19.4
PSH80PSD20	-0.32	126.7
	$\pm$	$\pm$
	0.04	17.7

As a result the magnitude of the constants A and B are of interest rather than the absolute values because of the large errors associated with them.

In the light of the results obtained for the high molecular weight isotopic diblock copolymers of polystyrene, it was decided to synthesise a lower molecular weight series of isotopic diblock copolymers of polystyrene with varying compositions and carry out the same experiment on these copolymer samples. The target set was a total molecular weight of 20000 because the maximum in the scattering profile from these samples would have been at  $Q \simeq 0.05 \text{ \AA}^{-1}$ . This is well within the resolution capabilities of the LOQ Instrument. These samples were synthesised (Ch. 2.3.2) and are characterised in Table 4.2.2. Data for this set of samples was collected over the temperature range 408K to 468K. Data correction for these lower molecular weight samples was made inaccurate by the need to estimate the copolymer film thickness for the samples at each temperature. Consequently the calculated absolute intensities for these samples have an undefined error associated with them due to this seepage problem. This does detract from the interaction parameters,  $\chi$ , calculated from these data sets which are dependent on the peak amplitude as well as the peak width. The peak

maximum position, however, is unaffected by the error in the peak amplitude as it is determined by the  $R_g$  of the whole copolymer. The scattering obtained from these samples, in general, showed no maxima in the scattered intensity, (Figure 4.2.8.), just an exponential-type decay from low to high  $Q$ . The only sample to show a maximum in its scattering profile was the PSH50PSD50B copolymer sample, (Figure 4.2.9.). Figure 4.2.10. shows a 'best' fit to a typical set of data obtained for the PSH50PSD50B sample. The PSH50PSD50B sample was the only data set to which a statistically 'good' fit could be obtained. These results are shown in Table 4.2.6..

Figure 4.2.8. Scattering Profile Obtained from PSH20PSD80 Sample at 413K

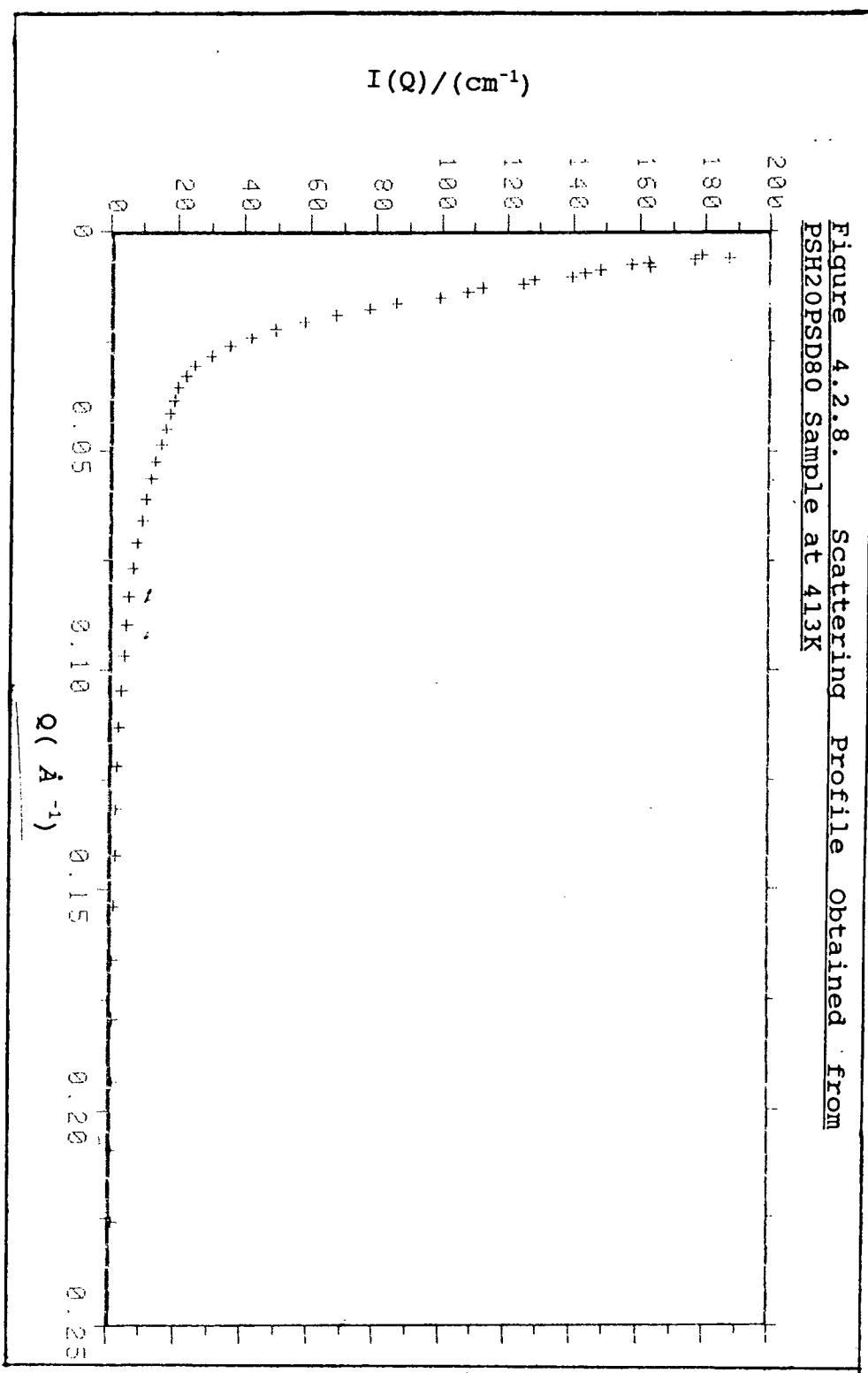


Figure 4.2.9. Scattering Profile for PSH50PSD50B  
Sample at 408K

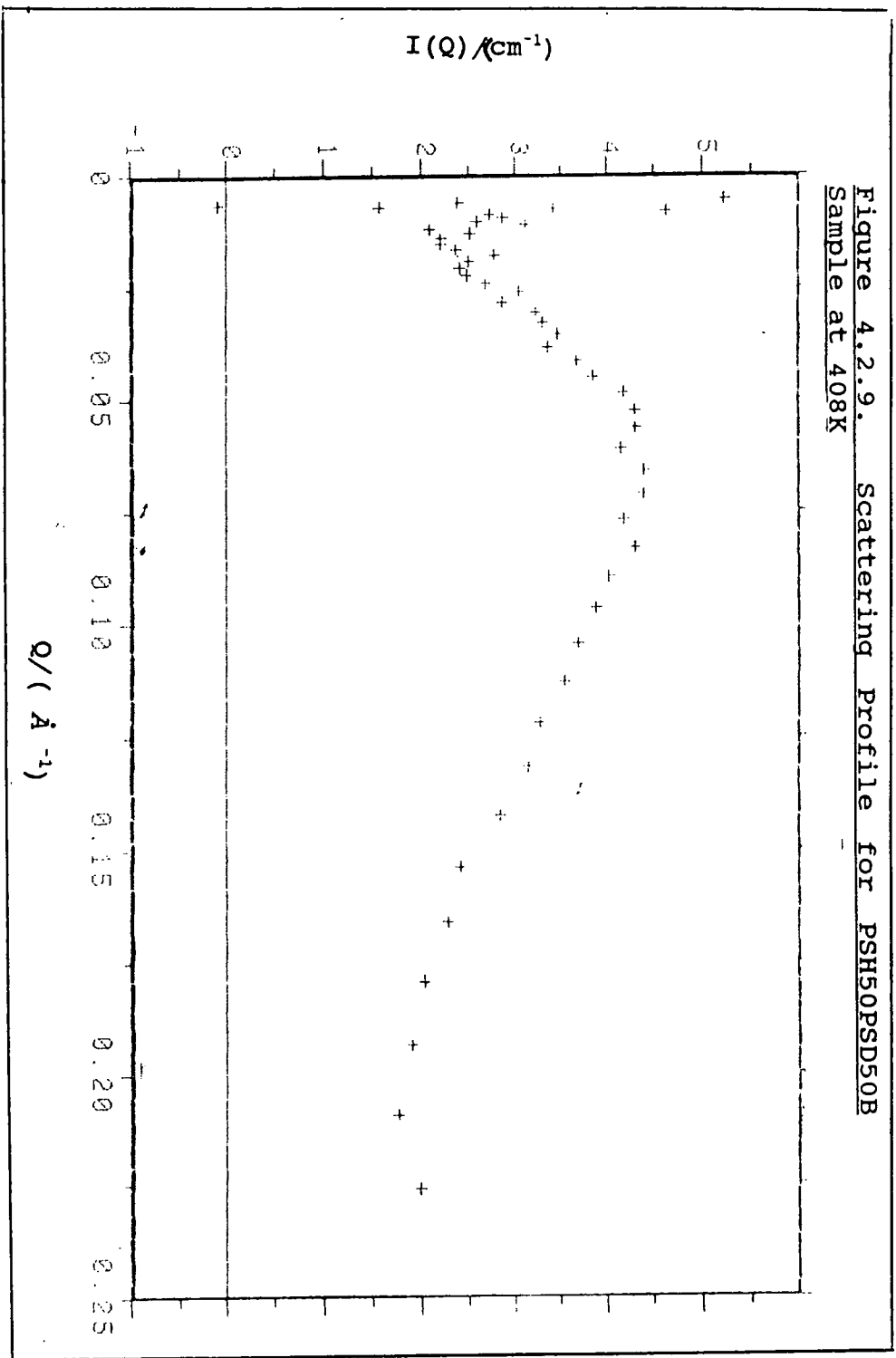


Figure 4.2.10. Scattering profile for PSH50PSD50B  
Sample at 443K showing best fit for data

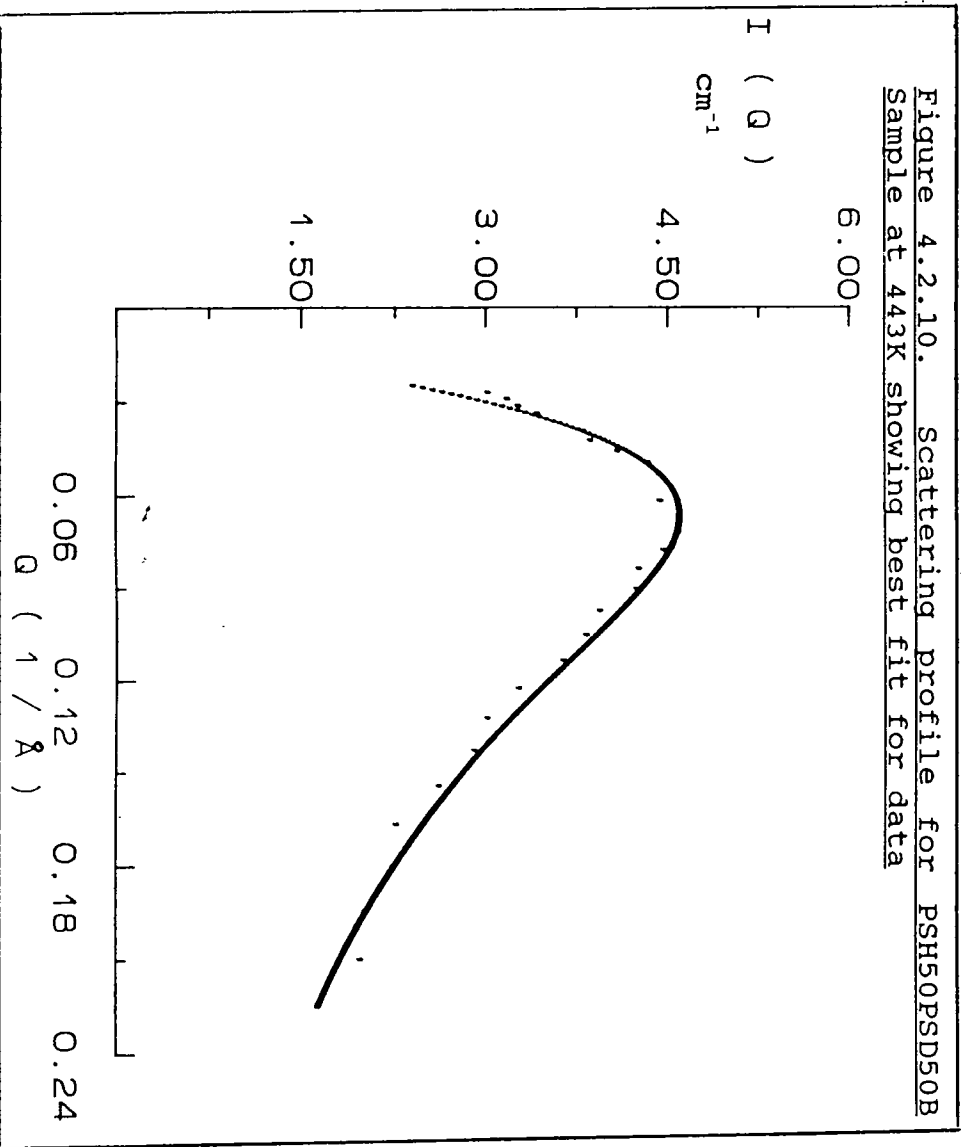


Figure 4.2.11. Plot of  $\chi$  vs.  $1/T$  for PSH50PSD50B  
Sample

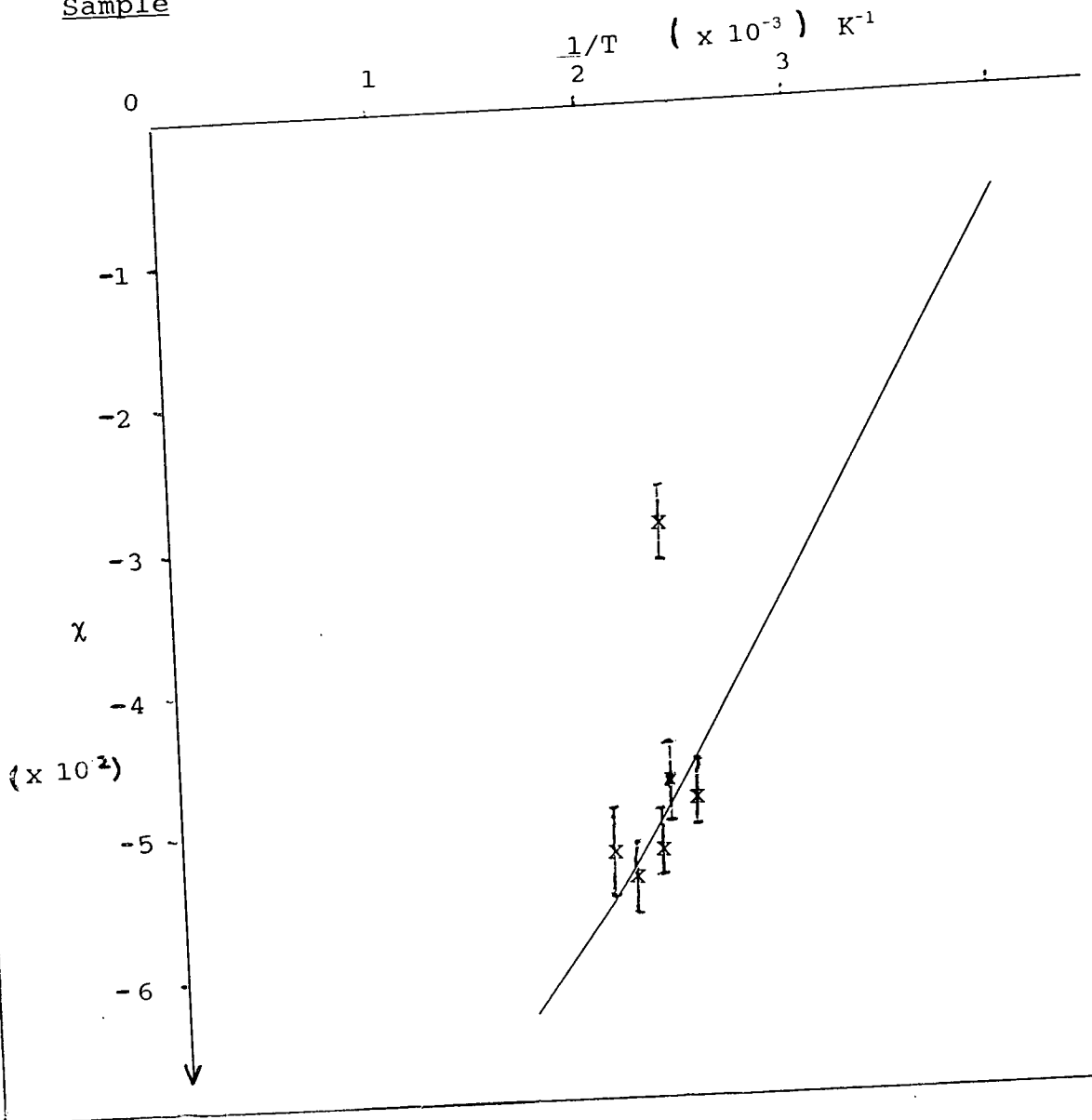


Table 4.2.6. - Results obtained for PSH50PSD50B Copolymer

	Temperature (K)						
	408	413	423	433	443	455	468
Interaction Parameters, $\chi$ ( $\times 10^2$ )	-4.82 $\pm$ 0.31	-4.74 $\pm$ 0.29	-2.86 $\pm$ 0.18	-5.35 $\pm$ 0.39	-5.05 $\pm$ 0.42	-5.47 $\pm$ 0.44	-4.10 $\pm$ 0.31
Radius of gyration, $R_g$ ( $\text{\AA}$ )	121.1	29.5	27.3	28.2	32.4	29.5	29.9

The results were used to plot  $\chi$  vs  $1/T$  for this PSH50PSD50B copolymer to evaluate constants A and B in equation (13). Fig 4.2.11. shows this data and a least squares fit to the data. From this plot the constants A and B were -0.11 and 25.44 respectively. The plots of  $\chi$  vs  $1/T$  in 4.2.6., 4.2.7. and 4.2.10. do not include the values obtained at 423K. The reason for this was that the values obtained for the interaction parameter,  $\chi$ , at this temperature were not consistent with the other results. The anomaly at 423K for both sets of copolymer samples led to an examination of the samples themselves using a Differential Scanning Calorimeter (D.S.C.). No exotherms or endotherms were observed for any of the samples at 423K and no further investigation was possible due to time restraints.

#### 4.2.2. Discussion of Diblock Copolymer Results

This study of two sets of isotopic diblock copolymer samples of polystyrene and deuteropolystyrene showed that, over all temperatures studied, the results obtained indicated that mixing was favoured for the PSH20PSD80, PSH80PSD20 and PSH50PSD50 samples. It should be pointed out that all other diblock copolymer samples did not have a single resolvable peak as had been previously expected. These samples showed a continual decrease in the scattered intensity with  $Q$ . One possible explanation of this phenomenon has been

put forward by Freed et al<sup>13</sup> who stated that the removal of the incompressibility restraint from the RPA theory for polymer molecules could account for the unexpected scattering profile. This work is not yet completed and should, in any case, only affect the  $Q \simeq 0$  intensity not the peak.

Previous work on copolymer systems is somewhat limited. The vast majority of work in this area has concentrated on polymer blends. Recently, Connell et al<sup>13</sup> performed SANS experiments on concentrated deuterostyrene-isoprene (SI) diblock copolymer solutions. The copolymers studied had molecular weight of around 85000 and a styrene weight fraction of 0.19 and 0.38 respectively. These workers found the values of constants A and B in equation (13) to be (-0.073, 40.49) and ( $0.32 \times 10^{-3}$ , 4.71) respectively. These results show that the composition of the copolymer affects the interaction parameter,  $\chi$  since the molecular weights are very similar. The value of the constant A for these two copolymers shows that for the latter, the interaction parameter will always be positive i.e. mixing is not favoured.

From the results obtained for A and B in equation (13) by Connell et al<sup>14</sup> for the first copolymer, the interaction parameter,  $\chi$ , will be negative (mixing is favoured) up to  $T = 555\text{K}$ , and positive (mixing not

favoured) thereafter. At this temperature the system will have degraded (degradation temperature for polystyrene is 500K). From the values of the constants A and B obtained for the copolymer samples PSH20PSD80, PSH80PSD20 and PSH50PSD50B an estimation of the spinodal temperature,  $T_S$ , can be made. In the case of the PSH20PSD80 sample the  $T_S$  is estimated to be around 363K and for the PSH80PSD20 samples, 385K. For the PSH50PSD50B sample the  $T_S$  is calculated to be around 153K. This latter value for the PSH50PSD50B has a very large error associated with it due to the problem discussed earlier in this chapter with regard to the sample seepage from holder. The values of  $T_S$  obtained for PSH20PSD80 and PSH80PSD20, do have a large error associated with the relatively few points used to obtain the values of constants A and B, but do show a close agreement. It is interesting to note that these values are in the same region as the glass transition temperatures,  $T_g$ , for deuteropolystyrene (378K) and polystyrene (363K).

The fact that only three samples, in total, gave data on which further analyses could be carried out meant that constructing a phase diagram for either the low or high molecular isotopic diblock copolymer was not possible. In the case of the high molecular weight system, carrying out the same series of experiments on

an instrument with better resolution in the low  $Q$  region, such as D17, would allow better resolution of the peak in the scattering profiles of these samples. This would be of benefit, for all copolymer compositions, since the scattering profiles obtained from LOQ suggested the presence of a peak in the scattered intensity of all samples. This would allow the phase diagram to be constructed and make the evaluation of constants A and B in equation (13) more accurate for the high molecular weight samples.

For the lower molecular weight samples, no obvious benefit could be obtained from using an instrument such as D17 since the peak position fell within the resolution limits of the LOQ instrument. The real problem to be resolved with these samples is the sample leaking from the sample-holder at all temperatures. Russell et al<sup>15</sup>, however, recently studied a low molecular weight (28000) diblock copolymer of perdeuterated polystyrene and polymethylmethacrylate. These workers reported no problems with sample leakage and found the values of constants A and B in equation (13) to be 0.028 and 3.9 respectively. These results are based on a linear least-squares fit to only three data points and so their accuracy is questionable. These results showed  $\chi$  was positive for all temperatures but more interestingly that the order - disorder transition for these

samples is below the  $T_g$  and therefore not observable. For a 10% increase in the total number of segments  $N$ , the microphase transition temperature was increased by 150K to a temperature where it could be observed. The effect of the polymer molecular weight on the interaction parameter can also be seen from the results obtained for the high and low molecular weight isotopic diblock copolymers of polystyrene in this study. As the molecular weight of the copolymer decreased so the interaction parameter,  $\chi$  became more negative i.e. mixing became more favourable. For the high molecular weight samples Tables 4.2.3. and 4.2.4. showed that as the volume fraction of the deuterated polystyrene in the diblock copolymer increased so mixing became more favourable. Other workers have also reported a molecular weight dependence of the interaction parameter. In conclusion, these studies on isotopic diblock copolymers have shown an Upper Critical Solution Temperature (UCST) for all samples and that mixing was favoured for all samples where calculation of the interaction parameter,  $\chi$  was possible. The values of  $\chi$  obtained were small but they tend to suggest that the assumption that selective deuteration had no effect on the mixing of hydrogenous and deuterated species was valid.

### 4.3. Polymer Blends

#### 4.3.1. Introduction

Alongside these studies of isotopic diblock copolymers of polystyrene a series of experiments were carried out on 50/50 (w/w) homopolymer blends of polystyrene and deuteropolystyrene of equivalent molecular weight to those studied as isotopic diblock copolymers. The characteristics of these samples are shown in Table 4.3.1.

Table 4.3.1. - Characteristics of Homopolymers used in Blends for study on LOO Instrument

	$M_w$ ( $\times 10^{-3}$ )	$M_w/M_n$
PSH100	96.0	1.05
PSD100	90.6	1.17
PSH100B	14.3	1.18
PSD100B	12.8	1.21

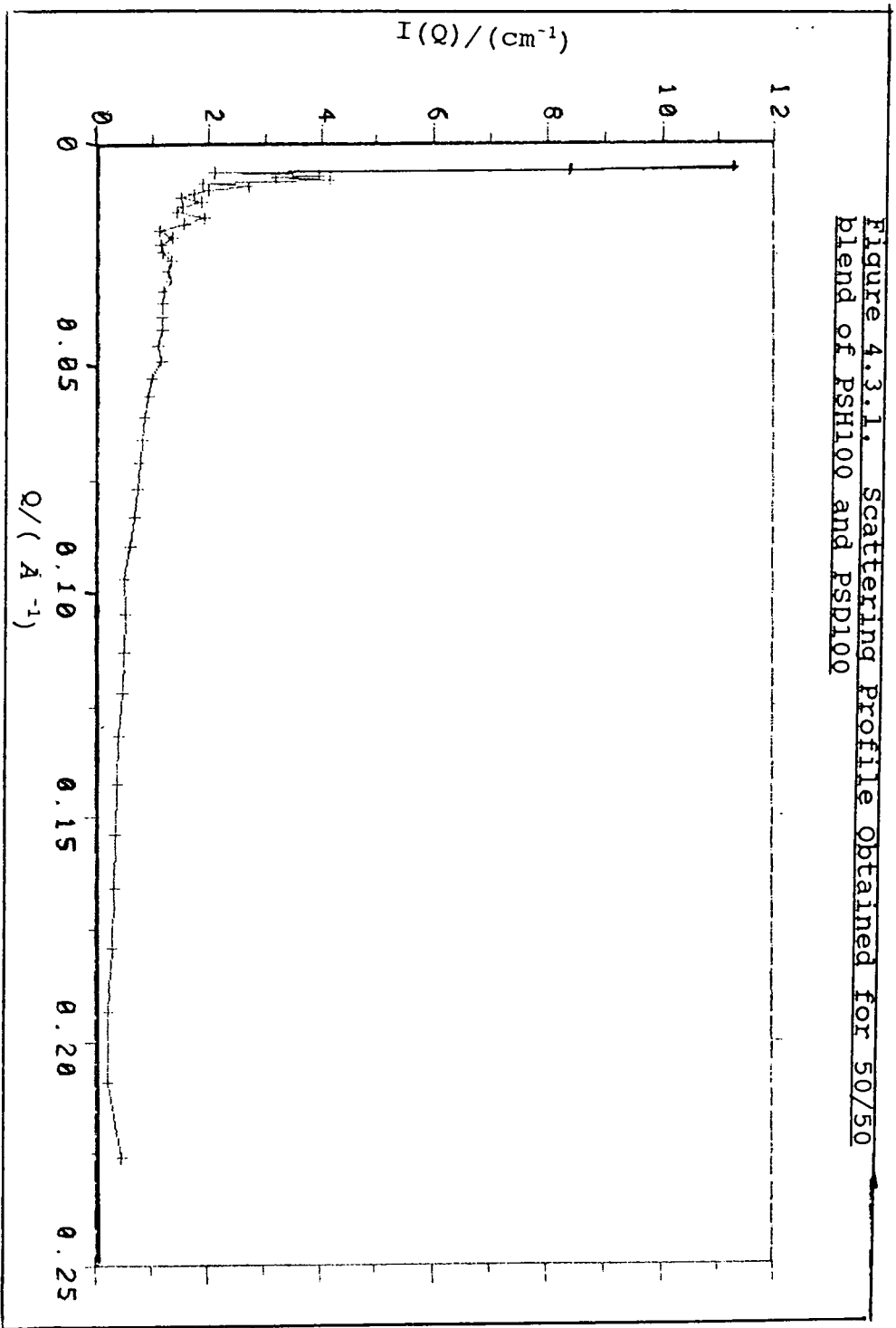
#### 4.3.2. Experimental

The samples were prepared by mixing the equivalent weights of the pure hydrogenous polystyrene and deuterated polystyrene and then pressing the sample into a disc in the same manner as was employed for the isotopic diblock copolymer described in Ch. 2.3.2(b).

#### 4.3.3. Results

The scattering profiles obtained for the polystyrene blends were as expected (Figure 4.3.1.). No peaks in the intensity were observed and the maximum occurred at  $q \approx 0$ . Attempts to fit this data to obtain interaction parameters were made but proved unsuccessful due to limitations of the computer program used.

Figure 4.3.1. Scattering Profile Obtained for 50/50 blend of PSH100 and PSD100



#### Chapter 4 - References

1. Bates, F.S.; Wignall, G.D.; *Macromolecules*, 19, 932, (1986)
2. Bates, F.S. et al; *Macromolecules*, 19, 1938 (1986)
3. Gervais, M.; Gallot, B.; *Makromol. Chem.* 171, 157 (1973)
4. Krause, S. et al; *Macromolecules*, 10, 786 (1977)
5. Widmaier, J.M.; Meyer, G.C.; *Polymer*, 19, 398 (1978)
6. Hadziioannon, G.; PhD Thesis, University of Strasbourg, (1973)
7. Gervais, M.; Gallot, B.; *Makromol. Chem.* 174, 193 (1973)
8. Green, P.F.; Doyle, B.; *Macromolecules*, 20, 2471, (1987)
9. De Gennes, P.G.; 'Scaling Concepts in Polymer Physics', (1979)
10. Leibler, L.; *Macromolecules*, 13, 1602 (1980)
11. Leibler, L.; *Macromolecules*, 22, 1238 (1989)
12. Mori, K.; Tanaka, H.; Hashimoto, T.; *Macromolecules*, 20, 1238 (1989)
13. Freed, K. et al; *Macromolecules*, 23, 255 (1990)
14. Connell, J.G.; Richards, R.W.; *Progr. Colloid and Polym. Sci.*, 80, 180 (1989)
15. Russell, T.P. et al; *Phys. Rev. Letts.* 62, 1852 (1989)

## CHAPTER 5 - NEUTRON REFLECTIVITY STUDIES OF THE ORDERING IN A SERIES OF DIBLOCK COPOLYMER FILMS

### 5.1. Introduction

Most experimental and theoretical work on block copolymers has focussed on the static and dynamic properties of the bulk species. The increasing use of block copolymers as surfactants and adhesives in the biomedical and microelectronics industries respectively has led to an increased interest in the behaviour of copolymers at interfaces.

In this study, a series of three poly(styrene-deuteroisoprene) and three poly(deuterostyrene-isoprene) diblock copolymers covering a range of molecular weights were synthesised. These are characterised in Table 5.1.1. and an account of their syntheses given in ch. 2.4.2. along with the sample preparation before performing reflectometry experiments on the CRISP instrument, Rutherford Appleton Laboratory (RAL), Oxford. A description of the CRISP reflectometer is given in Ch. 2.4.1.

Table 5.1.1. - Sample characteristics of Poly(h-styrene-d-isoprene) (HSDI series) and Poly(d-styrene-h-isoprene) (DSHI series)

SAMPLE	$M_{CP}^{(1)}$	$M_D^{(1)}$	$W_S^{(2)}$
HSDI1	29190	14360	0.527
DSHI1	30680	14850	0.485
HSDI2	95680	50710	0.510
DSHI2	36570	17070	0.490
DSHI3	13100	6470	0.531

(1) - Measured by G.P.C.

(2) - Obtained from weight of styrene used in polymer synthesis.

where:

$M_D$  = molecular weight of the domain - forming part of the copolymer.

$M_{CP}$  = molecular weight of the whole copolymer.

$W_S$  = weight fraction of styrene in each copolymer.

#### 5.1.1. Background

A description of neutron reflectivity is given in Chapter 1. As with Small Angle Neutron Scattering (SANS), neutron reflectivity relies on the very different scattering lengths of hydrogen and deuterium. A basic understanding of the behaviour of copolymers at interfaces and surfaces has become essential as the applications of block copolymers as surfactants and adhesives in industry have increased.

Information on the interfacial region from studies of bulk species using SANS were limited by density fluctuations. This limitation does not apply to neutron reflectivity so that a great deal of work examining surfaces and interfacial regions in chemical compounds have been made. Very few studies of block copolymers near surfaces<sup>1-4</sup> or interfaces<sup>5</sup> have been published. These results have led to an increased interest in utilizing neutron reflectivity to study various copolymer systems. Russell et al<sup>6</sup> studied a poly(styrene-deuteromethylmethacrylate) of low molecular weight (30,000) and a poly(deuterostyrene-methylmethacrylate) of similar molecular weight.

These workers found that both samples formed multilayered films parallel to the surface. The neutron reflectivity profiles both showed several Bragg peaks and, using the multilayered matrix method<sup>7</sup>, a 'fit' to the data was obtained. This showed the films were arranged as lamellar microdomains with an interfacial region of  $54 \pm 2 \text{ \AA}$  width, and uniform layer thicknesses. These results were in close agreement with the theoretical mean-field approach postulated by Fredrickson<sup>4</sup>.

## 5.2. Results and Discussion

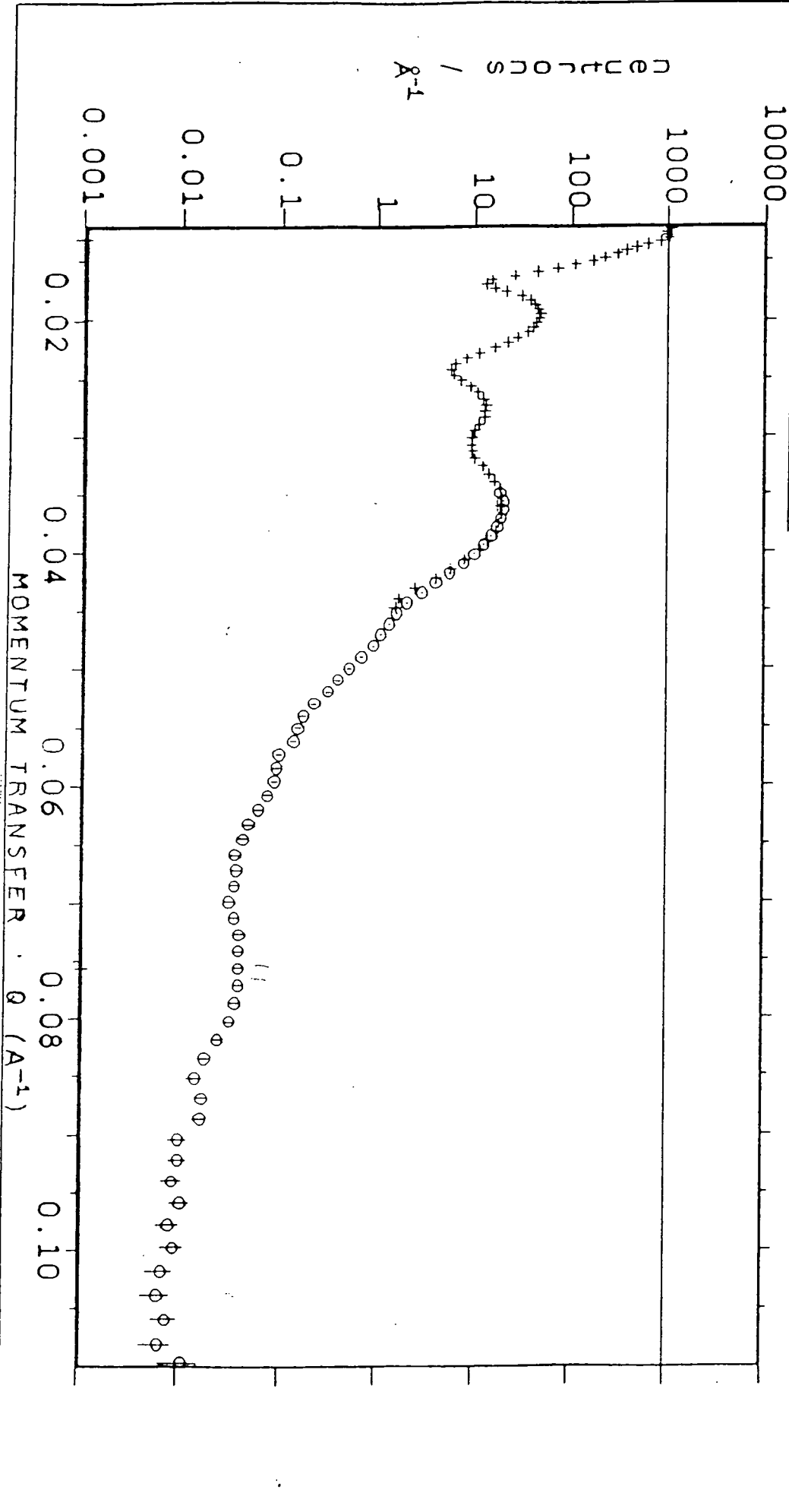
### 5.2.1. Results

The diblock copolymer films on optical flats were not annealed before being used in the reflectivity study. The reason for this was that when the first samples were spun-cast onto optical flats and annealed at 443K for 24 hours in a vacuum oven under nitrogen pressure, the samples went from a smooth layer to a pitted, broken film. This annealing procedure was repeated twice to ensure the first result was not the result of human error or mechanical failure but on each occasion the outcome was the same.

When the next set of spun cast samples were made these were simply placed in a vacuum oven a 333K for 12 hours to remove any excess solvent prior to being taken to R.A.L. for reflectivity studies.

The scattering profiles for each sample were obtained using two grazing angles of incidence for the neutrons,  $0.35^\circ$  and  $1.0^\circ$ , to give, when combined, a  $Q$  range of  $0.005 \text{ \AA}^{-1}$  to  $0.12 \text{ \AA}^{-1}$ . For each sample studied, the scattering profiles showed several maxima (Figures 5.1.1 and 5.1.2). From SANS studies of diblock copolymers<sup>8</sup> the ratio of the lower order Bragg peaks to the primary Bragg peak depends on the copolymer composition Ch. 1. For diblock copolymer with lamellar domain morphology the ratios are 0.5, 0.33, 0.25, 0.02....

-3 Figure 5.2.1 Reflectivity Profile Obtained for DSHI2  
Sample (Unannealed)



-3  
X10  
10000

Figure 5.2.2 Reflectivity Profile Obtained for DSH13  
Sample (Unannealed)

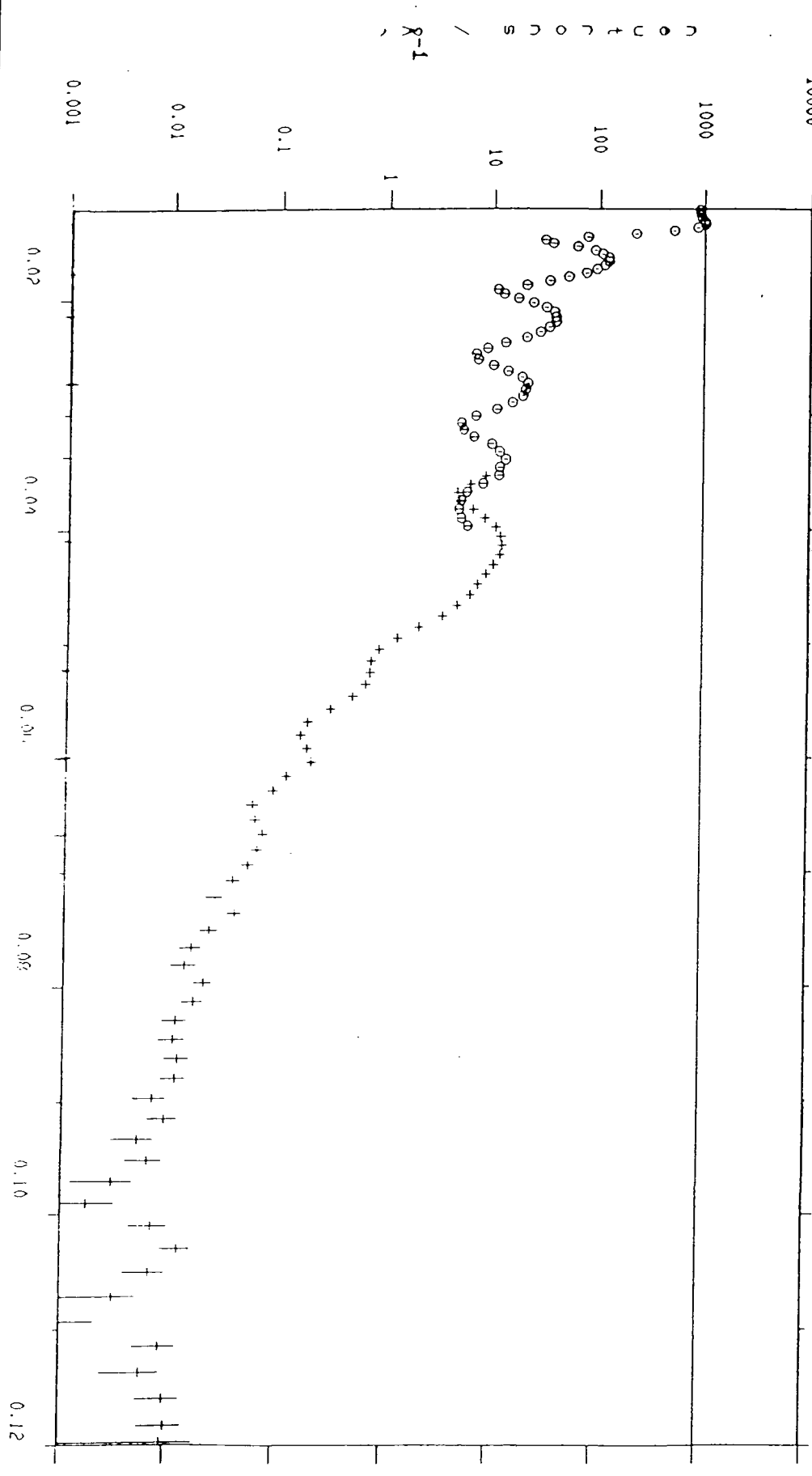


Table 5.2.1. shows the Q value at the maximum for each peak and its corresponding interdomain spacing, d. The theoretical d-spacing calculated from SANS for these samples<sup>9</sup> is shown as  $d_{\text{SANS}}$ . The  $d_{\text{SANS}}$  value is obtained from the relationship:

$$d_{\text{SANS}} = 0.997 M_{\text{CP}}^{0.56} \quad \text{EQ. (1)}$$

Table 5.2.1. shows that each sample showed at least three orders of Bragg peaks which would appear to confirm the lamellar nature of the copolymer films. The presence of other intermediate maxima in the reflectivity profiles of all the samples, except HSDI1, may be due to several factors. Firstly, they may be a result of interference due to regular arrangement of the samples.

Secondly, since the samples were examined without annealing then it cannot be assumed that they were in equilibrium when examined. Consequently several unexpected maxima could be found in the reflectivity profile.

Table 5.2.1. - Corrected Q values for each maximum (Q corr), its corresponding interdomain spacing (d), ratio of lower order peaks to primary peak (d/d<sub>0</sub>) and (d<sub>SANS</sub>) calculated from SANS

SAMPLE	Qcorr (Å)	d (Å)	d/d <sub>0</sub>	d <sub>SANS</sub> (Å)
HSDI1	0.034	184.8	1	315.7
	0.069	91.1	0.49	
	0.106	59.3	0.32	
DSHI1	0.012	523.6	1	324.6
	0.022	285.6	0.54	
	0.033	190.4	0.36	
	0.050	125.7	0.24	
	0.057	110.2	0.21	
	0.064	98.2	0.19	
	0.074	84.9	0.16	
	0.084	74.8	0.14	
HSDI2	0.011	571.2	1	613.7
	0.015	418.9	0.73	
	0.020	314.2	0.55	
	0.027	232.7	0.40	
	0.031	202.7	0.35	

Table 5.2.1. cont.

SAMPLE	Qcorr ( $\text{\AA}$ )	d ( $\text{\AA}$ )	d/d <sub>0</sub>	d <sub>SANS</sub> ( $\text{\AA}$ )
DSHI2	0.015	418.9	1	358.1
	0.024	261.8	0.62	
	0.032	196.3	0.47	
	0.075	83.8	0.20	
DSHI3	0.018	349.1	1	201.5
	0.024	261.8	0.75	
	0.039	161.1	0.46	
	0.059	106.5	0.31	

Finally, these intermediate peaks could indicate that the domain morphology in the sample was not 100% lamellar. To ascertain whether this final possibility was true for the diblock copolymers examined in this study, 'rocking-curve' profiles were obtained as described by Russell<sup>6</sup>. This involved fixing the detector at the angle corresponding to the primary Bragg peak and 'rocking' the sample around the angle of the peak. This moves the scattering vector to off-normal to off-normal positions. The half width at half maximum of the rocking curve obtained includes contributions from instrumental broadening and disorientation of the lamellae. Samples were inclined at 2°, 4°, 6°, 8° to the beam. Figures 5.2.3 and 5.2.4 show the 'normal' and 'rocked' profiles for DSH11 sample. The primary Bragg peak in Figure 5.2.3 is situated at  $0.018\text{\AA}^{-1}$  and for the 'rocked' sample the half width at half maximum occurs at  $0.0185\text{\AA}^{-1}$  indicating near-perfect lamellar domains parallel to the surface over large distances. Thus it may be concluded that the extra maxima in the scattering profile were not caused by the lamellar domain morphology being somewhat less than perfect. This conclusion was reached for all samples studied from examination of the 'rocking curve' profiles obtained. The experimentally obtained data was then fitted by a simulation using the multilayer matrix method<sup>10</sup>. This method states that the segment density profile

Figure 5.2.3 Reflectivity Profile Obtained for DSH11  
Sample (Unannealed) with no incline to beam

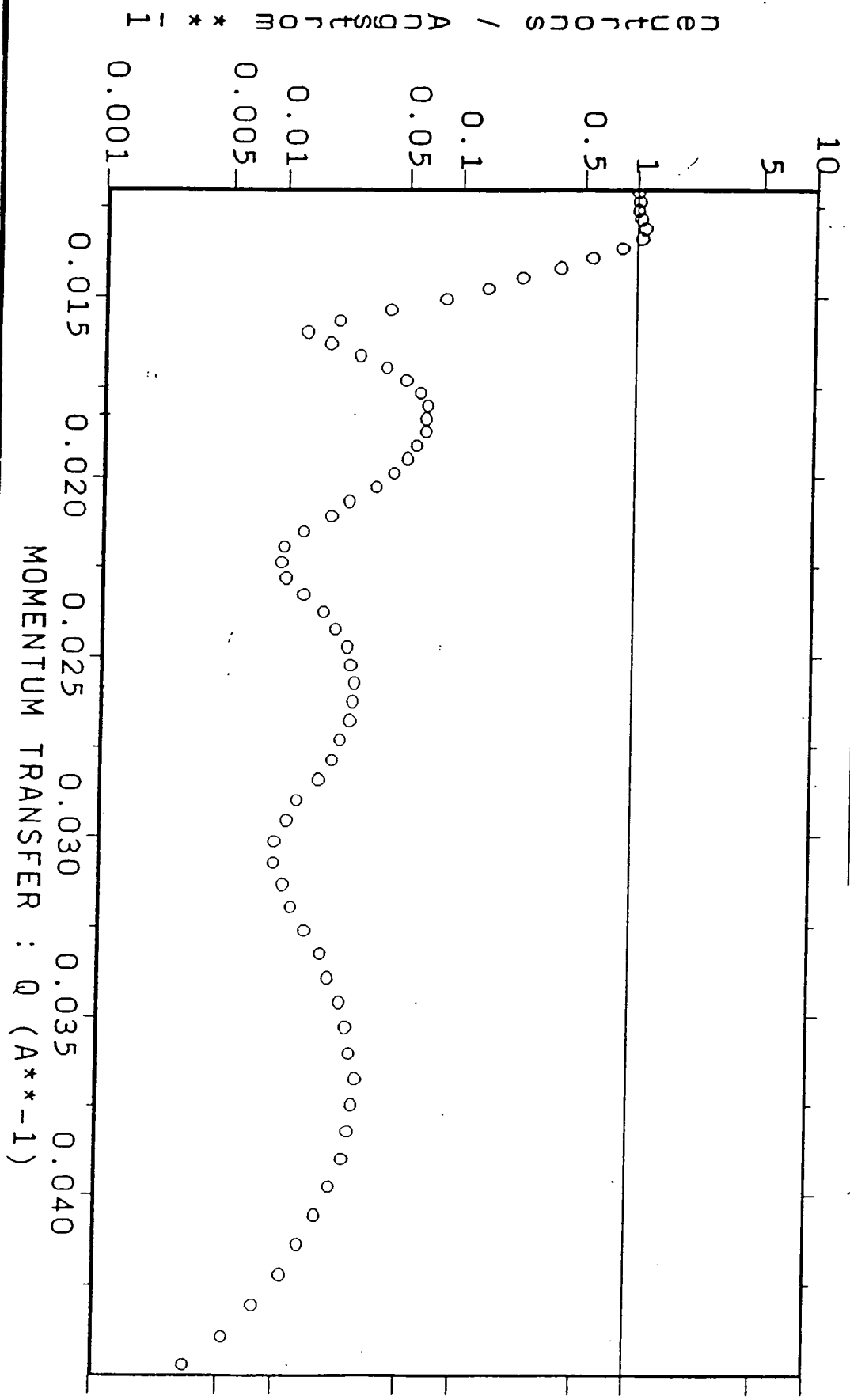
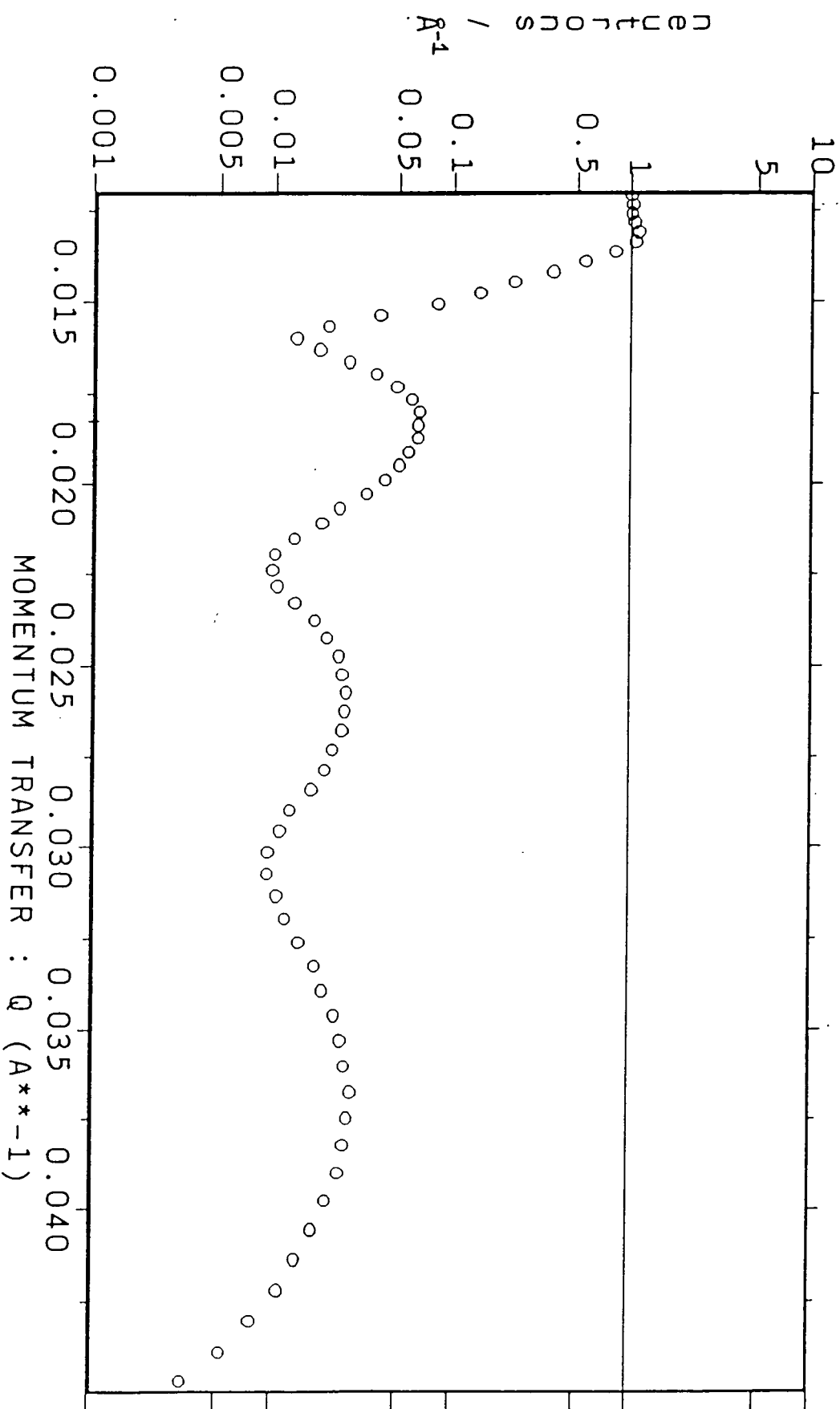


Figure 5.2.4 Reflectivity Profile Obtained for DSH11 Sample (Unannealed) with +2° incline to beam



perpendicular to the free surface can be approximated by a histogram with layers of different scattering length densities. Assuming that the sample films were made up of alternating layers of styrene and isoprene with a degree of mixing between layers, the data was simulated using the L-MULFIT program from the computer simulation programs available at R.A.L.. This simulation used the scattering length density, thickness and the roughness of each layer as variables to arrive at a 'best-fit' to the experimentally obtained data. Figs. 5.2.5 to 5.2.8. show a good agreement between simulation and experiment.

Table 5.2.2 shows the scattering length density ( $\lambda$ ), layer thickness (d) and roughness for each sample. It should be noted that layer number 1 is that at the air-copolymer interface. After studying the unannealed samples, each sample was then annealed at 433K under nitrogen in a vacuum oven and placed in the beam. Figure 5.2.9. shows the reflectivity profile obtained for the annealed and unannealed samples. This showed the loss of almost all order in the poly(styrene-deuteroisoprene) and poly(deuterostyrene-isoprene) samples of similar molecular weight.

Figure 5.2.5 Experimentally (-) and Theoretically (+)  
Obtained Reflectivity Profiles for DSHI2 Sample

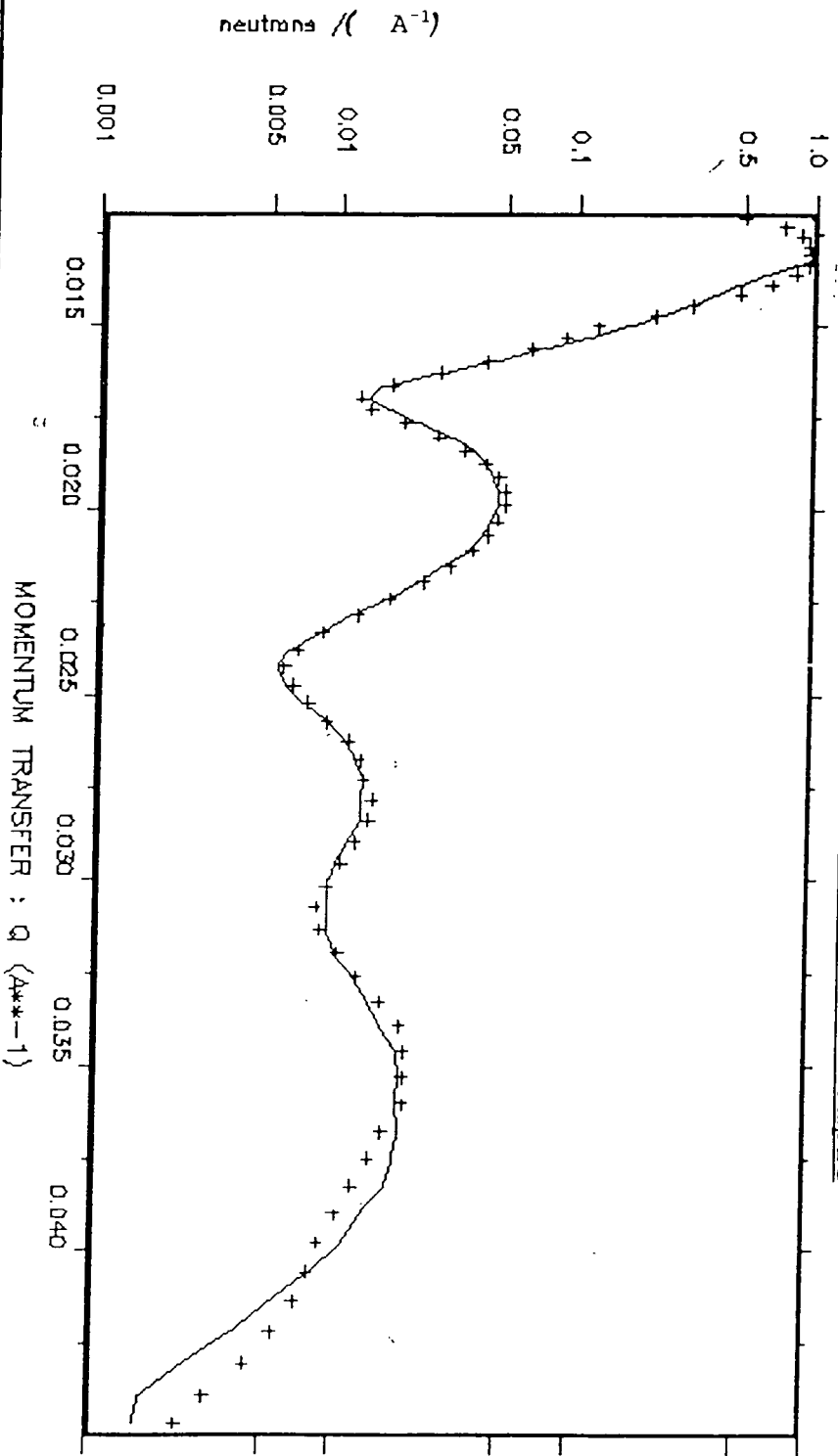


Figure 5.2.6 Experimentally (+) and Theoretically (-) Obtained Reflectivity Profiles for DSH11 Sample

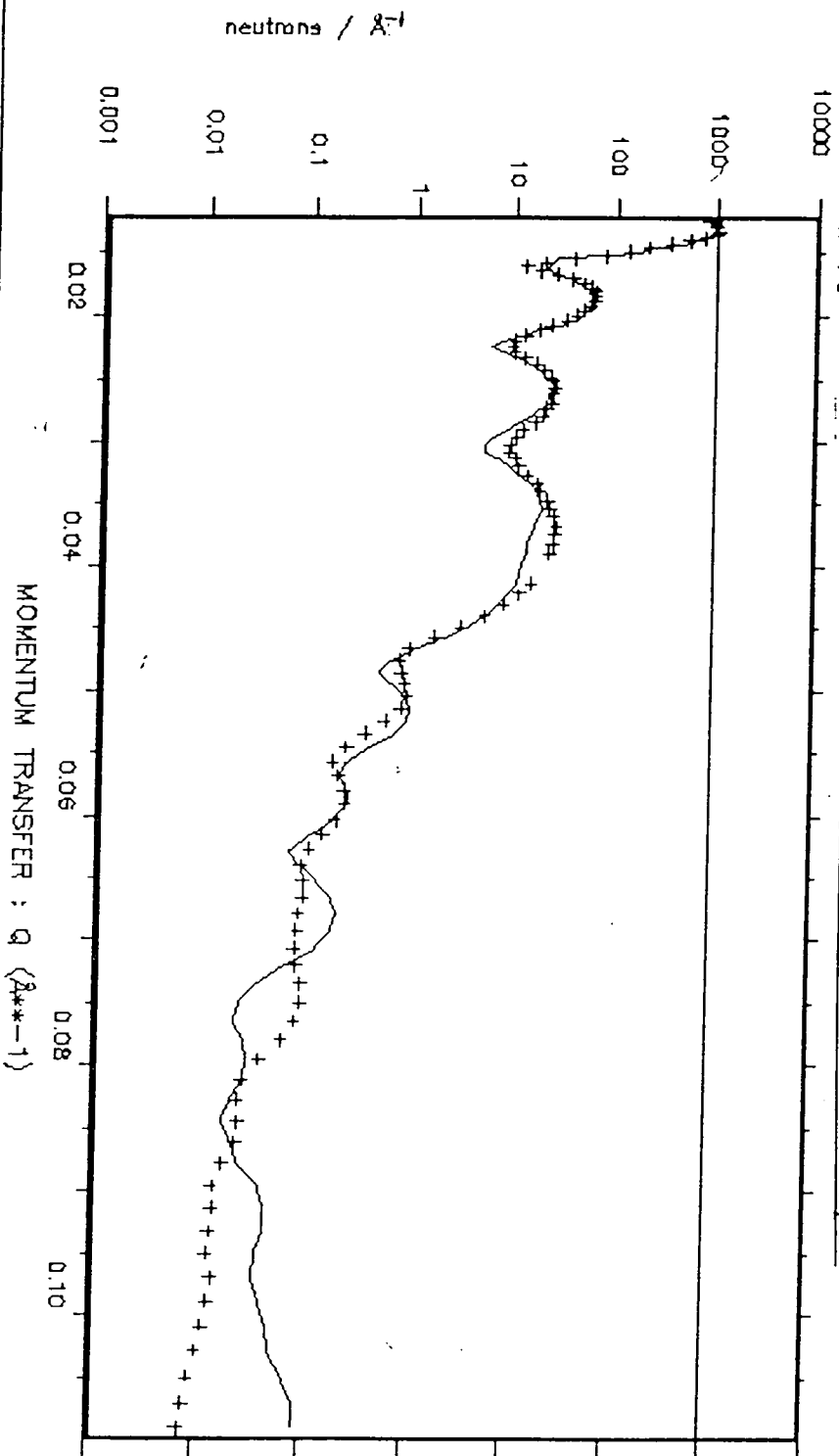


Figure 5.2.7 Experimentally (-) and Theoretically (+) Obtained Reflectivity Profiles for HSD11 Sample

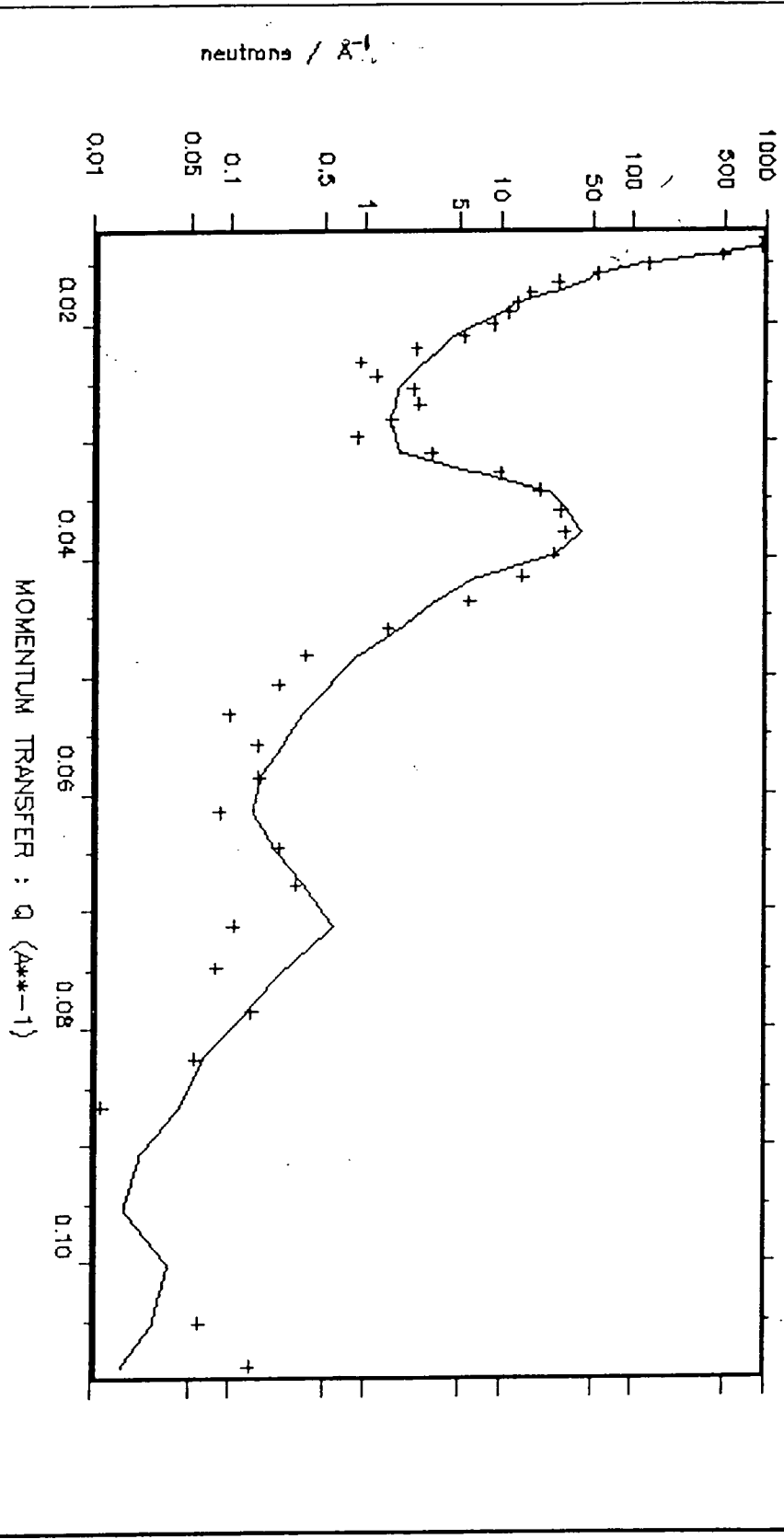


Figure 5.2.8 Experimentally (+) and Theoretically (-) Obtained Reflectivity Profiles for DSH13 Sample

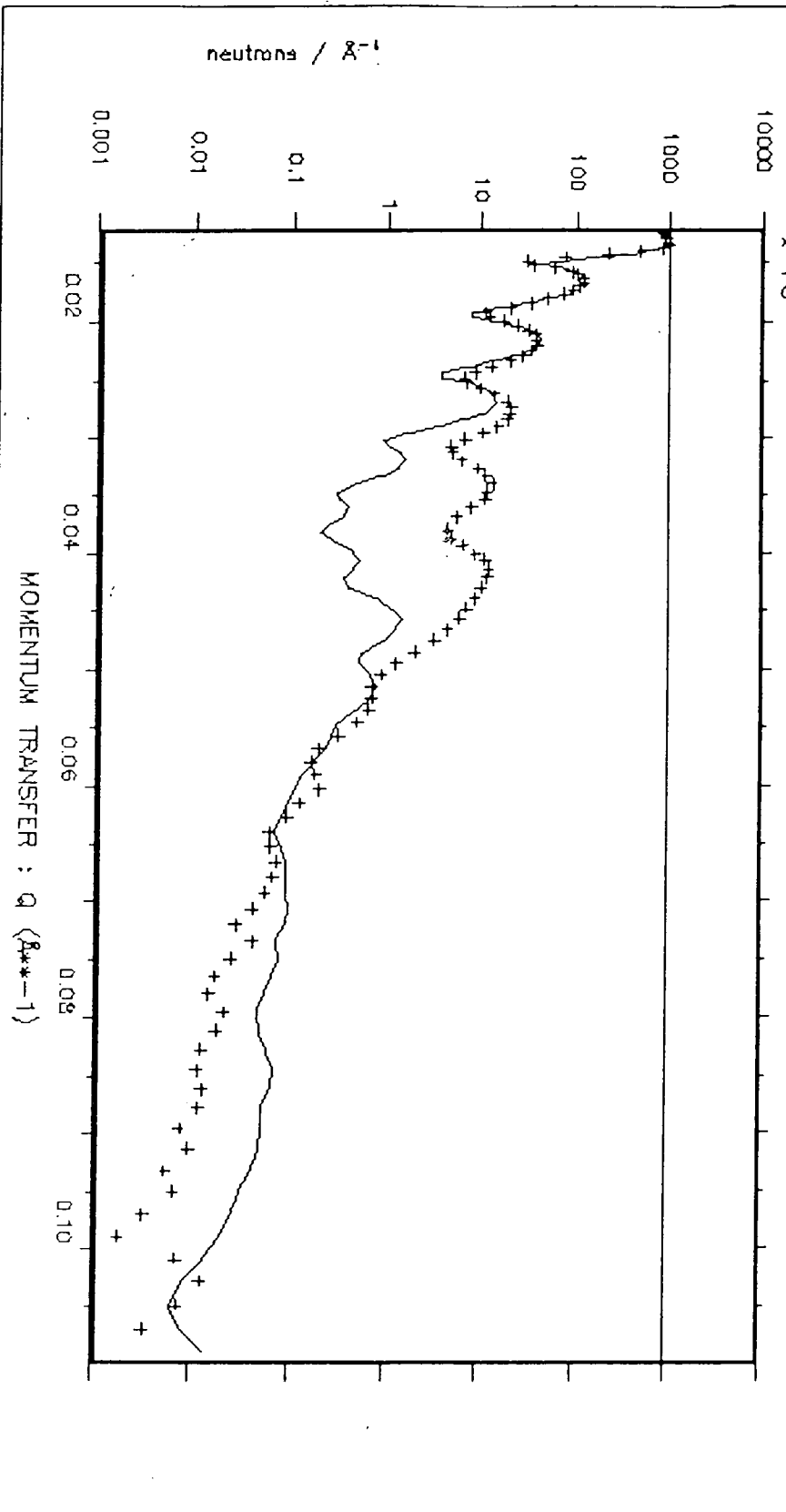


Figure 5.2.9 Reflectivity Profiles for Annealed ( $\phi$ )  
Unannealed (+) DSH12 Diblock Copolymer Sample

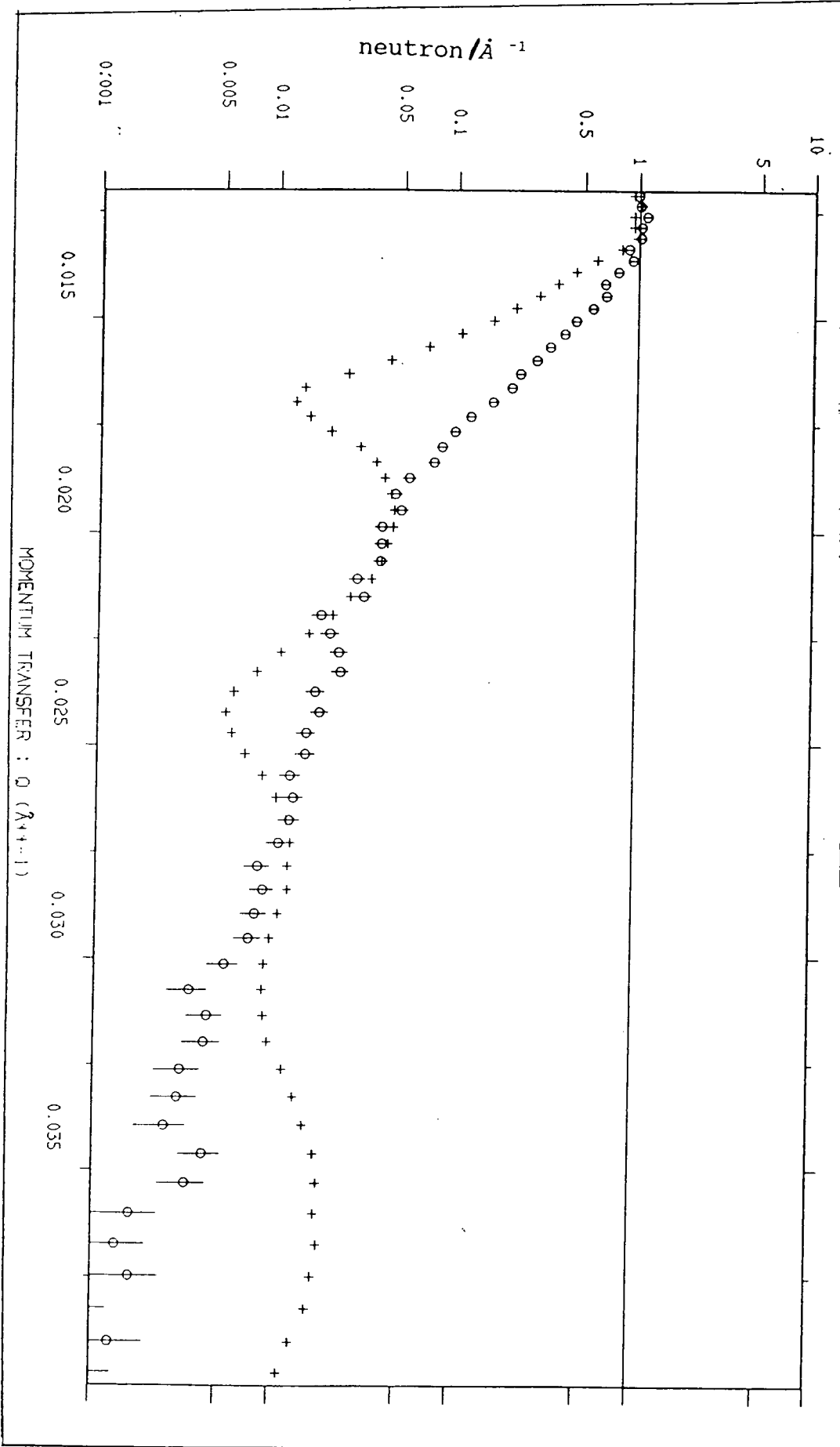


Table 5.2.2. - Layer thicknesses, (d), scattering length densities, ( $\lambda$ ) and roughnesses, (R) of diblock samples obtained from L-MULFIT program

SAMPLE	LAYER NUMBER	d ( $\text{\AA}$ )	$\lambda$ ( $\text{\AA}^{-2}$ ) ( $\times 10^{-6}$ )	R ( $\text{\AA}$ )
HSDI1	1	67.7	1.84	3.0
	2	102.8	0.61	3.0
	3	76.0	2.87	3.0
	4	89.0	0.92	3.1
	5	83.5	3.62	3.1
	6	81.0	0.88	3.1
	7	94.9	3.84	3.0
	8	67.5	1.12	3.0
DSHI1	1	52.3	1.20	5.1
	2	92.3	1.22	5.0
	3	116.7	2.07	5.2
	4	76.6	0.67	5.2
	5	85.4	4.26	5.3
	6	87.0	1.05	5.2
	7	80.7	2.91	5.1
	8	222.7	1.11	5.3
	9	111.8	2.42	5.2
	10	168.5	1.82	5.2

Table 5.2.2. cont.

SAMPLE	LAYER NUMBER	d (Å)	$\lambda$ (Å <sup>-2</sup> ) ( x 10 <sup>-6</sup> )	R (Å)
HSDI2	1	258.0	1.70	2.0
	2	239.6	0.44	2.5
	3	302.5	0.49	2.1
	4	106.6	2.45	2.1
	5	156.3	1.32	2.0
	6	269.9	2.52	2.0
DSHI2	1	62.6	1.47	5.0
	2	93.7	1.13	5.0
	3	119.9	2.80	5.0
	4	84.5	0.70	5.0
	5	87.2	3.19	5.0
	6	83.2	1.19	5.0
	7	78.4	2.46	5.0
	8	214.0	1.11	5.0
	9	100.6	2.17	5.0
	10	178.7	1.73	5.0
DSHI3	1	184.0	2.35	5.1
	2	275.0	1.08	4.9
	3	185.0	1.39	5.1
	4	130.0	0.87	5.0
	5	197.0	0.31	5.1
	6	270.0	1.79	5.1

The layer thicknesses obtained from L-MULFIT simulation in Table 5.2.2. show that for both polystyrene and polyisoprene there was a wide range in value for all samples studied. For the HSDI1 sample where layers 1,3,5,7 are deuteropolystyrene the layer became progressively larger on moving from air to the surface of optical flat and vice-versa for the polyisoprene layer. For the equivalent molecular weight DSHI sample, however, there was no obvious pattern for either the polystyrene or deuterioisoprene layers thicknesses.

In the case of the HSDI2 and DSHI2 samples there was no obvious pattern to the layer thickness similar to that found for the DSHI1 samples.

The DSHI3 sample, however, showed a uniform deuterostyrene layer of between 184Å to 197Å but with no similar uniformity for polyisoprene layers.

The scattering length densities for each layer calculated using L-MULFIT program showed, on a general inspection, that the polyisoprene and polystyrene layers in each sample were not pure but contained some mixing. Table 5.2.3. shows the scattering length densities of the various polystyrene and polyisoprene constituents as well as that for the solvent, toluene. It may be assumed that the polystyrene layer at the surface would incorporate some air ( $\lambda_{air}=0$ ) which would decrease the measured scattering length density but the presence of air beyond this first layer was

improbable. The presence of relatively large amounts of solvent was also unlikely since the samples had been placed in a vacuum oven at 333K for 12 hours which would have removed most of the excess solvent.

Table 5.2.3. - Scattering Length Density ( $\lambda$ ) Of the Constituents of Diblock Copolymers and Toluene

Constituent	Mean Scattering Length Density ( $\lambda$ ) ( $\text{\AA}^{-2}$ )
Polystyrene	$1.35 \times 10^{-6}$
Deuteropolystyrene	$5.73 \times 10^{-6}$
Polyisoprene	$0.295 \times 10^{-6}$
Deuteropolyisoprene	$6.86 \times 10^{-6}$
Toluene	$1.09 \times 10^{-6}$

The possibility remained, however, that some solvent remained trapped in each layer or at the interfaces as well as the possibility that some degree of mixing occurred between copolymer substituents. The latter would appear most unlikely due to the different chemical natures of the substituents. The extent of air penetration into block copolymer layers is a reasonable assumption for the first layer but beyond this seems much less likely. Of these possibilities, Fredrickson et al<sup>11</sup> put forward a theory which showed that solvent collects at interfaces in A-B diblock copolymers and screen unfavourable A-B interactions. The calculated scattering length density ( $\lambda$ ) for each

layer of each sample shown in Table 5.2.1 (except layer 1) can be described as:-

$$\lambda = \phi_s \lambda_s + \phi_c \lambda_c \quad \text{EQ. (2)}$$

where:

$\lambda_s$  = scattering length density of solvent (toluene)

$\lambda_c$  = scattering length density of layer constituent

$\phi_s$  = weight fraction of toluene

$\phi_c$  = weight fraction of layer constituent

$$\phi_c = 1 - \phi_s$$

The first layer was excluded since this layer would also have some air trapped within it. The results obtained using equation (2) in Table 5.2.4. showed a large proportion of solvent incorporated with each layer or the result could not be calculated since the experimentally obtained scattering length density was less than that of pure solvent and pure copolymer constituent respectively. For the former case, the results do not appear realistic since the amount of solvent present in these layers would have led to a 'wet' sample which was clearly not the case on physical examination of the sample which had been placed in a vacuum oven at 333K for 12 hours.

The lack of success with the solvent penetration approach above led to the exploration of the possibility of a less likely option. In this case, the possibility of there being a degree of mixing

between polystyrene and polyisoprene constituents. Using the same approach as described in equation (2) the degree of mixing in each layer was calculated using equation (3)

$$\lambda = \phi_s \rho_s + (1 - \phi_s) \rho_i \quad \text{EQ. (3)}$$

where:

$\rho_i$  = scattering length density of polyisoprene

$\rho_s$  = scattering length density of polystyrene

$\phi_s$  = weight fraction of polystyrene

These results are shown in Table 5.2.5 and, as previously, they show that this approach was not completely successful as some layer compositions were not calculable using equation (3). For those layers where a result was obtained, only three layers within all samples studied were made up of one pure constituent. In all other cases the layers were made

Table 5.2.4. - Weight Fractions of Polystyrene, Polyisoprene and Solvent in each Layer for Diblock Copolymers Studied

SAMPLE	LAYER NO.	WEIGHT FRACTION OF POLYISOPRENE	WEIGHT FRACTION OF POLYSTYRENE	WT. FRAC'N OF SOLVENT
HSDI1	2	-	N/C	N/C
	3	0.31	-	0.69
	4	-	N/C	N/C
	5	0.44	-	0.56
	6	-	N/C	N/C
	7	0.48	-	0.52
	8	-	0.12	0.88
	DSHI1	2	N/C	-
3		-	0.21	0.79
4		0.53	-	0.47
5		-	0.68	0.32
6		0.05	-	0.95
7		-	0.39	0.61
8		N/C	-	N/C
9		-	0.29	0.71
10		N/C	-	N/C

Table 5.2.4. cont.

SAMPLE	LAYER NO.	WEIGHT FRACTION OF POLYISOPRENE	WEIGHT FRACTION OF POLYSTYRENE	WEIGHT FRAC'N OF SOLVENT
HSDI2	2	-	N/C	N/C
	3	N/C	-	N/C
	4	-	0.24	0.76
	5	0.88	-	0.12
	6	-	0.25	0.75
DSHI3	2	N/C	-	N/C
	3	-	N/C	N/C
	4	N/C	-	N/C
	5	-	0.98	0.02
	6	N/C	-	N/C
DSHI2	2	N/C	-	N/C
	3	-	0.30	0.70
	4	0.49	-	0.51
	5	-	0.36	0.64
	6	N/C	-	N/C
	7	-	0.24	0.76
	8	N/C	-	N/C
	9	-	0.19	0.81
	10	N/C	-	N/C

Table 5.2.5 - Composition of Layers for Diblock Copolymers

SAMPLE	LAYER NUMBER	WT. FRAC'N	
		STYRENE	ISOPRENE
HSDI1	2	>1.0	<0.0
	3	0.74	0.26
	4	>1.0	<0.0
	5	0.59	0.41
	6	>1.0	<0.0
	7	0.55	0.45
	8	>1.0	<0.0
	DSHI1	2	0.17
3		0.33	0.67
4		0.07	0.93
5		0.73	0.27
6		0.14	0.86
7		0.48	0.52
8		0.15	0.85
9		0.39	0.61
10		0.28	0.72
HSDI2		2	>1.0
	3	>1.0	<0.0
	4	0.8	0.2
	5	1.0	0.0
	6	0.79	0.21

Table 5.2.5. cont.

SAMPLE	LAYER NUMBER	WEIGHT FRACTION STYRENE	WEIGHT FRACTION ISOPRENE
DSHI2	2	0.15	0.85
	3	0.46	0.54
	4	0.07	0.93
	5	0.53	0.47
	6	0.17	0.83
	7	0.40	0.60
	8	0.15	0.85
	9	0.35	0.65
	10	0.26	0.74
	DSHI3	2	0.14
3		0.20	0.80
4		0.11	0.89
5		0.0	1.0
6		0.28	0.72

up of a mixture of polystyrene and polyisoprene up to 50:50 mix.

In view of the two sets of results obtained using equations (2) and (3) it is clear that neither fully described the copolymer samples. The only feasible explanation was that the copolymer had adopted a non-equilibrium conformation which was disturbed when the samples were annealed and attempted to attain their equilibrium conformation.

The roughnesses,  $R$ , shown in Table 5.2.2. were an indication of the diffuse interface value given by:-

$$t = \sqrt{12}\sigma$$

where:

$t$  = diffuse interface thickness,  $\text{\AA}$

$\sigma$  = Roughness,  $\text{\AA}$

For the samples examined in this study the interfacial thicknesses were all in the range  $7.0\text{\AA}$  to  $18.4\text{\AA}$  which is similar to that found by Richards and Thomason<sup>13</sup> on a similar diblock copolymer using SANS. The nature of this diffuse interfacial layer was the major difference between the statistical dynamic theories of Meier<sup>14</sup> and Helfand. Helfand<sup>15,16</sup> and co-workers assumed that the interfacial layer, where mixing of the components takes place, was very small compared to the interdomain separation. Meier<sup>14</sup> derived relationships between domain dimensions and the molecular weight of

the domain - forming component,  $M_D$ . The results of this study, however, for the roughness and the diffuse interfacial thickness must be by the results obtained for the composition of the copolymer layers which proved inconclusive but did suggest that layers were formed of 'mixed' polystyrene and polyisoprene components.

In conclusion, the results obtained in this neutron reflectometry study were unique since they showed an ordered lamellar structure for the unannealed samples but a near complete loss of order on annealed samples. Thomason<sup>17</sup> suggested that the non-equilibrium results found in a study of styrene-isoprene diblocks that the domains may have been "locked" into non-equilibrium positions by some mechanism. For the diblock copolymers used in this study, the sample could have adopted a non-equilibrium conformation when cast which, on annealing, attempted to attain an equilibrium conformation. This rearrangement may have been hindered by the "locked" nature of the unannealed sample leading to the loss of order in the samples. This was only one possible explanation for the problems encountered with annealed samples. For all other copolymer films studied using reflectivity, no worker's have reported any problems on annealing samples.

Russell and coworkers<sup>6</sup> studied a polystyrene - deuteromethylmethacrylate diblock copolymer which,

after annealing, showed three Bragg peaks and was equivalent to alternate polystyrene and deuteromethylmethacrylate layers with partial mixing of components and a diffuse interfacial layer of magnitude  $54 \pm 2 \text{ \AA}$ . This result and those obtained for the correlation length and the period by Russell were consistent with the thermodynamic theory put forward by Fredrickson<sup>4</sup>. Reflectivity studies on block copolymer films were limited to the work carried out by Russell and the work described in this chapter. Higgins et al<sup>18</sup> studied polymer films using neutron reflectivity and obtained a similar set of results to those found by Russell in that they concurred with current thermodynamic theory.

The results obtained for the polystyrene-polyisoprene diblock copolymer samples are, in effect, unique. They cannot be directly compared with other workers results due to the question over their adoption of an equilibrium conformation before annealing.

Of the various possibilities put forward to explain the results obtained, the most plausible would appear to be a 'pseudo-equilibrium' existed in the samples which, when the samples were annealed, was lost as was the order in the system.

The overall layer thicknesses when measured by neutron reflectometry were in close agreement to those measured on the DEKTAK instrument prior to studies on the CRISP reflectometer. (Table 5.2.6.).

Table 5.2.6. - Layer Thickness from DEKTAK Measurement and L-MULFIT Simulations

SAMPLE	OVERALL THICKNESS (nm)	
	DEKTAK	L-MULFIT
HSDI1	-	66.24
HSDI2	130.00	133.29
DSHI1	115.00	109.90
DSHI2	105.50	110.28
DSHI3	-	124.10

## Chapter 5 - References

1. Thomas, H.R.; O'Mally, J.J.; *Macromolecules*, 12, 323, (1979)
2. Hasegawa, H.; Hashimoto, T; *Macromolecules*, 18, 589, (1985)
3. Henkee, C.S.; Thomas, E.L.; Fetters, J.L.; *J. Mater. Sci.*, 23, 1685 (1988).
4. Fredrickson, G.H.; *Macromolecules*, 20, 2535 (1987).
5. Noolandi, J.; Hong, K.M.; *Macromolecules*, 17, 1531 (1984).
6. Russell, T.P.; Anastasiadis, S.H. et al, *Phys. Rev. Letts.*, 62, (16), 1852, (1989).
7. Werner, S.A.; Klein, A.G.; Neutron Scattering edited by D.L. Price and K. Skold (Academic, New York, 1984).
8. Davidson, N.D.; PhD Thesis, Strathclyde University, (1984).
9. Thomason, J.L.; Richards, R.W.; *Macromolecules*, 16, 982, (1983).
10. Parratt, L.G.; *Phys. Rev.* 54, 359, (1954).
11. Fredrickson, G.H.; Leibler, L.; *Macromolecules*, 22, 1238, (1989).
12. Thomason, J.L.; Richards, R.W.; *Polymer*, 24, 275, (1983).
14. Meier, D.J.; *J. Polym. Sci., Part C*: 26, 81, (1969).

15. Helfand, E.; *Macromolecules*, 9, 879, (1976).
16. Helfand, E.; *Macromolecules*, 8, 552, (1975).
17. Thomason, J.L.; Richards, R.W.; *Macromolecules*, 18, 452, (1985).
18. Higgins, J.S. et al, *Polymer*, 29, 1923, (1988).

## CHAPTER 6 - GENERAL DISCUSSION

This study has been mostly devoted to using SANS technique to study block copolymer systems. The block copolymers studied were diblock poly(styrene-isoprene) and triblock poly(styrene-isoprene-styrene) respectively. These samples were synthesised by anionic polymerisation as described in Chapter 2 to give block copolymers with narrow molecular weight distributions.

The triblock samples were used to examine the effect of uniaxial deformation on the central polyisoprene block. In order that the polyisoprene block could be examined, the scattering due to the ordering of the polystyrene domains was eliminated using the 'contrast-matching' technique (Ch. 1). This technique proved quite successful on all triblock samples studied.

The first two sets of triblock copolymers studied using SANS technique, S15150 and S15150B respectively, did not show the expected anisotropy when subjected to extension (Ch. 3.1.) but did show a non-affine increase in the calculated radius of gyration,  $R_g$ , as the elongation ratio increased. The molecular weights calculated from the scattering data for these samples were around 30% below that calculated from G.P.C. measurement (Ch. 3.2). This fact, combined with the tacky nature of the S15150 and S15150B samples led to

the conclusion that the deuterioisoprene had degraded in these samples. The molecular conformation in these samples was examined using Kratky Plots and showed two maxima in the LOQ region for both sets of samples indicating that the orientation was the same in the S15150 and S15150B samples respectively.

The presence of the two peaks, however, could not be attributed to any known molecular configuration.

A third series of triblock copolymers were synthesised by Polymer Labs (Ch. 3.3) but instead of cylindrical polystyrene domains, as had been the case for the S15150 and S15150B, these had spherical polystyrene domains. In contrast to the S15150 and S15150B samples, these spherical samples, SPH150, were anisotropic on elongation (Ch. 3.3) and, furthermore, parallel to the stretch direction the deformation was affine for all extensions studied. The latter was not what had been expected since no other workers had obtained such results for block copolymer systems studied. Perpendicular to the stretch direction, the scattering obtained for the SPH150 series was non-affine and similar results have been obtained by other workers (Ch. 3.3) working on other block copolymer systems.

The SANS technique is based on the very different scattering obtained from hydrogen and deuterium molecules (Ch. 1). It also relies on the assumption that there is no excess free energy of mixing when the

deuterated and hydrogenous species' are mixed. Bates and co-workers, however, reported a small positive interaction parameter for a polystyrene system which, if correct, would mean that this would have to be accounted for in all SANS studies. In order to ascertain if this correction would be necessary, it was decided to examine an isotopic diblock copolymer of polystyrene of various compositions and molecular weights (Ch. 4). For the higher molecular weight series, the peak in the scattering data was not sufficiently resolved in most cases to allow a statistically significant interaction parameter,  $\chi$ , to be calculated. In those samples where the peak was sufficiently resolved to allow a 'fit' to be obtained with some statistical significance, a small negative interaction parameter was obtained for all temperatures studied, indicating that mixing was favoured for all these temperatures.

For the low molecular weight series, most of the samples did not show a resolvable peak. For those that did the values of  $\chi$  calculated were small and negative for all temperatures studied. The differences in the interaction parameters calculated for the high and low molecular weight series were due to a molecular weight dependence of the interaction parameter which had been reported by workers for other copolymer samples (Ch. 4).

The nature of the polymer-polymer interface was

examined in a reflectivity study on a series of styrene-isoprene diblock copolymers. These samples were not annealed prior to examination since the samples broke up and lost all their ordering when annealing was attempted. The unannealed samples showed several orders of Bragg peaks when studied on the CRISP reflectometer (Ch. 5) and some interference peaks. These reflectometry profiles were 'fitted' using a computer simulation which resulted in a layer thickness and a scattering length density being obtained for each layer. These showed that there was some residual solvent trapped within the substituent layers and that there was some mixing of layers. These results, however, must be tempered by the fact that the samples had not been annealed and so cannot be considered to have been at equilibrium.

A broad outline of what has been obtained in this SANS study of polymer systems has been given previously. The scope for future work based on these results is great. For the deformation study (Ch. 3), the SPH150 sample could be examined at extension ratios beyond those studied here to determine at what point, if any, the scattering parallel to the stretch direction becomes non-affine. Secondly, the apparent degradation of the S15150 and S15150B samples means that similar copolymers should be synthesised and used in a SANS study of deformation. This would allow data to be gathered for the effect of deformation on the central

polyisoprene block in a triblock copolymer with cylindrical styrene domains and enable comparison with the SPH150 data. For extruded samples studied a better design of extrusion apparatus is required, if any useful data is to be obtained.

For the isotopic diblock copolymers of polystyrene some time on the D11 Spectrometer could be utilised to resolve the peaks obtained for the higher molecular weight series. In the case of the lower molecular weight series, attempts to solve the leakage problem from the sample holder, would allow quantitative results to be obtained.

The reflectometry results obtained for the diblock copolymer obtained from the CRISP instrument (Ch. 5) require some examination of what happens to these samples when they are annealed that causes them to lose almost all their ordering. These are some areas where future work could be done to expand upon the work done in this study.

\$DEBUG

C

C

PROGRAM RPOLLY

C

C S.A.N.S. ANALYSIS PROGRAM

C WATER RUN SET FIRST FOR ALL RUNS

C LOQ: READS DATA NORMALISED FOR EMPTY CAN, TRANSMISSIONS,  
C SAMPLE THICKNESS AND MONITOR COUNTS.

C GRENOBLE : READS REGROUPED DATA FROM RCARD files i.e. Q,I,erri

C THE ERRORS READ IN FROM RNILS OR HREG REGROUPING PROGRAMS  
ARE

C STATISTICAL ESTIMATES OF THE STANDARD DEVIATION

C CALCULATED AS :  $\sqrt{\text{NO. OF COUNTS AT RADIUS , R}/\text{NO. OF CELLS}}$

c

c Corrected data are written automatically to an RCARD format file with  
c extension .crd.

c There is an option to write SPOLLY files with extension .LST

c

INTEGER RUNNUS,RUNUB,FAULT

INTEGER ECNO1,ECNO2,RUNNUB

REAL TRANS,TRANW,TAIL,ETAIL

CHARACTER\*25 TITLE

CHARACTER\*12 FTIT,FNAME,crdfil

CHARACTER\*1,CHH,SH,REP

LOGICAL L1,L2,L6,M2

LOGICAL L15,L12,L16

DIMENSION Q(500),W(500),EW(500),WB(500),EWB(500)

DIMENSION S(500),ES(500),SB(500),ESB(500)

DIMENSION SINV(500),SQ2(500),Q2(500),ERSC(500)

DIMENSION ERR(500),ERR1(500),NC(500)

DIMENSION QN(500)

DIMENSION ESINV(500),QLN(500),ERSC1(500),BG(500),ERBG(500)

DIMENSION SL10(500),SC3(500),BG1(500),ERBG1(500)

DIMENSION SL(500),SC(500),SC1(500),SC2(500)

C\*\*\*\*\*

\*\*

C SET UP SOME DEFAULT VALUES FOR USE LATER MAYBE

C FACTM =FACTOR TO MULTIPLY EACH BACKGROUND RUN BEFORE  
ADDING

C THEM TOGETHER

C BG FACT =FACTOR TO MULTIPLY COMBINED BACKGROUND BEFORE  
SUBTRACTION

C FROM SAMPLE INTENSITY

C ABCAT =ABSOLUTE CROSS SECTION FACTOR TO CONVERY DATA  
C TO ABSOLUTE UNITS IN 1/CM.

C CONCENTRATION OF SCATTERING SPECIES

102 rep='n'

FACTM=1.

BGFACT=1.

ABSCAT=1.

CD=1.

```
NLAST=1
NFIRST=1
FBG=0.
```

```
C
```

```
C*****
**
```

```
C INITIALISE SOME ARRAYS TO FORESTALL ANY STRANGE AFFECTS
LATER
```

```
C
```

```
DO 16 I=1,NOPTS
SC(I)=0.
SC1(I)=0.
SC2(I)=0.
SC3(I)=0.
Q(I)=0.
ERR1(I)=0.
ERR(I)=0.
SINV(I)=0.
SQ2(I)=0.
Q2(I)=0.
SL10(I)=0.
NC(I)=0.
QLN(I)=0.
ERBG1(I)=0.
  ERSC1(I)=0.
  ERBG(I)=0.
  ERSC(I)=0.
```

```
16 CONTINUE
```

```
C
```

```
C*****
*****
```

```
C
```

```
C THIS IS THE MAIN PART OF THE PROGRAMME WHERE DATA FILES
(AVERAGED AND
C IN ASCII FORMAT ARE READ INTO THE PROGRAMME AND
MANIPULATED IN
C VARIOUS WAYS AND COMBINATIONS OF QUANTITIES CALCULATED.
C ALLOWS INSERTION OF CONCENTRATION OF SCATTERING SPECIES
AND
C ABSOLUTE DIFFERENTIAL SCATTERING CROSS SECTION OF A
CALIBRANT
```

```
C
```

```
572 PRINT*,'ANALYSIS OF S.A.N.S. DATA '
  PRINT*,' '
573 write(6,211)' Name of file to write corrected data to'
  write(6,211)' the extension .crd will be added'
  read(5,211)crdfil
  INQUIRE(FILE=crdfil/' .crd',exist=l15)
  if(l15)then
  write(6,211)' A FILE ALREADY EXISTS WITH THAT NAME!
+TRY AGAIN'
  goto 573
```

```

endif
OPEN(15,FILE=crdfil//'.crd',STATUS='NEW')
PRINT*,' DO YOU WANT SPOLLY OUTPUT?'
CALL ANS(L1)
if(l1)goto 210
209 PRINT*,' ENTER FILENAME FOR SPOLLY DATA'
PRINT*,' THE FILENAME WILL BE WRITTEN WITH THE EXTENSION'
PRINT*,' .LST'
READ(5,211)FTIT
INQUIRE(FILE=FTIT//'.lst',exist=l15)
if(l15)then
write(6,211)' A FILE ALREADY EXISTS WITH THAT NAME!
+TRY AGAIN'
goto 209
endif
OPEN(14,FILE=FTIT//'.lst',STATUS='NEW')
210 PRINT*,' DATA FROM LOQ(R) OR GRENOBLE(G)?'
READ 103,CHH
103 FORMAT(1A1)
IF(CHH.EQ.'G'.or.chh.eq.'g')GOTO 217
C
C*****
C
C THIS PART IS ORGANISED TO DEAL WITH FILES PRODUCED
C FROM LOQ USING THE COLLETE/GENIE PACKAGE
C
C A NUMBER OF BACKGROUND RUNS CAN BE READ IN AND ADDED
TOGETHER AFTER
C WEIGHTING EACH BY A MULTIPLYING FACTOR.THIS MAY BE USEFUL
WHEN A
C PURE H SAMPLE AND PURE D SAMPLES ARE RUN TO ASSESE THE
CORRECT
C BACKGROUND FOR A SAMPLE WHICH HAS BOTH COMPONENTS
PRESENT IN SOME
C PROPORTION.
C AS AT 19/11/88 THIS OPTION IS NOT AVAILABLE FOR THE SAMPLE
RUNS;
C THESE ARE JUST ADDED TOGETHER
C THE BACKGROUND OBTAINED MAY BE MULTIPLIED BY A
FACTOR(TRANSM ETC)
CBEFORE SUBTRACTION FROM THE SAMPLE.THE RESULTANT ARRAY
MAY HAVE AN
C ADDITIONAL FLAT BACKGROUND SUBTRACTED BEFORE THE RESUKTS
ARE
C MULTIPLIED BY THE ABSOLUTE DIFFERENTIAL CROSS SECTION
FACTOR.
C
C ERRORS ARE PROPAGATED THROUGH AS THE SQRT OF THE SUM OF
THE
C INDIVIDUAL SQUARES.....THIS AMY NOT BE CORRECT(19/11/88) AS
C I COULDN'T REMEBER THE CORRECT FORMULA!!CHECK IT
C

```

C

```

PRINT*,' DATA SHOULD BE CORRECTED BY COLLETE BEFORE'
PRINT*,' USING THIS PROGRAM!!'
199 PRINT*,' SUPPLY FILENAME WHERE ALL RUNS ARE HELD'
PRINT*,' EXTENSION .DAT ASSUMED'
READ(5,211)FNAME
INQUIRE(FILE=FNAME//'.dat',EXIST= L15)
IF(.NOT.L15)THEN
WRITE(6,211)' FILE NOT PRESENT...TRY AGAIN'
GOTO 199
ENDIF
OPEN(20,FILE=FNAME//'.dat',STATUS='OLD')
PRINT*,' HAVE THESE DATA SETS HAD OTHER LOQ RUNS
SUBTRACTED FROM'
PRINT*,' THEM ALREADY? Y/N'
CALL ANS(L12)
211 FORMAT(A)
606 PRINT*,' SUPPLY BACKGROUND RUN NUMBER '
PRINT*,' A ZERO RUN NUMBER COMPLETES THE SET OF RUNS'
print*,' A NEGATIVE RUN STOPS THE PROGRAM'
READ(5,212)RUNUB
IF(RUNUB.EQ.0)GOTO 607
IF(RUNUB.LT.0)GOTO 999
RUNNUB=RUNUB
CALL READRAL(RUNUB,NOPTS,Q,BG1,ERBG1,L12,ECNO1,FAULT)
IF(FAULT.LT.1)GOTO 606
650 PRINT*,' ENTER FACTOR TO MULTIPLY EACH SET BY BEFORE
ADDING'
PRINT*,' THIS COULD INCLUDE EFFECTS OF THICKNESS,CONCN
ETC'
READ(5,*)FACTM
DO 604 I=1,NOPTS
BG(I)=BG(I)+FACTM*BG1(I)
ERBG(I)=SQRT(ERBG(I)**2+(FACTM*ERBG1(I))**2)
604 CONTINUE
GOTO 606
607 CONTINUE
PRINT*,'SAMPLE RUN NUMBER ENTRY'
655 PRINT*,'ENTER SAMPLE RUN NO.'
PRINT*,' A ZERO RUN NUMBER COMPLETES THE SET OF RUNS'
PRINT*,' A NEGATIVE RUN STOPS THE PROGRAMME'
READ(5,212)RUNNUS
212 FORMAT(I6)
IF(RUNNUS.EQ.0)GOTO 613
IF(RUNNUS.LT.0)GOTO 999
numS=RUNNUS
CALL READRAL(RUNNUS,NOPTS,Q,SC1,ERSC1,L12,ECNO2,FAULT)
IF(FAULT.LT.1)GOTO 607
DO 612,I=1,NOPTS
SC(I)=SC(I)+SC1(I)
ERSC(I)=SQRT((ERSC(I)**2)+ERSC1(I)**2)
612 CONTINUE

```

```

GOTO 655
613 PRINT*,' ENTER THE FACTOR TO MULTIPLY BACKGROUND BY
BEFORE'
PRINT*,' SUBTRACTION FROM SAMPLE SCATTERING'
READ(5,*)BGFACT
PRINT*,' ENTER ABSOLUTE CROSS SECTION FACTOR'
READ(5,*)ABSCAT
PRINT*,' ENTER THE CONCENTRATION (G/ML) OF SCATTERING
SPECIES'
READ(5,*)CD
PRINT*,' ENTER A VALUE FOR FLAT BACKGROUND '
READ(5,*)FBG
DO 660,I=1,NOPTS
SC(I)=((SC(I)-BGFACT*BG(I))-FBG)*ABSCAT
ERR(I)=(SQRT(ERSC(I)**2+(BGFACT*BG(I)**2))*ABSCAT
660 CONTINUE
PRINT*,'SUPPLY A TITLE FOR SAMPLE'
READ 116,TITLE
GOTO 705
C
C*****
C
C THIS SECTION DEALS WITH DATA AS OBTAINED AT GRENOBLE AND
C BROUGHT BACK IN RCARD FORMAT OF RADIALY AVERAGED DATA
C
C
217 SH='G'
C PART PUT IN TO ACCOUNT FOR FUNNY? D16 FILES
C
print*,' IS THIS D16 DATA Y/N?'
CALL ANS(L16)
C
C
PRINT*,' SUPPLY FILENAME FOR DATA PLEASE'
PRINT*,' THE EXTENSION .DAT WILL BE ASSUMED'
READ(5,211)FNAME
inquire(file=fname//'.dat',exist=l15)
if(.not.l15)then
write(6,211)' File not present...try again!'
goto 217
endif
OPEN(20,FILE=FNAME//'.dat',STATUS='OLD')
50 CONTINUE
PRINT*,' '
C
C ***** INPUT WATER RUN *****
C
106 PRINT*,'WATER RUN NUMBER,MONITOR '
CALL DATREAD(NUMW,NOPTS,Q,W,EW,MONW,NOWAT,L16)
C
C IF NO WATER RUN THEN SKIP ON TO BACKGROUND RUN INPUT
C

```

```

IF(NOWAT.LT.1) GOTO 111
IF(NUMW.LT.1) GOTO 106
CALL AGAIN(MONW,W,EW,NOPTS,L16)
PRINT*,'ABSOLUTE DIFFERENTIAL SCATTERING CROSS SECTION OF
WATER'
  READ(5,*)ABSCAT
107 PRINT*,'WATER CELL RUN NUMBER MONITOR '
  CALL DATREAD(NUMWB,NOPTS,Q,WB,EWB,MONWB,NOWB,L16)
C
C   IF NO BACKGROUND RUN FOR WATER THEN SKIP ON TO
BACKGROUND RUN
C   INPUT
  IF(NOWB.LT.1) GOTO 111
  IF(NUMWB.LT.1) GOTO 107
  CALL AGAIN(MONWB,WB,EWB,NOPTS,L16)
  PRINT*,'ENTER WATER TRANSMISSION FACTOR ?'
  READ (5,*)TRANW
111 CONTINUE
101 CONTINUE
C
C   ***** INPUT SAMPLE BACKGROUND DATA *****
C
  PRINT*,'SAMPLE BACKGROUND RUN NUMBER MONITOR '
  PRINT*,'A NEGATIVE RUN NUMBER STOPS THE PROGRAMME'
  CALL DATREAD(NUMSB,NOPTS,Q,SB,ESB,MONSB,NOBAC,L16)
  IF(NUMSB.LT.0)GOTO 999
  PRINT*,'SUBTRACT A CELL FIRST ? '
  CALL ANS(M2)
  IF(.NOT.M2) CALL SUBCELL(MONSB,SB,ESB,NOPTS,L16)
  PRINT*,'BACKGROUND RUNS CONTINUED : '
  CALL AGAIN(MONSB,SB,ESB,NOPTS,L16)
114 CONTINUE
C
C   ***** INPUT SAMPLE DATA *****
C
312 PRINT*,'SAMPLE RUN NUMBER MONITOR '
  PRINT*,'A NEGATIVE RUN NUMBER RETURNS TO SAMPLE
BACKGROUND INPUT'
  CALL DATREAD(NUMS,NOPTS,Q,S,ES,MONS,NOSAM,L16)
  IF(NOSAM.LT.1) GOTO 124
  IF(NUMS.LT.0) GOTO 101
  PRINT*,'SUBTRACT A CELL FIRST ? '
  CALL ANS(M2)
  IF(.NOT.M2) CALL SUBCELL(MONS,S,ES,NOPTS,L16)
  PRINT*,'SAMPLE RUNS CONTINUED : '
  CALL AGAIN(MONS,S,ES,NOPTS,L16)
  PRINT*,'SAMPLE TRANSMISSION FACTOR ?'
  READ (5,*)TRANS
  PRINT*,' INPUT THE CONCEN(g/ml) OF SCATTERING SPECIES'
  READ(5,*)CD
113 CONTINUE
C

```

```

C      ***** NO BACKGROUND GIVEN *****
C
      IF(NOBACK.LT.1)THEN
        PRINT*,'NO BACKGROUND - DEFAULT VALUES APPLIED'
        NUMSB=0
        MONSB=MONS
        TRANS=1.0
        DO 115 I=1,NOPTS
          SB(I)=0.0
          ESB(I)=0.0
115    CONTINUE
        END IF
        IF(NOWAT.GT.0) GOTO 109
C
C      ***** NO WATER RUN GIVEN *****
C
180  PRINT*,'NO WATER RUN GIVEN - DEFAULTS APPLIED'
      PRINT*,'ONLY NORMALISED TO SAMPLE MONITOR COUNTS !!!'
      MONW=MONS
      MONWB=MONS
      NUMW=0
      NUMWB=0
      TRANW=1.0
      DO 110 I=1,NOPTS
        W(I)=1.0
        EW(I)=0.0
        WB(I)=0.0
        EWB(I)=0.0
110  CONTINUE
        GOTO 112
109  CONTINUE
        IF(NOWB.GT.0) GOTO 112
C
C      ***** NO WATER CELL RUN GIVEN *****
C
      PRINT*,'NO WATER CELL RUN - DEFAULTS APPLIED'
      MONWB=MONW
      NUMWB=0
      TRANW=1.0
      DO 150 I=1,NOPTS
        WB(I)=0.0
        EWB(I)=0.0
150  CONTINUE
112  CONTINUE
        AMONS=MONS
        R1=AMONS/MONSB
        R2=AMONS/MONW
        R3=AMONS/MONWB
C
C      ***** SUBTRACTION OF FLAT LEVEL OR EXP BACKGROUND *****
C
      TAIL=0.0

```

```

B2=0.0
FL=0.0
ETAIL=0.0
PRINT*,'DO YOU WISH TO SUBTRACT A FLAT BACKGROUND ?'
  CALL ANS(L2)
  IF(L2) GOTO 117
  PRINT*,'LEVEL FOR FLAT BACKGROUND AND ERROR ,'
  PRINT*,'ENTER A NEGATIVE NUMBER IF WISH AN EXPONENTIAL'
PRINT*,'BACKGROUND.FREE FORMAT ENTRY OF DATA'
  READ(5,*)TAIL,ETAIL
  IF(TAIL.GT.0.0) GOTO 117
  PRINT*,'EXP BACKGROUND = F.EXP(B.Q^2) F,B ?'
  READ *,FL,B2
  ETAIL=0.0
117  CONTINUE
  PRINT*,'SUPPLY A TITLE FOR SAMPLE'
  READ 116,TITLE
116  FORMAT(20A)
C
C  CALCULATE NORMALISED INTENSITY
C
DO 119 K=1,NOPTS
  BX=B2*(Q(K)**2)
  BX=(FL*EXP(BX)) + TAIL
  WAT=(W(K)*R2) - (WB(K)*R3*TRANW)
IF(WAT.LE.0)THEN
  EWAT=0.0
  GOTO 119
ENDIF
  WAT=1.0/WAT
  EWAT=R2*EW(K) + R3*TRANW*EWB(K)
  EWAT=EWAT*WAT
IF(S(K).EQ.0)THEN
  ERR(K)=0.0
  GOTO 119
ENDIF
  SC(K)=S(K)-SB(K)*R1*TRANS
  ESAM=ES(K) + R1*TRANS*ESB(K)
  ESAM=ESAM/SC(K)
  ETOT=SQRT(EWAT**2 + ESAM**2)
  SC(K)=SC(K)*WAT
  ERR(K)=(ETOT*SC(K))
  ERR(K)=ERR(K) + ETAIL
  SC(K)=(SC(K) - BX)*ABSCAT
119  CONTINUE
705  write(15,70)nums,nopts
70  format(i6,19x,i5)
  do 72,i=1,nopts,2
  write(15,74)q(i),sc(i),err(i),q(i+1),sc(i+1),err(i+1)
72  continue
74  format((1x,2(e10.3,e11.4,e10.3)))
  IF(L1) GOTO 120

```

```

C
C   WRITE HEADER FOR SPOLLY DATA
C
      WRITE(14,118)TITLE
118  FORMAT(1X,20A)
      WRITE(14,1001)NOPTS
1001 FORMAT(1X,I3)
      IF(CHH.EQ.'G'.or.chh.eq.'g')THEN
          WRITE(14,121)NUMS,MONS,NUMSB,MONSB,NUMW,MONW,
          +NUMWB,MONWB,TAIL,ETAIL,TRANS,TRANW,FL,B2,CD,ABSCAT
121  FORMAT(/,5X,'SAMPLE',5X,'RUN',I6,5X,'MONITOR=',I10,
          +15X,'SAMPLE BACK',5X,'RUN',I6,5X,'MONITOR=',I10,
          +//,5X,'WATER',6X,'RUN',I6,5X,'MONITOR=',I10,
          +15X,'WATER CELL',6X,'RUN',I6,5X,'MONITOR=',I10,/,
          +5X,'INC. LEVEL=',F7.4,2X,'ETAIL=',F7.5,2X,'SAMPLE TRANS
          +=',F5.3,2X,'WATER TRANS=',F5.3,4X,'FL =',F6.2,4X,
          +'B2 =',F6.4,/,5X,'CONC OF SCATTERING SPECIES(g/ml)=',F7.4,/,
          +5X,'ABSOLUTE DIFFERENTIAL CROSS SECTION OF WATER=',F5.3,/)
          ELSE IF(CHH.EQ.'R'.or.chh.eq.'r')THEN
              WRITE(14,700)numS,ECNO2,RUNNUB,ECNO1,FBG,BGFACT,CD,ABSCAT
              ENDIF
700  FORMAT(/,5X,'SAMPLE',5X,'RUN',I6,5X,'EMPTY CAN RUN',5X,I6,
          1//,5X,'BGRD',5X,'RUN',I6,5X,'EMPTY CAN RUN',5X,I6,/,
          *' FLAT BACKGROUND LEVEL= ',F9.5,/,
          3' BACKGROUND FACTOR',5X,F7.4,
          *,5X,'CONC OF SCATTERING SPECIES(g/ml)=',F7.4,/,
          4' ABSOLUTE CROSS SECTION FACTOR',3X,F8.5,/)
120  CONTINUE
C
C   CALCULATE VARIOUS FUNCTIONS OF I AND Q
C
      DO 123 K=1,NOPTS
          NC(K)=K
          IF(SC(K).GT.0.0)GOTO 140
          SL(K)=0.0
          SINV(K)=0.0
          ESINV(K)=0.0
          GOTO 444
140  CONTINUE
          SL(K)=LOG(SC(K))
          SINV(K)=1.0/SC(K)
          ESINV(K)=(ERR(K)/SC(K))*SINV(K)
          SL10(K)=LOG10(SC(K))
444  CONTINUE
          Q2(K)=(Q(K)*Q(K))
          QN(K)=(Q(K)**1.67)
          SQ2(K)=Q2(K)*SC(K)
          IF(Q(K).GT.0.0) GOTO 90
          QLN(K)=0.0
          GOTO 123
90   QLN(K)=LOG10(Q(K))
123  CONTINUE

```

```

      IF(L1) GOTO 124
C
C   OUTPUT STANDARD SPOLLY DATA
C
      WRITE(14,125)
      WRITE(14,126)(NC(K),Q(K),SC(K),ERR(K),Q2(K),
+QN(K),SINV(K),SL10(K),SQ2(K),QLN(K),K=1,NOPTS)
126  FORMAT(2X,I3,1X,E11.4,1X,E11.4,1X,E9.2,1X,E10.3,
+1X,E10.3,1X,E10.3,1X,F8.4,1X,E10.3,1X,F8.4)
125  FORMAT(2X,'NC',6X,'Q',10X,'INT',8X,'ERROR',
+6X,'Q**2',7X,'Q**N',7X,'1/INT',5X,'LOG I',5X,'I*Q**2',
+4X,'LOG Q')
124  continue
      IF(CHH.EQ.'R'.or.chh.eq.'r')THEN
      GOTO 606
      ELSEIF(CHH.EQ.'G'.or.chh.eq.'g')THEN
      GOTO 312
      ENDIF

999  PRINT*,'CHANGE DATA FILE ?'
      CALL ANS(L6)
      IF(L6) GOTO 998
      close(20)
      GOTO 102
998  CLOSE(14)
      close(15)
      STOP
      END

C
C*****
C
C*****
      SUBROUTINE ANS(L)
      CHARACTER*1 NN
      LOGICAL I
      I=.false.
      READ 310,nn
310  FORMAT(1A1)
      if(NN.eq.'N'.or.NN.eq.'n')then
      I=.true.
      endif
c    L=MM.eq.NN
      RETURN
      END
C*****
      SUBROUTINE AGAIN(MONX,SX,EX,NOPTS,L16)
      DIMENSION SX(500),SNEW(500),Q(500),ENEW(500),EX(500)
      LOGICAL L9,M2,L16
500  PRINT*,'ANOTHER RUN TO BE ADDED ?'
      CALL ANS(L9)
      IF(L9) GOTO 501
504  PRINT*,'RUN NUMBER , (MON. CTS.) ?'

```

```

CALL DATREAD(NUM,NOPTS,Q,SNEW,ENEW,MONNEW,NONUM,L16)
IF(NONUM.LT.1) GOTO 501
IF(NUM.LT.1) GOTO 504
PRINT*,'SUBTRACT A CELL FIRST ? '
CALL ANS(M2)
IF(.NOT.M2) CALL SUBCELL(MONNEW,SNEW,ENEW,NOPTS,L16)
MONX=MONX + MONNEW
DO 503 K=1,NOPTS
SX(K)=SX(K) + SNEW(K)
EX(K)=EX(K) + ENEW(K)
503 CONTINUE
GOTO 500
501 RETURN
END
C C*****
SUBROUTINE DATREAD(NUM,NP,Q,Y,EY,MON,NONUM,L16)
DIMENSION Q(500),Y(500),EY(500)
LOGICAL L16
NONUM=100
15 READ(5,830)NUM,MON
830 FORMAT(I6,I10)
IF(NUM.EQ.0) GOTO 840
IF(NUM.LT.0) GOTO 835
IF(MON.EQ.0)THEN
WRITE(5,10)
MON=1
ENDIF
10 FORMAT(1X,' MONITOR COUNTS OMMITTED'./,
+' DEFAULT VALUE OF 1 APPLIED')
C C*****
REWIND 20
800 CONTINUE
C
C
IF(L16)THEN
READ(20,820,END=811)NORUN,NP
ELSE
READ(20,821,END=811)NORUN,NP
ENDIF
820 FORMAT(I6,19X,I5)
821 FORMAT(I5,21X,I3)
C
NPX=INT((NP + 1)/2.0)
IF(NORUN.EQ.NUM) GOTO 809
DO 802 I=1,NPX
READ(20,803,END=811)X
803 FORMAT(A3)
802 CONTINUE
GOTO 800
811 CONTINUE
PRINT*,'RUN CANNOT BE FOUND !!'
print*,' Enter run number and monitor counts again!'

```

```

      goto 15
      N=-1
      RETURN
C C ***** READ DATA *****
809 CONTINUE
      DO 805 I=1,NP,2
      J=I + 1
      IF(J.GT.NP)GOTO 806
      READ(20,*,END=817)Q(I),Y(I),EY(I),Q(J),Y(J),EY(J)
805 CONTINUE
806 CONTINUE
      NPX=NPX - INT(NP/2.0)
      IF(NPX.EQ.0) GOTO 817
      READ(20,*,END=817)Q(NP),Y(NP),EY(NP)
817 CONTINUE
      GOTO 835
840 CONTINUE
      NONUM= -1
835 CONTINUE
      RETURN
      END
C C*****
C*****
      SUBROUTINE
READRAL(RUNNUS,NOPTS,Q,SC1,ERSC1,L12,ECNO,FAULT)
      REAL Q(500),SC1(500),ERSC1(500),JUNK(500)
      LOGICAL L12
      INTEGER RUNNUS,ECNO,RUNNO,FAULT
      FAULT=1
      IF(RUNNUS.EQ.0)GOTO 613
      REWIND 20
609 CONTINUE
      IF(L12)THEN
      READ(20,215,END=605)RUNNO
      ELSE
      READ(20,213,END=605)RUNNO,ECNO
      ENDIF
      READ(20,216)GARBGE
      READ(20,214)NOPTS
      READ(20,216)GARBGE
      READ(20,216)GARBGE
      IF(RUNNO.EQ.RUNNUS)THEN
      DO 610,I=1,NOPTS
      READ(20,600)Q(I),SC1(I),ERSC1(I)
610 CONTINUE
      GOTO 613
      ELSE
      DO 611 I=1,NOPTS
      READ(20,602)JUNK(I)
611 CONTINUE
      GOTO 609
      ENDIF

```

```

605 WRITE(6,606)
606 FORMAT(1X,'!!!RUN NOT FOUND!!!')
      FAULT=-1
613 RETURN
600 FORMAT(F12.5,2(E16.6))
215 FORMAT(64X,I5)
213 FORMAT(33X,I6,15X,I6)
216 FORMAT(A)
214 FORMAT(1X,I4)
602 FORMAT(F12.5)
      END
C*****
****
C*****
****
      SUBROUTINE SUBCELL(MONXX,SXX,EXX,NOPTS,L16)
          DIMENSION SXX(500),EXX(500),Q(500)
          DIMENSION SCELL(500),ECELL(500)
          LOGICAL L16
850  PRINT*,'CELL RUN NO. , (MON. CTS.) ?'
          CALL
DATREAD(NUMCEL,NOPTS,Q,SCELL,ECELL,MONCEL,NOCELL,L16)
          IF(NOCELL.LT.1)GOTO 859
          IF(NUMCEL.LT.1)GOTO 850
          PRINT*,'CELL TRANSMISSION FACTOR ?'
          READ (5,*)TCELL
          AMONXX=MONXX
          RC=AMONXX/MONCEL
          DO 852 K=1,NOPTS
          SXX(K)=SXX(K) - TCELL*RC*SCELL(K)
          EXX(K)=EXX(K) + TCELL*RC*SCELL(K)
852  CONTINUE
859  RETURN
      END

```

```

$DEBUG
C
C
PROGRAM SASFIT
implicit double precision (a-h,o-z)
DIMENSION A(10)
DIMENSION SIGMAA(10),DELTA A(10),AT(10,120)
DIMENSION Q(500),SC(500),ERR(500),yfit(500)
REAL XX(500),YY(500),erry(500)
REAL DIFF(500)
real yint,ery,rg,errg,a2,era2,backg,erbak
CHARACTER*12 FNAME
CHARACTER*50 TITLE
LOGICAL I1,L4,L5,L6
common/cmol/pd,pdh,pdd,dph,dpd,vd
common/raw/q,sc,err
C
C ** PROGRAM TO ANALYSE DATA BY PARABOLIC EXTRAPOLATION OF
CHISQUARE
WRITE(6,800)
800 FORMAT(2X,/, ' This program takes corrected data as input from'
*,/, ' RCARD format data files.'
*,/, ' Currently 4 types of equations may be fitted to the data;'
*,//,
* ' 1 Debye eqn Rg, intercept and background are adjustable',/,
* ' parameters in the non-linear least squares fit.',/,
* ' 2 Random Phase Approximation for homopolymer blends in',/,
* ' addition to the parameters in the Debye fit,the interaction'
*,/, ' parameter is a variable',/,
* ' 3 Random phase approximation for linear diblocks',/,
* ' 4 Single Chain with virial coefficient',//)
C
C
100 DO 10,I=1,150
SC(I)=0.
YFIT(I)=0.
DIFF(I)=0.
10 CONTINUE
vd=1.0
C ***** SUPPLY TITLE FOR WORK *****
C
651 PRINT*, ' FILE NAME FOR STORING RESULTS '
PRINT*, ' THE EXTENSION .FIT WILL BE ADDED AUTOMATICALLY'
READ(5,101)TITLE
INQUIRE(FILE=TITLE//'.fit',EXIST=L4)
IF(L4)THEN
WRITE(6,101)' FILE ALREADY EXISTS!'
GOTO 651
ENDIF
OPEN(9,FILE=TITLE//'.fit',STATUS='NEW')
C
C

```

```

652 PRINT*,'INPUT FILE FROM WHICH DATA IS TO BE READ '
    print*,' include the extension i.e. name.dat'
    READ(5,101)FNAME
    INQUIRE(FILE=FNAME,EXIST=L4)
    IF(.NOT.L4)THEN
    WRITE(6,101)' THAT DATA FILE DOES NOT EXIST!'
    GOTO 652
    ENDIF
    OPEN(18,FILE=FNAME,STATUS='OLD')
300 call datread(num,npts)
    j=0
    do 850,i=1,npts
    if((q(i).le.0.).OR.(SC(I).LE.0.))then
    goto 850
    else
    j=j+1
    q(j)=q(i)
    xx(j)=q(j)
    sc(j)=sc(i)
    yy(j)=sc(j)
    err(j)=err(i)
    erry(j)=0.
    endif
850 continue
    npts=j
    j=0
c    write(6,101)' To see the data hit a key'
c    call qinkey(im,mi)
c    xmin=q(1)*0.95
c    xmax=q(npts)*1.05
c    ymin=sc(npts)*0.95
c    ymax=sc(1)*1.05
c    title3=' data'
c    call plot
C    ***** WEIGHTING OPTION FOR FIT ROUTINE *****
C
167 write(6,101)' Select weighting for fit'
    write(6,101)' no weighting = 0, statistical = -1, instrumental =1'
    read(5,*)mode
c    MODE=0
C    *** SELECT FITTING FUNCTION ***
C
    WRITE(6,41)
41 FORMAT(1X,'CHOOSE FITTING OPTION FROM FOLLOWING
MENU',/,12X,
1 '1-DEBYE PLOT-',/,12X,'2-RANDOM PHASE APPROX-homopolymers'
2,/,12X,'3-RANDOM PHASE APPROX-diblocks',/,
312x,'4-SINGLE CHAIN with 2nd virial coeff.')
```

PRINT\*,'INPUT YOUR CHOICE'

```

    READ(5,70)INP
70 FORMAT(BN,I3)
    DO 11,I=1,10
```

```

A(I)=0.
SIGMAA(I)=0.
DO 12,J=1,120
AT(I,J)=0.
12 CONTINUE
11 CONTINUE
pd=1.0001
pdh=pd
pdd=pd
GOTO (323,324,325,326),INP
323 continue
a(1)=sc(15)
print*,'enter starting RG value'
read(5,*)a(2)
c a(2)=a(2)**2
print*,' Enter polydispersity (Must be>1)'
read(5,*)pd
a(3)=sc(npts)-0.5*sc(npts)
c PRINT*,'INPUT STARTING VALUE FOR INTERCEPT AT Q=0/A(1)'
c READ(5,*)A(1)
c PRINT*,'INPUT STARTING VALUE FOR Rg /A(2)'
c READ(5,*)A(2)
c PRINT*,'INPUT STARTING VALUE FOR BACKGROUND /A(3)'
c READ(5,*)A(3)
NTERMS=3
GOTO 37
324 continue
c STARTING VALUE FOR Rg(H)/A(1)
print*,' Enter the Rg of the H component'
read(5,*)a(1)
print*,' Enter the polydispersity >1.0'
read(5,*)pdh
c STARTING VALUE FOR Rg(D)/A(2)
print*,' Enter the Rg of the D component'
read(5,*)a(2)
print*,' Enter the polydispersity'
read(5,*)pdd
PRINT*,'Enter the degree of polymerisation of the H polymer'
READ(5,*)dph
PRINT*,'Enter the degree of polymerisation of the D Polymer'
READ(5,*)dpd
PRINT*,'INPUT STARTING VALUE FOR CHI/A(3)'
READ(5,*)A(3)
c***** STARTING VALUE FOR SCALING FACTOR
A(4)=50.
c*****starting value for background
a(5)=sc(npts)-0.5*sc(npts)
PRINT*,'INPUT DEUTERATED VOL. FRAC'
READ(5,*)VD
NTERMS=5
GOTO 37
325 print*,' Input the volume fraction of the A block'

```

```

read(5,*)vd
jmax=0
print*,' Input the starting value for total RG(a(1))'
read(5,*)a(1)
print*,' Input starting value for CHIN(a(2))'
read(5,*)a(2)
print*,' Input the starting value for scale factor(a(3))'
read(5,*)a(3)
print*,' Input the starting value for the background(a(4))'
read(5,*)a(4)
nterms=4
goto 37
326 print*,' input the polymer concentration (g/ml)'
read(5,*)cpol
a(1)=sc(15)
a(2)=0.0001
a(3)=(1/sc(20)-1/sc(15))/((q(20)-q(15))**2)*3*sc(15)
a(3)=sqrt(a(3))
a(4)=sc(npts)-0.5*sc(npts)
nterms=4
37 NFREE=NPTS - NTERMS
IF(NFREE.GT.0)GOTO 107
WRITE(*,101)' NUMBER OF DEGREES OF FREEDOM NOT VALID '
GOTO 990
107 CONTINUE
DO 109 I=1,NTERMS
DELTA A(I)=0.05*A(I)
109 CONTINUE
C
C
C ***** CALL FITTING ROUTINE *****
C
DO 145 I=1,NTERMS
AT(I,1)=A(I)
145 CONTINUE
write(6,846)
846 format(1x,' The no of iterations and the fitted values',
&/,' are printed out. Last no is chi^2')
CALL CURFIT (Q,SC,err,NPTS,A,DELTA A,MODE,NTERMS,SIGMA A,
1 FL,YFIT,CHISQR,NC,AT,INP)
C ***** COMPUTE FINAL PARAMETERS OF FITTED FUNCTION *****
C
GOTO(150,151,152,153),INP
150 CUTQ=A(1)
ERRCUT=(SIGMA A(1))
RADG=A(2)
ERRADG=(SIGMA A(2))
BACKG=A(3)
ERRBAK=(SIGMA A(3))
GOTO 154
151 rgh=a(1)
ERRRGH=(SIGMA A(1))

```

```

    rgd=a(2)
    ERRRGD=(SIGMAA(2))
    CHI=A(3)
    ERRCHI=SIGMAA(3)
    SCALEF=A(4)
    ERRSCA=SIGMAA(4)
    backg=a(5)
    errbak=sigmaa(5)
    goto 154
152 rg=a(1)
    errg=0.6745*(sigmaa(1))
    chin=a(2)
    erchin=0.6745*(sigmaa(2))
    scfac=a(3)
    errssf=0.6745*(sigmaa(3))
    bkgrnd=a(4)
    errbg=0.6745*(sigmaa(4))
    goto 154
153 rg=a(3)
    errg=0.6745*sigmaa(3)
    yint=a(1)
    ery=sigmaa(1)
    a2=a(2)
    era2=0.6745*(sigmaa(2))
    backg=a(4)
    erbak=0.6745*sigmaa(4)
154 CONTINUE
C ***** CALCULATE THE RESIDUALS *****
C
    DO 116 I=1,NPTS
    DIFF(I)=SC(I)-YFIT(I)
116 CONTINUE
C
C ** TABULATE DATA **
WRITE(9,117)FNAME
write(9,121)num
if(mode.gt.0)then
write(9,101)' Instrumental weighting of points'
elseif(mode.lt.0)then
write(9,101)' Statistical weighting of points'
else
write(9,101)' No weighting'
endif
WRITE(9,118)
if(inp.eq.1)then
write(9,101)' Fit to Debye equation'
elseif(inp.eq.2)then
write(9,101)' Fit to RPA expression for homopolymer blend'
elseif(inp.eq.3)then
write(9,101)' Fit to RPA expression for diblock copolymer'
else
write(9,101)' Fit to single chain with 2nd Virial coefficient'

```

```

endif
write(9,118)
GOTO(128,129,400,420),INP
128
WRITE(9,413)NC,CHISQR,CUTQ,ERRCUT,RADG,ERRADG,BACKG,ERRBAK
WRITE(9,118)
WRITE(9,119)
WRITE(9,120)(Q(K),SC(K),YFIT(K),DIFF(K),
1K=1,NPTS)
40 WRITE(9,118)
GOTO 51
129 WRITE(9,136)NC,CHISQR,RGH,ERRRGH,RGD,ERRRGD,CHI,ERRCHI,
1 SCALEF,ERRSCA,backg,errbak
WRITE(9,118)
WRITE(9,119)
WRITE(9,120)(Q(K),SC(K),YFIT(K),DIFF(K),K=1,NPTS)
39 WRITE(9,118)
GOTO 52
400 write(9,436)nc,chisqr,rg,errg,chin,erchin,scfac,errssf,
&bkgrnd,errbg
write(9,118)
write(9,119)
write(9,120)(q(k),sc(k),yfit(k),diff(k),k=1,npts)
write(9,118)
goto 53
420 WRITE(9,438)NC,CHISQR,yint,ery,rg,errg,a2,era2,
&backg,erbak
WRITE(9,118)
write(9,440)cpol
write(9,118)
apmw=yint/cpol
a2=a2/cpol
write(9,445)apmw,a2
WRITE(9,119)
WRITE(9,120)(Q(K),SC(K),YFIT(K),DIFF(K),
1K=1,NPTS)
C **** VALUES OF PARAMETERS AT EACH STEP ****
51 WRITE(9,101)TITLE
WRITE(9,118)
WRITE(9,131)FNAME
WRITE(9,118)
WRITE(9,132)
WRITE(9,118)
DO 134 I=1,NC
WRITE(9,133)AT(1,I),AT(2,I),AT(3,I)
134 CONTINUE
WRITE(9,118)
WRITE(9,118)
GOTO 675
52 WRITE(9,101)TITLE
WRITE(9,118)
WRITE(9,131)FNAME

```

```

WRITE(9,118)
WRITE(9,467)
WRITE(9,118)
DO 138 I=1,NC
  WRITE(9,465)AT(1,I),AT(2,I),AT(3,I),AT(4,I),AT(5,I),AT(6,I)
138 CONTINUE
  WRITE(9,118)
  WRITE(9,118)
53 write(9,101)TITLE
  WRITE(9,118)
  WRITE(9,131)FNAME
  WRITE(9,118)
  WRITE(9,468)
  WRITE(9,118)
  WRITE(9,466)(AT(1,I),AT(2,I),AT(3,I),AT(4,I),I=1,NC)
  WRITE(9,118)
  WRITE(9,118)

```

C

C \*\*\*\*\* RETURN OPTIONS \*\*\*\*\*

c\*\*\*\*\*CHECK PLOTTING LIMITS \*\*\*\*\*

C\*\*\*\*\* RETURN OPTIONS \*\*\*\*\*

```

675  print*,'another fitting option y/n?'
      call ans(11)
      if(11)then
        goto 678
      else
        goto 167
      endif
678  PRINT*,'CHANGE SAMPLE RUN ?'
      CALL ANS(L5)
      IF(L5) GOTO 135
      GOTO 300
135  CLOSE(14)
      PRINT*,'CHANGE DATA FILE ?'
      CALL ANS(L6)
      IF(L6) GOTO 919
      GOTO 100
919  CONTINUE

```

C

```

990 CONTINUE
    CLOSE(9)
101 FORMAT(A)
98  FORMAT(BN,F6.1)
50  FORMAT(BN,F7.4)
61  format(i1,1x,g11.4)
132 FORMAT(7X,'A1',12X,'A2',12X,'A3')
133 FORMAT(5X,1PE11.4,3X,E11.4,3X,E11.4)
131 FORMAT(2X,' VALUES AT EACH CYCLE IN CALCULATION FOR DATA
SET'
  1,2x,A12)
120 FORMAT(3X,E11.4,3X,E11.4,3X,E11.4,3X,E11.4)
121 format(' Run number ',i6)

```

```

119 FORMAT(9X,'Q/A',11X,'SC',12X,'YFIT',9X,'DIFF',6X)
413 FORMAT(2X,' NO. OF ITERATIONS = ',I5,' CHISQR = ',1PE11.4/,
  1 2X,' INTERCEPT(AT Q=0) = ',1PE11.4,' ERROR IN INTERCEPT= ',
  2 1PE11.4/,2X,' RADIUS OF GYRATION = ',1PE11.4,' A',
  3 ' ERROR IN Rg='
  4 ,F10.4/,2X,' BACKGROUND= ',1PE11.4,' ERROR IN BACKGROUND= ',
  5 1PE11.4)
136 FORMAT(2X,' NO. OF ITERATIONS = ',I5,' CHISQR = ',1PE11.4/,
  1 2X,' Rg(HYD) = ',F10.4,' ERROR IN Rg(H) = ',F9.4/,2X,
  2 'Rg(DEU) = ',F10.4,' ERROR IN Rg(D) = ',F9.4/,2X,
  3 ' CHI= ',1PE15.4,1x,'ERROR IN CHI= ',1PE10.4/,2X,
  4 ' SCALING FACTOR = ',1PE10.4,1x,'ERROR IN SCALING FACTOR = ',
  5 1PE10.4/, ' Background = ',1pe10.4,1x,' Error = ',1pe10.4)
436 format(2x,' no. of iterations =',i5,' chisqr= ',1pe11.4/,
  &2x,' total Rg/A= ',f10.4,' error in Rg= ',f9.4/,2x,
  &' chiN= ',1pe12.4,' error in chiN= ',1pe12.4/,2x,
  &' Scale factor= ',1pe12.4,' error in scale factor= ',1pe12.4,
  &/,2x,' Background= ',1pe12.4,' error in bkgcmd= ',1pe12.4/)
438 format(2x,' Iterations ',i5,8x,'chisqr ',1pe11.4/,
  *' Int at Q=0 ',1pe11.4,1x,' error ',1pe11.4/,
  *' Rg ',1pe11.4,' A',6x,' error ',1pe11.4/,
  *' virial fact ',1pe11.4,1x,' error ',1pe11.4/,
  *' background ',1pe11.4,1x,' error ',1pe11.4)
445 format(1x,' App mol wt ',1pe11.4/, ' App 2nd virial coeff '
  *,1pe11.4,/)
440 format(1x,' Polymer concentration',1pe11.4,' g/ml')
465 FORMAT(6(1X,1PE11.4))
466 FORMAT(6(1X,1PE12.4))
467 FORMAT(8X,'A1',12X,'A2',12X,'A3',12X,'A4',12X,'A5',12X,'A6')
468 FORMAT(8X,'A1',12X,'A2',12X,'A3',12X,'A4')
118 FORMAT(/)
117 FORMAT(' DATA SET = ',A12,5X)
  82 FORMAT(I3,1X,F10.0,1X,1PE12.4,1X,E12.4)
103 FORMAT(BN,I3)
999 STOP
      END

```

```

C
C*****
C
C
C
FUNCTION FCHISQ(Y,EY,NP,NF,M,YF)
C *** EVALUATES REDUCED CHI SQUARE FOR FIT TO DATA ***
C +++ FCHISQ = SUM((Y-YFIT)**2/SIGMA**2)/NFFREE
C
implicit double precision (a-h,o-z)
DIMENSION Y(500),EY(500),YF(500)
CHISQ=0.0
IF(NF)401,401,402
401 FCHISQ=0.0
GOTO 404
C
C ***** ACCUMULATE CHISQUARE *****

```

```

C
402 CONTINUE
    DO 408 I=1,NP
        IF(M)405,406,407
405 IF(Y(I))410,406,411
411 WT=1.0/Y(I)
        GOTO 409
410 WT=1.0/(-Y(I))
        GOTO 409
406 WT=1.0
        GOTO 409
407 WT=1.0/EY(I)**2
409 CONTINUE
    CHISQ=CHISQ + WT*(Y(I)-YF(I))**2
408 CONTINUE
C
C   *** DIVIDE BY NUMBER OF DEGREES OF FREEDOM ***
C
    FREE=NF
    FCHISQ=CHISQ/FREE
404 RETURN
    END
C*****
C
    SUBROUTINE FUNC(X,A,YF,NP,INP)
    implicit double precision (a-h,o-z)
    DIMENSION X(500),A(10),YF(500)
    common/cmol/pd,pdh,pdd,dph,dpd,vd
    DO 501 I=1,NP
        XT=X(I)
        YF(I)=CALC(XT,A,INP)
501 CONTINUE
    RETURN
    END
C*****
C
    FUNCTION CALC(X,A,INP)
    implicit double precision (a-h,o-z)
    DIMENSION A(10)
    common/cmol/pd,pdh,pdd,dph,dpd,vd
    GOTO (711,712,713,714),INP
711 un=pd-1
    pow=-1./un
    qrg2=(X**2*A(2)**2)/(1+2*un)
    c1=(qrg2-1)+(1+un*qrg2)**pow
    c2=(un+1)*qrg2*qrg2
    calc=a(1)*(2*(c1/c2))+a(3)
    GOTO 769
712 uh=pdh-1
    powh=-1./uh
    qrgh=(X**2*A(1)**2)/(1+2*uh)
    c1=(qrgh-1)+(1+uh*qrgh)**powh

```

```

c2=(uh+1)*qrgh*qrgh
  c6=2*c1/c2
  CALC1=1/((1-VD)*dph*c6)
  ud=pdd-1
  powd=-1./ud
  qrgd=(X**2*A(2)**2)/(1+2*ud)
c3=(qrgd-1)+(1+ud*qrg2)**powd
c4=(ud+1)*qrgd*qrgd
c5=2*c3/c4
  CALC2=1/(VD*dpd*c5)
  FAC=(CALC1+CALC2-2*A(3))
  calc=(a(4)/fac)+a(5)
goto 769
713 uh=x*x*a(1)*a(1)
  g2=(2/(uh**2))*(vd*uh+exp(-vd*uh)-1)
  g3=(2/(uh**2))*((1-vd)*(uh+exp(-(1-vd)*uh)-1))
  g1=(2/(uh**2))*(uh+exp(-uh)-1)
  bl1=g2*g3
  bl2=(g1-g2-g3)**2
  fun=g1/(bl1-0.25*bl2)
  soq=1/(fun-2*a(2))
  calc=(soq*a(3))+a(4)
goto 769
714 u=x*x*a(3)*a(3)
  debye=(2.0/(u*u))*(u-1.0+exp(-u))
  calc=a(1)*debye/(1+2*a(2))+a(4)
769 RETURN
END
C
C*****
C
SUBROUTINE CURFIT(X,Y,ey,NP,A,DA,M,NT,EA,FL,YF,CHISQR,
INC,AT,INP)
implicit double precision (a-h,o-z)
double precision array
DIMENSION X(500),Y(500),EY(500),YF(500)
DIMENSION A(10),DA(10),EA(10),AT(10,120)
DIMENSION WT(500),ALPHA(10,10),BETA(10),DERIV(10)
DIMENSION ARRAY(10,10),B(10)
common/cmol/pd,pdh,pdd,dph,dpd,vd
NC=0
CHISQR=0.0
CHIOLD=0.0
do 500,i=1,np
ey(i)=ey(i)/0.6745
500 continue
DO 631 J=1,NT
DO 630 I=2,120
AT(J,I)=0.0
630 CONTINUE
631 CONTINUE
NF=NP - NT

```

```

C
C ***** EVALUATE WEIGHTS *****
C
  DO 601 I=1,NP
  IF(M)602,607,609
602 IF(Y(I))605,607,603
603 WT(I)=1.0/Y(I)
  GOTO 601
605 WT(I)=1.0/(-Y(I))
  GOTO 601
607 WT(I)=1.0
  GOTO 601
609 WT(I)=1.0/EY(I)**2
601 CONTINUE
C *** EVALUATE ALPHA AND BETA MATRICES ***
  10 GOTO(666,667,668,670),INP
666 CONTINUE
  WRITE(*,699)nc,A(1),A(2),A(3),chiold
  GOTO 497
667 WRITE(*,489)nc,A(1),A(2),A(3),A(4),A(5),chiold
  goto 497
668 write(*,669)nc,a(1),a(2),a(3),a(4),chiold
  goto 497
670 write(*,669)nc,a(1),a(2),a(3),a(4),chiold
669 format(1x,i3,5(1x,1pe11.4))
489 FORMAT(1x,i3,7(1X,1PE11.4))
699 FORMAT(1x,i3,4(1X,1PE11.4))
497 FL=0.001
  DO 610 J=1,NT
  BETA(J)=0.0
  DO 610 K=1,J
  ALPHA(J,K)=0.0
610 CONTINUE
  DO 620 I=1,NP
  XT=X(I)
  CALL FDERIV(XT,A,DA,NT,DERIV,INP)
  DO 616 J=1,NT
  BETA(J)=BETA(J)+WT(I)*(Y(I)-CALC(XT,A,INP))
  & *DERIV(J)
  DO 616 K=1,J
  ALPHA(J,K)=ALPHA(J,K) +WT(I)*DERIV(J)*DERIV(K)
616 CONTINUE
620 CONTINUE
  DO 613 J=1,NT
  DO 613 K=1,J
  ALPHA(K,J)=ALPHA(J,K)
613 CONTINUE
C
C *** EVALUATE CHISQUARE AT STARTING POINT ***
C
  CALL FUNC(X,A,YF,NP,INP)
  CHISQ1=FCHISQ(Y,EY,NP,NF,M,YF)

```

```

C
C   INVERT MODIFIED CURVATURE MATRIX TO FIND NEW PARAMETERS
C
621 CONTINUE
    DO 614 J=1,NT
    DO 615 K=1,NT
    ARRAY(J,K)=ALPHA(J,K)/SQRT(ALPHA(J,J)*ALPHA(K,K))
615 CONTINUE
    ARRAY(J,J)=1.0 + FL
614 CONTINUE
    CALL MATINV(ARRAY,NT,DET)
    DO 617 J=1,NT
    B(J)=A(J)
    DO 617 K=1,NT
    B(J)=B(J)+BETA(K)*ARRAY(J,K)/SQRT(ALPHA(J,J)*ALPHA(K,K))
617 CONTINUE
C
C   *** IF CHISQUARE INCREASED, INCREASE FL & TRY AGAIN ***
C
    CALL FUNC(X,B,YF,NP,INP)
    CHISQR=FCHISQ(Y,EY,NP,NF,M,YF)
    IF(CHISQ1 - CHISQR) 618,619,619
618 FL=10.0*FL
    GOTO 621
C
C   *** EVALUATE PARAMETERS AND UNCERTAINTIES ***
C
619 CONTINUE
    DO 622 J=1,NT
    A(J)=B(J)
    EA(J)=SQRT(ARRAY(J,J)/ALPHA(J,J))
622 CONTINUE
    FL=FL/10.0
C
C
    NC=NC + 1
    DO 632 I=1,NT
    AT(I,NC+1)=A(I)
632 CONTINUE
    IF(NC.GT.100)GOTO 624
    IF(NC.EQ.1) GOTO 623
    VAL=ABS(CHIOLD - CHISQR)
    VAL=VAL/CHIOLD
    IF(VAL.LE.0.0001) GOTO 625
623 CONTINUE
    CHIOLD=CHISQR
    GOTO 10
624 WRITE(*,600)'EXCEEDED LIMIT OF ITERATIONS AT LINE 6810'
625 CONTINUE
600 FORMAT(A)
    RETURN
    END

```

C

C\*\*\*\*\*

C

SUBROUTINE FDERIV(X,A,DA,NT,DERIV,INP)

implicit double precision (a-h,o-z)

DIMENSION A(10),DA(10)

DIMENSION DERIV(10)

common/cmol/pd,pdh,pdd,dph,dpd,vd

DO 701 J=1,NT

AJ=A(J)

DELTA=DA(J)

A(J)=AJ + DELTA

YFIT=CALC(X,A,INP)

A(J)=AJ - DELTA

DERIV(J)=(YFIT - CALC(X,A,INP))/(2.0\*DELTA)

A(J)=AJ

701 CONTINUE

RETURN

END

C

C\*\*\*\*\*

C

SUBROUTINE MATINV(ARRAY,NO,DET)

C

C \*\*\* INVERTS MATRIX AND COMPUTES ITS DETERMINANT \*\*\*

C

implicit double precision (a-h,o-z)

DIMENSION ARRAY(10,10),IK(10),JK(10)

DET=1.0

DO 700 K=1,NO

C

C \*\* FIND THE LARGEST ELEMENT ARRAY(I,J) IN REST OF MATRIX \*\*

C

AMAX=0.0

702 CONTINUE

DO 703 I=K,NO

DO 703 J=K,NO

IF(dABS(AMAX) - dABS(ARRAY(I,J)))704,704,703

704 AMAX=ARRAY(I,J)

IK(K)=I

JK(K)=J

703 CONTINUE

C

C INTERCHANGE ROWS &amp; COLUMNS TO PUT AMAX IN ARRAY(K,K)

C

IF(AMAX)705,706,705

706 DET=0.0

GOTO 799

705 I=IK(K)

IF(I-K)702,707,708

708 DO 709 J=1,NO

SAVE=ARRAY(K,J)

```
    ARRAY(K,J)=ARRAY(I,J)
    ARRAY(I,J)=-SAVE
709 CONTINUE
707 J=JK(K)
    IF(J-K)702,710,711
711 DO 712 I=1,NO
    SAVE=ARRAY(I,K)
    ARRAY(I,K)=ARRAY(I,J)
    ARRAY(I,J)=-SAVE
712 CONTINUE
C
C   *** ACCUMULATE ELEMENTS OF INVERSE MATRIX ***
C
710 DO 713 I=1,NO
    IF(I-K)714,713,714
714 ARRAY(I,K)=-ARRAY(I,K)/AMAX
713 CONTINUE
    DO 715 I=1,NO
    DO 715 J=1,NO
    IF(I-K)716,715,716
716 IF(J-K)717,715,717
717 ARRAY(I,J)=ARRAY(I,J) + ARRAY(I,K)*ARRAY(K,J)
715 CONTINUE
    DO 718 J=1,NO
    IF(J-K)719,718,719
719 ARRAY(K,J)=ARRAY(K,J)/AMAX
718 CONTINUE
    ARRAY(K,K)=1.0/AMAX
700 DET=DET*AMAX
C
C   *** RESTORE ORDERING OF MATRIX ***
C
720 CONTINUE
    DO 721 L=1,NO
    K=NO - L + 1
    J=IK(K)
    IF(J-K)722,722,723
723 DO 724 I=1,NO
    SAVE=ARRAY(I,K)
    ARRAY(I,K)=-ARRAY(I,J)
    ARRAY(I,J)=SAVE
724 CONTINUE
722 I=JK(K)
    IF(I-K)721,721,725
725 DO 726 J=1,NO
    SAVE=ARRAY(K,J)
    ARRAY(K,J)=-ARRAY(I,J)
    ARRAY(I,J)=SAVE
726 CONTINUE
721 CONTINUE
799 CONTINUE
    RETURN
```

END

```

C*****
C Subroutine where data is read in from the files
C*****
      SUBROUTINE DATREAD(NUM,NP)
      implicit double precision (a-h,o-z)
      DIMENSION Q(500),Y(500),EY(500)
      common/raw/q,y,ey
      10  write(6,100)' Enter run number'
      100 format(a)
      READ(5,830)NUM
      830 FORMAT(I6)
      IF(NUM.LE.0)then
      write(6,100)' Dummy! Enter a number > 0!!'
      goto 10
      endif
C*****
      REWIND 18
      800 CONTINUE
C
C
      READ(18,820,END=811)NORUN,NP
      820 FORMAT(I6,19X,I5)
      NPX=INT((NP + 1)/2.0)
      IF(NORUN.EQ.NUM) GOTO 809
      DO 802 I=1,NPX
      READ(18,803,END=811)X
      803 FORMAT(A3)
      802 CONTINUE
      GOTO 800
      811 CONTINUE
      PRINT*,'Run not found !!'
      write(6,100)' Try another number'
      goto 10
C C   ***** READ DATA *****
      809 CONTINUE
      DO 805 I=1,NP,2
      J=I + 1
      IF(J.GT.NP)GOTO 806
      READ(18,*,END=817)Q(I),Y(I),EY(I),Q(J),Y(J),EY(J)
      805 CONTINUE
      806 CONTINUE
      NPX=NPX - INT(NP/2.0)
      IF(NPX.EQ.0) GOTO 817
      READ(18,*,END=817)Q(NP),Y(NP),EY(NP)
      817 CONTINUE
      RETURN
      END
c
C*****
      SUBROUTINE ANS(L)
      CHARACTER*1 NN

```

```
LOGICAL I
I=.false.
READ 310,nn
310  FORMAT(1A1)
    if(NN.eq.'N'.or.NN.eq.'n')then
        I=.true.
    endif
c    L=MM.eq.NN
    RETURN
    END
```

```
C*****
```

```
C*****
```

## University of Durham

## Board of Studies in Chemistry

Colloquia, lectures and Seminars given by Invited Speakers

1st August 1989 to 31st July 1990

- ASHMAN Mr A (Durham Chemistry Teacher's Centre)  
The National Curriculum - An Update 11th Oct 1989
- BADYAL Dr J P S (Durham University)  
Breakthroughs on Heterogeneous Catalysis 1st Nov 1989
- BECHER Dr J (Odense University)  
Synthesis of New Macrocyclic Systems using  
Heterocyclic Building Blocks 13th Nov 1989
- BERCAW Prof J E (California Institute of Technology)  
Synthetic and Mechanistic Approaches to  
Ziegler-natta Polymerization of Olefins 10th Nov 1989
- BLEASDALE Dr C (Newcastle University)  
The Mode of Action of some Anti-tumour Agents 21st Feb 1990
- BOLLEN Mr F (formerly Science Advisor, Newcastle LEA)  
What's new in Satis, 16-19 27th Mar 1990
- BOWMAN Prof J M (Emory University)  
Fitting Experiment with Theory in Ar-OH 23rd Mar 1990
- BUTLER Dr A (St Andrews University)  
The Discovery of Penicillin: Facts and Fancies 7th Dec 1989
- CAMPBELL Mr W A (Durham Chemistry Teachers Centre)  
Industrial Catalysis - Some Ideas for  
the National Curriculum 12th Sep 1989
- CHADWICK Dr P (Dept of Physics, Durham University)  
Recent Theories of the Universe (with respect  
to National Curriculum Attainment Target 16) 24th Jan 1990
- CHEETHAM Dr A K (Oxford University)  
Chemistry of Zeolite Cages 8th Mar 1990

- CLARK Prof D T (ICI Wilton)  
Spatially resolved Chemistry (using Nature's Paradigm  
in the Advanced Materials Arena) 22nd Feb 1990
- COLE-HAMILTON Prof D J (St Andrews University)  
New Polymers from Homogeneous Catalysis 29th Nov 1989
- CROMBIE Prof L (Nottingham University)  
The Chemistry of Cannabis and Khat 15th Feb 1990
- DYER Dr U (Glaxo)  
Synthesis and Conformation of C-Glycosides 31st Jan 1990
- FLORIANI Prof C (University of Lausanne,  
Switzerland)  
Molecular Aggregates - A Bridge between  
Homogeneous and Heterogeneous Systems 25th Oct 1989
- GERMAN Prof L S (USSR Academy of Sciences,  
Moscow)  
New Syntheses in Fluoroaliphatic Chemistry:  
Recent Advances in the Chemistry of Fluorinated Oxiranes 9th Jul 1990
- GRAHAM Dr D (BP Research Centre)  
How Proteins Absorb to Interfaces 4th Dec 1989
- GREENWOOD Prof J H (University of Leeds)  
Novel Cluster Geometries in Metalloborane Chemistry 9th Nov 1989
- HOLLOWAY Prof J H (University of Leicester)  
Noble Gas Chemistry 1st Feb 1990
- HUGHES Dr M N (King's College, London)  
A Bug's Eye View of the Periodic Table 30th Nov 1989
- HUISGEN Prof R (Universitat Munchen)  
Recent Mechanistic Studies of [2+2] Additions 15th Dec 1989
- IDDON Dr B (University of Salford)  
Schools' Christmas Lecture - The Magic of Chemistry 15th Dec 1989
- JONES Dr M E (Durham Chemistry Teachers'  
Centre)  
The Chemistry A Level 1990 3rd Jul 1989

- JONES Dr M E (Durham Chemistry Teachers' Centre) 21st Nov 1989  
GCSE and Dual Award Science as a starting point for A level Chemistry - how suitable are they ?
- JOHNSON Dr G A L (Durham Teachers' Training Centre) 8th Feb 1990  
Some aspects of local Geology in the National Science Curriculum (attainment target 9)
- KLINOWSKI Dr J (Cambridge University) 13th Dec 1989  
Solid State NMR Studies of Zeolite Catalysts
- LANCASTER Rev R (Kimbolton Firreworks) 8th Feb 1990  
Fireworks - Principles and Practice
- LUNAZZI Prof L (University of Bologna) 12th Feb 1990  
Application of Dynamic NMR to the Study of Conformational Enantiomerism
- PALMER Dr F (Nottingham University) 17th Oct 1989  
Thunder and Lightning
- PARKER Dr D (Durham University) 16th Nov 1989  
Macrocycles, Drugs and Rock 'n' Roll
- PERUTZ Dr R N (York University) 24th Jan 1990  
Plotting the Course of C-H Activations with Organometallics
- PLARINOV Prof V E (USSR Academy of Sciences, Novosibirsk) 9th Jul 1990  
Polyfluoroindanes: Synthesis and Transformation
- POWELL Dr R L (ICI) 6th Dec 1989  
The Development of CFC Replacements
- POWIS Dr I (Nottingham University) 21st Mar 1990  
Spinning off in a huff: Photodissociation of Methyl Iodide
- RICHARDS Mr C (Health and Safety Executive, Newcastle) 28th Feb 1990  
Safety in School Science Laboratories and COSHH

- ROZHKOV Prof I N (USSR Academy of Sciences,  
Moscow) 9th Jul 1990  
Reactivity of Perfluoroalkyl Bromides
- STODDART Dr J F (Sheffield University) 1st Mar 1990  
Molecular Lego
- SUTTON Prof D (Simon Fraser University,  
Vancouver BC) 14th Feb 1990  
Synthesis and Applications of Dinitrogen and  
Diazo Compounds of Rhenium and Iridium
- THOMAS Dr R K (Oxford University) 28th Feb 1990  
Neutron Reflectometry from Surfaces
- THOMPSON Dr D P (Newcastle University) 7th Feb 1990  
The role of Nitrogen in Extending Silicate  
Crystal Chemistry

